AD_____

Award Number: DAMD17-99-1-9560

TITLE: Genetic Evaluation of Peripheral Nerve Sheath Tumors in Neurofibromatosis Type I

PRINCIPAL INVESTIGATOR: David H. Viskochil, M.D., Ph.D.

CONTRACTING ORGANIZATION: University of Utah
Salt Lake City, UT 84102

REPORT DATE: October 2003

TYPE OF REPORT: Final

PREPARED FOR: U.S. Army Medical Research and Materiel Command
Fort Detrick, Maryland 21702-5012

REPORT DOCUMENTATION PAGE

Form Approved OMB No. 074-0188

1. AGENCY USE ONLY (Leave blank)	2. REPORT DATE	3. REPORT TYPE AND DATES COVERED
	October 2003	Final (1 Oct 1999 - 30 Sep 2003)

4. TITLE AND SUBTITLE

Genetic Evaluation of Peripheral Nerve Sheath Tumors in Neurofibromatosis Type I

5. FUNDING NUMBERS

DAMD17-99-1-9560

6. AUTHOR(S)

David H. Viskochil, M.D., Ph.D.

7. PERFORMING ORGANIZATION NAME(S) AND ADDRESS(ES)

University of Utah
Salt Lake City, UT 84102

E-Mail: dave.viskochil@hsc.utah.edu

8. PERFORMING ORGANIZATION REPORT NUMBER

9. SPONSORING / MONITORING AGENCY NAME(S) AND ADDRESS(ES)

U.S. Army Medical Research and Materiel Command
Fort Detrick, Maryland 21702-5012

10. SPONSORING / MONITORING AGENCY REPORT NUMBER

11. SUPPLEMENTARY NOTES

Original contains color plates: ALL DTIC reproductions will be in black and white

12a. DISTRIBUTION / AVAILABILITY STATEMENT

Approved for Public Release; Distribution Unlimited

12b. DISTRIBUTION CODE

13. ABSTRACT (Maximum 200 Words)

The goal of this research project was to identify molecular changes associated with the progression of peripheral nerve sheath tumors in neurofibromatosis type 1 (NF1). Archival and prospectively acquired plexiform neurofibromas and malignant peripheral nerve sheath tumors (MPNSTs) were collected and evaluated by immunohistochemical stains and genetic analyses. Tumor heterogeneity has been assessed by both methodologies. The level of ras signal transduction activity in frozen tumor specimens was estimated by ras-GTP/ras-GDP ratios.

A number of archival specimens in paraffin blocks have been evaluated, whereas a relatively small number of MPNSTs have been collected for complete analysis. Immunohistochemical stains have been developed to distinguish high-grade versus low-grade MPNSTs and plexiform neurofibromas. The genome of plexiform neurofibromas is relatively stable, compared to the random genomic imbalances identified in low- and high-grade MPNSTs. There is minimal tumor heterogeneity in the plexiform neurofibromas, whereas there is increased tumor heterogeneity in MPNSTs. Ratios of ras-GTP to ras-GDP, in a subset of peripheral nerve sheath tumors, did not correlate well with level of malignancy.

14. SUBJECT TERMS

Tumor Suppressor gene, p53, immunohistochemistry, allele imbalance

15. NUMBER OF PAGES

156

16. PRICE CODE

17. SECURITY CLASSIFICATION OF REPORT	18. SECURITY CLASSIFICATION OF THIS PAGE	19. SECURITY CLASSIFICATION OF ABSTRACT	20. LIMITATION OF ABSTRACT
Unclassified	Unclassified	Unclassified	Unlimited

Table of Contents

INTRODUCTION

Peripheral nerve sheath tumors (PNSTs) are soft tissue tumors that are associated with neurofibromatosis type 1 (NF1). These tumors can undergo malignant transformation, however the mechanisms that are involved in this process are not known. The goal of this research project was to identify genetic and immunologic changes that are associated with the progression of a PNST from a benign to a malignant state. To carry out this project, archival and prospectively acquired PNSTs from NF1 individuals were examined for consistent immunohistochemical and genetic abnormalities. The samples were also examined for expression of a set of informative immunologic markers in multiple sites of individual tumors.

Relatively routine histologic analysis enables one to differentiate benign plexiform neurofibromas versus high-grade MPNSTs. It does not easily determine diagnosis of benign plexiform neurofibroma with atypia versus low-grade MPNST. Special immunohistochemical stains were applied to PNSTs to define immunophenotypes that could prove helpful for pathologists to assess malignant transformation. In addition, genetic analyses of corresponding immunostained sections were performed. Genetic analysis included screening for constitutional *NF1* mutations in white blood cells (if available) of patients with NF1-related PNST, identification of somatic loss of the normal *NF1* allele in tumor specimens, or allelic imbalance analyses of a subset of genomic markers representing each of the chromosome arms. Differences between benign PNSTs (plexiform neurofibromas) and malignant PNSTs were duly noted, and provided relevant data helpful in the identification of potential genomic regions that could play a role in the process of malignant transformation. As candidate genes, genetic analyses of the *TP53* and *INK4A/CDKN2A* genes were performed to identify somatic mutations in tumor tissue. In addition, a pilot study applying Comparative Genomic Hybridization (CGH) Microarray analysis was performed on two tumors from one individual with NF1. It demonstrated the utility of examination of DNA from PNST to assess genomic imbalances. Finally, evaluations of mast cell distribution in plexiform neurofibromas, low-grade MPNST and high-grade MPNSTs were performed to assess the potential role of the microenvironment in tumor progression.

BODY

ARCHIVAL SPECIMENS

Identify genetic changes associated with malignant transformation in archival specimens

Task 1: Months 1-15 Obtain tumor specimens and perform pathology studies

The University of Utah and Department of the Army provided human subjects approval for this study in August 2000. A system has been implemented to obtain and evaluate retrospectively acquired samples from the University of Utah and the Cooperative Human Tissue Network located in Columbus, Ohio. Tumor specimens are still currently being identified and collected. Pathology sections from several archived blocks of malignant PNSTs (MPNSTs) have been prepared for immunohistochemistry analysis of p53, p16, p27, Bcl-2, CD57 (Leu7), S100, CD34, Mib-1, topoisomerase I (TOPO1), and topoisomerase II-alpha (TOPO2). The immunohistochemical stains for over 50 archival tumor specimens have been evaluated by us and collaborators, Dr. Cheryl Coffin and Dr. Holly Zhou (pathologists at the University of Utah). There were over 20 plexiform neurofibromas and over 30 MPNSTs. Our work was initially presented at the United States and Canadian Academy of Pathology (Chicago, IL, 2/25/02), and resulted in a published manuscript in the American Journal of Surgical Pathology in 2003 (see appendix – Zhou et al., 2003). This was the first report comparing this set of immunohistochemical markers between benign, low-grade and high-grade peripheral nerve sheath tumors. It also examined differences between NF1-associated and nonNF1-associated peripheral nerve sheath tumors. We concluded that p53, p16, and p27 immunohistochemical staining is associated with tumor progression, however they do not distinguish low-grade MPNST from benign plexiform neurofibromas. Nevertheless, p53 expression is a consistent marker for high-grade tumors. There was also a higher frequency of p53 expression in NF1-related versus sporadic high-grade MPNSTs. This observation supports published work by Liapis *et al.* (1999), which is in contrast to Halling *et al.* (1996).

Additional studies on this same set of archived peripheral nerve sheath tumors continue and include antibodies directed against epidermal growth factor receptor (EGFR) and mast cells. In previous work, increased immunoreactivity of EGFR has been shown to be associated with PNST progression (DeClue *et al.* 2001; appended). An abstract regarding the EGFR immunohistochemical staining patterns of this set of tumors was presented at the United States and Canadian Academy of Pathology meeting in February 2003 (see item 3 in the appendix – Zhou et al., 2003). Genetic analysis of the *EGFR* locus on chromosome 7 was also performed by genotyping 5 polymorphic markers spanning the *EGFR* locus using DNA extracted from adjacent sections of paraffin sections that had shown increased EGFR expression by immunohistochemistry (see item 4 in the appendix - Table III in poster by Zhou *et al.*, 2003; CTOS meeting). The results of this study did not demonstrate allelic imbalance, which indicates that the *EGFR* locus may not be amplified in this set of tumors. These data suggest that overexpression of EGF receptors in MPNSTs is not due to genomic amplification as concluded by Perry *et*

al., (2000). These results were presented as a poster at the Connective Tissue Oncology Meetings in Barcelona, Spain in November 2003 (see item 4 in the appendix; Zhou *et al.*, 2003).

Mast cell infiltration in PNST formation has been proposed to play a central role in the initiation of neurofibromas (Zhu *et al.*, 2002); therefore we performed mast cell immunohistochemical staining of this same set of archived tumors. Formalin-fixed, paraffin-embedded archival tumors from 5 dermal neurofibromas, 6 plexiform neurofibromas, and 13 MPNSTs (7 with NF1) were immunostained with monoclonal antibodies to mast cell tryptase and CD31 using and automated staining system (Ventana). The mast cell density (MCD), cellularity of stroma fibrous cells, and microvessel count (MVC) were determined on 10 randomly selected high-power fields (HPF) and compared among dermal all the tumor types. Mast cells with tryptase activity were present in all cases, however significant differences in MCD were found among each tumor type. These differences appeared to be associated with the abundance of stroma fibrous cellular component. The highest MCD (>100/10 HPF) was found in all dermal neurofibromas and diffuse neurofibroma areas between nodules in plexiform neurofibromas, where abundant fibrous stroma was present. In plexiform neurofibroma nodular areas with less cellular, myxoid stroma, moderately MCD (50-100/10 HPF) was observed. The majority of high-grade MPNSTs, regardless of their NF1 status, contained minor MCD (<50/10 HPF) and generally had scant fibrous stroma. Increased microvessel count (>200/10HPF) was observed in all high-grade MPNSTs when compared to plexiform neurofibromas or dermal neurofibromas (MCV 50-100/10HPF). There was no significant difference between MCV between plexiform and dermal neurofibromas. These observations provide a baseline to dissect the microenvironment of NF1-related peripheral nerve sheath tumors. These data were presented in an abstract submitted to the United States and Canadian Academy of Pathology for presentation at the 2004 meeting (see item 5 in the appendix; Zhou *et al.*, 2003).

The findings that p53 immunoreactivity is abnormal in high-grade MPNSTs coupled with the *Nf1/Tp53* double mutant mouse model for high-grade, triton-like MPNSTs (Cichowski *et al.*, 1999; Vogel *et al.*, 1999) suggests that abnormal *TP53* is potentially the most important somatic mutation that leads to tumor progression in NF1-related MPNSTs. These observations refocused our efforts toward the dual analysis of the *TP53* locus for somatic mutations in DNA extracted from tumors (see tasks 6 and 20) and the detailed immunohistochemical staining for p53 and p16 in multiple sections of PNST tissue blocks. We submitted a proposal to the US Army Medical Research and Materiel Command NFRP02 (Log#NF020074; September 17, 2002) to expand these studies with respect to p53 analysis, however it was not approved for funding.

We have also developed an immunohistochemical stain against a potential marker for malignancy with respect to peripheral nerve sheath tumors. Osteopontin is expressed in murine bone tissue as a reflection of abnormal Ras signal transduction. It is also over-expressed in breast cancer, and has been used as a marker for malignancy (Kim *et al.*, 2002; Fedarko *et al.*, 2001). Based on our preliminary work demonstrating osteopontin expression by Western blot analysis in 2 MPNST cells lines, we decided to develop immunohistochemistry to assess its expression in plexiform neurofibromas and MPNSTs. Our initial data show that the osteopontin antibody is more highly expressed in MPNSTs than plexiform neurofibromas. In addition, staining in plexiform neurofibromas is

primarily localized to the nuclei, whereas in MPNST sections it is more diffuse within the cell. The staining pattern in MPNST is much more similar to breast adenocarcinoma (See figure 1). These data suggest osteopontin could be a potential marker for malignant transformation in NF1-related peripheral nerve sheath tumors, and additional experiments are ongoing.

Task 2: Months 1-24 Select and begin microdissection across transition zones of MPNSTs

Microdissection experiments have been carried out to determine the robustness of the technique to obtain DNA template for allelic imbalance analysis. These experiments have been carried out on a prospectively acquired MPNST, and on several dermal neurofibromas that were mentioned in the previous annual report. In the 2001 report we noted that the amount of DNA used in the genotyping and allelic imbalance analysis is critical to the reproducibility of data. Therefore, two strategies have since been implemented. The first was to harvest as much tissue from the section of interest as possible. This is accomplished by either harvesting more tissue by laser capture microdissection (LCM), or if the section appears homogeneous, by simply scraping off the section of tissue with a clean sterile syringe needle. The second strategy that has been implemented is the technique of primer-extension pre-amplification polymerase chain reaction (PEP-PCR) according to Paulson et al., (1999). This technique amplifies the whole genome using random oligomers 15 nucleotides in length. This second strategy is outlined in task 3.

We have identified 24 archived tumors that clearly show clonal areas of mitoses and nuclear atypia that signify high-grade MPNST. Likewise, we have identified tumors that have benign-appearing foci in the context of an MPNST (see figure 1 in item 1 of the appendix; Zhou *et al.,* 2003).

Task 3: Months 4-30 Genotyping and allelic imbalance analysis of microdissected DNA

In order to have reproducible microdissection data, the method of PEP-PCR has been implemented. Microdissected DNA is purified using the Puregene® DNA isolation kit from Gentra Systems. 500µl of cell lysis solution from the kit is added to 100µl of crude DNA extract. This is mixed by pipetting, 200µl of protein precipitation solution is added and vortexed for 20sec. The mixture is placed on ice for 5min, then centrifuged at 12000g for 3min at room temperature in a microfuge. 600µl of isopropanol is added to the supernatant and mixed gently by inverting the tube 50 times to precipitate the DNA. The DNA is then collected by centrifugation at 12000g, for 5min at 4°C in a microfuge. The DNA pellet is washed using 75%(v/v) ethanol, air-dried for 5min and resuspended in 30µl sterile H_20.

The isolated DNA serves as template in the PEP-PCR. The DNA is mixed with 400µM random 15mer random primers (Operon), 1×PCR buffer, 300µM dNTP mixture, 2.5mM $MgCl_2$, and 5U of *Taq* DNA polymerase (Gibco-BRL). Cycling conditions are 1min at 95°C, 2min at 37°C, ramp up to 55°C at 10sec/degree, hold at 55°C for 4min and repeat cycling for 49 cycles with a final hold at 4°C. The resulting product is subjected

to specific PCR reactions for each marker. There is a size limitation associated with this method, and the largest product we can amplify is in the range of 300 base pairs. This has limited our ability to use the ABI automated genotype analyzer for allelic imbalance studies. Therefore, PEP-PCR products from microdissected samples are limited in the number of genetic loci that can be tested. We have applied the technique to direct mutation analysis of TP53 from a subset of high-grade MPNSTs shown to have high p53 immunostaining.

Figure 2 shows the microdissected H&E section for tumor #1949713 and the *TP53* PCR-based single strand conformation polymorphism (SSCP) analysis of exon 5 to examine for somatic mutation of the *TP53* gene in a specimen that has aberrant p53 staining. This section corresponds to the tumor represented as figure 1 in the appended Zhou *et al.* manuscript. This analysis enables us to screen for *TP53* mutations in areas of the tumor that show high immunoreactivity for p53. In addition to SSCP analysis, we have been able to DNA sequence individual *TP53* exons. Figure 3 shows PCR products for *TP53* exons 4 – 8, and figure 4 shows the DNA sequence generated from the respective PCR products.

These sets of experiments failed to identify *TP53* mutations in the genomic DNA of MPNSTs. We conclude that *TP53* mutations are not common in MPNSTs, however these assays do not exclude functional abnormalities of the p53 at the protein level. We attempted to identify peptide abnormalities by Western blot analysis using a number of different antibodies directed against p53 as outlined in task 12.

Task 4: Months 12-30 Statistical analysis of allelic imbalance analysis in genomic regions that are candidates for harboring genes important in malignant transformation

The statistical analysis has not been completed. Tumor material from paraffin blocks is not adequate for robust genome-wide allelic imbalance studies. This material has been used to analyze specific loci rather than all chromosome arms. We have not attempted to use DNA from archival specimens for CGH microarray. Frozen versus paraffin-embedded archival samples are adequate for allelic imbalance studies, but the number of frozen specimens available precludes robust statistical analysis. We have obtained permission to extend our study to obtain more archival samples, and continue to obtain samples as they are identified. Due to changes in the protection of human subjects procedures, we have been constrained in the collection specimens that have associated blood DNA, therefore statistical power has not been achieved. Information regarding each specimen includes age, sex and NF1-affected status.

Task 5: Months 18-34 Expand allelic imbalance analysis in candidate regions

We have found that the genomes of the dermal neurofibromas and benign PNSTs appear very stable, and allelic imbalance at any given genomic locus is rare. On the other hand, MPNSTs demonstrate a number of marker loci that are in genomic imbalance. Consistent loci demonstrating imbalances have not been identified, however 2 potential candidate regions (17p for *TP53*; 9p21 for *INK4A/CDKN2A*) in MPNSTs have been

identified from published work (Berner *et al*, 1999; Kourea *et al*, 1999; Nielson *et al*, 1999). We have screened each locus by developing oligonucleotide primer sets for polymerase chain reaction (PCR) amplification of genomic DNA from archived and prospectively acquired tumor specimens (see tasks 6 and 20). We have not yet identified another locus that merits detailed expansion of the genetic marker analysis. Potential candidates are any loci that show allelic imbalance. One such candidate locus is the *EGFR* gene. The finding of over-expression of EGFR in MPNSTs (DeClue *et al*, 2000; item 2 in the appendix) suggests that the gene could be amplified in genomic DNA.

A comparison has been made between genomic imbalance at the *EGFR* locus and immunoreactivity against Epidermal Growth Factor Receptor (EGFR) in 16 plexiform neurofibromas versus 16 archival MPNSTs. Of the 16 plexiform neurofibromas, 12 were known to be from individuals with NF1. Of the 16 MPNSTs, 13 were high-grade and 9 were known to be from individuals with NF1. The tumors were scored for S100 staining and scaled for EGFR expression (0 to 3+). In 5 tumors, adjacent slides were microdissected for DNA derived from normal-appearing skin and tumor from the respective MPNST sections. The *EGFR* locus was evaluated for allelic imbalance using 5 genetic markers spanning the gene on chromosome 7. The normal tissue showed heterozygosity for the highly informative genetic markers (D7S2422, D7S506, D7S2550, D7S494, and D7S502) and no allelic imbalance in tumor tissue. See table III in the poster by Holly Zhou (item 4 in the appendix; Zhou et al., 2003; CTOS poster; and figures 11 and 12). This suggests that amplification of the genome encompassing the *EGFR* locus does not explain over-expression of the EGF receptor in MPNSTs. Other regulatory processes likely play a significant role.

Once consistent allelic imbalance has been demonstrated at any genetic marker locus, our intention was to use additional genetic markers on the same chromosome arm to delineate potential transitions from allele balance to allelic imbalance. The genotyping core at the University of Utah (The Utah Marker Development Group, 1995) has developed an adequate number of genetic loci for each chromosome arm (see figure 2 in poster by Hang et al., 2003; item 6 in the appendix), which enables us to provide them samples for further analysis, after loci are identified as having consistent allelic imbalance in high-grade tumor tissue.

Task 6: Months 6-18 Screen known candidate genes for mutations

One candidate gene that we investigated involved the t(X;18) chromosomal translocation, commonly observed in synovial sarcomas (Dos Santos *et al.* 2001). The breakpoint genes have been identified as *SYT* from chromosome 18, and *SSX* from the X chromosome (deLeeuw *et al.*, 1994; Clark *et al.*, 1994). However, it was recently reported that this chromosomal translocation was also observed in MPNSTs [1]. We determined that the t(X;18) chromosomal translocation could not be found in dermal neurofibromas, benign PNSTs or MPNSTs from patients with NF1. Our results have been published in the journal Pediatric and Developmental and Pathology (see Appendix).

The assays for candidate genes *TP53* and *INK4A/CDKN2A* are currently being optimized. As was mentioned in the first annual report, it was planned that a PCR product would be generated from genomic DNA for exons 4-8 of *TP53*, which could then be

sequenced to find mutations. At this stage, the PCR reaction works well for genomic DNA derived from tumor tissue, and we have sequenced some PCR products without identification of *TP53* mutations. We are presently screening DNA extracted from adjacent slide sections of high-grade MPNSTs that demonstrated abnormal p53 immunoreactivity (see task 3). This has turned out to be more challenging, because it is difficult to amplify large PCR products from the genomic DNA extracted from paraffin-embedded tissue. We have re-designed the primers used in the *TP53* screen to make several smaller PCR products spanning individual *TP53* exons instead of one large product. A high-grade MPNST and an adjacent section were microdissected and their respective genomic DNA templates were screened for *TP53* mutations by SSCP (single-strand conformation polymorphism) and direct DNA sequencing. Mutations in this candidate gene in MPNSTs were not identified. These finding are consistent with Lothe et al. (2001) who failed to identify *TP53* mutations in 16 PNSTs. The association of p53 immunoreactivity and lack of mutations of *TP53* in high-grade MPNSTs has yet to be explained.

Deletions of the *INK4A/CDKN2A* locus, also known as the *p16* gene, have been implicated in MPNST development (Kourea *et al.*, 1999). We have synthesized primer sets for 4 genetic markers that span the *P16* locus; *D9S274* (151-171bp), *D9S137* (133-149bp), *D9S156* (133-155bp), and *D9S162* (172-186bp). Three blood-MPNST (archived tumor tissue) paired DNA samples have been analyzed for allelic imbalance by denaturing gel electrophoresis of end-labeled PCR products. Only one of the blood samples was heterozygous (at *D9S137* and *D9S162*) and neither marker demonstrated allelic imbalance. Microdissection of this sample was not performed, but our demonstration that these markers are robust on tumor tissue enables us to apply this marker set to other archived PNST samples.

We have developed primers to amplify exons of the *P16* gene, however SSCP of PCR products failed to identify sequence variants by acrylamide electrophoresis. We have collaborations with the melanoma team at the University of Utah (Scott Florrell, Assistant Professor, Departments of Pathology and Dermatology) to optimize conditions to detect mutations, however PCR amplifications from DNA extracted from microdissected tumor specimens have not been robust. This raised the possibility that the mutation screen may not be sensitive enough to detect small mutations of the *P16* gene.

We have not developed assays for mutation analysis of the *EGFR* gene, however we have evaluated the locus for allelic imbalance (amplification and loss of heterzygosity). In our studies, the *EGFR* locus is relatively stable in peripheral nerve sheath tumors, both plexiform neurofibromas and MPNSTs.

In summary, we have completed screening of RNA samples collected from frozen MPNSTs for the t(X;18) chromosomal translocation, however none show such an abnormality (see Liew *et al*, 2002; item 7 in the appendix). We have designed rigorous screening techniques for *NF1* gene mutation analysis by high-throughput DNA sequencing (task 13). We have designed primer sets to screen the *P16* locus for allelic imbalance and altered migration in SSCP analysis. We have screened the *TP53* locus for somatic mutations in peripheral nerve sheath tumors. We have developed a genetic marker set spanning the *EGFR* locus to determine allelic imbalance.

Task 7: Months 24-36 Screen candidate genes identified in this proposal

Apart from the known candidate genes being tested, no novel candidate genes have been identified experimentally.

Establish the degree of tumor heterogeneity in archival PNSTs

Task 8: Months 1-15 Obtain specimens and select foci for microdissection

We have selected foci from the appropriate archival bank of tumors to complete this task. We used immunohistochemical phenotyping of different sites in single tumors to determine areas that may be most informative in linking the immunophenotype with genetic studies. We recognize that having blood DNA from patients in whom we are dissecting foci is most informative for the genetic studies.

Task 9: Months 4-12 Perform genotyping and allelic imbalance analysis

Genotyping and allelic imbalance analysis is currently underway on an expanded set of tumors, including prospectively acquired samples with matched blood DNA from the subject. Blood/tumor genotype analysis is also covered in task 14. We now have data from 19 dermal neurofibromas, 7 benign PNSTs and 3 MPNSTs. These samples have been screened for allelic imbalance at a subset of genomic loci representing different chromosomal arms. These data show few markers with allelic imbalance in benign PNSTs, suggesting that these tumors are, in general, stable throughout the genome (see Table 1). Only 1 of the benign PNSTs (36670) demonstrates LOH in this set of genetic markers (summarized in table 2). These data are comparable to the results from the dermal neurofibromas, which were also very stable as stated in the previous report (see summary table 3). The more interesting data come from high-grade MPNSTs, which clearly show allelic imbalance at a number of genetic marker loci.

Genotyping of the *NF1* locus has been initiated on the archival tumors. We have started genotyping these tumors at the markers *GXAlu*, *D17S960*, $(GATN)_n$, a CA/GT repeat in intron 38, a CA/GT repeat in intron 27b, and single nucleotide polymorphic markers found at positions *NF1* cDNA 702, 2034, and 10647. Our results indicate that the genomic DNA extracted from some PNSTs clearly undergo loss of heterozygosity at *NF1* genetic marker loci (see figure 5), however a number of tumors preserve heterozygosity even in microdissected regions of the tumor.

Task 10: Months 12-18 Compare foci to establish the degree of tumor heterogeneity

To determine the degree of tumor heterogeneity, different pieces from the same tumor have been analyzed. This analysis has been extended into the other 6 benign PNSTs, and we have preliminary data from one of the MPNSTs (table 1). The data demonstrate that in the benign PNSTs there are only subtle signs of tumor genetic

heterogeneity based on differential allelic imbalances between 5 different sampled sites in single PNSTs. Some of the markers have allelic imbalance in all of the sites sampled, while other markers have only a couple of sites with allelic imbalance. The best example of this experiment is shown for tumor 708429 (see table 1 and figure 6), whereby this benign PNST had but a few genetic loci demonstrating differences of allelic imbalance. Only genetic markers on chromosome 10p demonstrated allelic imbalance at all sampled sites. It implies that the somatic genetic mutation on 10p originated early in the clonal proliferation of Schwann cells, whereas other somatic genetic changes arise later in this particular tumor progression. In summating with other benign PNST data (table 1), there is only a mild degree of tumor heterogeneity in the benign plexiform neurofibromas.

In MPNST 306595, there are clear signs of intra-tumor genetic heterogeneity. Two markers have some sites that demonstrate allelic imbalance, whereas others are normal. The strongest evidence can be seen in the 2 markers with LOH, as there is only 1 site out of the 4 in each case that has LOH. There are 2 caveats to this data. The first is that there is presently no blood DNA data available to enable us to make a comparison with the tumor data. The second is that it is only 1 MPNST, and more tumors are needed to undergo this substantial analysis before genetic heterogeneity can be definitely concluded for malignant PNSTs.

PROSPECTIVE SPECIMENS

Identify common genetic alterations in prospectively acquired benign and malignant PNSTs

Task 11: Months 1-24 Obtain tumor/blood pairs

Tumor/blood pairs are still currently being collected. This has been difficult given the issues related to inter-institutional review board approval to collect and send pathologic specimens between non-affiliated academic centers. We are continuing our recruitment of other Centers, and we are also working with a consortium (items 8 and 9 in the appendix) to develop a tissue core facility for collection of MPNSTs as part of a multi-center project to integrate Sarcoma Centers with NF Centers in the diagnosis and treatment of MPNSTs in individuals with NF1.

Task 12: Months 1-24 Perform pathology analysis on PNSTs

Immunophenotyping has been performed on two prospectively acquired PNSTs (figures 7 and 8). Results from the immunohistochemical staining profiles of archived PNSTs (Zhou et al, appended manuscript) enabled us to select Mib-1, Topo IIa, p53, p16 and p27 as discriminating immunohistochemical markers in addition to the routine H&E and S100 stains used for every tumor specimen. Tumor 36670 (figure 7) has typical features of benign plexiform neurofibroma, and the allelic imbalance studies demonstrate that it has a very stable genome. Tumor 38628 (figure 8) shows a potential transition to malignancy, whereby increased p53 staining and nuclear atypia suggest changes associated with low-grade MPNST. Allelic imbalance studies performed on this tumor

showed loss of heterozygosity for a number of genetic marker loci (table 1), which alerted us to the possibility that this otherwise benign-appearing PNST could be different that other plexiform neurofibromas. In reviewing the clinical pathology report, this tumor has been classified on clinic-pathologic criteria as a low-grade MPNST. Tumor 38628-2 arose in the same individual as 38268. It was proximal to the original tumor and may reflect direct extension or metastasis rather than being an independent tumor. This work was presented as a poster at the CTOS meeting in Barcelona, Spain in 2003 (Hang et al., 2003; item 6 in the appendix; figures 9 and 10).

Western blot analyses using antibodies directed against different epitopes of the P53 protein were performed against MPNST cell lines and cell lysates from MPNSTs. Antibodies directed against the p53 peptide (DO-1), the phosphorylated serine 392 peptide, and the P53 phosphorylated threonine 155 peptide were positive in 3 cell lines, 881F, T265 and ST526T. In addition, by Western blot analysis, antibodies directed against insulin-like growth factor receptor, $TP27^{KIP1}$, and osteopontin showed positive signals in MPNSTs.

Task 13: Months 1-34 Perform *NF1* germline mutation analysis on blood samples from prospectively enrolled subjects who have a PNST

Currently, we still evaluate cDNA PCR products from *NF1* mRNA extracted from white blood cells. Since the previous report, new primers have been designed, and appear to work better (see figures 9-10). We continue to have problems amplifying product 1 from *NF1* cDNA. In addition to sequencing the coding region of *NF1*, we are also attempting to sequence the promoter region. This is turning out to be very difficult, as designing primers for this region is more difficult than the coding region of the gene.

There is a risk in screening cDNA for mutations; some mutations result in mRNA instability leaving only 1 normal allele in the analysis. Our laboratory has moved to a new location adjacent to the University of Utah Genome Center directed by Professor Robert Weiss, which has provided us with an opportunity to develop a genomic DNA sequencing protocol for *NF1* mutation detection. Dr. Weiss' laboratory team has established methodology for high throughput DNA sequencing for the detection of mutations in the Duchenne Muscular Dystrophy gene. With this success, his team agreed to collaborate on an effort to develop a genomic DNA mutation screen for germline *NF1* mutations in NF1 patients. This process was begun in Spring of 2002. We have designed primer sets that generate 1-kb fragments specific for the *NF1* locus from genomic DNA template. Automated, high-throughput sequencing has been performed on control DNA and 6 individuals with NF1 (see table 4).

NF1 mutations have been detected in 5 of the 6 individuals; 2 of which were known mutations used as a positive control. The five purported mutations include a frame-shift single-basepair deletion in exon 21, a frame-shift single-basepair deletion in exon 12b, nonsense mutation in exon 23-1, a frame-shift single-base deletion in exon 16 (corresponds to tumor 38628), and a frame-shift single-base deletion of exon 10a (corresponds to tumor 36670). These purported mutations detected by a high-throughput screen are now in the process of adjudication by focused DNA sequence analysis. This is

proof of principle that high-throughput DNA sequence analysis can detect mutations, even in the presence of a normal allele.

In addition to mutations, this technique is robust in the detection of polymorphisms that may prove useful in other genetic studies. As shown in table 4, each subject's *NF1* genome has between 6 and 14 sequence variants that could represent polymorphisms. Each exon is spanned by approximately 800 basepairs of intron sequence in each PCR product that is sequenced, therefore potential functional polymorphisms may be detected that could modify the expression of *NF1* transcripts.

This technique has been applied to another NF1 study for which Dr. Viskochil is the PI. It is focused on bone abnormalities in NF1, and high-throughput mutation detection of the mutant *NF1* allele in a cohort of individuals with NF1 being studied for skeletal dysplasia will be evaluated for genotype-phenotype correlation.

Task 14: Months 1-30 Genotype and perform allelic imbalance analysis blood/tumor pairs

Some genotyping or allelic imbalance analysis has been performed on prospectively acquired PNSTs (Table 1). Results from other tumors that have been collected are currently being processed.

Of keen interest is tumor 38628, which initially appeared as an atypical plexiform neurofibroma by immunophenotype, yet it had 10/36 genetic markers with LOH. The other MPNST 306595 had 2 sites of LOH when compared to other areas of the same tumor. There could be complete LOH at all four sampled sites for a number of loci that are presently scored as uninformative, but defining these additional sites requires a comparison to blood DNA to determine heterozygosity at such loci from constitutional genomic DNA. This tumor and second tumor from the same individual have been extensively evaluated for allelic imbalance at the subset of polymorphic sites selected for genotype analysis. Multiple sites in both tumors have been evaluated as shown in figure 4 in a poster presented at the 2003 CTOS meeting (item 6 in the appendix; Hang et al., 2003).

In addition to allelic imbalance analysis, we used DNA from both tumors to identify genomic imbalances by CGH microarray. This technique is a sensitive way to screen the entire genome at 1-3 megabase intervals to identify loss or gain of genomic material that can be mapped to its respective chromosomal location.

Briefly, genomic DNA is extracted from the tumor cell line and sonicated to smaller segments of DNA. High-copy genomic DNA is prehybridized, and genomic DNA enriched in low-copy and single copy DNA is labeled with a fluorescent dye and hybridized to cloned genomic DNA immobilized as an array on a "chip." Hybridization signals are collected by a scanner and fed to a software program that compares hybridization signals between tumor DNA versus normal DNA. Plots for 2 separate peripheral nerve sheath tumors are provided as item 10 in the appendix. The tumor DNA is scored for deletions and amplifications as depicted in figure 3 in item 6 (Hang *et al.*, 2003; poster presentation at CTOS meeting) in the appendix. This technique will be used in future studies.

Task 15: Months 1-18 Perform differential display by microarray analysis of PNST RNA

No further microarray analysis has been performed. However, we are currently looking into modifying the current protocol, to compare tumors to a MPNST cell line. This would provide a more stable control in order to make comparisons. The original chips used for microarray at the University of Utah are specific for certain cancers, not sarcomas. We could not compare our data with other investigators using other chips. Approximately 2 years ago, Dr. Lor Randall began using an Alphametrix chip for all sarcomas collected at the University of Utah. He has analyzed the data in 4 MPNSTs in addition to other soft tissue tumors. In a collaborative effort, Dr. Randall has agreed to perform microarray analysis as part of a sarcoma center service for those tumors that we use for immunohistochemical and genomic allelic imbalance studies. We have isolated RNA from all prospectively acquired PNSTs, and cDNA has been synthesized for long-term storage. Likewise, Dr. Randall has collected a large percentage of MPNSTs that have been surgically resected at the University of Utah. This joint endeavor will ensure that tumor tissue is collected and is now available for this new microarray service provided by laboratory personnel affiliated with the sarcoma center.

We have not performed any other studies related to RNA/cDNA microarray analysis. The core facility at the University of Utah is not providing a consistent service to rely on the data output at this time.

Task 16: Months 12-30 Identify candidates by combining allelic imbalance/differential display

We have not linked our genomic allelic imbalance data with Dr. Randall's data on differential expression of genes in MPNSTs versus the standard fibroblast cell line genes. Since Dr. Randall is evaluating differences between sarcomas, he will likely identify genes that are specifically associated with Schwann cell proliferation in MPNSTs versus other soft tissue tumors. The analysis of MPNST microarray gene expression data is presently being performed on jointly acquired tumors samples. We meet with Dr. Randall approximately once a month to review the sarcoma center projects, and gene expression microarray data is presented only after it has been evaluated by his laboratory personnel. We have not compared data sets for the prospectively acquired tumors obtained under our protocols. This data will not be obtained.

Task 17: Months 12-36 Compare allele imbalance differences of benign versus malignant PNSTs

More PNSTs are to be collected before statistically significant conclusions can be determined. In review of the data at hand, it appears that benign dermal and plexiform neurofibromas have few loci with allelic imbalance, whereas MPNSTs have much higher levels of allelic imbalance, including complete loss of heterozygosity. This is an expected result, as we suspect that benign tumors are genomically stable and malignant PNSTs accumulate a number of somatic mutations in the process of tumor progression.

Determine the level of *Ras*-activation in prospectively acquired PNSTs

Task 18: Months 3-30 Perform *Ras*-activation assays on frozen samples of PNSTs

Nine tumor samples have been assayed in the last year (see table 5). Of these, 3 are prospectively acquired PNSTs of which 2 were processed into liquid nitrogen immediately upon collection. We have not performed these assays.

Task 19: Months 12-36 Compare Ras GTP/GDP levels between benign and malignant PNSTs

The range of GTP/(GTP + GDP) ratios is quite variable. As a measure of ras activation, the data are not consistent. One MPNST (306595) is 3%, whereas a benign plexiform neurofibroma is 30%. We initially hypothesized that there would be higher GTP to (GTP+GDP) ratios for higher-grade PNSTs, even though it is known that benign plexiform neurofibromas have double inactivation of *NF1*. This data suggest that ras signaling may be influenced substantially by other genetic loci or gene expression patterns. We have a number of frozen samples that have not yet been analyzed, and before making any conclusions regarding this aberrance in expected data we will complete the studies on additional samples.

Determine somatic mutation status of candidate genes in PNST progression

Task 20: Months 1-30 Perform mutation analysis on known candidate genes

Mutation analysis has been performed on *TP53* as the PNSTs are acquired. In addition, we have developed primer sets to screen for mutations in *INK4A/CDKN2A*, also known as the *p16* gene. Mutations were screened by using a combination of single stranded conformational polymorphism (SSCP) analysis and direct sequencing. We have developed primer sets to screen for mutations in the gene known to cause Noonan syndrome, *PTPN11*. Individuals with NF1 who have a more remarkable phenotype, including higher numbers of dermal neurofibromas, sometimes fit a diagnosis of Noonan-NF syndrome. Likewise, individuals with Noonan syndrome have physical features found in NF1, and visa versa. This connection has suggested an overlapping biochemical pathway with neurofibromin and the *PTPN11* gene product, protein tyrosine phosphatase SHP-2. Noonan syndrome patients have recently been shown to have missense mutations in exon 3 (2/3 of all detectable mutations in Noonan syndrome patients), that lead to gain-of-function changes and excessive SHP-2 activity (Tartaglia *et al.*, 2001). For this reason, tumor DNA has been screened for mutations in exon 3 of the *PTPN11* gene as a candidate modifier gene of proliferating Schwann cells. We developed PCR primers (L:51211 and R:51748) to amplify a 537-bp product spanning the 207-bp exon. Using internal primers, DNA sequence analysis was carried out on both strands in 7 archived frozen PNST specimens. No *PTPN11* exon 3 mutations were identified.

Task 21: Months 18-36 Perform mutation analysis on candidate genes identified in this study

Once identified the candidate genes will be analyzed.

Task 22: Months 12-36 Compare mutation status of candidate genes in benign versus MPNSTs

Once acquired, the mutation status of candidate genes in benign versus MPNSTs will be compared.

Develop future NF1 investigators

Task 23: Months 1-18 Trainee develops, revises and streamlines protocols

Dr. Michael Liew started work on this project, June 1st, 2000. He attended the NNFF, Inc Consortium meeting in June 2000, and he has developed collaborations at the University of Utah to undertake additional techniques. He regularly attends seminar series at the Eccles Institute of Human Genetics and the Huntsman Cancer Institute. His protocols are continually being developed and streamlined. Last year, he attended the 51st Annual Meeting of the American Society of Human Genetics at San Diego, CA, from the 12th-16th of October 2001. He presented a talk at the Neurofibromatosis symposium before the meeting, as well as a poster at the actual meeting. Finally, he completed a manuscript that was published in the journal Pediatric Development and Pathology. He attended the NNFF Consortium Meeting in June 2002 and presented a poster entitled, a comparison of cell cycle/growth activation marker expression in plexiform neurofibromas and malignant peripheral nerve sheath tumors in NF1. Dr. Liew submitted 3 grant proposals during his tenure as trainee under this award. One proposal was funded by the Shriners Research Foundation (June 2002). It is entitled, Immunohistochemical and Genetic Analysis of Tibial Pseudarthrosis in NF1 (Total amount of award - $16,500). Work outlined in the proposal was a continuation of the molecular techniques that he had applied to the peripheral nerve sheath tumors in NF1. Dr. Liew completed his fellowship July 12th, 2002. This was about 9 months premature because he obtained a position as staff scientist at ARUP (Associated Regional University Pathologists), which is an affiliated Laboratory of the Department of Pathology at the University of Utah. His training, with respect to the molecular biology of tumors associated with NF1, is now being applied in a research and development laboratory at ARUP. He satisfied the goals of the traineeship award, although Dr. Viskochil had hoped he would have pursued an independent academic career evaluating the link between growth factor receptors (epidermal growth factor and insulin-like growth factor receptors) and cellular responses in cells derived from individuals with NF1.

In addition to work with a postdoctoral trainee, a dermatologist from Japan, Dr. Katsumi Tanito, has been training with David Viskochil and Michael Liew since

September 2000. He is using similar techniques to screen a set of peripheral nerve sheath tumors from Japan. Dr. Tanito completed his fellowship and returned to Japan in December 2002. He is preparing a manuscript for submission as part of his thesis.

David Viskochil has devoted a significant portion of his time developing a consortium with other investigators to address a number of issues with respect to MPNSTs in NF1. The consortium met in May 2001 in London and June 2002 in Aspen Colorado as a satellite meeting to the annual NNFF-sponsored Consortium meeting. David Viskochil was designated as the organizer of the June 2002 meeting, and a copy of the executive summary statement is provided in the appendix. This effort led to the submission of 2 separate multi-center proposals for which David Viskochil is the PI. One was submitted to the Department of Defense NF Program Announcement for proposals under the category of Clinical Trials Development Award (August, 2003). This was not approved for funding by the Programmatic Review Board. A second proposal with 3 clinical trials was submitted to the NIH on October 1, 2003. It has been assigned to the Neurological Sciences and Disorders K section. A copy of the abstract is submitted in the appendix.

Task 24: Months 12-36 Trainee analyzed likelihood of non-*NF1* loci role in PNSTs

Dr. Michael Liew initiated studies into the likelihood of non-*NF1* loci being involved in the development of PNSTs. So far he has ruled out the t(X;18) chromosomal translocation as having a role in the development of PNSTs. The preliminary data he has on the role of IGF-IR is interesting, and will require more work to determine whether it is causative or a result of tumor development. Dr. Liew completed his fellowship in July 2002. He has not applied his training in NF1 to seek extramural funding in the NF1 field.

KEY RESEARCH ACCOMPLISHMENTS

- Determined that, in addition to the dermal neurofibromas being stable across the genome, benign PNSTs (plexiform neurofibromas) are also very stable across the genome with few and inconsistent somatic changes in genetic marker loci.
- Early data suggests that MPNSTs, including low-grade MPNSTs are genetically unstable at selected genetic loci across the genome.
- Different foci in benign PNSTs harbor similar, and stable, genomic signatures.
- Different foci in benign PNSTs have similar immunohistochemical staining patterns.
- Mib-1, TopoII, and P53 are the most informative immunohistochemical markers for the distinction between benign and low-grade PNSTs.
- Genetic heterogeneity can be detected in different sites from within one MPNST.
- Have developed a robust protocol for the amplification of DNA from tissue sections suitable for genotyping.
- Developed primer sets for *NF1* cDNA sequence mutation screening.
- Developed primer sets for *NF1* genomic DNA sequence mutation screening and identification of single nucleotide polymorphisms upstream and downstream of intron-exon boundaries.
- Developed primer sets for *TP53* exons for gene mutation screening of DNA extracted from paraffin-embedded PNSTs.
- Could not identify *TP53* mutations in MPNSTs from NF1 patients.
- Developed primer sets *P16* genetic markers to detect allelic imbalance in PNSTs.
- Developed and screened PNST DNA for missense mutations in the Noonan gene, *PTPN11*. No mutations were found in plexiform neurofibromas.
- Developed a standard set of genetic markers to determine the size of *NF1* microdeletions with respect to the repetitive sequences that are associated with approximately half of *NF1* microdeletions.
- Contributed to the establishment of a working group focused on the detection and treatment of MPNSTs in individuals with NF1.
- Could not establish a specific Ras-GTP/Ras-GDP ratio indicative of malignant transformation in peripheral nerve sheath tumors.
- Could not establish functional protein abnormalities for p53 using a battery of p53 antibodies directed against multiple phosphorylated domains in Western blot analysis of MPNST cell lines.
- Identified osteopontin protein expression by Western blot analysis in an MPNST cell line.
- Demonstrated DNA from MPNSTs serves as adequate template for CGH microarray analysis to detect unbalanced regions across the entire genome.
- Determined that EGFR over-expression is not due to genomic duplication of the *EGFR* gene locus.

REPORTABLE OUTCOMES

Manuscripts

PERIPHERAL NERVE SHEATH TUMORS FROM PATIENTS WITH NEUROFIBROMATOSIS TYPE 1 (NF1) DO NOT HAVE THE CHROMOSOMAL TRANSLOCATION t(X;18)

Michael A. Liew, Cheryl M. Coffin, Jonathan A. Fletcher, Minh-Thu N. Hang, Katsumi Tanito, Michihito Niimura , David Viskochil

Pediatric and Developmental Pathology, April/May (2002). 5;165-169.

INTERNATIONAL CONSENSUS STATEMENT ON MALIGNANT PERIPHERAL NERVE SHEATH TUMORS IN NEUROFIBROMATOSIS 1

Rosalie Ferner and David Gutmann.

Cancer Research (2002).62;1573-1577

David Viskochil attended a Conference in London, UK that led to this consensus report. He chaired the Clinical Group Section.

PLEXIFORM NEUROFIBROMAS IN NF1: TOWARDS BIOLOGIC-BASED THERAPY

Roger Packer, David Gutmann, Alan Rubenstein, David Viskochil, Robert Zimmerman, Gilbert Vezina, Judy Small, and Bruce Korf

Neurology (2002) 58;1461-1470.

David Viskochil chaired a session on clinical trials and contributed to the synopsis of the Clinical Trial Design section, and he reviewed the consensus report prior to submission.

C TO U RNA EDITING OF NEUROFIBROMATOSIS 1 mRNA OCCURS IN TUMORS THAT EXPRESS THE TYPE II TRANSCRIPT AND THAT ALSO EXPRESS APOBEC-1, THE CATALYTIC SUBUNIT OF THE APOLIPOPROTEIN B mRNA EDITING ENZYME

Debnath Mukhopadhyay, Shrikant Anant, Robert Lee, Susan Kennedy, David Viskochil, and Nicholas Davidson

American J Human Genetics. (2002) 70;38-50.

Some of the retrospectively acquired PNSTs in Dr. Viskochil's lab were tested in the assays performed in this work. Dr. Viskochil also provided intellectual effort in the review and discussion of pertinent data.

Poster presentations

51st Annual Meeting of the American Society of Human Genetics, San Diego CA, October 12th-16th, 2001.

GENOME-WIDE SCREEN WITH TETRA-NUCLEOTIDE REPEATS DEMONSTRATES INFREQUENT ALLELIC IMBALANCE IN BENIGN PERIPHERAL NERVE SHEATH TUMORS IN NF1.

Michael Liew, Katsumi Tanito, Yan Zhang, Minh-Thu Hang, Linda Ballard, Shunichi Sawada, Michihito Niimura and David Viskochil

ABSTRACT

Approximately 20-25% of patients with neurofibromatosis type 1 (NF1) have benign peripheral nerve sheath tumors (PNSTs), also known as plexiform neurofibromas. Some of these tumors undergo transformation into malignant PNSTs (MPNSTs), however pathogenesis of malignant transformation has not been determined. Stable benign PNSTs have double inactivation of NF1, therefore we hypothesize that additional genetic changes must occur to lead to malignant transformation. A genome-wide tetra-nucleotide genotyping screen was implemented to evaluate allelic imbalance in DNA derived from different sites within 8 benign PNSTs from 8 individuals with NF1. Using GenotyperTM software the area under the allele-specific peaks and the ratio of the areas for two alleles were compared between blood and tumor DNA to estimate allelic imbalance in tumor-derived DNA template. A ratio of peak areas for informative alleles that was either less than 0.75 or greater than 1.25 in tumor versus blood DNA samples was scored as allelic imbalance. Loss of heterozygosity (LOH) was scored by a ratio less than 0.2, or greater than 5.0. This allele imbalance could reflect either LOH or extensive amplification of one allele.

39 tetra-nucleotide markers from the distal arms of 22 chromosomes were genotyped. 2/8 PNSTs had LOH, one with one marker demonstrating LOH and 3 markers with allelic imbalance, while the other had 9 markers with LOH and 12 markers with allelic imbalance. The latter tumor is currently under re-evaluation, and is not included in this current study. The remaining PNSTs had 1-8 sites of allelic imbalance. These data were unable to identify common markers that have LOH in PNSTs, but possibly could be used to potentially classify the malignant state of a tumor based on the number of markers that show a change. Use of these markers with adjacent sets of markers in an extended set of tumors would better define candidate genes that might contribute to NF1-related tumor formation, growth and transformation.

NNFF Consortium on NF1 and NF2; Aspen Colorado; June, 2002

Liew M, Tanito K, Hang M-T, Ballard L, Sawada S, Niimura M, Viskochil D. Genome-wide screen with tetranucleotide repeats demonstrating infrequent allelic imbalance in benign peripheral nerve sheath tumors in NF1.

American and Canadian Pathology Society Meeting; February, 2003

Zhou H, **Viskochil D**, Perkins S, Tripp S, Coffin C. Expression of epidermal growth factor receptor and vascular endothelial growth factor receptor in plexiform neurofibroma, and malignant peripheral nerve sheath tumors.

Connective Tissue Oncology Meeting; Barcelona, Spain; November 2003

Zhou H, Hang M-T, Coffin C, Tripp S, **Viskochil** D. EGFR Expression and Genetic Analysis in plexiform neurofibromas (PNF) and malignant peripheral nerve sheath tumors (MPNSTs).

CONCLUSIONS

Since the previous report we have implemented some of the protocols developed, as well as refining others. Our main accomplishments have been in the realm of immunohistochemical phenotyping of benign plexiform neurofibromas, low-grade MPNSTs, and high-grade MPNSTs. We have identified a set of immunostains directed against potential modifying proteins of MPNST progression. When applied in a standardized way they lead to more uniform analysis of PNSTs. However, by Western blot analysis using antibodies directed against different epitopes of p53, we were unable to identify the molecular moiety of p53 that populates MPNSTs. We were also unable to detect aberrant p16 and p27 expression patterns in malignant peripheral nerve sheath tumors by Western analysis. We were able to detect an unusual expression pattern of a breast cancer marker, osteopontin. It is not expressed in benign peripheral nerve sheath tumors, however it is expressed in MPNSTs. This will require follow-up studies.

As before, our analysis of the coding region of *NF1* and now the promoter region, has been slowed by the difficulties faced in designing primer sets for the PCR reactions from cDNA transcribed from *NF1* mRNA. Nevertheless, we have developed a set of overlapping oligonucleotide primer sets that enable one to screen the *NF1* cDNA for mutations. We have also worked with the genome center at the University of Utah to develop a screen to detect *NF1* mutations from genomic DNA by direct sequencing. We have developed a set of genetic markers spanning the *NF1* locus that enable us to prescreen patient DNA for whole-gene deletions by simple, automated genotype analysis.

In addition, the protocols for DNA extraction and genome-wide screen we have developed are robust and informative. The DNA from MPNSTs serves as adequate template for comparative genomic hybridization microarray analysis to detect genomic imbalances by fluorescence *in situ* hybridization. We now have more results that support our data from the previous annual reports that genetic heterogeneity can be detected in

benign and malignant PNSTs. These data also indicate that benign PNSTs are very stable across the genome, like the dermal neurofibromas. However, from the MPNST data, it appears that once malignant transformation occurs the genome of these tumors becomes very unstable. This probably means that there are other genetic changes outside of *NF1* that may lead to their development, and that some of the markers could indicate a progression in the tumor. It must be stressed however, that, at this point, the data for the MPNSTs are not sufficient to make statistically valid conclusions.

We observed that highly expressed EGFR in MPNSTs does not correlate with allelic imbalance. This is an important observation because genomic amplification may not be the explanation as indicated from other investigators. It will be important to continue this analysis to decipher the etiology of EGFR overexpression, as it may play a significant role in future therapeutic trials.

We have developed assays to screen for somatic mutations of *TP53*, *P16*, and *PTPN11* in addition to *NF1*. We have assessed a lack of correlation between immunohistochemical staining, Western blot analysis, *TP53* mutations, and genome screening for allelic imbalance in an attempt to decipher the role p53 plays in tumor progression in NF1-related MPNSTs.

REFERENCES

Berner J, Sorlie T, Mertens F, et al. Chromosome band 9p21 is frequently altered in malignant peripheral nerve sheath tumors: studies of CDKN2A and other genes of the pRB pathway. Genes Chromosomes Cancer 1999; 26:151-160.

Cichowski K, Shih T, Schmitt E, Santiago S, Reilly K, McLaughlin M, Bronson R, Jacks T. Mouse models of tumor development in neurofibromatosis type 1. Science 1999;286:2172-2176.

Clark J, Rocques PJ, Crew AJ, et al. Identification of novel genes SYT and SSX, involved in the t(X;18)(p11.2;q11.2) translocation found in human synovial sarcoma. Nat Genet 1994; 7: 502-508.

DeClue J, Heffelfinger S, Benvenuto G, Ling B, Li S, Rui W, Vass W, Viskochil D, Ratner N. Epidermal growth factor receptor expression in neurofibromatosis type 1-related tumors and NF1 animal models. J Clin Invest 2000;105:1233-1241.

de Leeuw B, Balemans M, Olde Weghuis D, et al. Molecular cloning of the synovial sarcoma-specific translocation (X;18)(p11.2;q11.2) breakpoint. Hum Mol Genet 1994; 3: 745-749.

Dos Santos NR, De Bruijn DRH and Van Kessel AG. Molecular mechanisms underlying human synovial sarcoma development. Genes Chrom Cancer 2001; 30: 1–14.

Fedarko N, Jain A, Karadag A, Van Eman M, Fisher L. Elevated serum bone sialoprotein and osteopontin in colon, breast, prostate and lung cancer. Clin Cancer Res 2001;7:4060-4066.

Ferner R, Gutmann D. Meeting Report; International consensus statement on malignant peripheral nerve sheath tumors in neurofibromatosis 1. Cancer Research 2002:62;1573-1577.

Halling K, Scheithauer B, Halling A, et al. p53 expression in neurofibroma and malignant peripheral nerve sheath tumor. An immunohistochemical study of sporadic and NF1-associated tumors. Am J Clin Pathol 1996;106:282-288.

Kim J, Skates S, Uede T, Wong K, Schorge J, Feltmate C, Berkowitz R, Mok S. Osteopontin as a potential diagnostic biomarker for ovarian cancer. JAMA 2002;287:1671-1679.

Kourea HP, Orlow I, Scheithauer BW, Cordon-Cardo C and Woodruff JM. Deletions of the *INK4A* gene occur in malignant peripheral nerve sheath tumors but not in neurofibromas. Am J Path. 1999; 155: 1855-1860.

Liapis H, Marley E, Lin Y, et al. p53 and Ki-67 proliferating cell nuclear antigen in benign and malignant peripheral nerve sheath tumors in children. Pediatric and Developmental Path 1999:2;377-384.

Liew M, Coffin C, Fletcher J, Hang M-T, Tanito K, Niimura M, and Viskochil D. Peripheral nerve sheath tumors from patients with neurofibromatosis type 1 do not have the chromosomal translocation t(X;18). Pediatric and Developmental Path 2002:5;165-169.

Lothe R, Smith-Sorensen B, Hektoen M, Stenwig A, Mandahl N, Saeter G, Mertens F. Biallelic inactivation of TP53 rarely contributes to the development of malignant peripheral nerve sheath tumors. Genes, Chromosomes & Cancer 2001;30:202-206.

Nielson G, Stemmer-Rachamimov A, Ino Y, et al. Malignant transformation of neurofibromas in neurofibromatosis 1 is associated with CDKN2A/p16 inactivation. Am J Pathol 1999; 155:1879-1884.

Paulson TG, Galipeau PC and Reid BJ. Loss of heterozygosity analysis using whole genome amplification, cell sorting, and fluorescence-based PCR. Genome Res. 1999; 9: 482-491.

Tartaglia M, Mehler E, Goldberg R, Zampino G, Brunner H, Kremer H, van der Burgt I, Crosby A, Ion A, Jeffery S, Kalidas K, Patton M, Kucherlapati R, Gelb B. Mutations in PTPN11, encoding the protein tyrosine phosphatase SHP-2, cause Noonan syndrome. Nature Genetics 2001:29;465-468.

The Utah Marker Development Group. A collection of ordered tetranucleotide-repeat markers from the human genome. Am. J. Hum. Genet. 1995; 57: 619-628.

Vogel K, Klesse L, Belasco-Miguel S et al. Mouse tumor model for neurofibromatosis type 1. Science 1999;286:2176-2179.

Zhu Y, Ghosh P, Charnay P, Burns D, Parada L. Neurofibromas in NF1: Schwann cell origin and role of tumor environment. Science 2002:296;920-922.

APPENDICES Tables: 1a-1b, 2-6 and Figures: 1-12

Published manuscript: Zhou H, Coffin C, Perkins S, Tripp S, **Liew M, Viskochil D.** Malignant Peripheral Nerve Sheath Tumor (MPNST): A comparison of grade, immunophenotype, and cell cycle/growth activation marker expression in sporadic and neurofibromatosis 1 (NF1)-related lesions. Am J Surgical Pathology 2003:

Published manuscript: DeClue J, Heffelfinger S, Benvenuto G, Ling B, Li S, Rui W, Vass W, **Viskochil D**, Ratner N. Epidermal growth factor receptor expression in neurofibromatosis type 1-related tumors and NF1 animal models. J Clin Invest 2000;105:1233-1241.

Poster abstract: Zhou H, **Viskochil D**, Perkins S, Tripp S, Coffin C. Expression of epidermal growth factor receptor and vascular endothelial growth factor receptor in plexiform neurofibroma, and malignant peripheral nerve sheath tumors. United States and Canadian Academy of Pathology Meeting 2003.

Poster: Zhou H, Hang Minh-Thu, Coffin C, Tripp S, **Viskochil D**. EGFR expression and genetic analysis in plexiform neurofibromas (PNF) and malignant peripheral nerve sheath tumors (MPNSTs). Connective Tissue Oncology Meeting CTOS, November 2003.

Submitted abstract: Mast cells in peripheral nerve sheath tumors: Association with histology, NF1 status, angiogenesis, and fibrous stroma cells. Zhou H, **Viskochil D**, Minh-Thu H, Tripp S, Coffin C. American and Canadian Pathology Meetings, 2004.

Poster: Hang Minh-Thu, Liew M, Cowley B, Brothman A, Zhou H, Coffin C, **Viskochil D**. Genetic evaluation of malignant peripheral nerve sheath tumors in neurofibromatosis type 1 using quantitative genotyping and comparative genomic hybridization (CGH) microarray analysis. Connective Tissue Oncology Meeting, November 2003.

Published manuscript: **Liew M**, Coffin C, Fletcher J, Hang M-T, Tanito K, Niimura M, and **Viskochil D**. Peripheral nerve sheath tumors from patients with neurofibromatosis type 1 do not have the chromosomal translocation t(X;18). Pediatric and Developmental Path 2002:5;165-169.

Executive summary statement: MPNST symposium, Aspen 06/2002 (organizer, **David Viskochil**)

Published manuscript: Ferner R and Gutmann D. Meeting Report; International consensus statement on malignant peripheral nerve sheath tumors in neurofibromatosis 1 Cancer Research 2002:62;1573-1577. (Acknowledgement to **David Viskochil**)

Human Genomic Profiling Ratio Plots – tumor 38628: years 2000 and 2003.

Accepted commentary: **Viskochil D**. It takes 2 to tango: Mast cells and Schwann cells in neurofibromas. J Clinical Investigation 2003:in press.

Abstract for submitted proposal to the NINDS. PI: **D. Viskochil**. MPNSTs in NF1: 3 clinical trials. Submitted October 1, 2003.

Published manuscript: Muknopadhyay D, Anan S, Lee R, Kennedy S, **Viskochil D**, Davidson N. C-> U Editing of neurofibromatosis 1 mRNA occurs in tumors that express both the type II transcript and aobec-1, the catalytic subunit of the apolipoprotein B mRNA-editing enzyme. Am J Hum Genet. 2002:70;38-50.

Published manuscript: Packer R, Gutmann D, Rubenstein A, **Viskochil D**, Zimmerman R, Vezina G, Small J, Korf B. Plexiform neurofibromas in NF1. Toward biologic-based therapy. Neurology 2002:58;1461-1470.

Technical Abstract in proposal to the US Army Medical Research and Materiel Command NFRP02 (Log#NF020074; September, 17, 2002; PI: **David H. Viskochil**). Not recommended for funding

Technical Abstract in proposal to the US Army Medical Research and Materiel Command NFRP02 (Log#NF030073; August, 23, 2003; PI: **David H. Viskochil**). Under review.

TABLES:

1a - 1b

2 - 6

Table 1a. Genome-wide screen results using tetra-nucleotide repeats. Blank squares indicates that there is no data available, ○-allelic balance, ● -not informative or homozygous, ●-allelic imbalance and ●-loss of heterozygosity.

			BENIGN PNSTs																											MPNSTs				
PATIENT	36670		588289					595171					708429					U105					U140					U142					38628	306595			
	A	B	A	B	C	D	E	A	B	C	D	E	A	B	C	D	E	A	B	C	D	E	A	B	C	D	E	A	B	C	D	E		A	B	C	D
D1S396	○	○	○	○	○	○	○	●	○	○	○	○	○	○	○	○	○	○	○	○	○	○	●	●	●	●	●	○	○	○	○	○	●	●	●	●	●
D1S517	○	●	○	○	○	○	○	○	○	○	○	○	○	○	○	○	○	●	●	●	●	●	○	○	○	○	○	●	●	●	●	●	●	○	○	○	○
D2S262	○		○	○	○	○	○	○	○	○	○	○	○	○	○	○	○	●	●	●	●	●	○	○	○	○	○	○	○	○	○	○	○	○	○	●	○
D2S1242			○	○	○	○	○	○	○	○	○	○	○	○	○	○	○																	●	●	●	●
D3S1539	○	○	○	○	○	○	○	○	○	○	○	○	○	○	○	○	○	○	○	○	○	○	●	●	●	●	●	○	○	●	○	○	○				
D3S2309	●	●	○	○	○	○	○	○	○	○	○	○	○	○	○	○	○	●	●	●	●	●	●	●	●	●	●	○	○	●	○	○	●	●	●	●	●
D4S2289	○	○	○	○	○	○	○	●	●	●	●	●	○	○	○	○	○	●	●	●	●	●	○	○	○	○	○	○	○	○	○	○	●	○	○	○	○
D4S1529			○	○	○	○	○	○	○	○	○	○	●	●	●	●	●	●	●	●	●	●	○	○	○	○	○	○	○	○	○	○		○	○	○	○
D5S580	●	●	○	○	○	○	○	○	○	○	○	○	○	○	○	○	○	○	○	○	○	○	○	○	○	○	○	○	○	○	○	○	●	○	○	○	○
D5S592	●	●	○	○	○	○	○	○	○	○	○	●	○	○	○	○	●	○	○	○	○	○	○	○	○	○	○	○	○	○	○	○	●	○	○	○	○
D5S1349	○	○	○	○	○	○	○	○	○	○	○	○	○	○	○	○	○	●	●	●	●	●	○	○	●	○	●	○	○	○	○	○	●	○	○	○	○
D6S399	●	●	●	●	●	●	●	●	●	●	●	●	○	○	○	○	○	○	○	○	○	○	●	●	●	●	●	○	○	○	○	○	●	●	●	●	●
D6S392	○	○	○	○	○	○	○	●	●	●	●	●	●	●	●	●	●	○	○	○	○	○	○	○	○	○	○	○	●	○	○	○	●	●	●		●
D7S1506			○	○	○	○	○	○	○	○	○	○	○	○	○	○	○	○	○	●	○	○	○	○	○	○	○	○	○	○	○	○	○	●	●		●
D8S492	●	●	●	●	●	●	●	○	○	○	○	○	○	○	○	○	○	●	●	●	●	●	○	○	○	○	○	○	○	○	○	○	●	●	●	●	●
D8S378	○	○	○	○	○	○	○	○	○	○	○	○	●	●	●	●	●	○	○	○	○	○	○	○	○	○	○	○	○	○	○	○	●	●	●	●	●
D9S759	○	○	○	○	○	○	○	●	●	●	●	●	○	○	○	○	○	○	○	●	○	○	●	●	●	●	●	○	○	○	○	○	●	○	○	○	○
D9S241			●	○	○	○	○	○	○	○	○	○	○	○	○	○	○	○	○	○	○	○	●	●	●	●	●	○	○	○	○	○		○	○	○	○
D9S744	○	○	○	○	○	○	○	○	○	○	○	○	○	○	○	○	○																●	○	○	○	○
D10S526	○	○	●	●	●	●	●	○	○	○	○	○	●	●	●	●	●	○	○	○	○	○	○	○	○	○	○	○	○	○	○	○	●	●	●	●	●
D10S528	○	○	○	○	○	○	○	○	○	○	○	○	○	○	○	○	○	○	○	○	○	○	●	●	●	●	●	○	○	○	○	○	●				

PATIENT	36670		588289					595171					708429					U105					U140					U142					38628	306595			
	A	B	A	B	C	D	E	A	B	C	D	E	A	B	C	D	E	A	B	C	D	E	A	B	C	D	E	A	B	C	D	E		A	B	C	D
D11S1923	●	●	●	●	●	●	●	○	○	○	○	○	○	○	○	○	○	○	○	○	○	○	○	○	○	○	○	●	●	●	●	●	●	○	○	○	○
D11S1298	●	○	○	○	○	○	○	○	○	○	○	○	○	○	○	○	○	○	○	○	○	○	○	○	○	○	○	○	○	○	○	○	●	○	○	○	○
D11S1304		○	●	●	●	●	●	○	○	○	○	○	●	●	●	●	●	○	○	○	○	○	○	○	○	○	○	●	●	●	●	●	●	○	○	○	○
D12S827																		●	●	●	●	●	●	●	●	●	●	●	●	●	●	●	○	●	●	●	●
D12S297	●	●																															●				
D12S807	○	○	○	○	○	○	○	○	○	○	○	●	○	○	○	○	○	●	●	●	●	●	○	○	○	○	○	○	○	○	○	○	●	○	○	○	○
D13S258	●	●	○	○	○	○	○	○	○	○	○	○	●	●	●	●	●	○	○	○	○	○	●	●	●	●	●	○	○	○	○	○	●	○	○	○	○
D14S122	○	○	●	●	○	○	○	●	●	●	●	●	○	●	●	○	○	○	○	○	○	○	○	○	○	○	○	○	○	○	○	○	○	○	○	○	○
D15S195	○	○	○	○	○	○	○	●	●	●	●	●	●	●	○	●	●	○	○	○	○	○	○	○	○	○	○	○	○	○	○	○	●	●	●	●	●
D16S475	○	○	○	○	○	○	○	○	○	○	○	○	○	○	○	○	○	●	●	●	●	●	●	●	●	●	●	○	○	○	○	○	○	○	○	○	○
D16S476	○	○	○	○	○	○	○	○	○	○	○	○	●	●	○	○	○	○	○	○	○	○	●	●	●	●	●	○	○	○	○	○	●	○	○	●	○
D17S695	●	○	○	○	○	○	○	○	○	○	○	○	●	●	●	●	●	●	●	●	●	●	○	○	○	○	○	●	●	●	●	●	●	○	○	○	○
GXAlu	●	●																										○	○	●	○	○	●	●	●		●
D17S960	○	○																										○	○	●	○	○	●	○	○	○	○
GATN													●	●	●		●																●				
D17S722	○	○																															●				
D18S818	●	●	●	●	●	●	●	○	○	●	○	●	●	○	●	○	○	○	○	○	○	○	○	○	○	○	○	○	○	○	○	○		○	○	○	○
D18S380	●	●	●	●	●	●	●	●	●	○	○	○	●	●	●	●	●	●	●	●	●	●	○	○	○	○	○	●	●	●	●	●	●					
D19S581	○	○	○	○	○	○	○	○	○	○	○	○	○	○	○	○	○	○	○	○	○	○	●	●	●	●	●	○	○	○	○	○	○	○	●	●	●
D19S544	○	●	●	●	●	●	●	○	○	○	○	○	●	●	●	●	●	○	○	○	○	○	●	●	●	●	●	●	●	●	●	●	●	○	○	○	○
D20S438	●	●	○	○	○	○	○	○	○	○	○	○	○	○	○	○	○	○	○	○	○	○	○	○	○	○	○	○	○	○	○	○	●	○	○	○	○
D21S1411	○	○	○	○	○	○	○	○	○	○	○	○	○	○	○	○	○	○	○	●	○	○	○	○	○	○	○	●	●	●	●	●	●	●	●	●	●
D22S417	●	●	○	○	○	○	○	○	○	○	○	○	○	○	○	●	●	○	○	○	○	○	○	○	○	○	○	○	○	○	○	○	●	●	●	●	●

Table 1b. Genotypes of a PNST tumor and a low-grade MPNST tumor from two different patients. The markers used are indicated along the side of the table, while patient samples are across the top of the table. Symbols used are as follows. = allelic balance; - not determined; F failed sample; I allelic imbalance; LOH loss of heterozygosity; N not informative.

Markers	PNST (#36670 tumor)	Low-grade MPNST (#38628 tumor)
UT5144-1p	=	LOH
UT5170-1q	=	N
UT595-2p	=	=
UT1360-3p	=	=
UT6129-3q	N	N
UT878-4p	=	I
UT615-5p	N	N
UT5013-5q	N	LOH
UT886-5q	=	N
UT2018-6p	N	I
UT897-6q	=	N
UT5189-7p	F	=
UT5412-8p	N	I
UT909-8q	=	I
UT873-9p	=	LOH
UT913-9q	F	F
UT7422-9q	=	N
UT1699-10p	=	N
UT5419-10q	=	I
UT8115-11p	N	LOH
UT5150-11	LOH	LOH
UT2095-11q	F	LOH
UT5029-12p	N	I
UT6136-12	-	=
UT931-12q	=	N
UT2413-13	N	LOH
UT1392-14	=	=
UT1232-15	=	I
UT581-16p	=	=
UT703-16q	=	I
UT269-17p	I	LOH
UT40-17q	=	I
UT7162-18p	N	F
UT576-18q	N	I
UT5187-19p	=	=
UT1342-19q	=	LOH
UT236-20	N	I
UT1355-20q	=	I
UT1091-22q	N	LOH

Table 2. Genotypes of a PNST tumor and a low-grade MPNST tumor from two different patients. The markers used are indicated along the side of the table, while patient samples are across the top of the table. Symbols used are as follows. = allelic balance; - not determined; F failed sample; I allelic imbalance; LOH loss of heterozygosity; N not informative.

Markers	PNST (#36670 tumor)	Low-grade MPNST (#38628 tumor)
UT5144-1p	=	LOH
UT5170-1q	=	N
UT595-2p	=	=
UT1360-3p	=	=
UT6129-3q	N	N
UT878-4p	=	I
UT615-5p	N	N
UT5013-5q	N	LOH
UT886-5q	=	N
UT2018-6p	N	I
UT897-6q	=	N
UT5189-7p	F	=
UT5412-8p	N	I
UT909-8q	=	I
UT873-9p	=	LOH
UT913-9q	F	F
UT7422-9q	=	N
UT1699-10p	=	N
UT5419-10q	=	I
UT8115-11p	N	LOH
UT5150-11	LOH	LOH
UT2095-11q	F	LOH
UT5029-12p	N	I
UT6136-12	-	=
UT931-12q	=	N
UT2413-13	N	LOH
UT1392-14	=	=
UT1232-15	=	I
UT581-16p	=	=
UT703-16q	=	I
UT269-17p	I	LOH
UT40-17q	=	I
UT7162-18p	N	F
UT576-18q	N	I
UT5187-19p	=	=
UT1342-19q	=	LOH
UT236-20	N	I
UT1355-20q	=	I
UT1091-22q	N	LOH

Table 3. Summary of genome wide results.

PATIENT NO.	TUMOR TYPE	ALLELIC IMBALANCE	LOH
U100	Dermal	1/39	0/39
U125	Dermal	0/39	0/39
U129	Dermal	1/39	0/39
U135	Dermal	1/39	0/39
58 8289	Plexiform	2/38	0/38
59 5171	Plexiform	7/38	0/38
70 8429	Plexiform	7/38	0/38
U105	Plexiform	4/37	0/37
U140	Plexiform	1/37	0/37
U142	Plexiform	3/37	0/37
36670	Plexiform	3/36	1/36
21508	MPNST	-	7/40
38628	MPNST	12/37	10/37
306595	MPNST	-	**2/37**

Table 4. NF1 genomic sequencing with results from six NF1 patients.

PCR product #	Exon #	PCR product size (bp)	Sequencing Coverage	Patient 38628	Patient 42908	Patient 42907
1	1	1322	optimizing	NA	NA	NA
2	2	1281	single strand	3' sp +300 C to T 3' sp +122 G to A	xx	xx
3	3	1126	double strand	3'sp + 42 -G to A	3'sp + 42 -G/A	3'sp + 42 -G to A
4	4a	1146	double strand	xx	xx	xx
5	4b	1080	double strand	3'sp +89 - c to t	5' sp 90 nts C/T	3'sp +89 - c to t
6	4c & 5	1011	double strand	xx	xx	xx
7	5	1337	single strand	xx	in exon A/T -syn	both bad
8	6	1123	double strand	xx	xx	both dead
9	79	1328	double strand	xx	xx	xx
10	8 & 9	1177	double strand	xx	xx	both dead
11	9	1359	double strand	xx	xx	xx
12	10a	1153	double strand	xx	xx	xx
13	10b	1207	double strand	xx	xx	both dead
14	10c	1184	double strand	xx	3' sp +39 C/T	both dead
15	11	1312	optimizing	NA	NA	NA
16	12a	1072	double strand	xx	xx	marginal
17	12b	1325	optimizing	xx		NA
18	13	1164	optimizing	NA	NA	NA
19	14 & 15	1338	optimizing	NA	NA	NA
20	15	1242	double strand	xx	xx	both dead
21	16	1102	double strand	- C het in exon	Xx	xx
22	17	1222	single strand	xx	both mixed	both mixed
23	18	1209	optimizing	NA	NA	NA
24	19a	1175	optimizing	NA	NA	NA

25	19b	1344	optimizing	NA	NA	NA
26	20 & 21	1358	double strand	xx	both bad	both dead
27	20 & 21	1170	double strand	xx	-G het in exon	xx
28	22 & 23-1	1160	double strand	xx	xx	xx
29	22 & 23-1	1351	single strand	xx	R is dead, 3' sp +39 T to G	xx
30	23-2	1226	single strand	xx	xx	both bad
31		1334	double strand	xx	xx	both mixed
32	24	1361	optimizing	NA	NA	NA
33	25	1333	optimizing	NA	NA	both mixed
34	26	1351	optimizing	NA	NA	NA
35	27a	1188	double strand	xx	xx	xx
36	27b	1141	double strand	5'sp + 52 - C to A	5'sp + 52 - C to A, R read was dead	5'sp + 52 - C to A
37	28	1176	double strand	R is fine, 3' sp +24 T to C	R is fine, 3' sp +24 T/C	both dead
38	29	1295	double strand	3' sp + 20 - T to A	xx	both dead
39	30	1470	double strand	xx	xx	xx
40	31	1273	double strand	xx	both bad	both mixed
41	32 & 33	1361	optimizing	NA	NA	NA
42	33	1267	single strand	xx	xx	-TT/+A +28,29 in runs
43	34 & 35	1279	double strand	3' sp -T in run ~ 240nts	xx	xx
44	35 & 36	1313	double strand	5' sp -2 -T	5' sp -2 -T	5' sp -2 -T
45	36	1174	single strand	xx	both dead	3' sp -A in run ~ 330nts
46	37	1238	double strand	5' sp -A ~230nts	5' sp -A ~230nts	xx
47	38	1253	single strand	G to C in exon, syn,	G to C in exon, syn,	G to C in exon, syn,

				ACG to ACC (Thr)	ACG to ACC (Thr)	ACG to ACC (Thr)
48	39	1341	double strand	xx	xx	xx
49	40	1350	single strand	xx	5' sp +~165 A/T	xx
50	41	1240	double strand	xx	xx	both dead
51	42	1171	double strand	5' sp +28nts G to A	5' sp het +28nts G/A	xx
52	43	1151	single strand	both reads bad	5' sp +225 C to G	5' sp +225nts C to G
53	44 & 45	1230	single strand	xx	xx	both bad
54	44 & 45	1342	double strand	xx	xx	xx

xx = good read and no polymorphism detected; NA = not available, still optimizing the protocol

Table 4 cont.

PCR product #	Exon #	Exon #	PCR product size (bp)	Sequencing Coverage	Patient 42730	Patient 46265	Patient 36670
1	1	1	1322	optimizing	NA	NA	NA
2	2	2	1281	single strand	3' sp +52 het G/C	both dead	5' sp +122 G to A
3	3	3	1126	double strand	3'sp + 42 -G to A	both dead	3'sp + 42 -G/A
4	4a	4	1146	double strand	xx	both dead	xx
5	4b	5	1080	double strand	3'sp +89 - c to t	both dead	3' sp +89 C to T
6	4c & 5	6	1011	double strand	xx	both dead	xx
7	5	7	1337	single strand	both dead	both dead	NA
8	6	8	1123	double strand	both dead	both dead	xx
9	79	9	1328	double strand	xx	xx	xx
10	8 & 9	10	1177	double strand	both bad	xx	xx
11	9	11	1359	double strand	xx	xx	xx
12	10a	12	1153	double strand	xx	xx	G het, 5' sp +99 and 3'sp + 34
13	10b	13	1207	double strand	xx	5'sp +A 21nts, 5'sp	NA

						129nts T to A, 5'sp 32nts C to T	
14	10c	14	1184	double strand	xx	5'sp –A 28nts, 3' sp +40 C/T	xx
15	11	15	1312	optimizing	NA	NA	NA
16	12a	16	1072	double strand	marginal	xx	xx
17	12b	17	1325	optimizing	NA	NA	xx
18	13	18	1164	optimizing	NA	NA	NA
19	14 & 15	19	1338	optimizing	NA	NA	NA
20	15	20	1242	double strand	both dead	both dead	xx
21	16	21	1102	double strand	xx	xx	xx
22	17	22	1222	single strand	xx	incomplete coverage	both bad
23	18	23	1209	optimizing	NA	NA	NA
24	19a	24	1175	optimizing	NA	NA	NA
25	19b	25	1344	optimizing	NA	NA	NA
26	20 & 21	26	1358	double strand	3'sp 34nts C to A	both bad	xx
27	20 & 21	27	1170	double strand	5'sp +85nts C to A	-G het in exon	xx
28	22 & 23-1	28	1160	double strand	xx	xx	xx
29	22 & 23-1	29	1351	single strand	both bad	3'sp +G ~40nts, 3'sp +G ~50nts	xx
30	23-2	30	1226	single strand	both bad	xx	xx
31		31	1334	double strand	marginal	xx	xx
32	24	32	1361	optimizing	NA	NA	NA
33	25	33	1333	optimizing	NA	NA	NA
34	26	34	1351	optimizing	NA	NA	NA
35	27a	35	1188	single strand	xx	xx	
36	27b	36	1141	double strand	5'sp + 52 - C to A	xx	5'sp + 52 - C to A
37	28	37	1176	double strand	xx	xx	xx

38	29	38	1295	double strand	L is fine, R is mixed	both dead	no reads
39	30	39	1470	double strand	xx	xx	xx
40	31	40	1273	double strand	both bad	xx	mixed
41	32 & 33	41	1361	optimizing	NA	NA	NA
42	33	42	1267	single strand	both bad	xx	xx
43	34 & 35	43	1279	double strand	xx	xx	3' sp -T in run ~ 240nts
44	35 & 36	44	1313	double strand	5' sp -2 -T	R is dead	5' sp -2 -T
45	36	45	1174	single strand	xx	xx	3' sp -A in run ~ 330nts
46	37	46	1238	double strand	xx	5' sp -A ~230nts	xx
47	38	47	1253	single strand	G to C in exon, syn, ACG to ACC (Thr)	G to C in exon, syn, ACG to ACC (Thr)	G to C in exon, syn, ACG to ACC (Thr)
48	39	48	1341	double strand	xx	xx	xx
49	40	49	1350	single strand	xx	both dead	xx
50	41	50	1240	double strand	xx	xx	xx
51	42	51	1171	double strand	xx	xx	5' sp het +28nts G/A
52	43	52	1151	single strand	both bad	both mixed	xx
53	44 & 45	53	1230	single strand	xx	both dead	xx
54	44 & 45	54	1342	double strand	xx	xx	xx

xx = good read and no polymorphism detected; NA = not available, still optimizing the protocol

Table 5. Ras activity in MPNST in tumor samples from 9 NF1 patients.

Sample ID	Tumor type	GTP (fmol/mg prot)	GTP + GDP (fmol/mg prot)	GTP (GTP+ GDP) (%)
21508	Neurofibrosarcoma	21	359	6
BG8	Dermal neurofibroma	17	660	3
P301	MPNST	39	1817	2
306595	MPNST	82	1746	5
U1001	Plexiform neurofibroma	60	735	8
42908	Plexiform neurofibroma	336	1120	30
U100nf	Dermal neurofibroma	41	1595	3
P309	MPNST	122	1143	11
42907	Plexiform neurofibroma	14	488	3

Table 6. Informative genotyping markers used to screen DNA extracted from the different sites of the 2000 and 2002 tumors from an individual with NF1. All chromosomes with exception of the acrocentric chromosomes have a marker on both the p and q arm. The marker position, size and percentage of heterozygosity was obtained from the University of Utah genomic core facility web site. The marker forward and reverse primer sequence was obtained from the NCBI UniSTS web site.

Marker ID	position (mega base)	Size	Het	Forward primer	Reverse Primer	
D1S517	267.5	198-241	85	GTACATAGTGGAATGCCTGG	GTAACTCACAAAGGCAAAGAC	Tetra
D1S396	65.6	119-139	79	CAGCCTGGGTGACAGAGT	CACTGCTAACTGGTAGCAGC	
D2S262	29.2	175-216	79	ACCCTGCCAAATCCCCCTC	TGCGCCCCCTTTACAGAGG	
D2S1242	225.6	136-172	88	TGACATAGCGAGACCCTGTC	CCATTCTCATCCAGCAGGA	
D3S1539	0.0	262-308	89	CTTTCCATTACTCTCTCCATA	CCAGTGCTGTTTTAGCTTC	
D3S1512	162.0	294-356	88	TCAGTTCAGGGAGAGACTC	CTGTATTATATAGCCCTGGTA	
D4S1529	185.2	192-220	86	GCAAAAGAGTGAAATTCTATC	TTCTGATATATAGTGAGGGC	
D4S2289	32.6	266-313	81	TTGGAATATCAGATGGAAAGG	GCATGGCATTCCTATGACAC	
D5S630	18.6	287-395	89	CATGACGATGTGGGCAG	CCTTTCAGTGTAGAAGTGTGTGTGT	ABI MD10
D5S592	0.0	162-198	81	AGACAGACAGAGAGATTAGA	AGTAAAGTGAGTGGAGAGC	
D6S399	23.9	351-377	72	CTGCAGTGAGACATGATTGC	TGTTGGAAGAGGAAAAATGAC	
D6S979	120.4	180-222	82	GCCTAGGTGATAGAGCAAAAC	CCCGCCTTTCTGCCTCTC	
D7S628	47.9	309-340	76	ATGGATACCAAAGGACTACT	GACTCACTCCGTAATCAGT	
D7S618	110.0	138-163	86	AAGACCCAGTCTCAAAGAAG	TTTCAGATGATGAAACCGATG	
D8S492	0.0	285-316	77	CCTACAACTGTCTTGGTACATTTGT	AGTTGAGACGCTGTGTATGTCTTG	
D8S378	145.9	123-157	87	TGTTCTGCACATGTATCCCA	CATTCATTAGCCACAGGCC	
D9S248	53.8	336-399	91	GGGCAACAAAGCAAGACTC	CCAGAAATTTGCCAGTATATC	
D9S241	125.6	178-238	82	GGAGGTTGCAGTGAGCAG	TTTATTTTCCAAGATTTTGCCA	
D10S506	33.7	260-332	90	AACACCACACTCCAGCCTG	GATTCACCAACACCACTGGT	
D10S528	143.9	386-446	72	TGACAGAGCAAGACTCCAT	GGGTTTTTTTCAACAATGCTC	

D11S1923	8.3	375-472	94	GTGTTTGCTTTGGAGAGAG	ATTTTCCGTAGGCTTGAATG	
D11S1298	63.3	185-230	86	GCCTGGGACAACAAGAGTG	AAGCCTGCCTCTGTGCAAC	
D11S1304	147.2	176-234	82	TTGGCATTTGGCTTTTTCAGA	TTAAGTGACCTGGGCTGCA	
D12S799	41.2	293-396	95	TGGGTGCAGAGAAAGACCT	CCTTTCCGCTTTCTCCATG	
D12S297	66.8	202-292	90	TTGGCATTTGGCTTTTTCAGA	TTAAGTGACCTGGGCTGCA	
D13S258	56.6	219-298	87	ACCTGCCAAATTTTACCAGG	GACAGAGAGAGGGAATAAACC	
D14S122	3.0	193-229	84	CCAGCCTGGGTGAGACTC	CGTTCATGTACCACTGCATG	
D15S195	52.0	136-164	75	AAGCAAAATTAATAAGAAGGAT	TCATCACATGGGCTAATTC	
D16S475	5.6	157-213	84	GGTTGACAGAGTGAGACTC	GGAACAGAAAATACTGCACG	
D16S476	126.5	139-188	87	TTGCACTCCACTCTGGGCA	TTGCCTTGGCTTTCTGTTGG	
D17S695	3.2	172-285	93	CTGGGCAACAAGAGCAAAATTC	TTTGTTGTTGTTCATTGACTTCAGTCT	
D17S966	58.8	263-325	93	GGGTGACAGAGTGAGACTCCATC	GCTCTGTGTCAGGGATGAGTTCA	
D17S722	106.0	128-194		AGCTGGGGGAATAGAGTGAGATTC	AATTGCATGTCTCTGGGGTACGGA	
D18S59	0.1	154-176	81	GGGGCACAAGACAGATAGAT	CCTACCAGAATGTGAACGAC	
D18S380	109.9	109.9	53	CACTGCATTCTGGGCAAC	AGGCTCTTGCTCCTGGAAT	
D19S581	0.0	189-287	90	TCGAGACTACAGTGAGCTG	ATTATGGGTGTCTTCCTGAC	
D19S544	104.8	263-323	84	AGAAGAGGAAATCCTGCCT	GGAAATTCAGATATATGTGTG	
D20S438	53.6	99-157	82	GAGTATCCAGAGAGCTATTA	ATTACAGTGTGAGACCCTG	
D21S1409	21.1	180-200	70	GGAGGGGAATACATTTGTG	TTGCCTCTGAATATCCCTAT	
D21S1411	56.6	263-310	89	ATGATGAATGCATAGATGGATG	AATGTGTGTCCTTCCAGGC	
D22S417	40.1	158-205	80	CCTGGGAAGTTAAGACTGC	TCTACCGCTTATTTCTTCCCT	

FIGURES

1 - 12

Figure 1. Osteopontin Antibody Staining

MPNST (38628-TMC) showing cytoplasmic staining

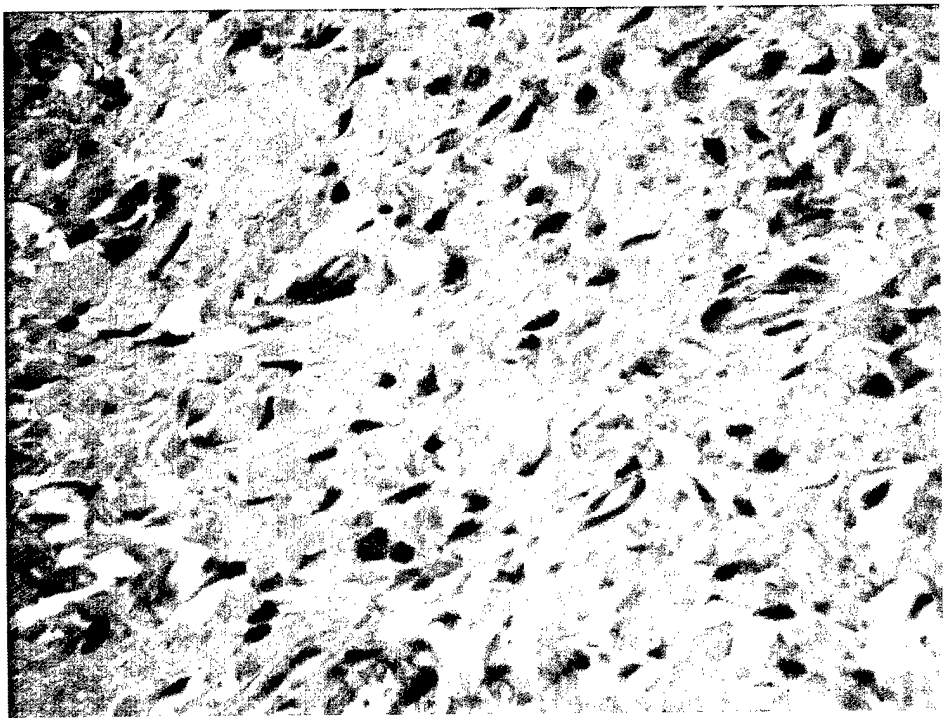

Plexiform neurofibroma (38628C) with focal, weak nuclear staining

Figure 2. Analysis of tumor specimen from patient #1949713. A) An H&E section showing the area that was scraped and DNA extracted for genetic analysis. B) SSCP results of human *tP53* exon 5 from DNA extracted from H&E paraffin section. The asterik denotes the sample that was part of the manuscript submitted for publication and the immunohistochemical staining shown in Figure 2 of the manuscript.

A)

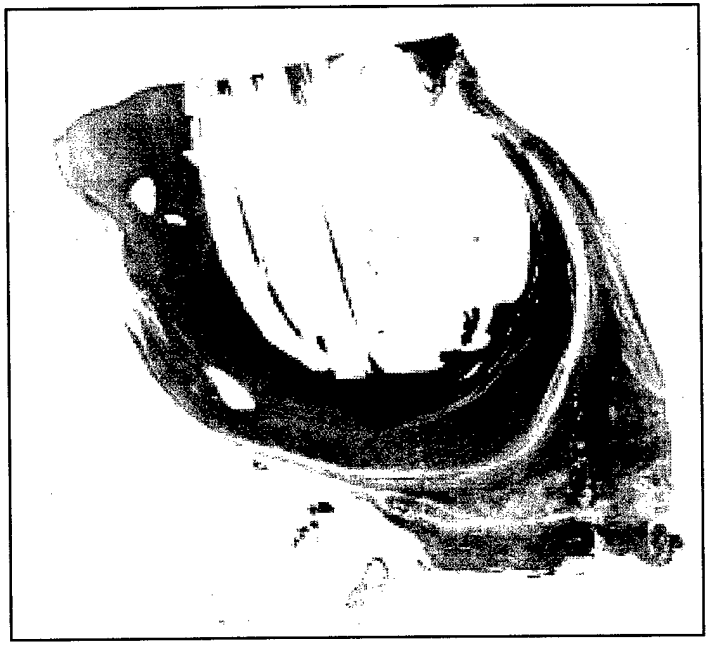

B)

A)	500-068751F	E)	501-05042	I)	42730
B)	PS278-830	F)	1949713 *	J)	1972-931A
C)	48299012	G)	P309		
D)	89575400	H)	U135		

Figure 3. Exon 4 to 8 of the *tP53* gene was amplified with specific primers. The first sample in each group is a water control (*). The remaining samples are PCR products from DNA template extracted from H&E tumor sections. Each lane contains 5µl of PCR product + 2µl of sample buffer. The samples were separated on a 1% agarose gel containing EtBr.

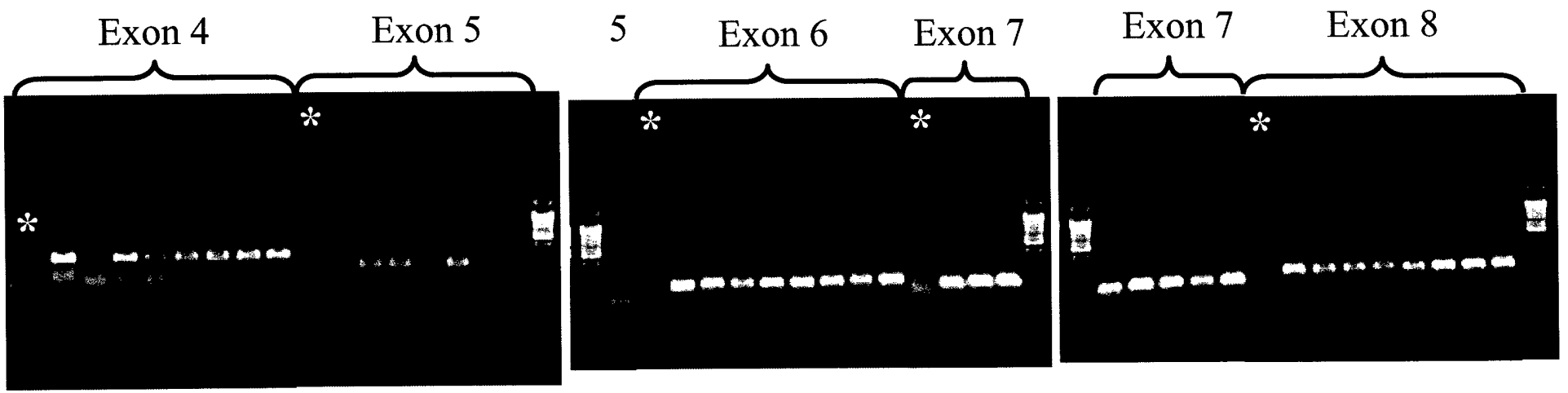

Figure 4. Sequencing results from PCR products for exon 4-8 of human *tP53*. Sequencing was carried out at core facility in the University Hospital.

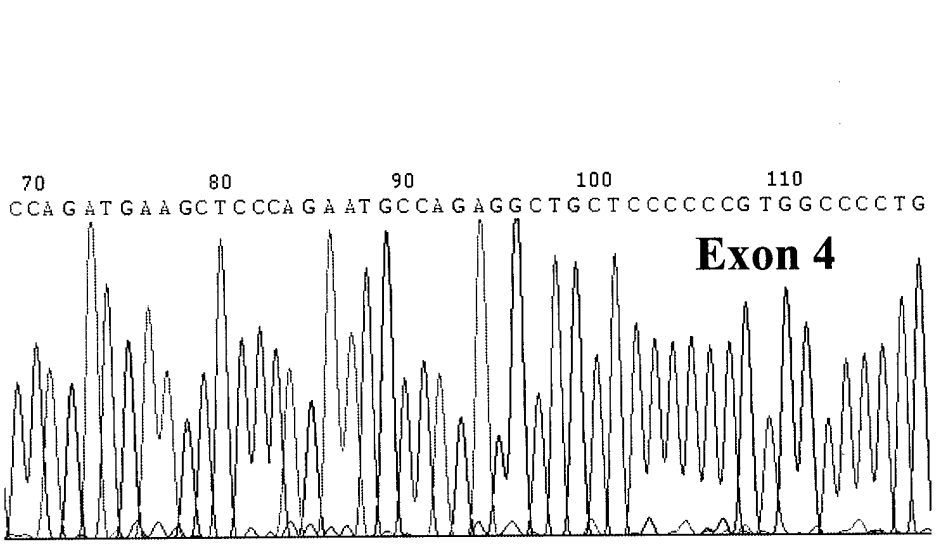

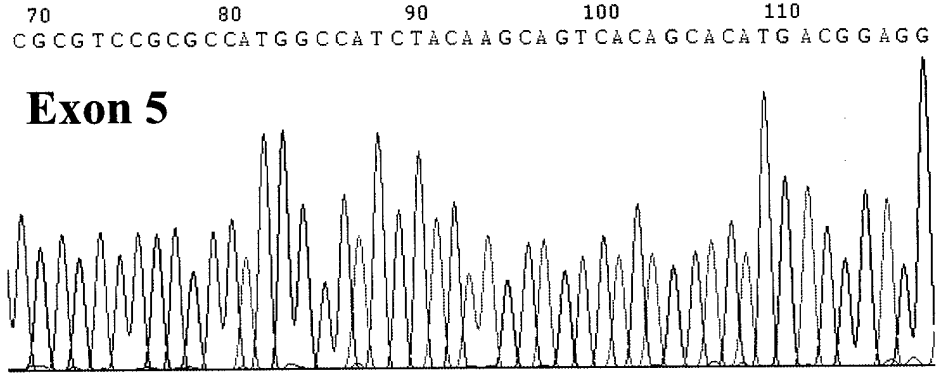

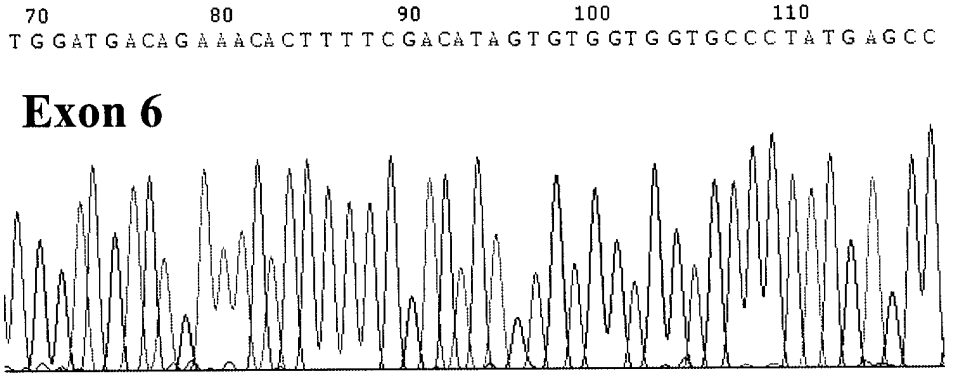

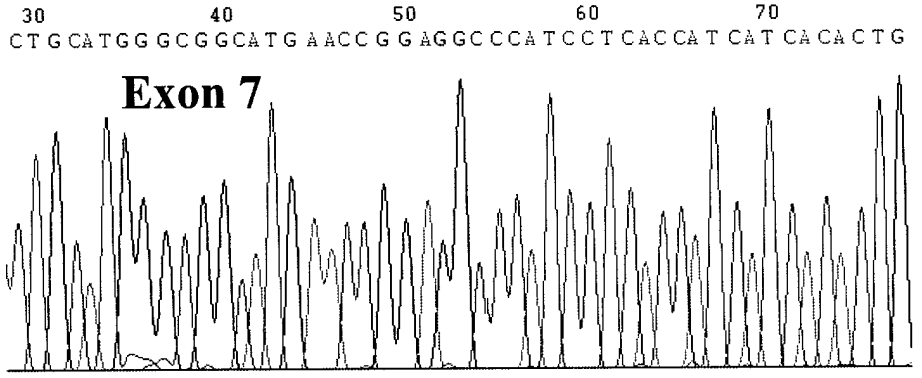

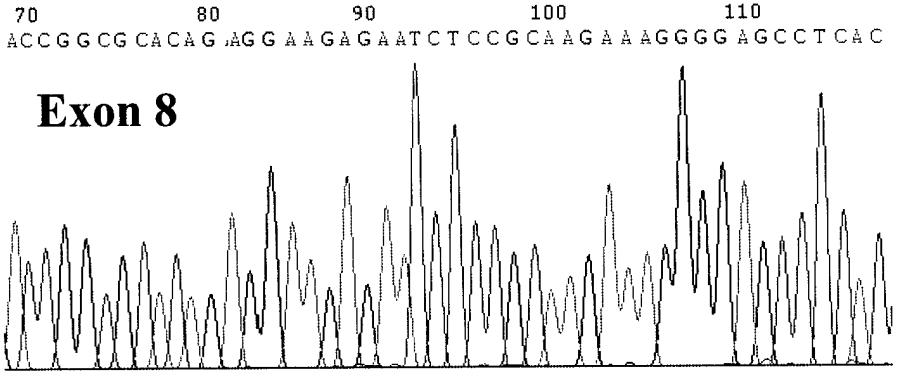

Figure 5. LOH analysis at the *NF1* gene shown for two different patients. The upper panel shows the marker GxAlu. The middle panel shows the marker GATN. The bottom panel shows the marker 28.4.

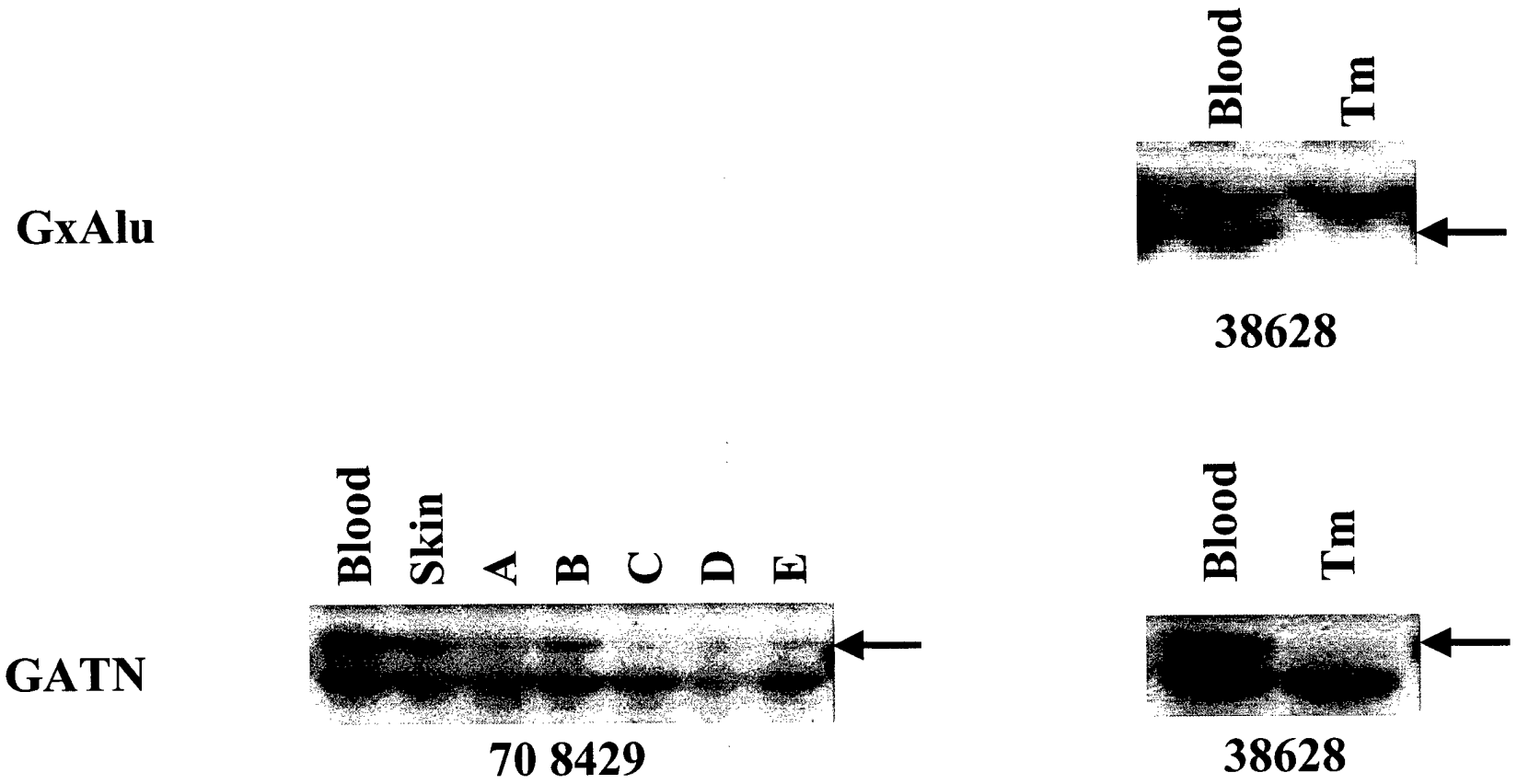

Figure 6. Intra-tumor genetic heterogeneity. A plexiform neurofibroma from patient #708429 showing the 5 different sites in which genetic analysis was carried out on the DNA extracted from the tumor site. The inset in each corner shows the general morphology with H&E staining.

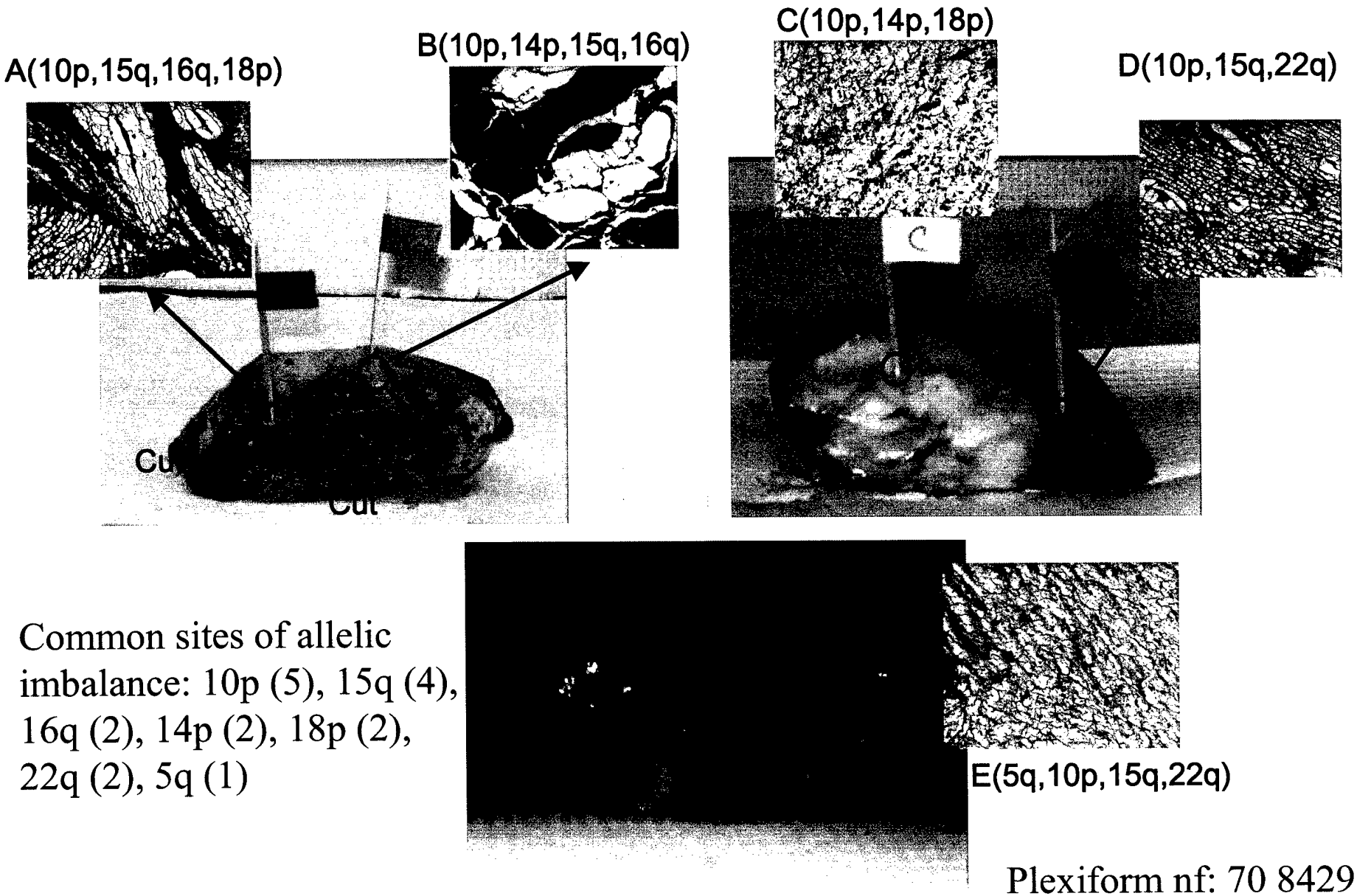

Common sites of allelic imbalance: 10p (5), 15q (4), 16q (2), 14p (2), 18p (2), 22q (2), 5q (1)

Plexiform nf: 70 8429

Figure 7. Immunohistochemical staining of tumor 1 from patient #36670. A) Shows the general morphology of the tumor section with H & E staining. B) - F) are the various immunohistochemical stains for specific antigens as cited. The insert in the corner is the photograph of the tumor after removal.

A) H & E

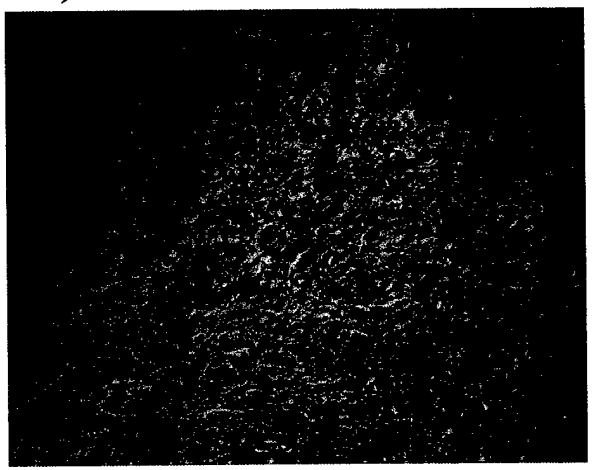

B) Mib-1

C) Topo IIa

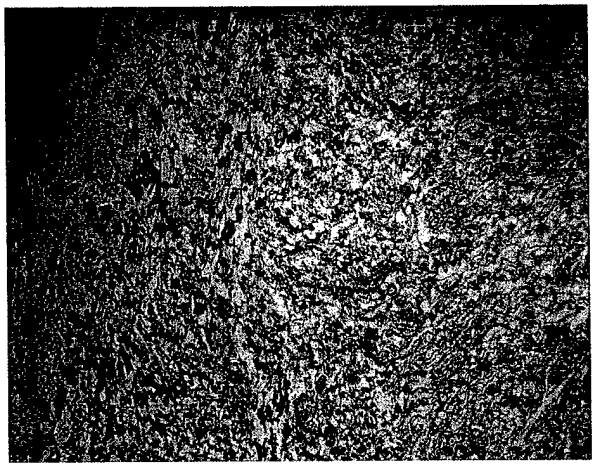

D) p53

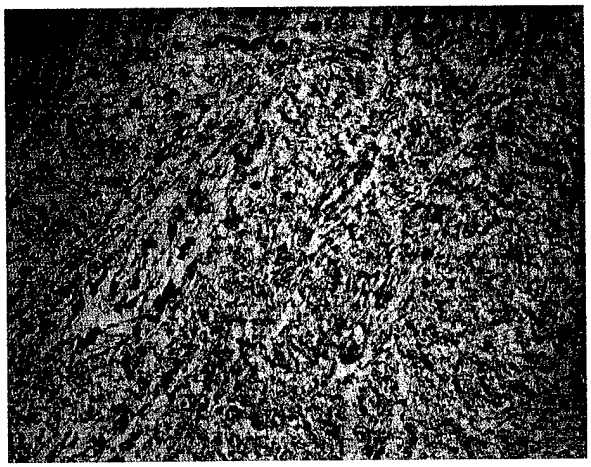

E) p16

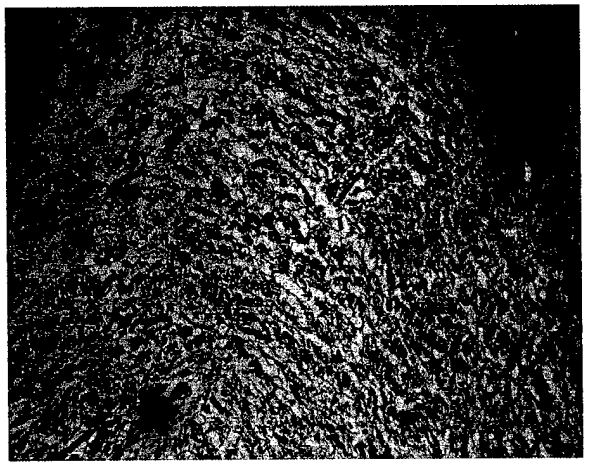

F) p27

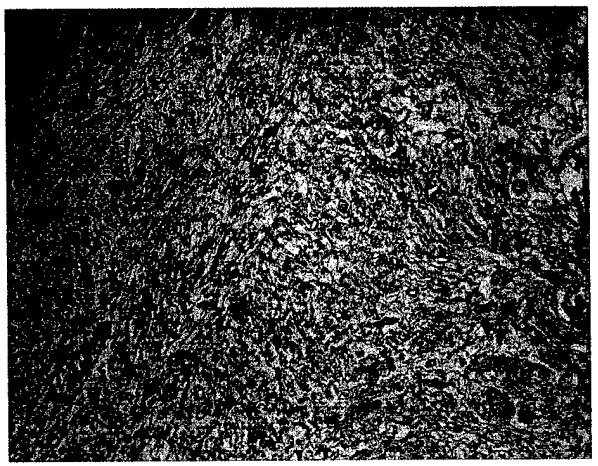

Figure 8. Immunohistochemical staining of tumor C from patient #38628. A) Shows the general morphology of the tumor section with H & E staining. B) - F) are the various immunohistochemical stains for specific antigens as cited. The insert in the corner is a photograph of the tumor after removal.

A) H & E

B) Mib-1

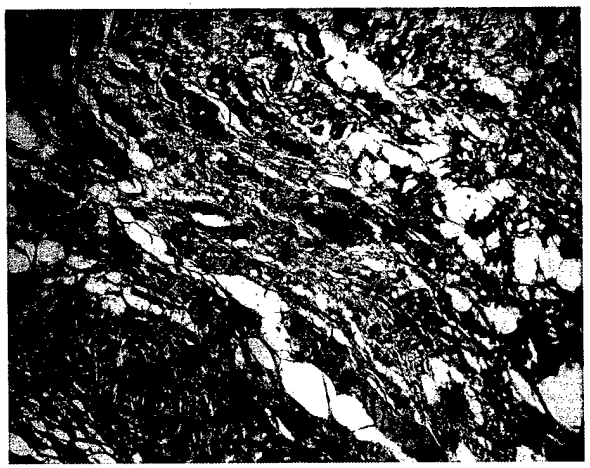

C) Topo IIa

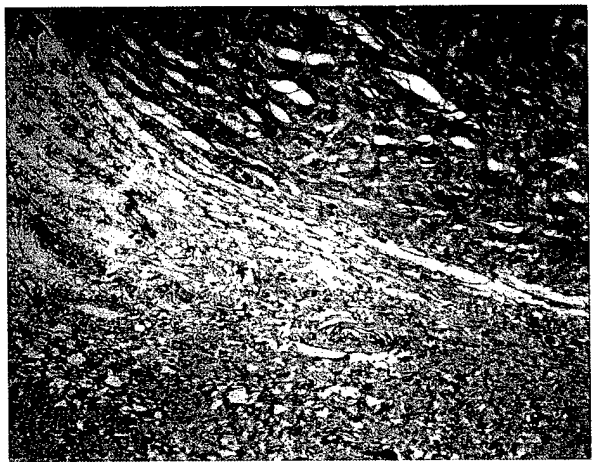

D) p53

E) p16

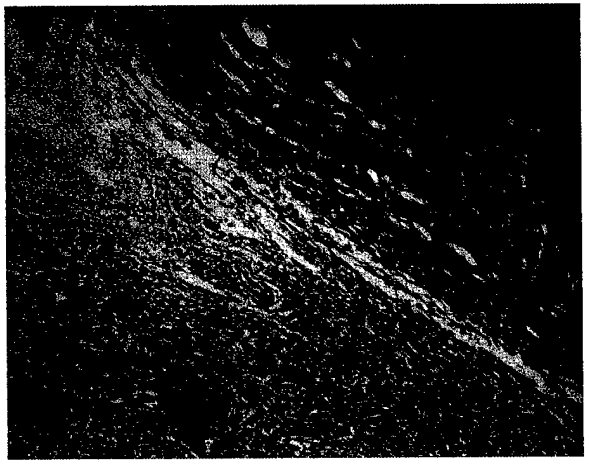

F) p27

Figure 9. Genotyping results from the different areas from T2000 and T2002. The markers used are on the left. The open circles are show allelic balance at informative heterozygous loci. Loci with loss of heterozygosity (LOH) are represented by the filled circles. Loci with allelic imbalance (AI) are represented by half-filled circles.

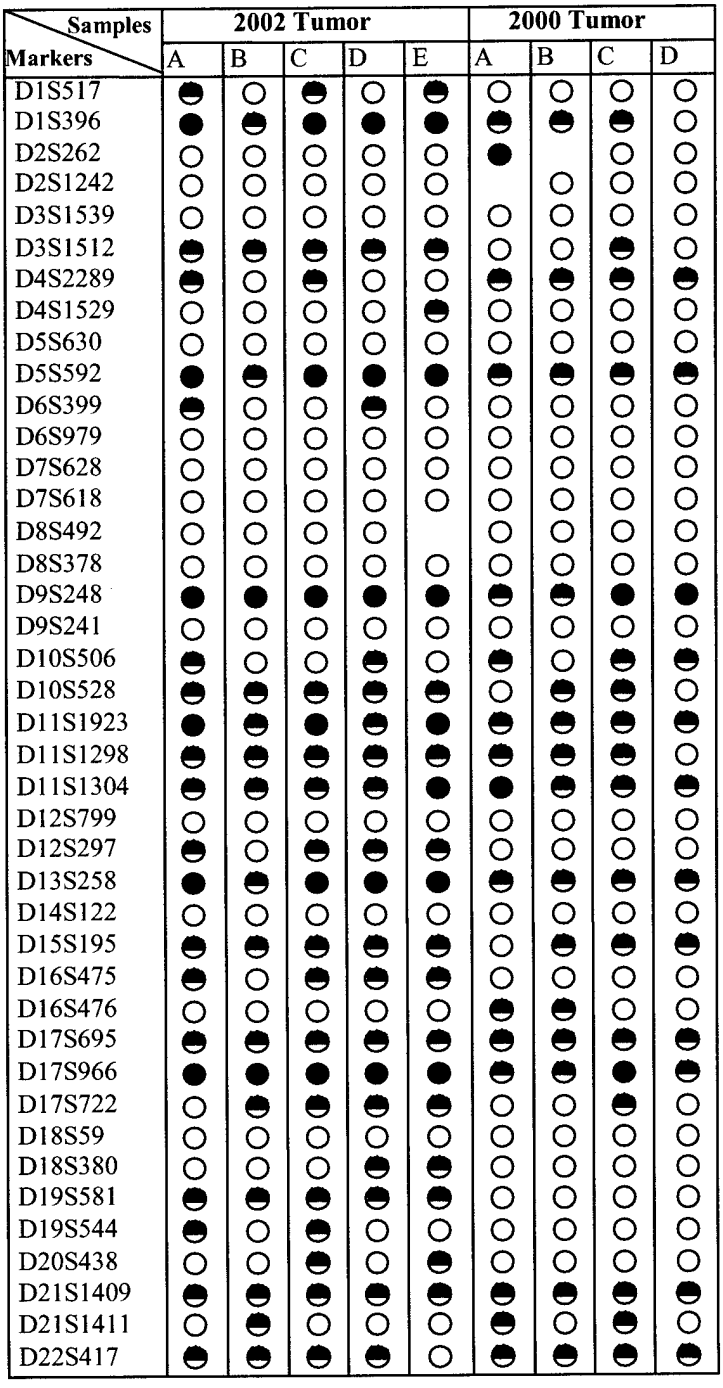

Figure 10. CGH Microarray results from DNA extracted from T2002. **A.** An array showing hybridization of the DNA to the clones on the chip. The left panel with the arrow is an example where a loss is observed (red dot). The right panel with the arrow is indicating a gain (green dot). **B.** The ratio plot of DNA from T2002 showing the "signature" of clonal expansion in chromosome 5 taken from the above array hybridization. Arrows correspond to clones depicting gain and loss on the ratio plot. T2000 had the same chromosome 5 "signature".

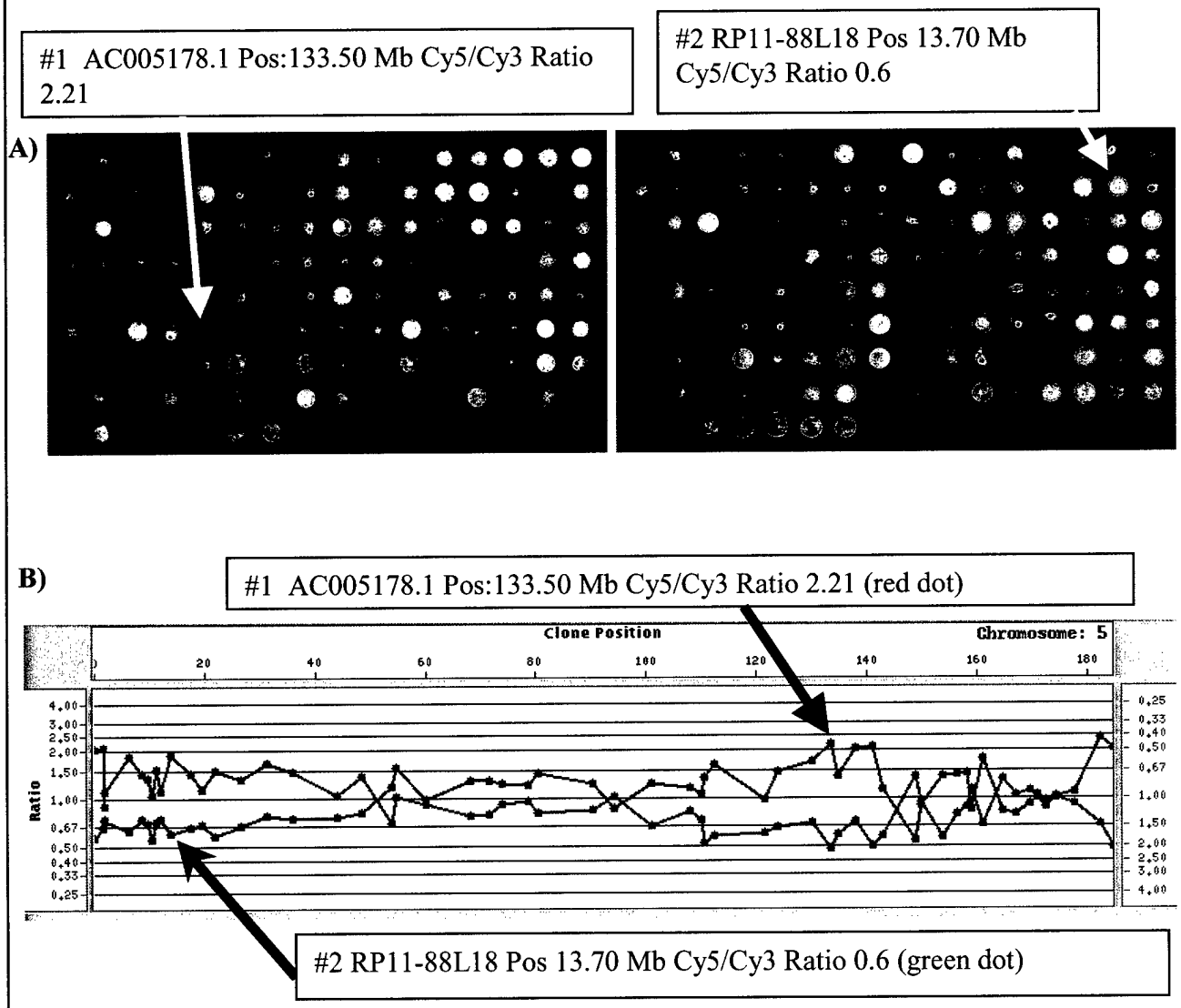

FIG. 11

EGFR EXPRESSION AND GENETIC ANALYSIS IN PLEXIFORM NEUROFIBROMAS (PNF) AND MALIGNANT PERIPHERAL NERVE SHEATH TUMORS (MPNSTS)

Holly Zhou[1], Minh-Thu N. Hang[1], Cheryl Coffin[1], Sheryl Tripp[1], David H. Viskochil[1]

[1]University of Utah, Utah, United States

EGFR protein expression detected by immunohistochemnistry.

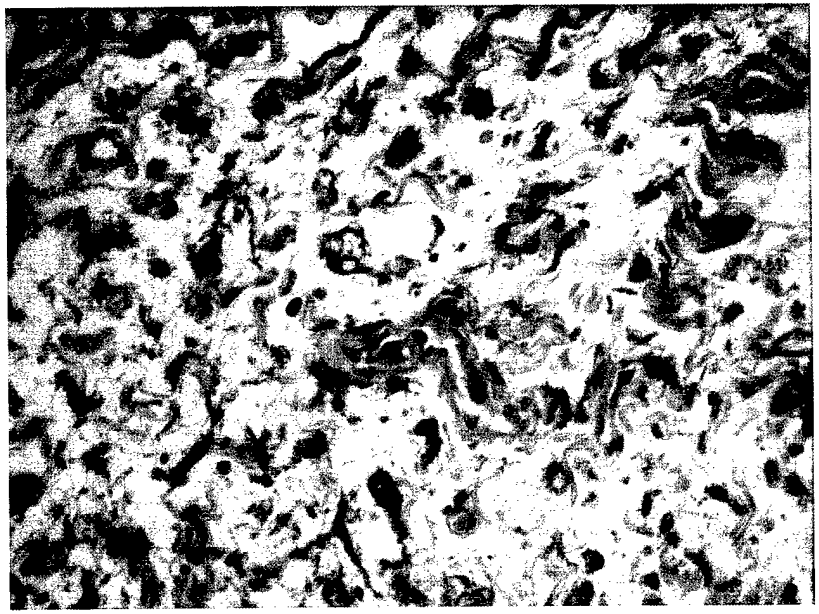

Plexiform Neurofibroma

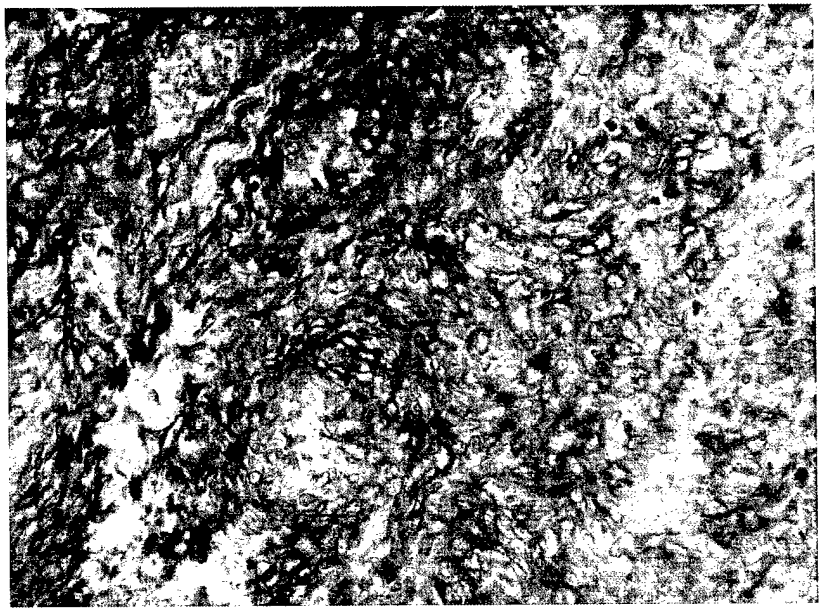

High-grade MPNST

EGFR overexpession was present in a high percentage of neoplastic cells in high-grade MPNSTs and in a subset of cells within PNF and low-grade MPNSTs.

FIG 12

EGFR EXPRESSION AND GENETIC ANALYSIS IN PLEXIFORM NEUROFIBROMAS (PNF) AND MALIGNANT PERIPHERAL NERVE SHEATH TUMORS (MPNSTS)

Holly Zhou[1], Minh-Thu N. Hang[1], Cheryl Coffin[1], Sheryl Tripp[1], David H. Viskochil[1]
[1]*University of Utah, Utah, United States*

Genotyping results from four MPNST and one PNF tumor using PCR-based genetic markers with a fluorescein tag. Allelic balance was observed at the 5 genetic markers spanning the EGFR locus.

	Ratio of normal control tissue vs tumor tissue				
Markers	**2139971A**	**194973**	**448891e**	**1362981b**	**2629992b**
D7S2422	1.08	1.02	0.96	1.69	0.65
D7S506	0.97	0.99	0.97	0.87	0.96
D7S2550	1.00	1.18	0.83	1.27	0.88
D7S494	1.09	0.98	0.97	1.21	1.08
D7S502	NA	NA	0.71	0.68	1.00

Allelic imbalance and LOH were assessed from the calculated peak ratios. Ratios higher than 2.0 and lower than 0.5 were termed allelic imbalance. The presence of only one peak indicated by a ratio higher than 5.0 and lower than 0.2 were termed LOH.

Conclusion: The overexpression of EGFR in PNF and MPNST may be mediated by mechanisms other than gnomic amplification of the EGFR locus.

Published manuscript: Zhou H, Coffin C, Perkins S, Tripp S, **Liew M**, **Viskochil D**. Malignant Peripheral Nerve Sheath Tumor (MPNST): A comparison of grade, immunophenotype, and cell cycle/growth activation marker expression in sporadic and neurofibromatosis 1 (NF1)-related lesions. Am J Surgical Pathology 2003:

Malignant Peripheral Nerve Sheath Tumor

A Comparison of Grade, Immunophenotype, and Cell Cycle/Growth Activation Marker Expression in Sporadic and Neurofibromatosis 1-Related Lesions

Holly Zhou, MD, Cheryl M. Coffin, MD, Sherrie L. Perkins, MD, PhD, Sheryl R. Tripp, Michael Liew, PhD, and David H. Viskochil, M.D, PhD

Abstract: This study investigates differences in expression of the cell cycle/growth activation markers p53, p16, and p27, and their relationship with nerve sheath cell and proliferation markers among plexiform neurofibromas (PNF), NF1-related and non-NF1 MPNSTs of different histologic grades and between benign-appearing and malignant areas in the MPNSTs associated with PNFs. Formalin-fixed, paraffin-embedded archival tissue from PNFs and MPNSTs were immunostained using the avidin-biotin-complex method with antibodies to S-100 protein (S-100), Leu7 (CD57), CD34, p16, p27, p53, Mib-1, and topoisomerase II-alpha (TopoIIα), with appropriate controls. All PNFs and most low-grade MPNSTs displayed diffuse or focal reactivity for S-100, Leu7, CD34, p16, and p27 and negative reactivity for p53, Mib-1, and TopoIIα. Most high-grade MPNSTs displayed decreased or negative reactivity to S-100, Leu7, CD34, p16, and p27 but increased reactivity to p53 (59%), Mib-1 (72%), and TopoIIα (72%). In addition, combined nuclear and cytoplasmic (nucleocytoplasmic) p27 staining, which was not seen in the PNF or low-grade MPNST, was observed in 33% of high-grade MPNSTs. These findings suggest that p53, p16, and p27 may be involved in tumor progression in the PNF-MPNST sequence. However, alterations in p53, p16, and p27 do not distinguish between low-grade MPNST and PNF, including PNF adjacent to high-grade MPNST. Although p53, p16, and p27 are unlikely to be reliable markers for early detection of tumor progression in MPNST, p53 reactivity was more frequent in NF1-associated high-grade MPNST and appeared to be a marker for high tumor grade. Combining immunohistochemical stains with histologic grading with careful examination of mitotic activity may provide insight into the progression of peripheral nerve sheath tumors.

From the Departments of Pathology (H.Z., C.M.C., S.L.P., S.R.T.) and Pediatrics (M.L., D.H.V.), University of Utah School of Medicine, Salt Lake City, UT.

Presented in part at the United States and Canadian Academy of Pathology, Chicago, IL, February 25, 2002. Abstract published in *Mod Pathol.* 2002; 15:24A.

Supported by grant from the Department of the Army Neurofibromatosis Program, DAMD-NF980007 (D.H.V.).

Reprints: Holly Zhou, MD Department of Pathology, Primary Children's Medical Center, 100 N. Medical Drive, Salt Lake City, UT 84113; e-mail: pchzhou@ihc.com

Key Words: p53, p16, p27, plexiform neurofibroma, malignant peripheral nerve sheath tumor, tumor progression/malignant transformation, immunophenotype

(*Am J Surg Pathol* 2003;27:1337–1345)

Malignant peripheral nerve sheath tumors (MPNST) often occur in association with neurofibromatosis type 1 (NF1), an autosomal dominant condition resulting from inactivating *NF1* gene mutations.[7,50,53] The function of the *NF1* gene product, neurofibromin, is to reduce cell signal transduction by accelerating inactivation of the proto-oncogene p21-ras.[32,51,59] Mutations in *NF1* generally lead to increased ras signaling, and individuals with NF1 have an increased risk of developing both benign and malignant tumors, especially peripheral nerve sheath tumors.[16,41] Approximately 20% to 25% of individuals develop plexiform neurofibroma (PNF), which usually arise at an early age and may undergo malignant transformation and progress to MPNST.[14,43] Clinically, MPNST is difficult to detect in NF1 patients and has a poor prognosis because of the high likelihood of local recurrence and distant metastasis. At present, there are no reliable indicators of early detection of tumor progression or malignant transformation of PNF to MPNST apart from classic histopathologic criteria, which remain somewhat controversial at the low-grade end of the spectrum.

Recent studies suggest that the development of MPNST is a multistage process that may involve a number of altered cell cycle regulators in addition to double inactivation of the *NF1* gene.[2,3,10,18,21–23,34,37] Among these cell cycle regulators, *TP53* is known for its critical role in arresting cells in the G1 phase of the cell cycle following DNA damage and negative regulation of cellular proliferation. Deletions involving chromosome 17p, including the *TP53* locus and mutation of the *TP53* gene, have been observed in a proportion of MPNSTs but not in neurofibromas.[18,23,34] p16, encoded by the *CDKN2A/p16* gene on the short arm of chromosome 9 (9p21),

inhibits the function of the cell cyclin kinase CDK4- and CDK6-cyclin D complexes, thus controlling cell proliferation through the retinoblastoma (pRB) pathway.[26,31,45] Inactivation of *CDKN2A/p16* has been observed in a wide variety of human tumors, including MPNST.[2,5,6,10,21,26,28,37,48] p27 is a multifunctional cyclin-dependent kinase inhibitor and not only directly inhibits cell proliferation but also functions as an important promoter of apoptosis and has a role in cell differentiation.[13,19,25,30,40,47] Recent studies suggest that predominant localization of p27 to the cytoplasm is associated with tumorigenesis in epithelial tumors[1,8,49] and MPNST.[22]

In this study, we compared the immunohistochemical expression of cell cycle regulators p53, p16, and p27 between PNF and both sporadic and NF1-related low- and high-grade MPNSTs. We also compared the sarcomatous and benign areas in MPNSTs arising in PNFs. The expression of nerve sheath cell markers S-100 protein, Leu 7, and CD34 and the cell proliferation markers Mib-1 and TopoIIα,was also assessed. The purposes of this study were to investigate alterations of cell cycle regulators in MPNST of different histologic grades, to assess their relationship to tumor cell cytodifferention and proliferation, and to identify possible markers for early detection of tumor progression and malignant transformation from PNF to MPNST.

MATERIALS AND METHODS

Case Selection

Institutional Review Board (University of Utah School of Medicine) approval was granted for this study. Formalin-fixed, paraffin-embedded archival tissue from 19 PNFs and 27 MPNSTs were obtained from institutional surgical pathology files. The diagnosis was based on the light microscopic examination with hematoxylin and eosin and immunohistochemical stains. With an appropriate clinical history and presentation, the diagnosis of a low-grade MPNST was made when atypical features in a PNF, such as increased cellularity, nuclear atypia, and low levels of mitotic activity, were present.[56] The diagnosis of a high-grade MPNST was made when a tumor was composed of pleomorphic, dense fascicles of spindle cells with brisk mitoses, focal necrosis, and histologic or immunohistochemical evidence of focal Schwannian cell differentiation with exclusion of other high-grade sarcomas.[57] Cases with heterologous or epithelial elements were not included in this study. MPNST grade was classified as either low (grade 1) or high (grade 2 or 3), using the Pediatric Oncology Group Non-Rhabdomyosarcoma Soft Tissue Sarcoma Grading System.[38]

Immunohistochemical Study

A representative tissue block for immunohistochemical analysis from each case was selected after all hematoxylin and eosin-stained sections were reviewed. Immunohistochemical analysis was performed with a Ventana 320 automated stainer (Ventana, Tucson, AZ) with use of a standard indirect avidin-biotin peroxidase detection method. The tissue was cut into 3-μm sections onto silanated slides and incubated at 56°C for 30 minutes. The sections were dewaxed and hydrated through diluted ethanol solutions to distilled water. The dilutions and sources of these antibodies are summarized in Table 1. The sections for S-100 and CD 34 antibodies were microwaved for 15 minutes in 10 mM citrate buffer. The sections for Leu7 (CD57) had no pretreatment. The sections for all of the other antibodies received antigen retrieval in an electric pressure cooker for 3 minutes. Sections were then stained against antibodies to S-100 protein (S-100), Leu7, CD34, p16, p27, p53, Mib-1, and topoisomerase II-alpha (TopoIIα), with appropriate controls. p27 also included an amplification kit (Amplification kit from Ventana). Among these antibodies, the expression of S-100, CD34, Mib-1, TopoIIa, p53, p16, and p27 was further compared and analyzed among PNF and low-grade and high-grade MPNSTs.

The staining patterns of S-100, Leu 7, and CD34 were determined by examination of cellular reactivity in the entire section. Positivity of S-100, Leu 7, and CD34 staining was scored as diffuse (majority of cells positive), focal (individual and focal cluster of cells positive), or absent (no positive cells identified). Staining for Mib-1, TopoIIα, p53, and p16 was scored by average numbers of nuclear reactivity in 10 microscopic fields. The following percentages of positive nuclear staining were used as cutoff points[11,21,22,27,35]: Mib-1 >5%, TopoIIα >5%, p53 >5%, p16 >10%, and p27 >10%. Additionally, the localization of p27 staining was recorded separately as nuclear versus nuclear and cytoplasmic (nucleocytoplasmic).

Statistical Methods

χ^2 test was used to compare immunohistochemical expression of S-100, Leu7, CD34, p16, p27, p53, Mib-1, and TopoIIα among PNF, NF1-related, and non-NF1 MPNSTs of different histologic grades. Significance of correlation for the presence of p53, p16, and p27 with the Mib-1 labeling index was tested by Fisher exact test. All comparisons were made at a significance level of $P < 0.05$.

TABLE 1. Antibodies and Sources

Antibody	Working Dilution	Source
S-100	1:2000	Dako Corporation, Carpinteria, CA
CD34	1:200	Biosource International, Camarillo, CA
Leu7	1:40	Becton Dickinson, NJ
Mib-1	1:200	Dako Corporation, Carpinteria, CA
TopoIIα	1:1000	Joe Holden, MD, Salt Lake City, UT
p53	1:80	Dako Corporation, Carpinteria, CA
p27	1:60	Dako Corporation, Carpinteria, CA
p16	1:100	Santa Cruz Biotechnology, Inc. CA

RESULTS

Clinicopathologic Data

Of 19 PNFs, 15 were from confirmed NF1 patients and 4 had unknown NF1 status. Of 27 MPNSTs, 13 patients had NF1 and 7 were non-NF1, according to a review of medical records. The NF1 status could not be determined by medical record review in the remaining 7 MPNSTs. The MPNST patients without NF1 (age range 2–61 years, mean 35 years) were generally older than those with NF1 (age range 7–21years, mean 16.4 years). The PNF patients had a mean age of 13.4 years (age range 2–18 years). Histologically, 5 MPNSTs were low-grade (3 with NF1, 1 without NF1, 1 with unknown NF1 status) and the remaining 22 were high-grade (10 with NF1, 6 without NF1, and 6 with unknown NF1 status). Six high-grade MPNST specimens demonstrated adjacent areas of PNF.

Immunohistochemical Data

Results of immunohistochemical stains are summarized in Tables 2 and 3. Distinct differences between high-grade MPNSTs and PNFs were noted for S-100, Leu7, CD34, Mib-1, TopoIIα, p16, p27, and p53 reactivity. In high-grade MPNSTs where focal PNF areas with an abrupt transition to MPNST were seen, staining patterns similar to the either isolated PNFs or high-grade MPNSTs were seen on each side of the transition areas (Fig. 1). While diffuse S-100 and Leu7 staining was present in 89% and 84%, respectively, of PNFs, it was observed in only 14% and 32%, respectively, of high-grade MPNSTs ($P < 0.001$). In the remaining high-grade MPNSTs, the S-100 and Leu7 staining was focal in 50% and 55%, and absent in 36% and 13% of cases, respectively. In contrast, the pattern and frequency of S-100 and Leu7 immunoreactivity was similar between PNFs and low-grade MPNSTs ($P > 0.05$ for S-100, $P > 0.05$ for Leu 7). Similarly, diffuse CD34-positive spindle cells were observed in 95% of the PNFs and 80% of low-grade MPNSTs. In comparison, only 9% of high-grade MPNSTs displayed diffuse CD34 reactivity ($P < 0.001$; for high-grade MPNST vs. PNF). Proliferation marker expression differed between PNF and high–grade MPNST, and low-grade MPNST staining was similar to PNF. Mib-1 nuclear staining ranging from 1% to 80% was seen in most high-grade MPNSTs; 72% of high-grade MPNSTs had Mib-1 expression in >5% of nuclei. In contrast, none of the PNFs had Mib-1 expression in >1% of nuclei ($P < 0.001$). Although one of five low-grade MPNSTs demonstrated an increased Mib-1 labeling index of 10%, the difference between low-grade MPNSTs and PNFs was not statistically significant. TopoIIα reactivity paralleled that of Mib-1; 72% of high-grade MPNSTs had >5% of nuclear stain positive for TopoIIα, whereas none of the PNFs displayed TopoIIα expression in >1% nuclei ($P < 0.001$).

TABLE 2. Clinicopathologic Data of 19 Plexiform Neurofibromas (PNFs)

Case No.	Age (yr)/Sex	Site	NF1	S-100	Leu7	CD34	p16	p27	p53	Mib-1	TopoIIα
1	7/M	Knee	Yes	D	D	D	P	N	N	N	N
2	12/M	Chest	Yes	D	D	D	P	P	N	N	N
3	14/M	C4	Yes	F	D	D	N	P	N	N	N
4	12/F	Thigh	Yes	D	D	F	P	P	N	N	N
5	14/M	Nose	Yes	D	D	D	P	N	P	N	N
6	8/F	Shoulder	Yes	D	F	D	P	P	N	N	N
7	21/M	Neck	Yes	D	D	D	P	P	N	N	N
8	13/M	Supraclavicular	Yes	D	D	D	P	P	N	N	N
9	17/F	Arm	Yes	F	F	D	N	P	N	N	N
10	19/F	Cheek	Yes	D	D	D	P	P	N	N	N
11	15/F	Thigh	Yes	D	F	D	P	P	N	N	N
12	12/F	Shoulder	Yes	D	D	D	P	N	N	N	N
13	16/F	Shoulder	Yes	D	D	D	N	N	N	N	N
14	11/F	Arm	Yes	D	F	D	P	N	N	N	N
15	17/F	Foot	Yes	D	D	D	P	P	N	N	N
16	9/F	Abdominal wall	Un	D	D	D	P	P	N	N	N
17	15/F	Back	Un	D	D	D	P	P	N	N	N
18	11/M	Hip	Un	D	D	D	P	P	N	N	N
19	14/M	Hand	Un	D	D	D	P	P	N	N	N

Un, unknown; D, diffuse; F, focal; P, positive; N, negative.

TABLE 3. Clinicopathologic Data of 27 MPMSTs

	Age (yr)/Sex	Site	Grade	NF1	S-100	Leu7	CD34	p16	p27	p53	Mib-1	TopoIIα
1	3/F	Leg	H	Un	N	D	D	P	n-c	N	N	N
2	3/F	Leg	H	Un	N	D	D	P	n-c	N	N	N
3	2/F	Unknown	H	No	D	D	N	P	P	N	P	P
4	13/F	Arm	H	Yes	F	F	F	N	N	P	P	P
5	13/F	Arm	H	Yes	F	F	F	N	N	P	P	P
6	11/F	Neck	H	Yes	N	D	N	P	N	N	P	P
7	15/M	Thigh	H	Yes	F	F	F	N	n-c	P	P	P
8	16/M	Shoulder	L	Yes	F	F	D	P	P	N	N	N
9	18/F	Neck	L	Yes	D	D	D	P	P	P	N	N
10	16/M	Lung	H	Yes	F	D	N	p	n-c	P	P	P
11	13/F	Neck	L	Yes	D	F	D	P	P	N	N	N
12	15/M	Chest	H	Un	F	F	N	N	n-c	N	P	P
13	20/F	Arm	H	Yes	D	F	F	N	N	P	N	N
14	21/M	Tibia	H	Yes	F	F	N	N	N	P	P	P
15	27/F	Back	H	Yes	F	F	N	N	N	P	P	P
16	35/F	Knee	H	No	F	F	N	P	n-c	N	N	N
17	65/M	Neck	H	Un	F	F	N	P	N	N	N	N
18	61/M	Back	H	No	N	N	F	N	N	P	P	P
19	30/M	Leg	L	No	N	F	N	N	N	N	N	N
20	43/M	Thigh	H	Yes	F	F	F	P	N	P	P	P
21	40/M	Arm	L	Un	D	F	D	P	N	N	N	N
22	59/F	Thigh	H	Un	N	F	N	N	N	N	P	P
23	25/M	Neck	H	No	F	D	N	N	n-c	N	P	P
24	44/M	Back	H	No	N	N	N	N	N	P	P	P
25	44/M	Back	H	No	N	N	N	N	N	P	P	P
26	20/M	Knee	H	Yes	F	D	N	P	n-c	P	P	P
27	74/M	Unknown	H	Un	P	F	F	P	n-c	P	N	N

Un, unknown; D, diffuse; F, focal; P, positive; N, negative; n-c, nuclear and cytoplasmic staining present.

Low-grade MPNSTs and PNFs did not differ significantly in TopoIIα expression ($P > 0.05$).

Increased p53 nuclear staining (Fig.1) and decreased p16 nuclear staining were frequently present in high-grade MPNSTs but not in low-grade MPNSTs or PNFs. p53 nuclear reactivity ranging from 5% to >50% of tumor cells were seen in 59% of high-grade MPNSTs but in none of 19 PNFs ($P < 0.01$). In contrast to the high-grade MPNSTs, only one of the five low-grade MPNSTs showed p53 nuclear staining of >5% nuclei. p53 expression between PNFs and low-grade MPNSTs did not differ significantly ($P > 0.05$). p16 nuclear staining ranging from 5% to >50% of cells was seen in PNFs. p16 positivity in >10% nuclei was present in 84% of the PNFs and in 46% of high-grade MPNST ($P < 0.025$). PNFs and low-grade MPNSTs were similar in their p16 reactivity (84% vs. 70%, $P > 0.05$).

Different p27 subcellular localization (nuclear vs. nuclear and cytoplasmic) was observed among high-grade MPNSTs, low-grade MPNSTs, and PNFs. p27 nuclear reactivity was present in 74% of PNFs (Fig. 2C), 60% of low-grade MPNSTs ($P > 0.05$), but only 15% of high-grade MPNSTs ($P < 0.01$). In contrast, variable nuclear and cytoplasmic p27 staining that was not observed in PNFs or low-grade MPNSTs was present in 33% of high-grade MPNSTs (Fig. 2E, F). Although scattered cells with only p27 cytoplasmic staining were noted, they usually were intermixed with more prominent combined nuclear and cytoplasmic staining patterns; therefore, they were recorded as nuclear and cytoplasmic staining. In addition, 52% of high-grade MPNSTs did not display p27 staining of any kind (Fig. 2D).

The presence of p53 reactivity correlated with Mib-1 and TopoIIα expression in high-grade MPNSTs ($P < 0.01$). No statistically significant correlations, however, were identified between p16 and p27 expression and proliferation markers Mib-1 and TopoIIα.

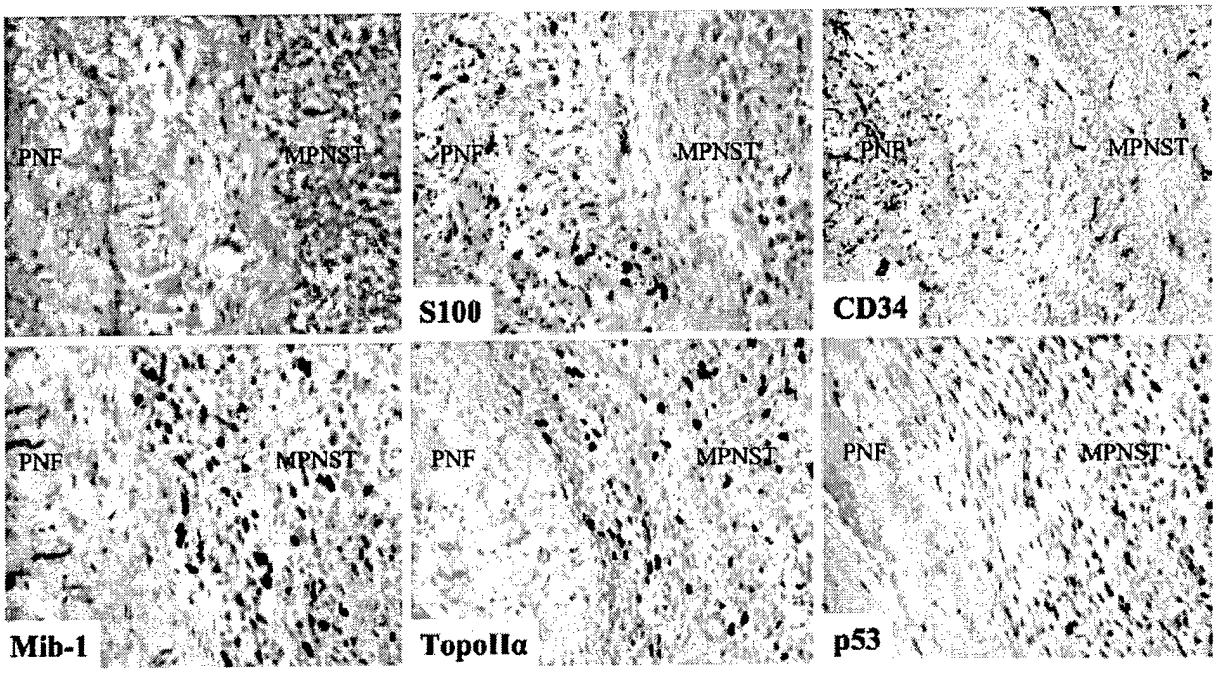

FIGURE 1. Immunohistochemical staining for S-100, CD34, Mib-1, Topollα, and p53 demonstrated distinct differences between high-grade MPNST (right) and adjacent PNF area (left).

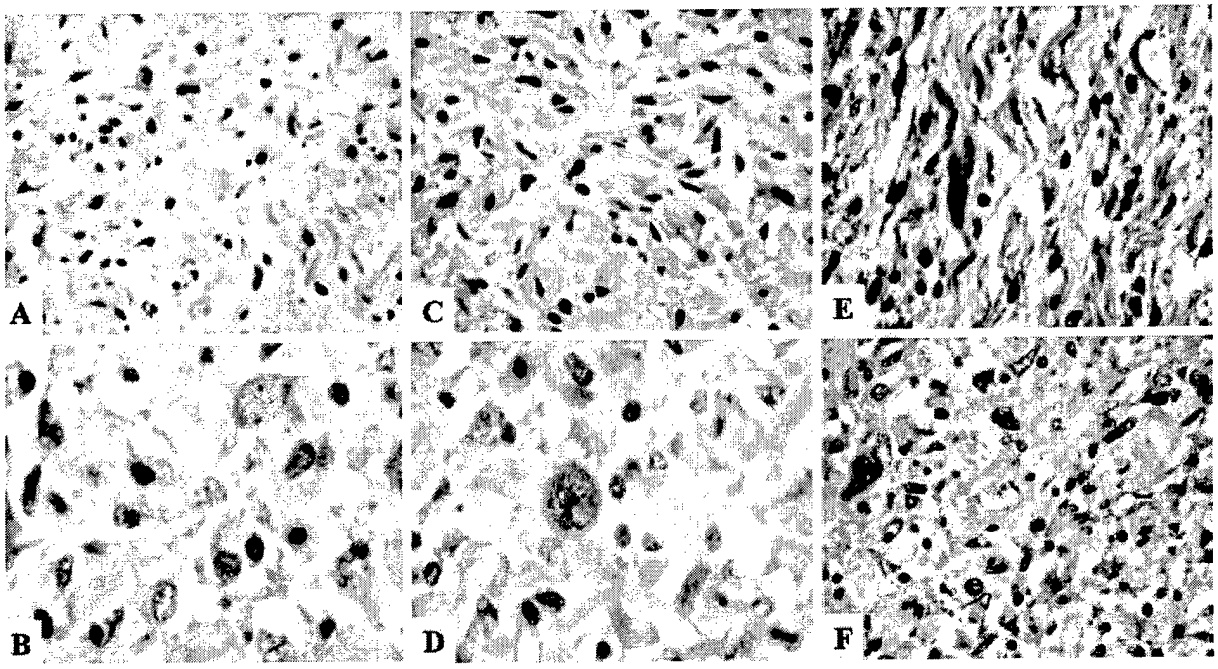

FIGURE 2. Representative immunohistochemistry results of p16 and p27. A, Diffuse p16 nuclear reactivity in PNF. B, Lack of p16 nuclear reactivity in high-grade MPNST. C, Diffuse p27 nuclear reactivity in PNF. D, Lack of p27 reactivity in 52% of high-grade MPNSTs. E and F, Variable p27 nuclear and cytoplasmic reactivity in 33% of high-grade MPNSTs.

Comparison of p53, p16, and p27 expression between NF1-related and non-NF1 high-grade MPNSTs revealed a higher frequency of p53 immunoreactivity present in the NF1-related MPNSTs than in the sporadic cases (89% vs. 43%, $P < 0.025$). Although p16 immunoreactivity was lower in NF1-related high-grade MPNSTs, it did not reach statistical significance ($P > 0.1$). Similarly, no significant differences were present in the expression of S-100, CD34, Mib-1, TopoIIα, and p27 between NF1-related and sporadic high-grade MPNSTs. There was no significant difference in the above-mentioned stains between NF1–related and non-NF1 low-grade MPNSTs, although the number of cases in this group was small (3 NF1-related and 1 non-NF1).

DISCUSSION

Although the neoplastic origin of PNF and MPNST remains unsettled, most studies suggest that Schwann cells that harbor inactivating *NF1* gene mutations in both alleles are the primary neoplastic component in both PNF and most MPNSTs.[20,39,44] Dual-color fluorescence in situ hybridization has provided evidence that S-100-positive Schwann cells harbor *NF1* deletions as somatic inactivating mutations ("second hits") in PNFs derived from patients with NF1.[39] This suggested that S-100-negative cells in both sporadic and NF1-associated MPNSTs represent dedifferentiated Schwann cells that lack functional neurofibromin. Our observation that the diffuse S-100 protein and Leu 7 expression in PNFs was diminished, or lost, in the majority of high-grade MPNSTs supports the concept of Schwann cell dedifferentiation during MPNST tumor progression. The decreased CD34 reactivity in our study parallels the change in S-100 protein and most likely represents a loss of distinctive CD34-positive, fibroblast-like, "dendritic interstitial" cells in the high-grade MPNSTs.[36,46] The CD34-positive cell population, which was present in both normal peripheral nerve and benign peripheral nerve sheath tumors, was diminished in high-grade MPNSTs, as has been previously described.[58] Although the underlying mechanism for significantly decreased CD34-positive cells in the high-grade MPNST remains unknown, the CD34-positive stromal component may play a role in MPNST tumor formation.[54]

The high-grade MPNSTs analyzed in this study displayed a distinctive pattern of increased proliferation and frequent alterations of the cell cycle regulators p53, p16, and p27. Interestingly, coexpression of proliferation markers Mib-1 and TopoIIα was also found in 72% of high-grade MPNSTs. Mib-1 is a monoclonal antibody to a nuclear proliferating antigen Ki-67, which is present in all phases of the cell cycle, except for G0. A high labeling index, >25%, correlated with a reduced survival rate and has been proposed as a significant indicator for poor prognosis.[55] TopoIIα is a nuclear enzyme whose reactivity has been linked with cellular dedifferentiation and a potentially aggressive tumor phenotype in various neoplasms.[11,35] Notably, the loss of diffuse staining patterns for S-100, Leu7, and CD34 and the increased proliferative activity were restricted to the high-grade MPNST areas in those tumors with both MPNST and PNF components. Furthermore, an identical topographical difference in the p53, p27, and p16 immunohistochemical expression between PNF areas with adjacent MPNST was also present. These observations support the hypothesis that altered p53, p16, and p27 protein expression is associated with malignant transformation from PNF to MPNST.

The underlying mechanism of p53 dysfunction in MPNST is incompletely understood. A shorter survival was documented in a study of 28 cases among the subgroup of MPNSTs with p53 immunohistochemical positivity.[17] However, another study failed to demonstrate a correlation between p53 immunoreactivity and prognosis for MPNST.[55] Our data, like a previous report,[55] demonstrated that p53 reactivity in the high-grade MPNSTs correlated with proliferative activity, suggesting that p53 alteration might play a role in tumor progression associated with cell proliferation. However, significant p53 nuclear expression was absent in the majority of the low-grade MPNSTs and or in the PNFs adjacent to high-grade MPNSTs. This absence of p53 reactivity mitigates against the hypothesis that p53 abnormalities are an early event in human tumor progression. This is in contrast to mouse tumor models where double inactivation of *Nf1* and *Tp53* in mice is sufficient to generate MPNSTs.[9,52]

Relatively few studies compare p53 immunohistochemical expression in MPNST of different histologic grades. A study of NF1-related and sporadic peripheral nerve sheath lesions in pediatric patients[27] reported a significant difference in p53 reactivity among different histologic grades of MPNST, which suggested that p53 accumulation with secondary *TP53* mutations may be a late event in tumor progression. Among 54 MPNSTs, with or without associated PNF, the immunohistochemical detection of p53 protein was common in malignant areas but rare in the PNF regions.[33] Among 17 NF1 patients with either PNF or MPNST arising from PNF, *TP53* mutations were identified in 4 of 6 MPNSTs with p53 overexpression but not in any of PNFs.[24] Thus, the late appearance of *TP53* mutations[24] and the rarity of p53 staining in the PNF regions[33] preclude the clinicopathologic use of p53 immunostaining to predict transformation of PNF to MPNST.

In the present study, we observed more frequent p53 immunoreactivity in NF1-related versus non-NF1 high-grade MPNSTs (89% vs. 43%, $P < 0.025$). These results agree with a previous study in which p53 accumulation was observed more frequently in NF1-associated MPNSTs.[27] In contrast, others reported no difference in the frequency or degree of p53 staining between MPNSTs from patients with or without NF1.[17] Comparison of p53 protein expression and *TP53* mutations between NF1-related and sporadic MPNSTs revealed that the

TP53 mutation, loss of heterozygosity involving the *TP53* locus, and p53 protein overexpression were mainly restricted to sporadic MPNSTs.[3] These divergent findings point out the need for further studies and careful documentation of NF1 status in the assessment and treatment of MPNST.

Loss of p16 has been reported in 50% to 75% of MPNSTs in different series, although tumor grade was not specifically analyzed.[3,22,45] We demonstrate that p16 expression is lost to a significant extent in high-grade MPNSTs but not in low-grade MPNSTs. No significant difference was found between p16 expression in PNF and low-grade MPNST or in PNF areas adjacent to high-grade MPNST, nor was there a significant correlation between the loss of p16 reactivity in high-grade MPNST and the proliferation markers. p16 regulates the G1-S phase checkpoint of the cell cycle through the pRB pathway,[3,26,45] and recent studies also demonstrate that inactivation of *INK4A*, the gene encoding both p16 and p19, is present in 60% to 75% of MPNSTs.[2,21] Because p16 and p19 affect the cell cycle through pRB and p53 pathways, respectively, this is further evidence that co-inactivation of different pathways may be an important step in MPNST tumor progression.[2]

The mechanism underlying p27 deregulation in human cancer is not well understood. Alteration of p27 protein immunostaining patterns during tumor progression may be at the posttranslational level with protein degradation by the ubiquitin-proteasome pathway[40] or nuclear-to-cytoplasmic relocation by oncogene-activated pathways (Ras, ErbB2).[4,15,29,42] A significant decrease in or loss of nuclear expression of p27 in MPNST versus PNF has been reported, with the majority of MPNSTs displaying strong cytoplasmic p27 staining.[22] These observations suggest that p27 might be involved in tumor progression in the PNF–MPNST pathway. In support of this hypothesis, our result also demonstrated a significant loss of p27 nuclear expression in high-grade MPNSTs, although preferential cytoplasmic p27 staining could not be distinguished from the combined nuclear and cytoplasmic (nucleocytoplasmic) p27 staining, which was present in 33% of high-grade MPNSTs and not in either low-grade MPNSTs or PNFs. If the nucleocytoplasmic p27 reactivity observed in our study represents a p27 nuclear-to-cytoplasmic translocation associated with tumor progression, then the observations also support the hypothesis that, like epithelial cancers,[1,8,49] exclusion of p27 from the nucleus contributes to tumor progression in MPNST.

No significant difference was found in the expression of either p16 or p27 in sporadic or NF-1-related MPNST. Others have showed that altered p16, represented by either *p16/INK-4A* gene homozygous deletion or loss of heterozygosity at the relative 9p21 locus and lack of p16 immunostaining, was similar between NF1-associated and sporadic MPNST.[3] There is no previous study comparing p27 expression between NF1-related and sporadic MPNST.

In summary, frequent alterations of cell cycle regulators p53, p16, and p27 are present in high-grade MPNST. The synchronous presence of p53, p16, and p27 alterations, decreased S-100 protein, Leu 7, and CD34 immunoreactivity patterns, and increased proliferation markers Mib-1 and TopoIIα in high-grade MPNST supports the concept that these altered cell cycle regulators influence tumor progression in the PNF–MPNST sequence. The p53 expression in high-grade MPNSTs is associated with concomitant expression of the proliferation marker Mib-1, and it appears to be more frequent in NF1-related MPNSTs. However, the lack of significant alterations of these cell cycle regulators in PNF adjacent to high-grade MPNST, or in the majority of low-grade MPNST, indicates that the alterations are unlikely to be initial events in malignant transformation. Therefore, they are not reliable for early detection of tumor progression in MPNST. Recently, DeClue et al reported that epithelial growth factor receptor, which regulates the cell cycle through both pRB-dependent and -independent pathways, might also play an important role in NF1 tumorigenesis and Schwann cell transformation.[12] The question remains as to whether there are as yet unidentified genetic events that initiate progression from PNF to MPNST. A study by Zhu et al provided genetic evidence that the *Nf1* haplo-insufficient state of the somatic tissue surrounding peripheral nerve sheath tumors, including fibroblasts and mast cells, provides a functional contribution to tumor formation, either through initiation or progression of tumorigenesis.[60] Studies are needed on genetic factors that, if detected, could provide insight to critical events that initiate tumor progression and malignant transformation. In the meantime, histologic criteria, though imperfect, remain the basis for clinically distinguishing PNF from MPNST, and determination of p53 reactivity may prove useful to discriminate low-grade and high-grade MPNST in a small biopsy.

REFERENCES

1. Baldassarre G, Belletti B, Bruni P, et al. Overexpressed cyclin D3 contributes to retaining the growth inhibitor p27 in the cytoplasm of thyroid tumor cells. *J Clin Invest*. 1999;104:865–874.
2. Berner JM, Sorlie T, Mertens F, et al. Chromosome band 9p21 is frequently altered in malignant peripheral nerve sheath tumors: studies of CDKN2A and other genes of the pRB pathway. *Genes Chromosomes Cancer*. 1999;26:151–160.
3. Birindelli S, Perrone F, Oggionni M, et al. Rb and TP53 pathway alterations in sporadic and NF1-related malignant peripheral nerve sheath tumors. *Lab Invest*. 2001;81:833–844.
4. Blagosklonny MV. Are p27 and p21 cytoplasmic oncoproteins? *Cell Cycle*. 2002;1:391–393.
5. Burns KL, Ueki K, Jhung SL, et al. Molecular genetic correlated of p16, cdk4 and pRb immunohistochemistry in glioblastomas. *J Neuropathol Exp Neurol*. 1998;57:122–130.
6. Caldas C, Hahn SA, da Costa LT, et al. Frequent somatic mutation and homozygous deletions of the p16 (MTS1) gene in pancreatic adenocarcinoma. *Nat Genet*. 1994;8:27–32.
7. Cawthon RM, Weiss R, Xu GF, et al. A major segment of the neurofibromatosis type 1 gene: cDNA sequence, genomic structure, and point mutations. *Cell*. 1990;62:193–201.
8. Chiappetta G, Vento MT, Spiezia S, et al. Overexpressed cyclin D3 con-

tributes to retaining the growth inhibitor p27 in the cytoplasm of thyroid tumor cells. *J Clin Invest.* 1999;104:865–874.
9. Cichowski K, Shih TS, Schmitt E, et al. Mouse models of tumor development in neurofibromatosis type 1. *Science.* 1999;286:2172–2176.
10. Cohen JA, Geradts J. Loss of RB and MTS1/CDKN2 (p16) expression in human sarcomas. *Hum Pathol* 1997;28:893–898.
11. Costa MJ, Hansen CL, Holden JA, et al. Topoisomerase II alpha: prognostic predictor and cell cycle marker in surface epithelial neoplasms of the ovary and peritoneum. *Int J Gynecol Pathol.* 2000;19:248–257.
12. DeClue JE, Heffelfinger S, Benvenuto G, et al. Epidermal growth factor receptor expression in neurofibromatosis type 1-related tumors and NF1 animal models. *J Clin Invest.* 2000;105:1233–1241.
13. Durand B, Gao FB, Raff M. Accumulation of the cyclin-dependent kinase inhibitor p27/Kip1 and the timing of oligodendrocyte differentiation. *EMBO J.* 1997;16:306–317.
14. Ferner RE, Gutmann DH. International consensus statement on malignant peripheral nerve sheath tumors in neurofibromatosis. *Cancer Res.* 2002; 62:1573–1577.
15. Fujita N, Sato S, Katayama K, et al. Akt-dependent phosphorylation of p27Kip1 promotes binding to 14-3-3 and cytoplasmic localization. *J Biol Chem.* 2002;277:28706–28713.
16. Gutmann DH, Collins FS. Von Recklinghausen neurofibromatosis. In: Driver CR, Beaudet AL, Sly WS, et al, eds. *The Metabolic and Molecular Bases of Inherited Disease.* New York: McGraw-Hill, 1995:677–696.
17. Halling KC, Scheithauer BW, Halling AC, et al. p53 expression in neurofibroma and malignant peripheral nerve sheath tumor: an immunohistochemical study of sporadic and NF1-associated tumors. *Am J Clin Pathol.* 1996;106:282–288.
18. Jhanwar SC, Chen Q, Li FP, et al. Cytogenetic analysis of soft tissue sarcomas: recurrent chromosome abnormalities in malignant peripheral nerve sheath tumors (MPNST). *Cancer Genet Cytogenet.* 1994;78: 138–144.
19. Katayose Y, Kim M, Rakkar AN, et al. Promoting apoptosis: a novel activity associated with the cyclin-dependent kinase inhibitor p27. *Cancer Res.* 1997;57:5441–5445.
20. Kluwe L, Friedrich R, Mautner VF. Loss of NF1 allele in Schwann cells but not in fibroblasts derived from an NF1-associated neurofibroma. *Genes Chromosomes Cancer.* 1999;24:283–285.
21. Kourea HP, Orlow I, Scheithauer BW, et al. Deletions of the *INK4A* gene occur in malignant peripheral nerve sheath tumors but not in neurofibromas. *Am J Pathol.* 1999;155:1855–1860.
22. Kourea HP, Cordon-Cardo C, Dudas M, et al. Expression of p27 (kip) and other cell cycle regulators in malignant peripheral nerve sheath tumors and neurofibromas: the emerging role of p27 (kip) in malignant transformation of neurofibromas. *Am J Pathol.* 1999;155:1885–1891.
23. Legius EL, Dierick H, Wu R, et al. TP53 mutations are frequent in malignant NF1 tumors. *Genes Chromosomes Cancer.* 1994;10:250–255.
24. Leroy K, Dumas V, Martin-Garcia N, et al. Malignant peripheral nerve sheath tumors associated with neurofibromatosis type 1: a clinicopathologic and molecular study of 17 patients. *Arch Dermatol.* 2001;137: 908–913.
25. Levkau B, Koyama H, Raines EW, et al. Cleavage of p21Cip1/Waf1 and p27Kip1 mediates apoptosis in endothelial cells through activation of Cdk2: role of a caspase cascade. *Mol Cell.* 1998;1:553–563.
26. Li Y, Nichols MA, Shay JW, et al. Transcriptional repression of the D-type cyclin-dependent kinase inhibitor p16 by the retinoblastoma susceptibility gene product pRb. *Cancer Res.* 1994;54:6078–6082.
27. Liapis H, Marley EF, Lin Y, et al. p53 and Ki-67 proliferating cell nuclear antigen in benign and malignant peripheral nerve sheath tumors in children. *Pediatr Dev Pathol.* 1999;2:377–384.
28. Liew CT, Li HM, Lo KW, et al. High frequency of p16 *INK4A* gene alterations in hepatocellular carcinoma. *Oncogene.* 1999;18:789–795.
29. Liu X, Sun Y, Ehrlich M, et al. Disruption of TGF-beta growth inhibition by oncogenic ras is linked to p27Kip1 mislocalization. *Oncogene.* 2000; 19:5926–5935.
30. Lloyd RV, Erickson LA, Jin L, et al. p27kip1: a multifunctional cyclin-dependent kinase inhibitor with prognostic significance in human cancers. *Am J Pathol.* 1999;154:313–323.
31. Lukas J, Aagaard L, Strauss M, et al. Oncogenic aberrations of p16INK4/CDKN2 and cyclin D1 cooperate to deregulate G1 control. *Cancer Res.* 1995;55:4818–4823.
32. Martin GA, Viskochil D, Bollag G, et al. The GAP-related domain of the neurofibromatosis type 1 gene product interacts with ras p21. *Cell.* 1990; 63:843–849.
33. McCarron KF, Goldblum JR. Plexiform neurofibroma with and without associated malignant peripheral nerve sheath tumor: a clinicopathologic and immunohistochemical analysis of 54 cases. *Mod Pathol.* 1998;11: 612–617.
34. Menon AG, Anderson KM, Riccardi VM, et al. Chromosome 17p deletions and p53 gene mutations associated with the formation of malignant neurofibrosarcomas in von Recklinghausen neurofibromatosis. *Proc Natl Acad Sci USA.* 1990;87:5435–5439.
35. Nakopoulou L, Lazaris AC, Kavantzas N, et al. DNA topoisomerase II-alpha immunoreactivity as a marker of tumor aggressiveness in invasive breast cancer. *Pathobiology.* 2000;68:137–143.
36. Nickoloff BJ. The human progenitor cell antigen (CD34) is localized on endothelial cells, dermal dendritic cells, and perifollicular cells in formalin-fixed normal skin, and on proliferating endothelial cells and stromal spindle-shaped cells in Kaposi's sarcoma. *Arch Dermatol.* 1991;127: 523–529.
37. Nielsen GP, Stemmer-Rachamimov AO, Ino Y, et al. Malignant transformation of neurofibromas in neurofibromatosis 1 is associated with CDKN2A/p16 inactivation. *Am J Pathol.* 1999;155:1879–1884.
38. Parham DM, Webber BL, Jenkins JJ 3rd, et al. Nonrhabdomyosarcomatous soft tissue sarcomas of childhood: formulation of a simplified system for grading. *Mod Pathol.* 1995;8:705–710.
39. Perry A, Roth KA, Banerjee R, et al. NF1 deletions in S-100 protein positive and negative cells of sporadic and neurofibromatosis 1 (NF1)-associated plexiform neurofibromas and malignant peripheral nerve sheath tumors. *Am J Pathol.* 2001;159:57–61.
40. Polyak K, Lee MH, Erdjument-Bromage H, et al. Cloning of p27Kip1, a cyclin-dependent kinase inhibitor and a potential mediator of extracellular antimitogenic signals. *Cell.* 1994;78:59–66.
41. Riccardi VM. *Neurofibromatosis: Phenotype, Natural History, and Pathogenesis,* 2nd ed. Baltimore: Johns Hopkins University, 1992.
42. Rodier G, Montagnoli A, Di Marcotullio L, et al. p27 cytoplasmic localization is regulated by phosphorylation on Ser10 and is not a prerequisite for its proteolysis. *EMBO J.* 2001;20:6672–6682.
43. Scheithauer BW, Woodruff JM, Erlandson RA. Tumors of the peripheral nervous system. In: *Atlas of Tumor Pathology,* 3rd series, fascicle 24. Washington, DC: Armed Forces Institute of Pathology, 1999.
44. Serra E, Rosenbaum T, Winner U, et al. Human Schwann cells harbor the somatic NF1 mutation in neurofibromas: evidence of two different Schwann cell subpopulations. *Mol Genet.* 2000;9:3055–3064.
45. Serrano M, Hannon GJ, Beach D. A new regulatory motif in cell-cycle control causing specific inhibition of cyclin D/CDK4. *Nature* 1993;16: 366:704–707.
46. Suster S, Fisher C, Moran CA. Expression of bcl-2 oncoprotein in benign and malignant spindle cell tumors of soft tissue, skin, serosal surfaces, and gastrointestinal tract. *Am J Surg Pathol.* 1998;22:863–872.
47. Toyoshima H, Hunter T. p27, a novel inhibitor of G1 cyclin-Cdk protein kinase activity, is related to p21. *Cell.* 1994;78:67–74.
48. Ueki K, Ono Y, Henson JW, et al. CDKN2/p16 or RB alterations occur in the majority of glioblastomas and are inversely correlated. *Cancer Res.* 1996;56:150–153.
49. Viglietto G, Motti ML, Bruni P, et al. Cytoplasmic relocalization and inhibition of the cyclin-dependent kinase inhibitor p27 (Kip1) by PKB/Akt-mediated phosphorylation in breast cancer. *Nat Med.* 2002;8:1136–1144.
50. Viskochil D, Buchberg AM, Xu G, et al. Deletions and a translocation interrupt a cloned gene at the neurofibromatosis type 1 locus. *Cell.* 1990; 62:187–192.
51. Viskochil D, White R, Cawthon R. The neurofibromatosis type 1 gene. *Annu Rev Neurosci.* 1993;16:183–205.
52. Vogel KS, Klesse LJ, Velasco-Miguel S, et al. Mouse tumor model for neurofibromatosis type 1. *Science.* 1999;286:2176–2179.
53. Wallace MR, Marchuk DA, Andersen LB, et al. Type 1 neurofibromatosis gene: identification of a large transcript disrupted in three NF1 patients. *Science.* 1990;249:181–186.

54. Watanabe T, Oda Y, Tamiya S, et al. Malignant peripheral nerve sheath tumour arising within neurofibroma: an immunohistochemical analysis in the comparison between benign and malignant components. *Clin Pathol.* 2001;54:631–636.
55. Watanabe T, Oda Y, Tamiya S, et al. Malignant peripheral nerve sheath tumours: high Ki67 labelling index is the significant prognostic indicator. *Histopathology.* 2001;39:187–197.
56. Weiss SW, Goldblum JR. Benign tumors of peripheral nerves. In: Weiss SW, Goldblum JR, eds. *Enzinger and Weiss's Soft Tissue Tumor*, 4th ed. St. Louis: Mosby, 2001:1137–1142.
57. Weiss SW, Goldblum JR. Malignant tumors of peripheral nerves. In: Weiss SW, Goldblum JR, eds. *Enzinger and Weiss's Soft Tissue Tumor*, 4th ed. St. Louis: Mosby, 2001:1209–1263.
58. Weiss SW, Nickoloff BJ. CD-34 is expressed by a distinctive cell population in peripheral nerve, nerve sheath tumors, and related lesions. *Am J Surg Pathol.* 1993;17:1039–1045.
59. Xu GF, O'Connell P, Viskochil D, et al. The neurofibromatosis type 1 gene encodes a protein related to GAP. *Cell.* 1990;62:599–608.
60. Zhu Y, Ghosh P, Charnay P, et al. Neurofibromas in NF1: Schwann cell origin and role of tumor environment. *Science.* 2002;296:920–922.

Published manuscript: DeClue J, Heffelfinger S, Benvenuto G, Ling B, Li S, Rui W, Vass W, **Viskochil D**, Ratner N. Epidermal growth factor receptor expression in neurofibromatosis type 1-related tumors and NF1 animal models. J Clin Invest 2000;105:1233-1241.

Epidermal growth factor receptor expression in neurofibromatosis type 1–related tumors and NF1 animal models

Jeffrey E. DeClue,[1] Sue Heffelfinger,[2] Giovanna Benvenuto,[1] Bo Ling,[3] Shaowei Li,[1] Wen Rui,[3] William C. Vass,[1] David Viskochil,[4] and Nancy Ratner[3]

[1]Laboratory of Cellular Oncology, National Cancer Institute, Bethesda, Maryland, USA
[2]Department of Pathology, and
[3]Department of Cell Biology, Neurobiology, and Anatomy, University of Cincinnati College of Medicine, Cincinnati, Ohio, USA
[4]Department of Genetics, University of Utah, Salt Lake City, Utah, USA

Address correspondence to: Jeffrey E. DeClue, Laboratory of Cellular Oncology, National Cancer Institute, Building 36, Room 1D-32, Bethesda, Maryland 20892, USA.
Phone: (301) 496-4732; Fax: (301) 480-5322; E-mail: jd99f@nih.gov.

Giovanna Benvenuto's present address is: Department of Cellular and Molecular Biology and Pathology, Faculty of Medicine, University of Naples, Naples, Italy.

Received for publication June 16, 1999, and accepted in revised form March 20, 2000.

We have found that EGF-R expression is associated with the development of the Schwann cell–derived tumors characteristic of neurofibromatosis type 1 (NF1) and in animal models of this disease. This is surprising, because Schwann cells normally lack EGF-R and respond to ligands other than EGF. Nevertheless, immunoblotting, Northern analysis, and immunohistochemistry revealed that each of 3 malignant peripheral nerve sheath tumor (MPNST) cell lines from NF1 patients expressed the EGF-R, as did 7 of 7 other primary MPNSTs, a non-NF1 MPNST cell line, and the $S100^+$ cells from each of 9 benign neurofibromas. Furthermore, transformed derivatives of Schwann cells from *NF1*$^{-/-}$ mouse embryos also expressed the EGF-R. All of the cells or cell lines expressing EGF-R responded to EGF by activation of downstream signaling pathways. Thus, EGF-R expression may play an important role in NF1 tumorigenesis and Schwann cell transformation. Consistent with this hypothesis, growth of NF1 MPNST lines and the transformed *NF1*$^{-/-}$ mouse embryo Schwann cells was greatly stimulated by EGF in vitro and could be blocked by agents that antagonize EGF-R function.

J. Clin. Invest. **105**:1233–1241 (2000).

Introduction

Neurofibromatosis type 1 (NF1) is a dominantly inherited human disease affecting one in 2,500 to 3,500 individuals (1, 2). The NF1 phenotype is highly variable, and its clinical course is unpredictable. Several organ systems are affected, including the bones, skin, iris, and central nervous system (manifested in learning disabilities and gliomas) (3). The hallmark of NF1 is the development of benign tumors of the peripheral nervous system (neurofibromas), which vary greatly in both number and size among patients (1, 4). Neurofibromas are heterogeneous tumors composed of Schwann cells, neurons, fibroblasts and other cells, with Schwann cells being the major (60–80%) cell type (5, 6). Neurofibroma-derived Schwann cells have been demonstrated to possess abnormal properties, including increased invasiveness and the induction of angiogenesis (7). NF1 patients are also at increased risk for the development of certain malignancies, including pheochromocytomas, childhood myeloid leukemias, and in about 5% of patients, malignant peripheral nerve sheath tumors (MPNST) (8–10). Although still a point of some debate, it is widely held that MPNST arise from large (plexiform) neurofibromas and are probably derived from Schwann cells, because many MPNST stain positive for Schwann cell markers such as S100 (4, 11).

The *NF1* gene lies on chromosome 17 (12–14), and the great majority of patient mutations prevent expression of the intact *NF1* product, designated neurofibromin (15). Neurofibromin contains a central domain homologous to a family of proteins known as Ras-GTPase–activating proteins (Ras-GAPs), which function as negative regulators for Ras proteins (16). Ras-GAPs attenuate signaling from Ras, thus blocking the transmission of signals leading to increased growth or differentiation. The role of neurofibromin as a tumor suppressor that inactivates Ras-dependent signals has been confirmed. Primary neurofibromas and cell lines derived from NF1 MPNST show high levels of Ras-GTP, and in MPNST cell lines lacking neurofibromin, elevated Ras-GTP leads to constitutive growth activation (17–19).

Targeted disruption of *NF1* in mice has provided an experimental system for analyzing the role of neurofibromin in growth regulation (20, 21). The importance of Schwann cells to tumor development in NF1 is sug-

gested by the altered properties of Schwann cells from heterozygous (+/-) or homozygous mutant (-/-) embryos (22). Mutant Schwann cells have elevated Ras-GTP, are more invasive than wild-type cells, and when cultured in low serum yield transformed derivatives (TXF) that display altered morphology, reduced growth factor dependence, and reduced adherence (23). These transformed derivatives, which fail to develop in cultures of wild-type (+/+) littermates, retain expression of the Schwann cell markers P75 and S100 (23).

Schwann cell growth in vivo is normally regulated through interactions with neurons (4). The family of small peptides known as heregulins/neuregulins, including glial growth factor (GGF), probably serve as in vivo Schwann cell mitogens. Neuregulins, which robustly stimulate Schwann cell growth in vitro (24), bear homology to EGF and activate transmembrane tyrosine kinase receptors (erbB2, -3, and -4) that are structurally and functionally related to the EGF-R (reviewed in ref. 25). Schwann cells, which express little if any erbB4, use erbB2-3 heterodimers for GGF signaling (26). Stimulation of Schwann cells with GGF in vitro leads to increases in Ras-GTP, demonstrating a link between Ras regulation and Schwann cell proliferation (27).

Both *NF1* alleles are disrupted in MPNST and in at least a proportion of benign neurofibromas (28–30). Whereas mutation or loss of the *p53* gene occurs in about one third of MPNST (31), it is likely that additional alterations are present in these tumors. Here we report evidence indicating that aberrant expression of the EGF-R is associated with tumor development in NF1 and in animal models of NF1, suggesting a role in pathogenesis and representing a novel potential therapeutic target.

Methods

Cell culture and biochemical assays. MPNST lines were grown as described (17), and the embryo-derived mouse Schwann cells and TXF derivatives were isolated and grown as described (22, 23). Agar colony formation assays were carried out as described (17). For MAP kinase assays, cells were grown until confluent, serum-starved for 24 hours, stimulated with mitogen for 5 minutes at 37°C, then lysed, and MAP kinase assays were carried out as described (23). For Western blotting, cells were grown until confluent and lysed. Lysates with 50 μg protein (human) or 100 μg protein (mouse) were subjected to SDS-PAGE using 6% gels. Immunoblotting was carried out as described (17) using the following antibodies from Santa Cruz Biotechnology (Santa Cruz, California, USA): for EGF-R, sc03; for erbB2, sc284; for erbB3, sc285; for erbB4, sc283. Antibodies were used at a dilution of 1:2,000 for human and 1:1,000 for mouse lysates. Blots were developed with an enhanced chemiluminescence detection kit (Kirkegaard & Perry Laboratories, Gaithersburg, Maryland, USA).

Northern blotting. Cells were grown until confluent and lysed, and total RNA was extracted using the RNeasy system (QIAGEN Inc., Valencia, California, USA). Twenty micrograms of total RNA from each line was electrophoresed in an agarose gel and transferred to a nylon filter (Millipore Corp., Bedford, Massachusetts, USA). Human EGF-R probe was derived from the plasmid pCO12 (32) by digestion with *Sst*II and *Xho*I. The probe was labeled with ^{32}P in a nick translation system (Promega Corp., Madison, Wisconsin, USA), and hybridization was carried out using Quickhyb buffer (Stratagene, La Jolla, California, USA) with 1.4×10^7 cpm of probe.

Immunohistochemistry. All immunohistochemistry was performed on 4–6-micron paraffin sections using the Ventana ES immunostaining system (Ventana Instruments, Tuscon, Arizona, USA). Following deparaffinization in xylenes and trypsinization (for EGF-R detection), slides were placed in the instrument that adds the primary antibody, the biotinylated anti-mouse or rabbit second antibody, and avidin-conjugated peroxidase or alkaline phosphatase as dictated by a bar code. Primary antibodies were incubated for 32 minutes at 37°C. The instrument performed all washes. Primary antibodies were rabbit polyclonal anti-bovine S100 (Dakopatts Inc., Carpinteria, California, USA) diluted to 1:1000; mouse monoclonal anti-EGF-R 31G7 (1:8; Zymed Inc., South San Francisco, California, USA); or PG-M1, a mouse monoclonal anti-macrophage marker (Dakopatts) diluted to 1:100. Slides were counterstained with hematoxylin or with nuclear fast red by hand. In all cases irrelevant mouse or rabbit immunoglobulin was used instead of a primary antibody as a negative control.

Dissociated cell preparations. Normal human nerves (n = 2) and neurofibroma (n = 3) specimens were digested overnight in enzymes as described (6). Cells (10^6) were washed twice in L15 medium (GIBCO/BRL, Grand Island, New York, USA) then fixed in non-buffered formalin, pelleted, and centrifuged into a cassette (Cytoblock; Shandon Inc., Pittsburgh, Pennsylvania, USA) for embedding.

Patient information. Adult normal nerves were used as controls. When NF1 diagnosis (NF1 dx) was made, it was based on family history, café-au-lait macules, and neurofibromas as described (33). Cutaneous neurofibromas were obtained from: 69-year-old man (non-NF1); 50-year-old woman (non-NF1); adult (non-NF1); 30-year-old woman (NF1). Plexiform neurofibromas were obtained from: 17-year-old man (NF1 dx); 6-year-old boy (NF1 dx); 15-year-old girl (NF1 dx); 14-year-old girl (NF1 dx); and a patient (mid-20s) with segmental NF1. Neurofibromas used for cell dissociation were obtained from: adult woman, cutaneous neurofibroma (NF1 dx); 3-year-old child, cervical neurofibroma (NF1 dx). For MPNST used see Table 1.

Results

NF1 patient tumor lines respond to EGF and express EGF-R. Stimulation of primary Schwann cells with GGF (10 ng/mL) led to a dramatic (approximately 80-fold) activation of mitogen-activated protein kinase (MAP kinase) (Figure 1a), consistent with the role of GGF as

a major Schwann cell mitogen, whereas EGF (50 ng/mL) had no effect. Compared with primary Schwann cells, the basal level of MAP kinase in serum-starved cells was substantially elevated (5–12-fold) in NF1 patient MPNST-derived cell lines (Figure 1a). Surprisingly, treatment of these lines with GGF failed to elicit activation of MAP kinase in two of three lines tested (lines 90-8 and 88-14), whereas only the 88-3 line responded to GGF (three- to fourfold). In contrast to primary Schwann cells, treatment of all three MPNST lines with EGF led to MAP kinase activation (six- to ninefold) (Figure 1a). These results suggested that the NF1 patient lines express the EGF receptor, but only the 88-3 line expresses the GGF receptor. To analyze directly the expression of receptors for EGF and GGF in these cells, we prepared lysates from growing cells and probed them by immunoblotting with antibodies specific for EGF-R and for erbB2, -3, and –4 (Figure 1b). The 88-3, 90-8, and 88-14 lines all expressed a strong band at approximately 170 kDa corresponding to EGF-R and also expressed abundant levels of erbB2, whereas only the 88-3 line expressed

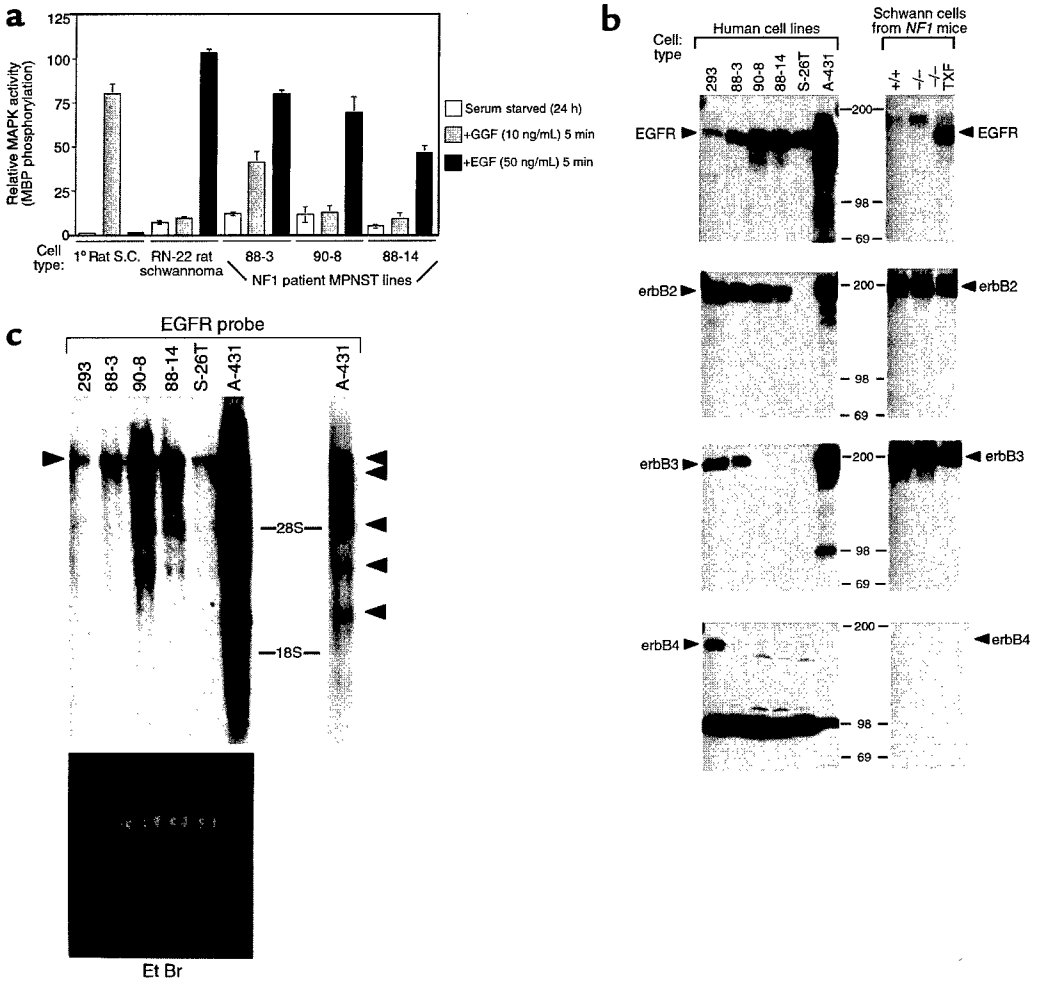

Figure 1

Response of primary rat Schwann cells, RN-22 rat schwannoma line, and human NF1 patient MPNST lines to GGF and EGF, and expression of EGF-R and erbB2, -3, and -4 proteins and *EGFR* mRNA. (**a**) The indicated cells were grown until nearly confluent, serum starved for 24 hours, then left untreated (–) or stimulated with 10 ng/mL recombinant human GGF (G) or 50 ng/mL recombinant human EGF (E) for 5 minutes at 37°C. The cells were lysed and the endogenous MAP kinase activity was assayed. Following the reaction, incorporation of $^{32}P_i$ into exogenous myelin basic protein was determined. Values were normalized to unstimulated primary rat Schwann cells (1.0) and represent the results of two experiments, carried out in duplicate, with error bars shown. (**b**) Expression of EGF-R and erbB2, -3, and -4 proteins in human and mouse cells. Cells were grown until confluent and lysed, and lysates containing 50 μg human or 100 μg mouse cell protein were subjected to analysis by SDS-PAGE and immunoblotting using antibodies specific for each protein indicated (arrows). 293, human embryonic kidney cells; 88-3, 90-8, 88-14, human NF1 MPNST lines; S-26T, human non-NF1 MPNST line; A-431, human epidermoid carcinoma line. Migration of molecular standards (kDa) is indicated at center. A strong nonspecific band of approximately 90 kDa appeared in the erbB4 blot of human but not mouse lysates. (**c**) Expression of *EGFR* mRNA in human MPNST and control cell lines. Cells were grown until confluent and lysed, and 20 μg of total RNA from each line was subjected to electrophoresis, transferred to a filter, and hybridized to a human *EGFR* probe labeled with ^{32}P. The predominant 10.5-kb mRNA is indicated with an arrow at left, as is the approximate location of the 28S and 18S RNAs (top). At right is a shorter exposure of the A-431 line, with arrows designating the different mRNAs detected. The filter was photographed under ultraviolet light before hybridization (bottom).

erbB3. None of the NF1 patient lines expressed significant levels of erbB4. The S-26T line is a S100$^+$ line from a non-NF1 patient (34) that displayed EGF-responsive MAP kinase activation, but this line failed to respond to GGF (G. Benvenuto and J.E. DeClue, unpublished data). This line expressed EGF-R but not erbB2, -3, or -4 (Figure 1b). Control lines included human embryonic kidney cells (line 293), which expressed all four proteins, and A-431 carcinoma cells, which contain amplified and rearranged copies of the *EGFR* gene (35) and expressed very high levels of EGF-R and smaller, related peptides, as well as erbB2 and -3. EGF treatment of all four MPNST lines yielded a 170-kDa tyrosine-phosphorylated band corresponding to the EGF-R, whereas GGF treatment led to the appearance of a 180–190 kDa tyrosine-phosphorylated erbB3 band in lysates from primary Schwann cells and the 88-3 cell line, but not in lysates from the 88-14, 90-8, or S26-T lines (data not shown). We conclude that human NF1 MPNST lines express EGF-R and respond to EGF, whereas only one of the lines expresses erbB3 and responds to GGF. To confirm the expression of EGF-R in these lines at the level of messenger RNA, we carried out Northern analysis using a human *EGFR*-specific probe (Figure 1c). A specific mRNA corresponding to the 10.5-kb, full-length *EGFR* mRNA (36) was detected in each of the MPNST lines (left arrow), as well as in 293, and the intensity of the band provided a striking parallel to the immunoblotting data for EGF-R in Figure 1b. A-431 cells expressed a variety of forms as described previously, including the 10.5-kb band (right panel; top arrow) and a 2.9-kb mRNA resulting from a rearranged copy of the gene (bottom arrow) (35). Based on these results, it is clear that the MPNST lines contain both EGF-R mRNA and protein and display a strong correlation between the levels of mRNA and protein expressed.

The ethylnitrosourea-induced rat schwannoma cell line RN-22, which expresses the Schwann cell marker S100 and normal levels of the neurofibromin, and likely contains a mutation in the *neu* gene encoding rat erbB2, was also analyzed in these experiments (25, 37). Similar to the human NF1 MPNST lines, the elevated basal level of MAP kinase activity in these cells was dramatically stimulated (15-fold) by EGF, whereas GGF had no effect (Figure 1a). Direct immunoblotting of RN-22 lysates with anti-phosphotyrosine antiserum revealed a 170-kDa, EGF-stimulated band, as well as a constitutive 185-kDa band (erbB2) (data not shown). Thus, an alternative route of Schwann cell tumorigenesis in a different species also led to expression of the EGF-R and loss of GGF responsiveness.

Primary benign and malignant NF1 patient tumors express EGF-R. The experiments described above suggest that one of the events leading to malignant tumorigenesis in NF1 is the acquisition of EGF-R expression. To test whether EGF receptors are expressed in primary tumors associated with NF1 disease, and not just in

Table 1
MPNST sections analyzed for EGF-R and S100 expression

Patient information	EGF-R expression	S100β expression
MPNST: 14-year-old girl; NF1 status unknown	Regions of high cellularity robustly EGF-R-positive: other areas EGF-R-negative	S100-negative
MPNST: 42-year-old woman; NF1 status unknown (Figure 2, a and b)	Uniform moderate EGF-R staining in at least 70% of tumor cells	Scattered robustly S100-postive cells (may be macrophages); other areas patch weak S100-positive; some areas S100-negative
MPNST: 31-year-old woman; NF1 status unknown	Multiple foci robustly EGF-R-positive cells	S100-negative
MPNST/Triton tumor: 13-year-old boy; NF1 dx	Robustly EGF-R-positive	S100-negative to uniform trace S100-positive in 1/3 of tumor
MPNST: adolescent Non-NF1	Weak EGF-R-positive staining in up to 10% of cells	Robust S100-positive staining most or all tumor cells
MPNST: 44-year-old man; NF1 dx	Uniform moderate EGF-R-positive staining throughout	S100-negative to uniform trace S100-positive in patches
MPNST: 30-year-old woman; NF1 dx (Figure2, c and d)	Very rare islands of weak EGF-R-positive staining: majority of tumor is negative	Strongly positive throughout

Immunohistochemistry was carried out as described in Methods. Two individuals read each slide (S. Heffelfinger and N. Ratner). In total, only one of seven tumors was almost entirely EGF-R-negative, and even that tumor may have some positive regions. For S100, three of seven are positive, two of seven are negative, and two of seven show trace or no expression. dx: NF1 diagnosis; non-NF1, failed to meet consensus criteria and no evidence of *NF1* mutation.

cultured cell lines, we immunostained sections from normal human nerves, benign neurofibromas, and MPNST with anti-EGF-R or anti-S100. Seven primary MPNST specimens were analyzed for expression of S100 and EGF-R. All seven tumors showed some EGF-R expression, but a range of expression patterns was evident (Table 1). Some tumors showed robust staining in nearly all cells, whereas others contained only rare, weakly positive cells. For example, sections from a tumor in which the majority of the cells showed strong EGF-R immunoreactivity is shown in Figure 2b. This tumor was negative for expression of S100 (Figure 2a). The other extreme example is shown in Figure 2, c and d. The majority of cells in this tumor were negative for EGF-R expression (Figure 2d), whereas many cells were positive for S100 expression (Figure 2c). In another case, focal areas within a single MPNST section had robust EGF-R immunoreactivity, whereas neighboring areas in the same section were negative (data not shown). We conclude that primary MPNST contain varying proportions of cells that express the EGF-R, with some tumors expressing high levels of EGF-R in most of their cells. These results reinforce the findings described above for the MPNST-derived cell lines.

In normal nerves, $S100^+$ cells are found only in the endoneurial compartment (Figure 2e), whereas $EGF\text{-}R^+$ cells (fibroblasts) make up the perineurium (Figure 2f). Sections from nine neurofibromas were analyzed, four from cutaneous neurofibromas, and five from the much larger plexiform neurofibromas. All showed both $S100^+$ cells (Schwann cells) and distinct $EGF\text{-}R^+$ cells (likely fibroblasts) (Figure 2g). In nine of nine neurofibroma specimens, occasional cells appeared to express both antigens. To verify this, we dissociated cells from three additional neurofibromas, isolated the cells, and embedded them in paraffin. Staining sections with anti-S100 and anti-EGF-R demonstrated a population of $S100^+/EGF\text{-}R^+$ cells (Figure 2h). We found that 1.8% of cells expressed both antigens (6/190, 1/110, and 3/216 double-labeled cells in three independent counts). In contrast, normal nerve samples completely lacked double-labeled cells and contained 99% $S100^+$ Schwann cells, and 1% $EGF\text{-}R^+$ cells (fibroblasts/perineurial cells) (Figure 2i). When sections were stained with an anti-macrophage marker (PG-M1) and anti-S100, no double-labeled cells were observed (not shown). We conclude that certain cells in neurofibromas, most likely Schwann cells, express both S100 and EGF-R, whereas such cells are absent in normal nerves.

In vitro transformation of mouse NF1-deficient Schwann cells leads to EGF-R expression. Mice with targeted mutations in the *NF1* gene represent a model system for investigating NF1 tumorigenesis (20, 21). Although homozygous mutant (-/-) embryos die by day 14.5, we have developed techniques to purify Schwann cells from day-12.5 embryos (22, 23). To investigate MAP kinase signaling, these Schwann cells were serum starved, stimulated with GGF, and lysed (Figure 3a). Although Schwann cells lacking one (+/-) or both (-/-) copies of *NF1* have elevated Ras-GTP, there was little or no enhancement of basal MAP kinase activity compared with wild-type cells (Figure 3a). Cells of all genotypes responded to GGF stimulation with large increases in MAP kinase activity. The TXF Schwann cells isolated from (-/-) embryos displayed an increased basal level of MAP kinase activity and responded to GGF.

We hypothesized that the in vitro transformation of *NF1*-deficient mouse Schwann cells might be associated with EGF-R expression. To test this, we examined MAP kinase activity following EGF stimulation of serum-starved (-/-) or TXF cells (Figure 3b). Whereas EGF elicit-

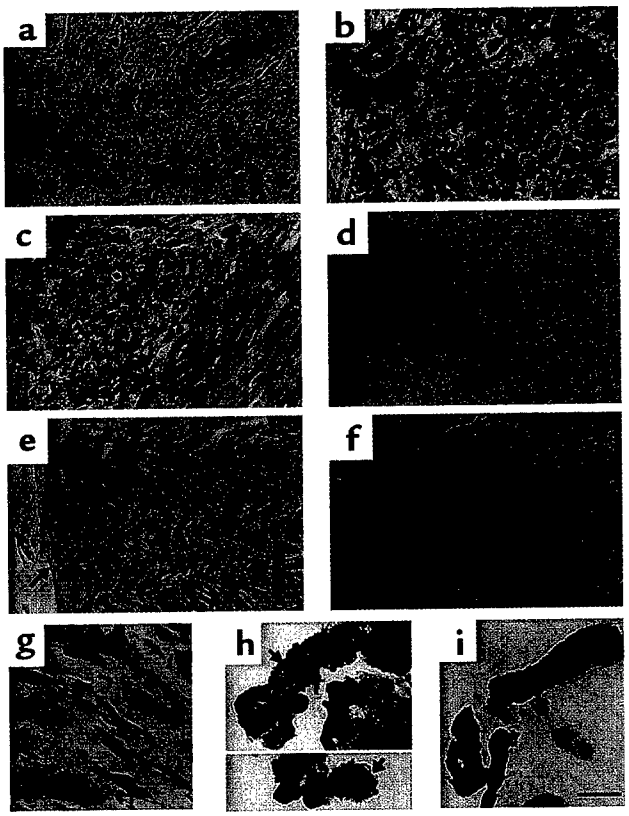

Figure 2
EGF-R expression in NF1 tumor sections. Paraffin sections were stained with anti-EGF-R (**b**, **d**, and **f**) or anti-S100 (**a**, **c**, and **e**) or with both antibodies (**g**, **h**, and **i**). Visualization of single antibodies was with 3'3-diaminobenzidine HCl (DAB; brown) (**a–f**). Double labeling used nitroblue tetrazolium (NBT/BCIP; blue) for anti-S100, and DAB (brown) for anti-EGF-R (**g–i**). In **a**, **b**, and **d–f**, the counterstain is hematoxylin (blue); in **c** and **g–i**, the counterstain is nuclear fast red (pink). (**a–d**) Sections from MPNST. In **a**, the arrow points to a normal nerve within the tumor, containing $S100^+$ cells, whereas the tumor matrix is $S100^-$. An adjacent section from the same tumor in **b** shows that most cells are $EGF\text{-}R^+$. Another MPNST contains $S100^+$ cells (**c**) and is mostly negative for EGF-R (**d**). (**e** and **f**) Sections of normal human nerve (arrow points to perineurium). (**g**) A section of a cutaneous neurofibroma with $EGF\text{-}R^+/S100^+$ cells. (**h**) A section from a dissociated neurofibroma cell preparation. The arrow designates a group of cells double stained by anti-S100 and anti-EGF-R. (**i**) A section from a dissociated normal nerve preparation. No double-labeled cells are detected. **a–g**, bar: 34.2 μm; **h** and **i**, bar: 16.3 μm.

ed no increase in MAP kinase activity in the (-/-) cells, TXF derivatives displayed a dramatic increase, even greater than the response to GGF. Schwann cells from wild-type (+/+) or heterozygous (+/-) embryos failed to respond to EGF (data not shown). To examine the expression of EGF-R and erbB2, -3, and -4, we carried out immunoblotting with antibodies against these proteins (Figure 1b). Lysates of (+/+) and (-/-) cells expressed erbB2 and -3, but not EGF-R. In contrast, the (-/-) TXF cells expressed abundant levels of EGF-R, as well as erbB2 and -3. None of the cells expressed erbB4, consistent with studies published previously (26). Immunoblotting of the lysates from Figure 3b confirmed the activation of EGF-R in the (-/-) TXF cells following EGF treatment, as well as tyrosine phosphorylation of erbB3 in GGF-stimulated lysates from TXF and (-/-) cells (data not shown). We conclude that acquisition of EGF-R expression is associated with in vitro transformation of *NF1*-deficient Schwann cells. These results represent a striking parallel to the results obtained from our analysis of human NF1-related tumors.

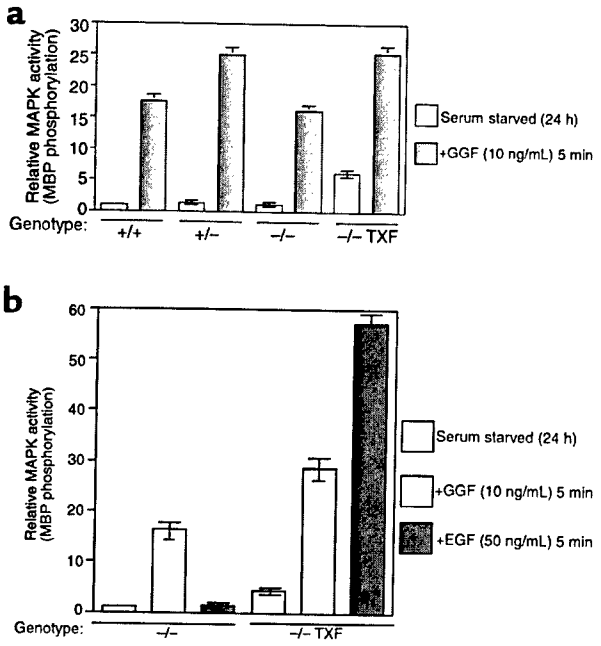

Figure 3

Transformed derivatives of *NF1* (-/-) mouse embryo-derived Schwann cells have elevated basal MAP kinase activity and respond to EGF. (**a**) Mouse Schwann cells were isolated from day 12.5 embryos with wild-type *NF1* (+/+) or targeted disruption of one *NF1* allele (+/-), or both alleles (-/-), and compared with transformed derivatives of (-/-) (TXF). The cells were serum starved for 24 hours, then left untreated or stimulated with GGF, as indicated. Cells were lysed and MAP kinase activity was determined as for Figure 1. Results are the mean of two experiments carried out in duplicate, with error bars shown. Results were normalized to the level of activity present in serum-starved wild-type (+/+) cells (1.0). (**b**) Schwann cells from (-/-) embryos and TXF were treated and assayed as above, except additional samples were prepared after stimulation with 50 ng/mL EGF for 5 minutes. Results are the mean of two experiments carried out in duplicate, with error bars shown. Results were normalized to the level of activity present in serum-starved homozygous null (-/-) cells (1.0).

Growth of NF1 patient tumor lines is EGF dependent and can be blocked by EGF-R antagonists. We wished to determine whether expression of the EGF-R in NF1 tumors and cell lines affected the growth of these cells. When the 88-14 cell line was grown in limiting amounts of FBS (0.1%), cells lacking EGF remained viable (as judged by trypan blue exclusion and replating under growth conditions) but did not grow, whereas cells treated with 10 ng/mL EGF grew at a rapid rate (Figure 4a). The EGF-dependent growth of the 88-14 line suggested that blocking the EGF-R might inhibit the growth of the cells. Therefore, we tested EGF-R antagonists for their ability to suppress growth of 88-14 cells under the same conditions (Figure 4a). Treatment with mAb 225, an antibody that blocks EGF-R activation (38), significantly inhibited cell growth, whereas even more dramatic inhibition was achieved with chemical inhibitors of EGF-R tyrosine kinase activity, the tyrphostins A-25 and AG-1478 (39). All of the EGF-R antagonists displayed significantly greater inhibition than that observed for the potent farnesyltransferase inhibitor B581 (40). Whereas previous studies demonstrated that farnesyltransferase inhibitors slow the growth of the 88-14 line in vitro, most likely by blocking Ras or RhoB activity (41), these results demonstrate that antagonizing the EGF-R also can block their growth.

As an additional test for these agents to antagonize EGF-dependent growth of the 88-14 tumor line, we carried out assays of anchorage-independent growth in soft agar (Figure 4b). When plated in moderate levels (7%) of serum, no significant growth was observed after 4 weeks. However, the presence of 100 ng/mL EGF supported the formation of small- to medium-sized colonies under these conditions (Figure 4b). Furthermore, the presence of mAb 225 or tyrphostin AG-1478 strongly inhibited the formation of such colonies (Figure 4b), whereas B581 had no significant effect (data not shown). We conclude that under limiting conditions, the growth of 88-14 is dependent on EGF and can be blocked by EGF-R antagonists. In other experiments, we found that the addition of EGF dramatically stimulated the growth of (-/-) TXF cells in vitro, and that tyrphostin A-25 could block this effect (data not shown). In contrast, EGF had no effect on nontransformed (-/-) Schwann cells or on Schwann cells from (+/-) or (+/+) embryos (data not shown). We conclude that EGF-R expression has a significant biological effect on the growth of both NF1 patient tumor-derived cells and TXF cells from *NF1*-deficient mice.

The experiments just described were carried out in conditions where exogenous EGF was essential for the growth of the cells. Whereas the availability of EGF-related peptides and other growth factors in the tumor environment is unknown, we nevertheless wished to determine the effect of EGF-R antagonists on the growth of NF1 patient lines under other growth conditions. Therefore, we examined the growth of the 88-14 and the 90-8 MPNST lines in the presence of 2% FBS with no EGF added (Figure 4, c and d). Whereas

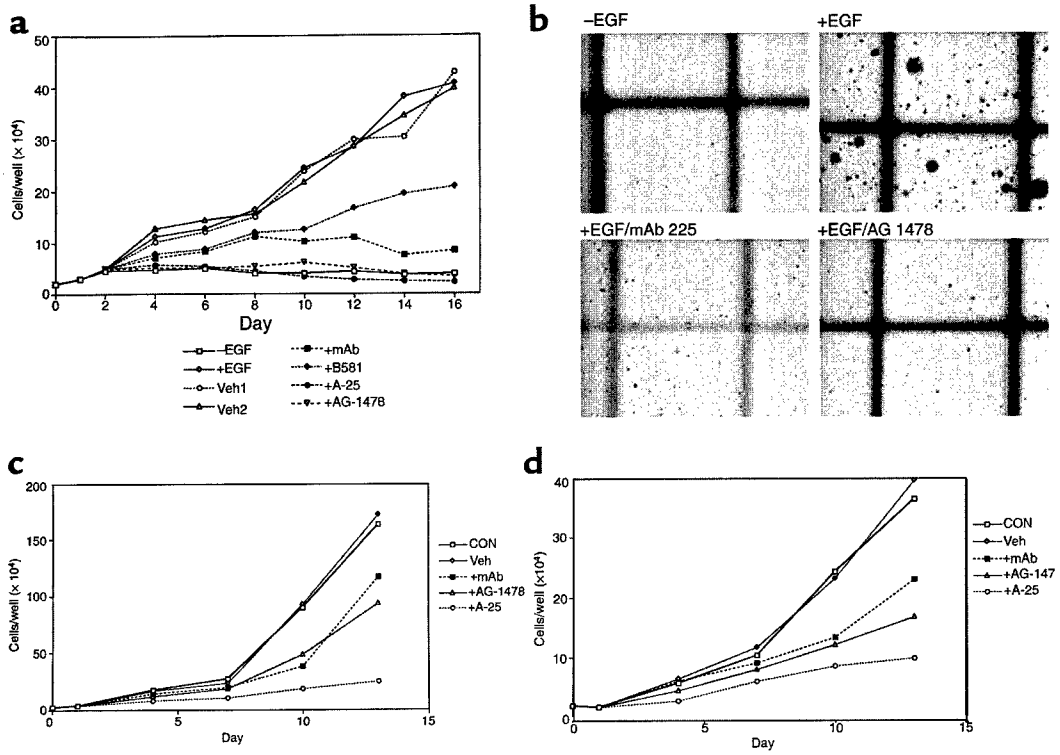

Figure 4

Growth of NF1 patient MPNST lines is EGF dependent and is inhibited by EGF-R antagonists. (**a**) MPNST line 88-14 was plated at 2×10^4 per 35-mm well. The next day (day 1) cells were switched to medium without (–EGF) or with 10 ng/mL EGF (+EGF), and on day 2 cells were switched to medium containing 10 ng/mL EGF and 3% PBS (Veh1); 0.1% DMSO (Veh2); 3 μg/mL mAb 225 in PBS (3% vol/vol; mAb); 40 μM farnesyltransferase inhibitor B581 in water; 10 μM tyrphostin A-25 in DMSO; or 400 nM tyrphostin AG-1478, also in DMSO. Cells were re-fed with medium containing fresh inhibitor and counted in duplicate every 2 days, beginning at day 2. (**b**) Growth of MPNST 88-14 line in soft agar. Cells were plated at 10^5/mL in a 0.4% (wt/vol) agar suspension with 7% FBS with or without 100 ng/mL EGF, as indicated; mAb 225 was included at 5 μg/mL and AG-1478 at 400 nM. Cells were photographed after 4 weeks. × 25. (**c** and **d**) Growth of 88-14 (**c**) and 90-8 (**d**) in 2% serum is inhibited by EGF-R antagonists. Cells were plated as in **a**, and switched on day 1 to medium containing 2% FBS (CON) or 2% serum plus 0.1% DMSO (Veh); 3 μg/mL mAb 225 (mAb); 10 μM tyrphostin A-25; or 400 nM tyrphostin AG-1478. Thereafter, cells were re-fed with medium containing fresh inhibitor every 2 days, and duplicate wells of cells were counted every three days.

the 88-14 line grew much more robustly than 90-8 under these conditions (Figure 4, c and d), the growth of both lines was significantly inhibited by the addition of tyrphostin A-25 and to a lesser extent by tyrphostin AG-1478. The anti–EGF-R mAb also inhibited the growth of these lines in serum, although the effect was somewhat less pronounced (Figure 4, c and d). These results demonstrate that EGF-R expression affects the growth of tumor cell lines derived from NF1 patients under conditions where EGF is not the primary factor driving growth of the cells.

Discussion

Here we have described aberrant expression of the EGF-R in primary tumors from patients with NF1, in cell lines derived from those tumors, in a cell line from a non-NF1 patient with MPNST, in a chemically induced rat schwannoma line, and in in vitro–transformed Schwann cells from mouse embryos lacking an intact *NF1* gene. The congruence of the animal model systems with the results from NF1 patient materials suggests that aberrant expression of the EGF-R might play an important role in the development of peripheral nerve tumors in NF1 patients and that mutation of *NF1* may predispose the tumor progenitor cells to express EGF-R. In the cells tested, we found a perfect correlation between expression of EGF-R and EGF responsiveness and also between expression of erbB2/erbB3 and GGF responsiveness. Additionally, the level of *EGF-R* mRNA in the human MPNST lines correlated well with the level of protein expression. There is a strong precedent for involvement by the EGF-R and other members of the erbB family in human cancer, because over 60% of all solid tumors overexpress at least one of these proteins or their ligands (reviewed in refs. 42 and 43). Furthermore, a negative correlation has been demonstrated between EGF-R expression and survival in certain cancers and with progression to malignancy in others (43). We have found that the growth of cell lines derived from MPNSTs and transformed mouse Schwann cells in vitro was highly EGF dependent and could be blocked by EGF-R antagonists under conditions where EGF was the primary growth factor. This demonstrates that the expressed EGF-R is capable of transmitting

mitogenic signals in these cells. We also found that EGF-R antagonists could block the growth of MPNST lines growing in serum without added EGF. This inhibition may be due to the blocking of potential autocrine growth stimulation pathways in the cells; alternatively, it may indicate that the EGF-R is involved (directly or indirectly) in mitogenic signaling by serum factors that induce growth of the cells.

Other than mutation or loss of the second (normal) *NF1* allele (10), little is known of the specific genetic and epigenetic events involved in the development of NF1-related neurofibromas and MPNSTs. Earlier work suggested a possible involvement of *p53* in NF1-related MPNST formation (31), and it was recently shown that *p53* and *NF1* cooperate in tumor formation in mice (44, 45). Furthermore, the hypothesis of a Schwann cell origin for both benign neurofibromas and MPNSTs remains to be proven. However, our data support other studies suggesting that deregulation of Schwann cell growth is a primary defect driving the development of both benign neurofibromas and MPNST in NF1 patients (4). The immunohistochemical analyses revealed that at some point during or after the formation of neurofibromas, a subset of the ($S100^+$) Schwann cells acquire EGF-R expression. Such cells were not observed in normal control nerves, although a previous analysis of tissue sections of benign schwannomas from non-NF1 patients revealed some EGF-R expression (46). Our analysis of Schwann cells isolated from *NF1*-mutant mouse embryos demonstrated that one of the events occurring concomitant with transformation of (-/-) cells is expression of the EGF-R. The TXF cells, which do not arise from wild-type (+/+) embryos, remained $S100^+$, GGF responsive and expressed other Schwann cell markers (23). Thus both the human and mouse systems indicate that mutational loss of *NF1* may lead to the development of altered Schwann cells with EGF-R expression. It is difficult at present to assess the role of the $EGF\text{-}R^+/S100^+$ cells in the development and progression of benign neurofibromas. Although these cells make up only a small portion of the total population, they may be altered in their interactions with other cells in the tumor environment or may release factors that help drive the growth of benign tumors, which typically undergo periodic bursts of growth. Alternatively, the $EGF\text{-}R^+$ cells may only arise after the benign tumor is formed. Similarly, it is unknown what potential ligands for the EGF-R may be present in benign neurofibromas, although they do contain a rich diversity of cell types, one or more of which may produce an EGF-R ligand. Whereas the vast majority of neurofibromas do not progress to malignancy, they represent the primary burden for many patients, and the role of the $EGF\text{-}R^+/S100^+$ cells in these tumors demands further investigation.

These studies also raise questions about the role of EGF-R in tumor progression, specifically whether EGF-R expression is a necessary step in MPNST formation. All three NF1 patient's MPNST lines expressed EGF-R, and seven of seven primary NF1 MPNST analyzed by immunohistochemistry contained $EGF\text{-}R^+$ cells. However, the relative levels of EGF-R expression in individual cells varied, as did the proportion of cells expressing EGF-R in each tumor. The existence of microdomains defined by EGF-R expression suggests heterogeneity within individual MPNSTs. It is possible that EGF-R expression is transient and occurs at particular stages in tumorigenesis or that expression of the EGF-R represents only one of several routes to formation of MPNST. The significance of EGF-R expression in Schwann cell tumorigenesis is strengthened by our finding that both the $S100^+$, Schwann cell-derived rat RN-22 line and the $S100^+$, non-NF1 human MPNST line S-26T express EGF-R. The finding of EGF-R expression in such a diversity of settings strongly implicates a role for it in the pathogenesis of malignant nerve sheath tumors.

One important distinction between the mouse and human systems was that the three NF1 MPNST lines were $S100^-$, and two of three lacked erbB3 expression and GGF-responsiveness. If these results are interpreted in terms of the Schwann cell origin model, they suggest that subsequent to acquisition of EGF-R expression, the cells begin to dedifferentiate and lose markers such as erbB3 and S100. Such a model may also help explain the general (though not complete) discordance between S100 and EGF-R expression among cells in primary MPNST samples and the fact that 5 of the 7 samples lacked S100 expression. Interestingly, both RN-22 and S-26T were unresponsive to GGF, suggesting that loss of erbB3 may contribute to the dedifferentiation of cells during tumorigenesis even without loss of S100. Our finding that *NF1*-deficient mouse Schwann cells, human $S100^+$ Schwann cells from neurofibromas, and RN-22 cells all express EGF-R leads us to favor the hypothesis that loss of Schwann cell markers is a feature of MPNST formation that can occur subsequent to expression of EGF-R. An alternative model would suggest that the cells giving rise to the $S100^+/EGF\text{-}R^+$ cells in benign neurofibromas and/or to the cells in MPNST, represent a different lineage arising from the neural crest. Such an argument could also be applied to the mouse TXF (-/-) cells. In each case, the loss of *NF1* would lead to a sub-population of cells that acquire EGF-R and various combinations of Schwann cell markers that might change during the evolution of the tumor. This alternative model is being evaluated in our current studies employing microchip gene arrays to compare and contrast the overall pattern of genes expressed in (+/+), (-/-), and TXF (-/-) cells. Another area of future investigation will be to determine the degree to which the EGF-R exerts its mitogenic effects through the Ras pathway. It is interesting that the expression of EGF-R occurs in the context of cells that already have high levels of Ras-GTP because of loss of *NF1*, and this may suggest that the signaling from the EGF-R also involves non-Ras pathways, thereby augmenting the high Ras activity present in the cells.

Acknowledgments

We thank Doug Lowy, Isabel Martinez-Lacaci, and David Salomon for comments and suggestions; Ricardo Dreyfuss for excellent assistance with photography; and Mary Ann Miller for expert assistance with immunohistochemistry. We are grateful to Bruce Korf and Gretchen M. Schneider (Boston Children's Hospital, Boston, Massachusetts, USA) and the University of Miami Human Tissue Bank (Miami, Florida, USA) for providing neurofibromas. We thank Patrick Wood (The Miami Project, Miami, Florida, USA) for normal human nerves, and Diya Mutasim (University of Cincinnati, Department of Dermatology, Cincinnati, Ohio, USA) and Kevin Bove (Cincinnati Children's Hospital, Department of Pathology, Cincinnati, Ohio, USA) for neurofibroma sections. The University of Alabama (Birmingham, Alabama, USA) and the Childhood Cancer Tissue Network (Columbus, Ohio, USA) provided MPNST. N. Ratner is supported by National Institutes of Health grant NS-28840.

1. Huson, S.M., Harper, P.S., and Compston, D. 1988. Von Recklinghausen neurofibromatosis: a clinical and population study in south-east Wales. *Brain.* **111**:1355–1381.
2. Upadhyaya, M., and Cooper, D.N. 1998. *Neurofibromatosis type 1: from genotype to phenotype.* BIOS Scientific Publishers Ltd. Oxford, United Kingdom. pp. 230.
3. Ferner, R.E. 1998. Clinical aspects of neurofibromatosis 1. In *Neurofibromatosis type 1: from genotype to phenotype.* M. Upadhyaya and D.N. Cooper, editors. BIOS Scientific Publishers Ltd., Oxford, United Kingdom. 21–38.
4. Rosenbaum, T., Petrie, K.M., and Ratner, N. 1997. Neurofibromatosis type 1: genetic and cellular mechanisms of peripheral nerve tumor formation. *The Neuroscientist.* **3**:412–420.
5. Stefansson, K., Wollmann, R., and Jerkovic, M. 1982. S-100 protein in soft tissue tumours derived from Schwann cells and melanocytes. *Am. J. Pathol.* **106**:261–268.
6. Peltonen, J., et al. 1988. Cellular differentiation and expression of matrix genes in type 1 neurofibromatosis. *Lab. Invest.* **59**:760–761.
7. Sheela, S., Riccardi, V.M., and Ratner, N. 1990. Angiogenic and invasive properties of neurofibroma Schwann cells. *J. Cell Biol.* **111**:645–653.
8. Ducatman, B.S., Scheithauer, B.W., Piepgras, D.G., and Reiman, H.M. 1984. Malignant peripheral nerve sheath tumors in childhood. *J. Neurooncol.* **2**:241–248.
9. Zoller, M.E., Rembeck, B., Oden, A., Samuelsson, M., and Angervall, L. 1997. Malignant and benign tumors in patients with neurofibromatosis type 1 in a defined Swedish population. *Cancer.* **79**:2125–2131.
10. Side, L.E., and Shannon, K.M. 1998. The *NF1* gene as a tumor suppressor. In *Neurofibromatosis type 1: from genotype to phenotype.* M. Upadhyaya and D.N. Cooper, editors. BIOS Scientific Publishers Ltd. Oxford, United Kingdom. 133–152.
11. Morioka, N., Tsuchida, T., Etoh, T., Ishibashi, Y., and Otsuka, F. 1990. A case of neurofibrosarcoma associated with neurofibromatosis: light microscopic, ultrastructural, immunohistochemical and biochemical investigations. *J. Dermatol.* **17**:312–316.
12. Wallace, M.R., et al. 1990. Type 1 neurofibromatosis gene: identification of a large transcript disrupted in three NF1 patients. *Science.* **249**:181–186.
13. Cawthon, R., et al. 1990. A major segment of the neurofibromatosis type 1 gene; cDNA sequence, genomic structure, and point mutations. *Cell.* **62**:193–201.
14. Viskochil, D., et al. 1990. Deletions and a translocation interrupt a cloned gene at the neurofibromatosis type 1 locus. *Cell.* **62**:187–192.
15. Upadhyaya, M., and Cooper, D.N. 1998. The mutational spectrum in neurofibromatosis 1 and its underlying mechanisms. In *Neurofibromatosis type 1: from genotype to phenotype.* M. Upadhyaya and D.N. Cooper, editors. BIOS Scientific Publishers Ltd. Oxford, United Kingdom. 65–88.
16. Boguski, M.S., and McCormick, F. 1993. Proteins regulating Ras and its relatives. *Nature.* **366**:643–654.
17. DeClue, J.E., et al. 1992. Abnormal regulation of mammalian $p21^{ras}$ contributes to malignant tumor growth in von Recklinghausen (type-1) neurofibromatosis. *Cell.* **69**:265–273.
18. Basu, T.N., et al. 1992. Aberrant regulation of ras proteins in malignant tumour cells from type-1 neurofibromatosis patients. *Nature.* **356**:713–715.
19. Guha, A., et al. 1996. Ras-GTP levels are elevated in human NF1 peripheral nerve tumors. *Oncogene.* **12**:507–513.
20. Jacks, T., et al. 1994. Tumor predisposition in mice heterozygous for a targeted mutation in *NF1*. *Nat. Genet.* **7**:353–361.
21. Brannan, C.I., et al. 1994. Targeted disruption of the neurofibromatosis type-1 gene leads to developmental abnormalities in heart and various neural crest-derived tissues. *Genes Dev.* **8**:1019–1029.
22. Kim, H., et al. 1995. Schwann cells from neurofibromin deficient mice exhibit activation of $p21^{ras}$, inhibition of cell proliferation and morphological changes. *Oncogene.* **11**:325–335.
23. Kim, H.A., Ling, B., and Ratner, N. 1997. *NF1*-deficient mouse Schwann cells are angiogenic and invasive and can be induced to hyperproliferate: reversion of some phenotypes by an inhibitor of farnesyl transferase. *Mol. Cell. Biol.* **177**:862–872.
24. Levi, A.D., et al. 1995. The influence of heregulins on human Schwann cell proliferation. *J. Neurosci.* **15**:1329–1340.
25. Pinkas-Kramarski, R., Alroy, I., and Yarden, Y. 1997. ErbB receptors and EGF-like ligands: cell lineage determination and oncogenesis through combinatorial signaling. *J. Mammary Gland Biol. Neoplasia.* **2**:97–107.
26. Burden, S., and Yarden, Y. 1997. Neuregulins and their receptors: a versatile signaling molecule in organogenesis and oncogenesis. *Neuron.* **18**:847–855.
27. Kim, H., DeClue, J.E., and Ratner, N. 1997. cAMP-dependent protein kinase A is required for Schwann cell growth: interaction between cAMP and neuregulin/tyrosine kinase pathways. *J. Neurosci. Res.* **49**:236–247.
28. Colman, S.D., Williams, C.A., and Wallace, M.R. 1995. Benign neurofibromas in type 1 neurofibromatosis (NF1) show somatic deletions of the *NF1* gene. *Nat. Genet.* **11**:90–92.
29. Sawada, S., et al. 1996. Identification of *NF1* mutations in both alleles of a dermal neurofibroma. *Nat. Genet.* **14**:110–112.
30. Serra, P., et al. 1997. Confirmation of a double-hit model for the *NF1* gene in benign neurofibromas. *Am. J. Hum. Genet.* **61**:512–519.
31. Menon, A.G., et al. 1990. Chromosome 17p deletions and *p53* gene mutations associated with the formation of malignant neurofibrosarcomas in von Recklinghausen neurofibromatosis. *Proc. Natl. Acad. Sci. USA.* **87**:5435–5439.
32. Velu, T.J., et al. 1989. Retroviruses expressing different levels of the normal epidermal growth factor receptor: biological properties and new bioassay. J. Cell. Biochem. 39:153–166.
33. Gutmann, D.H., et al. 1997. The diagnostic evaluation and multidisciplinary management of neurofibromatosis 1 and neurofibromatosis 2. *JAMA.* **278**:51–57.
34. Dahlberg, W.K., Little, J.B., Fletcher, J.A., Suit, H.D., and Okunieff, P. 1993. Radiosensitivity *in vitro* of human soft tissue sarcoma cell lines and skin fibroblasts derived from the same patients. *Int. J. Radiat. Biol.* **63**:191–198.
35. Merlino, G.T., et al. 1985. Structure and localization of genes encoding aberrant and normal epidermal growth factor receptor RNAs from A431 human carcinoma cells. *Mol. Cell. Biol.* **5**:1722–1734.
36. Merlino, G.T., et al. 1984. Amplification and enhanced expression of the epidermal growth factor receptor gene in A431 human carcinoma cells. *Science.* **224**:417–419.
37. Pfeiffer, S.E., and Wechsler, W. 1972. Biochemically differentiated neoplastic clone of Schwann cells. *Proc. Natl. Acad. Sci. USA.* **69**:2885–2889.
38. Peng, D., et al. 1996. Anti-epidermal growth factor receptor monoclonal antibody 225 up-regulates $p27^{KIP1}$ and induces G_1 arrest in prostatic cancer cell line DU145[1]. *Cancer Res.* **56**:3666–3669.
39. Levitzki, A., and Gazit, A. 1995. Tyrosine kinase inhibition: an approach to drug development. *Science.* **267**:1782–1788.
40. Garcia, A.M., Rowell, C., Ackermann, K., Kowalczyk, J.J., and Lewis, M.D. 1993. Peptidomimetic inhibitors of Ras farnesylation and function in whole cells. *J. Biol. Chem.* **268**:18415–18418.
41. Yan, N., et al. 1995. Farnesyltransferase inhibitors block the neurofibromatosis type I (NF1) malignant phenotype. *Cancer Res.* **55**:3569–3575.
42. Salomon, D.S., Brandt, R., Ciardiello, F., and Normanno, N. 1995. Epidermal growth factor-related peptides and their receptors in human malignancies. *Crit. Rev. Oncol. Hematol.* **19**:183–232.
43. Bridges, A.J. 1996. The epidermal growth factor receptor family of tyrosine kinases and cancer: can an atypical exemplar be a sound therapeutic target? *Curr. Med. Chem.* **3**:167–194.
44. Cichowski, K., et al. 1999. Mouse models of tumor development in neurofibromatosis type 1. *Science.* **286**:2172–2176.
45. Vogel, K.S., et al. 1999. Mouse model for neurofibromatosis type 1. *Science.* **286**:2176–2179.
46. Sturgis, E.M., Woll, S.S., Aydin, F., Marroji, A.J., and Amedee, R.G. 1996. Epidermal growth factor receptor expression by acoustic neuromas. *Laryngoscope.* **106**:457–462.

Poster abstract: Zhou H, **Viskochil D**, Perkins S, Tripp S, Coffin C. Expression of epidermal growth factor receptor and vascular endothelial growth factor receptor in plexiform neurofibroma, and malignant peripheral nerve sheath tumors. United States and Canadian Academy of Pathology Meeting 2003.

Title: EXPRESSION OF EPIDERMAL GROWTH FACTOR RECEPTOR AND VASCULAR ENDOTHELIAL GROWTH FACTOR RECEPTOR IN PLEXIFORM NEUROFIBROMA AND MALIGNANT PERIPHERAL NERVE SHEATH TUMORS

H Zhou [1], D H Viskochil [2], S L Perkins [1], S R Tripp [1] and C M Coffin [1]. [1]Pathology, and [2]Pediatrics, University of Utah, Salt Lake City, UT, .

Background: Malignant peripheral nerve sheath tumor (MPNST) may arise in association with neurofibromatosis type I (NF1) or sporadically, and some evidence suggests a role for epidermal growth factor receptor (EGFR) in pathogenesis. EGFR is a transmembrane glycoprotein with intrinsic tyrosine kinase activity. In cancer cells, activation of the EGFR signaling pathway has been linked with increased cell proliferation, aberrant cell differeniation, and angiogenesis through modulation of vascular endothelial growth factor (VEGF) expression. VEGF and its receptor (VEGFR) are implicated in tumor neovascularization, growth and metastasis. This study investigates immunohistochemical expression of EGFR and VEGFR among plexiform neurofibroma (PNF), and NF1-related and non-NF1 malignant peripheral nerve sheath tumor (MPNST).

Design: Formalin-fixed, paraffin-embedded archival tissue from 4 PNFs, and 13 MPNSTs (7 with NF1) were immunostained with monoclonal antibodies to EGFR (Zymed), and VEGFR (Dako) using an automated staining system (Ventana). Positivity was scored semi-quantitatively as 0 to 3. (0=<5%, 1+ =5-25%, 2 + =25-50%, 3 + = >50% positive cells).

Results: All MPNSTs had intense cytoplasmic EGFR staining ranging from 2-3+. Cytoplasmic VEGFR staining ranging from 1-2+ was also observed in both vascular endothelial and tumor cells in these MPNSTs. In PNFs, a subset of S100-positive tumor cells also demonstrated distinct membranous/cytoplasmic EGFR staining. Compared to EGFR-negative tumor cells in the same lesion, the EGFR-positive cells were typically dissociated Schwann cells with vacuolated cytoplasm. In PNF, occasional cytoplasmic VEGFR expression was present in the vascular endothelial cells but absent in the tumor cells.

Conclusion: EGFR is expressed in a high percentage of neoplastic cells in NF1-related and non-NF1 MPNST and in a subset of Schwann cells within PNF. These data indicate that EGFR may play a role in tumor progression of Schwann cell-derived tumors and may be associated with VEGF/VEGFR expression in MPNST. Further studies are needed to determine whether the EGFR-positive Schwann cells in the PNF represent an aggressive cell phenotype that may undergo malignant transformation to MPNST.

Poster: Zhou H, Minh-Thu H, Coffin C, Tripp S, **Viskochil D**. EGFR expression and genetic analysis in plexiform neurofibromas (PNF) and malignant peripheral nerve sheath tumors (MPNSTs). Connective Tissue Ocology Meeting, November 2003.

EGFR EXPRESSION AND GENETIC ANALYSIS IN PLEXIFORM NEUROFIBROMAS (PNF) AND MALIGNANT PERIPHERAL NERVE SHEATH TUMORS (MPNSTS)

Holly Zhou[1], Minh-Thu N. Hang[1], Cheryl Coffin[1], Sheryl Tripp[1], David H. Viskochil[1]

[1]University of Utah, Utah, United States

Introduction

Epidermal growth factor receptor (EGFR) is a transmembrane glycoprotein with intrinsic tyrosine kinase activity and oncogenic properties (1). Aberrant signaling through EGFR is associated with neoplastic cell proliferation, migration, stromal invasion, resistance to apoptosis, and angiogenesis (2). Recent studies suggested that EGFR protein expression was commonly present in NF1 related tumors and activation of the EGFR signaling pathway may be associated with tumorigenesis of plexiform neurofibroma (PNF) and malignant peripheral nerve sheath tumor (MPNST) in patients with neurofibromatosis type I (NF1) (3, 4). However, by FISH analysis, EGFR gene amplification was found in 0% -26% of MPNSTs (5, 6). The molecular mechanisms for EGFR over expression in NF1 related tumors are unknown. This study is designed to investigate whether EGFR protein expression assessed by immunohistochemistry (IHC) is associated with genomic imbalance involving EGFR gene.

Figure 1. Schematic representation of the interaction between EGFR and Ras in the process of oncogenesis.

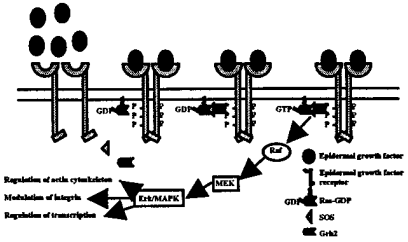

Methods

•Formalin-fixed, paraffin-embedded archival tissue were retrieved from the surgical pathology files at the Primary Children's Hospital, Salt Lake City and University of Utah Health Science Center, Salt Lake City.

•**Immunohistochemistry:** Immunoreactivity of EGFR from 16 PNFs, and 16 MPNSTs was evaluated with monoclonal antibodies to EGFR (Zymed) using an automated staining system (Ventana). Immunoreactivity of the tumors was scored subjectively from 0-3+: 0 = <10% cells with focal, faint staining; 1+ = >10% cells with cytoplasmic and membrane staining; 2+ = > 10% cells with moderate cytoplasmic and membrane staining; 3+ = majority of cells with strong cytoplasmic and membrane staining.

•**DNA extraction from paraffin embedded tissue:** Paraffin blocks from 7 MPNSTs and 5 PNFs with the matched non-tumor tissue controls were further selected for EGFR genomic analysis. The areas of tumor and non-tumor were identified on the H&E stained slides and corresponding areas in unstained slides were microdissected. DNA was extracted from tissue sections and subjected to PCR-based fluorescent genotyping of size polymorphisms at 5 genetic markers spanning the EGFR gene.

Table I. Primers used for PCR-based genotyping spanning the EGFR gene.

EGFR marker	Forward primer	Reverse primer
D7S2422	GCTCCACATTCCTTGGGTA	AAGTGAGGGCCTTTCAAAC
D7S506	CCCTTCAAATGCACAGATA	GCGTCAGTTACTGGAACTT
D7S2550	AAGTTCCATTTGTCTCGGTT	AGTCTCCTCGTCTCACACCT
D7S494	CCTGGGTGACAGAGATTCTT	AATCCTGTTGTTATTAACTTGGTTT
D7S502	GGAAGGTATGTTGCGG	TAAGCCACCAAGAACACC

Results

Table II. Clinicopathologic data of 16 MPNST and 16 PNF.

	Age/Sex	Site	Grade	NF1	S100	EGFR
MPNST	2/F	Un	H	No	D	0
	13/F	Arm	H	Yes	F	3+
	13/F	Arm	H	Yes	F	3+
	15/M	Thigh	H	Yes	F	2+
	16/M	Shoulder	L	Yes	F	2+
	18/F	Neck	L	Yes	D	3+
	16/M	Lung	H	Yes	F	3+
	13/F	Neck	L	Yes	D	1+
	15/M	Chest	H	Un	F	0
	21/M	Tibia	H	Yes	F	1+
	35/F	Knee	H	No	F	3+
	25/M	Neck	H	No	F	3+
	44/M	Back	H	No	N	3+
	44/M	Back	H	No	N	3+
	20/M	Knee	H	Yes	F	2+
	Un	Un	H	Un	D	2+
PNF	12/M	Chest		Yes	D	0
	14/M	C-4		Yes	F	1+
	12/F	Thigh		Yes	D	2+
	14/M	Nose		Yes	D	0
	11/F	Neck			D	2+
	21/M	Neck		Yes	D	0
	13/M	Supraclavicular		Yes	D	0
	17/F	Arm		Yes	F	0
	19/F	Cheek		Yes	D	2+
	11/F	Arm		Yes	D	0
	17/F	Foot		Yes	D	0
	9/F	Abdominal wall		Un	D	2+
	15/F	Back		Un	D	1+
	11/M	Hip		Un	D	0
	14/M	Hand		Un	D	1+
	11/F	Neck		Yes	D	0

Un- unknown; D-diffuse; F-focal; P-positive; N-negative; Bold- cases submitted or genomic analysis

Results

Figure 2. General histology and immunohistochemistry of sections from a plexiform nerve sheath tumor. A) A photograph of a plexiform nerve sheath tumor. B) H & E staining showing the general morphology of a plexiform nerve sheath tumor with spindle cells interspersed between extracellular matrix. C) S100 staining in a plexiform nerve sheath tumor. D) EGFR staining in a plexiform nerve sheath tumor.

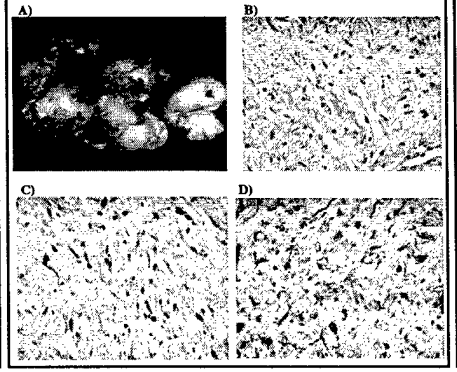

Results

Figure 3. General histology and immunohistochemistry of sections from a low-grade malignant peripheral nerve sheath tumor. A) A H& E of a low-grade malignant peripheral nerve sheath tumor with more cells compared to the plexiform nerve sheath tumor. B) S100 staining of a low-grade malignant peripheral nerve sheath tumor. C) EGFR staining of a low-grade malignant peripheral nerve sheath tumor.

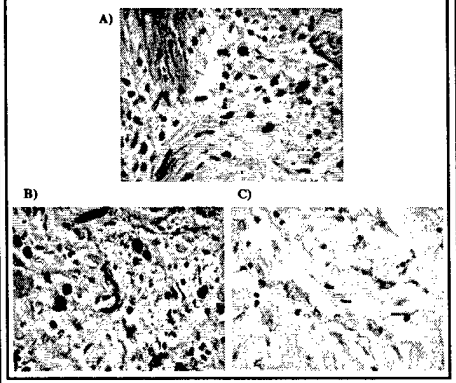

Results

Figure 4. General histology and immunohistochemistry of section from a high-grade malignant peripheral nerve sheath tumor. A) A photograph of a high-grade malignant peripheral nerve sheath tumor. B) H&E staining showing the hypercellularity of a high-grade malignant peripheral nerve sheath tumor. C) S100 staining in a high-grade malignant peripheral nerve sheath tumor. D) EGFR staining in a high-grade malignant peripheral nerve sheath tumor.

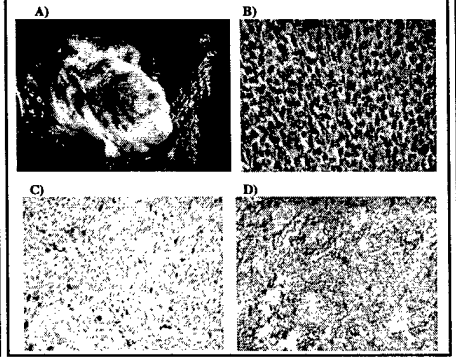

Results

Figure 5. Examples of the peaks from genotyping analysis for two of the tumor tissue (lower peaks) with a corresponding normal control tissue (top peaks). The two markers in this data are D7S502 in green and D7S2422 in blue. The peak size and area underneath each peak which is used to calculate the ratio to determine allelic imbalance or LOH are given underneath the peaks.

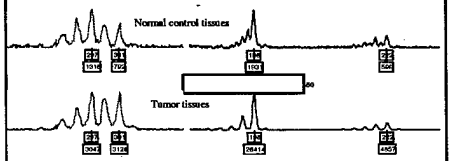

Table III. Genotyping results from five of the tumors with corresponding normal control tissue. The first four samples are MPNST while the last sample is a PNF. Allelic imbalance is defined as ratios of ≤0.5 or ≥2.0. Loss of heterozygosity is the loss of one allele. There were no allelic imbalance or LOH in the samples tested with the specific markers below.

	Ratio of normal control tissue vs tumor tissue				
Markers	2139971A	194973	448891e	1362981b	2629992b
D7S2422	1.08	1.02	0.96	1.69	0.65
D7S506	0.97	0.99	0.97	0.87	0.96
D7S2550	1.00	1.18	0.83	1.27	0.88
D7S494	1.09	0.98	0.97	1.21	1.08
D7S502	NA	NA	0.71	0.68	1.00

Discussion

EGFR RNA and /or protein over expression is frequently observed in human tumors and the increased EGFR expression has been found to be associated with a poorer clinical outcome in cancers of breast, head and neck, lung, and bladder (7, 8, 9, 10). In addition, EGFR gene amplification has been observed in 40% glioblastomas (11) and is often in association with rearrangement of the gene to produce a truncated, constitutively activated receptor (12). In contrast, gene amplification is not a commonly reported finding in other EGFR positive tumors, indicating that the tumor cells may have additional EGFR activation mechanisms. In a recent study, a novel molecular pathway in peripheral nerve sheath tumor tumorigenesis, in which NF1 mutation leads to aberrant EGFR expression that results in elevated levels of Brain lipid bonding protein(BLBP) and loss of axonal contact has been suggested (13). In this study, we confirmed that EGFR overexpansion was present in a high percentage of neoplastic cells in high-grade MPNSTs and in a subset of cells within PNF and low-grade MPNSTs. Furthermore, the intensity of EGFR expression was associated with tumor grade with highest expression was seen in high-grade MPNST. The majority of high- grade, EGFR positive MPNST cells and a subset of EGFR positive cells in PNF and low-grade MPNST had decreased or negative reactivity for S100. These data support that EGFR may play a role in tumorigenesis of PNF and MPNST. We further hypothesized that EGFR protein expression was associated with genomic imbalance involving the EGFR gene. However, genomic analyses revealed allelic balance at the 5 genetic markers spanning the EGFR locus and thus do no support that genomic amplification of the EGFR locus is responsible for the EGFR protein expression in these tumors. The over expression of EGFR in PNF and MPNST may be mediated by mechanisms other than genomic amplification of the EGFR locus.

Acknowledgements

Thank-you to Margaret Robertson, Rebecca Scholl and Michael Klein at the Genomics Core Facility at the University of Utah for the genotyping analysis. This work was supported by ARUP laboratory service and Division of US Army.

Submitted abstract: Mast cells in peripheral nerve sheath tumors: Association with histology, NF1 status, angiogenesis, and fibrous stroma cells. Zhou H, **Viskochil D**, Minh-Thu H, Tripp S, Coffin C. American and Canadian Pathology Meetings, 2004.

Title: Mast cells in peripheral nerve sheath tumors: Association with histology, NF1 status, angiogenesis, and fibrous stroma cells.

H Zhou [1], DH Viskochil [2], MN Hang[2], SR Tripp [1], CM Coffin [1]. [1]Pathology, and [2]Pediatrics, University of Utah, Salt Lake City, UT.

Background: Peripheral nerve sheath tumors (PNST), including dermal and plexiform neurofibromas and malignant peripheral nerve sheath tumors (MPNST), are cardinal features of neurofibromatosis 1 (NF1). Recent studies in animal and in vitro models suggest that NF1-mediated tumorigenecity requires both neoplastic (*Nf1-/-)* Schwann cells and non-neoplastic (*Nf1+/-)* cellular components that may provide landscaping factors to facilitate tumor growth. In mice studies, one of these non-neoplastic cellular components, the *Nf1+/-*mast cell (MC), demonstrates increased proliferation and survival in response to Kit ligand (Ingram D et al., 2001). Interestingly, MC hyperplasia is also a common observation in human peripheral nerve sheath tumors. The pathogenesis and significance of MC proliferation and infiltration in these tumors is not known. We hypothesized that in human NF1, *NF1+/-* mast cells play an active role in promoting angiogenesis as is observed in several other tumors (Ribatti D, et al., 2003, Crivellato E, et al., 2002), where increased numbers of MCs are associated with an increase in microvessels, tumor invasion and tumor progression. Our study is designed to determine the association of mast cells with tumor histology, NF1 status, and microvessel formation.
Design: Formalin-fixed, paraffin-embedded archival tissue from 5 dermal neurofibromas (NF), 6 plexiform neurofibromas (PNF) and 13 MPNSTs (7 with NF1) were immunostained with monoclonal antibodies to mast cell tryptase and CD31 using an automated staining system (Ventana). The mast cell density (MCD), cellularity of stroma fibrous cells, and microvessel count (MVC) were determined on 10 randomly selected high power field (HPF) and compared among dermal NFs, PNFs and MPNSTs; and between NF1-related and sporadic MPNSTs.
Results: Mast cells with tryptase activity were present in all cases. However, significant differences in MCD were found among NFs, PNFs and MPNSTs ($p<0.01$, MPNST vs NFs and PNFs) and appeared to be associated with the abundance of stroma fibrous cellular component. The highest MCD (>100/10 HPF) was found in all NFs and diffuse NF areas between nodules in PNF where abundant fibrous stroma was present. In PNF nodular areas with less cellular, myxoid stroma, moderately MCD (50-100/10 HPF) was observed. Similarly, the majority of high grade MPNSTs, regardless of their NF1 status, contained usually a MCD that <50/ 10HPF, and generally had very scant fibrous stroma. Increased MVC (>200/10HPF) were observed in all high-grade MPNSTs when compared to PNFs or NFs (MVC 50-100/10HPF) ($P<0.05$). There was no significant difference in MVC between PNFs and NFs.
Conclusion: MC proliferation in peripheral nerve sheath tumors, regardless of their NF1 status, is not directly associated with increased microvessels as seen in other human malignancies such as malignant melanoma, Hodgkin's and non- Hodgkin's lymphomas. The lack of significantly increased MCs in malignant versus benign PNSTs suggests that mast cells do not play a significant role in the propagation of high-grade MPNST. However, MCs might cooperate with stroma cellular components such as fibroblasts, to facilitate tumor growth and enhance subsequent malignant transformation.

Poster: Minh-Thu H, Liew M, Cowley B, Brothman A, Zhou H, Coffin C, **Viskochil D**. Genetic evaluation of malignant peripheral nerve sheath tumors in neurofibromatosis type 1 using quantitative genotyping and comparative genomic hybridization (CGH) microarray analysis. Connective Tissue Oncology Meeting, November 2003.

GENETIC EVALUATION OF MALIGNANT PERIPHERAL NERVE SHEATH TUMORS IN NEUROFIBROMATOSIS TYPE 1 USING QUANTITATIVE GENOTYPING AND COMPARATIVE GENOMIC HYBRIDIZATION (CGH) MICROARRAY ANALYSIS

Minh-Thu N. Hang[1], Michael Liew[1], Brett Cowley[1], Arthur Brothman[1], Holly Zhou[1], Cheryl Coffin[1], David H. Viskochil[1]

[1]University of Utah, Utah, United States

Introduction

NF1 is an autosomal dominant condition that affects 1 in 3,500 individuals world wide. Hallmark features of this disease include dermal neurofibromas, café-au-lait spots, and peripheral nerve sheath tumors, plexiform neurofibromas and MPNSTs. Approximately 10% of NF1 patients followed in longitudinal cohort develop MPNST at sometime in their lifetime, usually 2 decades earlier than those who develop MPNST without NF1. As a tumor suppressor gene, double inactivation of the *NF1* gene by somatic mutation of the normal allele in Schwann cells is necessary for the development of benign neurofibromas, but not sufficient for their progression to MPNSTs. Other genes, including *TP53*, *P27*, *P16*, and *EGFR* have been implicated in tumor progression in NF1-related malignancies. We hypothesize that additional genes undergo mutation before benign plexiform neurofibromas transform to MPNSTs. In order to identify these genes we looked for consistent genome-wide imbalances in NF1-associated tumors. In this study we use 2 methods to identify genome instability, allelic imbalance analysis with tetra-nucleotide genetic markers mapping to the distal arms of each chromosome and comparative genomic hybridization (CGH) microarray analysis to detect imbalances with higher resolution throughout the genome.

The aims of this project were to assess intra-tumor genetic heterogeneity in 2 MPNSTs from an individual with NF1 and to compare quantitative genotype analysis versus CGH microarray analysis to establish genetic "signatures" of clonal expansion.

Results

Figure 1. General morphology of the different areas from the two tumors extracted from an individual with NF1. The upper panel is a set of H&E sections from 5 different sites of a pelvic tumor removed from an individual with NF1 in 2002. The lower panel is a set of H&E sections from 4 different sites from an ipsilateral distal leg tumor which was removed previously in 2000 from the same individual. Images were taken at 40X magnification. DNA was also extracted from each site.

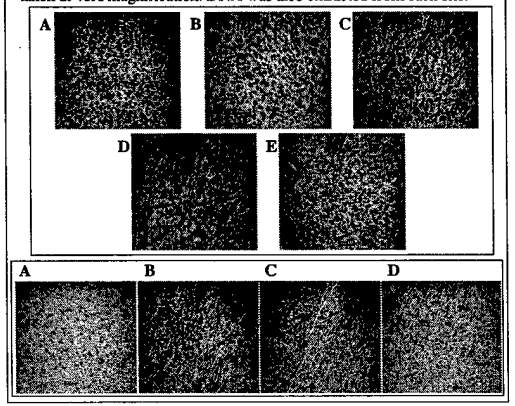

Results

Figure 2. Genotyping data from an area of Tm2000 and Tm2002. **A)** The markers used for genotyping and their approximate location of the respective chromosomes. **B)** The left panel shows the blood samples where the alleles are balanced. The middle panel is an example of LOH and the right panel shows allelic imbalance.

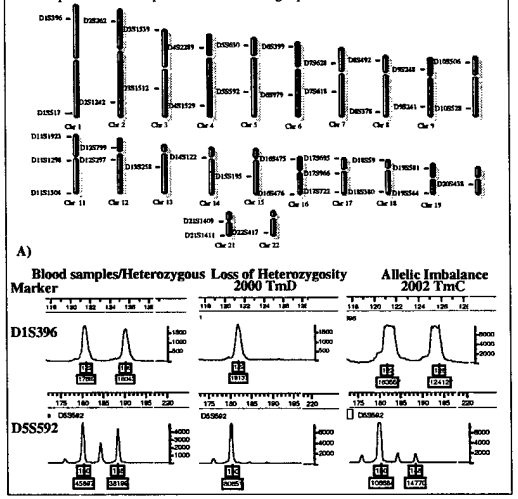

Results:

Figure 3. CGH Microarray results from DNA extracted from T2002. **A.** An array showing hybridization of the DNA to the clones on the chip. The left panel with the arrow is an example where a loss is observed (red dot). The right panel with the arrow is indicating a gain (green dot). **B.** The ratio plot of DNA from T2002 showing the "signature" of clonal expansion in chromosome 5 taken from the above array hybridization. Arrows correspond to clones depicting gain and loss on the ratio plot. T2000 had the same chromosome 5 "signature".

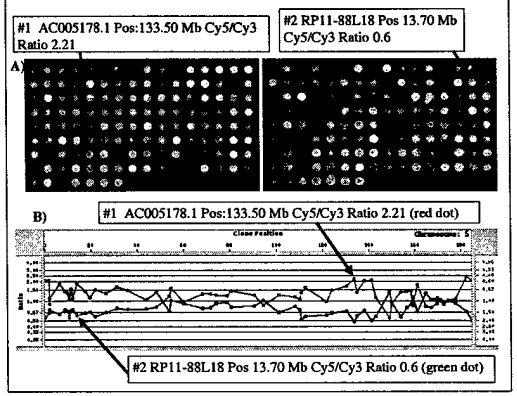

Methods

- A low-grade MPNST (T2000) was removed from the left thigh of an individual with NF1.
- Two years later a high-grade MPNST (T2002) was removed from the same individual.
- Each tumor was randomly dissected into 4 and 5 areas for histology, immunohistochemical analysis and DNA extraction.

Histology and Immunohistochemistry

- Paraffin sections from each site from T2000 and T2002 were stained with H&E for general morphology.
- The sections were also stained with various antibodies for specific antigen expression via immunohistochemistry including S100, p16, p27, p53, Mib1 and EGFR.

Comparative Genomic Hybridization Microarray

- DNA from two areas of each tumor were pooled and subjected to CGH microarray (Spectral Genomics).

Genotyping analysis

- PCR-based quantitative genotyping at 32 selected informative markers spanning the entire genome was performed.

Results

Table I. Immunohistochemistry results for areas of T2000 and T2002.

		S100	p16	p27	p53	Mib1	EGFR
T2000	TmA	P(10%)	P(60%)	P(W15%)	N(ef)	NA	P(25%)
	TmB	P(30%)	P(60%)	P(W10%)	N(ef)	N	P(30%)
	TmC	P(10%)	P(60%)	P(W15%)	N(ef)	N	P(25%)
	TmD	P(30%)	P(60%)	P(W5%)	N(ef)	N	P(30%)
T2002	TmA	N	P(80%)	P(>80%)	N	P(30%)	P(65%)
	TmB	N	P(80%)	P(>50%)	N	P(30%)	P(65%)
	TmC	N	P(80%)	P(>50%)	N	P(30%)	P(65%)
	TmD	N	P(80%)	P(>50%)	N	P(30%)	P(65%)
	TmE	N	P(80%)	P(>50%)	N	P(30%)	P(65%)

P- positive; P(W)-weak staining; N-negative; N(ef)-edge effect

Results

Figure 4. Genotyping results from the different areas from T2000 and T2002. The markers used are on the left. The open circles are show allelic balance at informative heterozygous loci. Loci with loss of heterozygosity (LOH) are represented by the filled circles. Loci with allelic imbalance (AI) are represented by half-filled circles.

DNA was extracted from tumor foci corresponding to each of the sections depicted in figure 1.

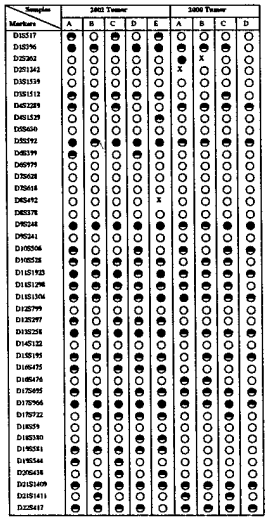

Discussion

In the present case, 2 separate tumors were excised from an individual with NF1 within a period of two years. We obtained tissue from multiple sites in both tumors for immunohistochemical staining and DNA analysis to assess tumor heterogeneity. The initial tumor, clinically diagnosed as a plexiform neurofibroma in the left thigh, was removed in 2000 (T2000) and pathologically diagnosed as a low-grade MPNST. The second tumor presented as a painful mass in the left pelvis and was removed in 2002 (T2002). It was diagnosed as high-grade MPNST.

T2002 is more hypercellular with a moderate mitotic index as compared to T2000. Different immunohistochemical staining patterns were noted between the 2 tumors, however the different foci within each tumor were relatively homogeneous with respect to patterns of protein immuno-expression for S100, p16, p27, p53, mib1 and EGFR. There was little tumor heterogeneity.

Of the 41 loci evaluated by allelic imbalance analysis, T2000 showed abnormalities in 20 (LOH in 4), and T2002 showed abnormalities in 25 (LOH for 7). Approximately 76% (31/41) of loci in T2000 and 68% (28/41) of loci in T2002 showed identical genotype analysis in each of their respective intratumor sites. Thus, approximately 1/4-to-1/3 of genetic loci demonstrated some degree of intratumor heterogeneity across the different sites from these tumors.

CGH microarray data confirmed most of the changes that were observed with the allelic imbalance analysis. This validates the use of the technique as a valuable high-resolution tool to screen genomic DNA from PNSTs for genomic imbalances. For example, we identified a "signature" for chromosome 5 that demonstrates a common origin of the predominant cell clone for both tumors. T2002 did not arise as an independent event, rather it could have developed either as a metastatic event or, more likely, direct subclinical extension of T2000 along the femoral and sciatic nerve sheath.

Thank-you to Margaret Robertson, Rebecca Scholl and Michael Klein from the Genomic Core facility at the University of Utah for the Genotyping results. This project was supported by funding from the DOD grant - DAMD17-99-1-9560.

Published manuscript: **Liew M**, Coffin C, Fletcher J, Hang M-T, Tanito K, Niimura M, and **Viskochil D**. Peripheral nerve sheath tumors from patients with neurofibromatosis type 1 do not have the chromosomal translocation t(X;18). Pediatric and Developmental Path 2002:5;165-169.

Pediatric and Developmental Pathology 5, 165–169, 2002
DOI: 10.1007/s10024-001-0126-y

Peripheral Nerve Sheath Tumors from Patients with Neurofibromatosis Type 1 Do Not Have the Chromosomal Translocation t(X;18)

MICHAEL A. LIEW,[1]* CHERYL M. COFFIN,[2] JONATHAN A. FLETCHER,[3] MINH-THU N. HANG,[1] KATSUMI TANITO,[1,4] MICHIHITO NIIMURA,[4] AND DAVID VISKOCHIL[1]

[1]Department of Pediatrics, Division of Medical Genetics, University of Utah, 50 North Medical Drive, Salt Lake City, UT 84132, USA
[2]Department of Pathology, Primary Children's Medical Center and University of Utah, 100 North Medical Drive, Salt Lake City, UT 84132, USA
[3]Department of Pathology, Brigham and Women's Hospital, 75 Francis Street, Boston, MA 02115, USA
[4]Department of Dermatology, The Jikei University School of Medicine, Tokyo, Japan

Received July 29, 2001; accepted October 15, 2001.

ABSTRACT

Neurofibromatosis type 1 (NF1) is a common autosomal dominant genetic disorder that is caused by a mutation in the *NF1* gene. Hallmark characteristics include dermal neurofibromas, café-au-lait spots, and learning disabilities. In approximately 25% of NF1 cases, plexiform neurofibromas, or peripheral nerve sheath tumors (PNSTs) that involve large segments of nerve sheath and nerve root, can form, of which a small percentage become malignant (MPNST). Most MPNSTs are composed of spindled neoplastic cells, and they can resemble other spindle-cell sarcomas, including leiomyosarcoma and monophasic synovial sarcoma. Histological diagnosis of MPNST is not always straightforward, and various immunohistochemical and molecular adjuncts can be critical in establishing a correct diagnosis. One example of genetic testing is the assay for the t(X;18) chromosomal translocation, which has been found to be common in synovial sarcomas. The aim of this study was to determine whether MPNSTs contain the t(X;18) chromosomal translocation. To detect the t(X;18) translocation product, SYT-SSX, total RNA was extracted from frozen archival tumors (15 dermal neurofibromas, 4 plexiform neurofibromas, and 7 MPNSTs) using Trizol. The RNA was then subjected to reverse-transcriptase polymerase chain reaction (RT-PCR) to specifically amplify SYT-SSX. None of the dermal neurofibromas, plexiform neurofibromas, or MPNSTs analyzed were positive for SYT-SSX mRNA. The results indicate that the t(X;18) translocation is absent in neurofibromas and is not a marker for MPNST in patients with NF1.

Key words: neurofibromatosis type 1, polymerase chain reaction, synovial sarcoma

INTRODUCTION

Neurofibromatosis type 1 (NF1) is an autosomal dominant disorder that affects approximately 1/3500 individuals. The *NF1* gene was identified as a tumor suppressor and cloned in the early 1990s; it maps to location 17q11.2 and spans 60 exons [1–3]. The *NF1* gene encodes a 2818–amino acid protein called neurofibromin. Hallmark clinical features of this disease are café-au-lait spots, der-

*Corresponding author, at University of Utah, Building 570, BPRB, Room 308, 20S 2030E, Salt Lake City, UT 84112-9454, USA.

mal neurofibromas, and learning disabilities. Approximately 25% of patients with NF1 develop plexiform neurofibromas, which are peripheral nerve sheath tumors (PNSTs) involving large segments of nerve sheath and nerve root. It is estimated that approximately 2%–4% of individuals with NF1 will develop a malignant PNST (MPNST) [4]. MPNSTs have complete inactivation of the *NF1* gene [5,6], as do many plexiform and dermal neurofibromas. In addition, gains in chromosomes [7], overexpression of p53 [8–10], inactivation of $p16^{INK4A}$ [8,11], and a change in the cellular compartmentalization of $p27^{KIP1}$ [12] in MPNSTs have been reported. Therefore, it appears that other important genetic modifiers, in addition to *NF1* inactivation, are responsible for MPNST development.

Many synovial sarcomas are histologically similar to MPNSTs. Both tumors can belong to the group of soft tissue sarcomas known as spindle cell sarcomas, which includes spindle cell rhabdomyosarcomas, leiomyosarcomas, malignant fibrous histiocytomas, and other neoplasms. Synovial sarcomas comprise 7%–10% of all soft tissue sarcomas [13] and were originally named to describe tumors that form near the joints and resemble synovial tissue [14,15], in contrast to MPNSTs, which are associated with nerve sheath or nerve root. Synovial sarcoma frequently arises in paraarticular regions, in close association with tendon sheaths, bursae, and joint capsules, but it is now known that it can arise frequently in other anatomical areas, such as the head, neck, and trunk [13,16–19]. It is important to clinically distinguish different spindle cell sarcomas so that the appropriate treatment can be implemented. For example, synovial sarcomas are known to be relatively sensitive to the chemotherapeutic agent ifosfamide [20]. There are also prognostic differences.

It has been clearly demonstrated that most synovial sarcomas carry the t(X;18) chromosomal translocation [21–25]. The breakpoint genes have been identified as *SYT* from chromosome 18 and *SSX* from the X chromosome [26,27]. It has now been found that the original *SSX* locus consists of three genes: *SSX1*, *SSX2*, and *SSX4* [28–30]. Recently, in addition to being observed in synovial sarcomas, the SYT-SSX fusion transcript was detected by reverse-transcriptase polymerase chain reaction (RT-PCR) in dermal neurofibromas and MPNSTs [31]. Two of three dermal neurofibromas and 15 of 20 MPNSTs expressed SYT-SSX fusion genes; this expression is indicative of the chromosomal translocation t(X;18). This was the first report of a large number of MPNSTs having an apparent t(X;18) chromosomal translocation. The presence of the t(X;18) chromosomal translocation in MPNSTs could play a major role in tumor progression and potential therapy. Therefore, the aim of this study was to confirm that the t(X;18) chromosomal translocation does occur in MPNSTs from patients with NF1.

METHODS

Patient identification

NF1 patients participating in this study met the criteria established at the consensus conference at the National Institutes of Health [32]. Tissue samples used in this study were obtained with permission from the University of Utah Institutional Review Board. Twenty-five of the 26 samples used in this study were from 25 patients with NF1 (15 dermal neurofibromas, 4 plexiform neurofibromas, and 6 MPNSTs). The other sample was a MPNST from a patient who was not diagnosed with NF1. All samples except one were frozen. The exception was the MPNST from the non-NF1 patient, which was placed in RNA later™ and stored at 4°C. All samples were evaluated histologically by hematoxylin and eosin (H&E) sectioning.

Cell culture

As a positive control for SYT-SSX expression, a synovial sarcoma cell line, SYN792, was cultured and harvested for fresh RNA. This cell line was established by Jonathan Fletcher from a biphasic synovial sarcoma. It has been examined cytogenetically and has the t(X;18) chromosomal translocation (J. Fletcher, unpublished observation). Cells were grown in RPMI + 15% (v/v) fetal bovine serum (FBS) and maintained at 37°C in 5% (v/v) CO_2 in a humidified incubator.

RNA extraction

Total RNA was extracted from frozen tissues using TRIZOL® (Invitrogen, Carlsbad, CA), according to the manufacturer's instructions. In brief, total RNA extraction was conducted following TRIZOL specifications. First 50–100 mg of tissue sample

was homogenized in 1 ml of TRIZOL reagent and then incubated at room temperature for 5 min. Then 0.2 ml of chloroform was added, followed by vigorous shaking and incubation at room temperature for 2–3 min. The sample was then centrifuged for 15 min at 12,000 × *g* at 4°C for phase separation. After this procedure 0.5 ml of isopropyl alcohol was added to the aqueous phase at room temperature for 10 min, followed by centrifugation at 12,000 × g at 4°C to precipitate out the RNA. The RNA pellet was washed once with 1 ml of 75% (v/v) ethanol and centrifuged at 7,500 × g for 5 min at 4°C. The RNA pellet was then air dried for 10 min at room temperature and dissolved in DEPC-treated distilled water, incubated at 60°C for 10 min, and stored at −70°C.

First-strand cDNA synthesis

First-strand synthesis of cDNA from the isolated total RNA was performed using the reverse transcriptase, Superscript II (Invitrogen, Carlsbad, CA). The following components were combined: 1 μl of random hexamer (1 μg/μl; Pharmacia, Peapack, NJ), 5 μg of total RNA, and sterile distilled water to 12.5 μl. This was then incubated at 70°C for 10 min and then quickly chilled on ice. Then the following components were added: 5 μl of 5 × first-strand buffer, 2 μl of 0.1 mM DTT, 1 μl of 25 mM dNTP (25 mM of each), 0.5 μl of RNasin (Promega, Madison, WI), 1 μl of single-strand DNA binding protein (0.5 μg/μl; USB), and 1.5 μl of water. This was then mixed and incubated at room temperature for 10 min. Then 1.5 μl of SuperScript II Rnase H-Reverse Transcriptase (Invitrogen, Carlsbad, CA) was added. This was then incubated at 37°C for 1 h. The enzyme was then inactivated at 65°C for 10 min and the cDNA was stored at −20°C.

Polymerase chain reaction

The polymerase chain reaction (PCR) method was adapted from O'Sullivan et al. [31]. To ensure the integrity of the cDNA synthesis, β2-microglobulin was amplified using the primers ACCCCCACTGAAAAAGATGA and ATCTTCAAACCTCCATGATG for a predicted product size of 120 base pairs. Contaminating genomic DNA would result in a predicted product size of 730 base pairs. The primers used for the t(X;18) translocation product (SYT-SSX) were AGACCAACACAGCCTGGACCAC and TCCTCTGCTGGCTTCTTG, for a predicted size of 87 base pairs. PCR reactions amplifying β2-microglobulin cDNA were carried out in 25 μl reaction volumes containing 1× PCR buffer, 143 μM dNTP, 200 μM spermidine, 1.5 mM $MgCl_2$, and 0.5 U *Taq* DNA polymerase (Invitrogen, Carlsbad, CA). Thermal cycling conditions for the β2-microglobulin PCR were 94°C for 5 min; 94°C for 40 s, 60°C for 1 min, and 72°C for 30 s, repeated for 38 cycles, followed by 72°C for 5 min. PCR reactions amplifying SYT-SSX cDNA were carried out in 25 μl reaction volumes containing 1 × PCR buffer, 143 μM dNTP, 200 μM spermidine, 0.5 mM $MgCl_2$, and 0.5 U *Taq* DNA polymerase. Thermal cycling conditions for the SYT-SSX PCR were 94°C for 5 min, 94°C for 40 s, 60°C for 1 min, and 72°C for 30 s, repeated for 40 cycles, followed by 72°C for 5 min. The PCR products were electrophoresed on a 2% (w/v, 3:1 Nusieve:Seakem LE) agarose gel.

RESULTS

The integrity of the cDNA synthesis and PCR assays was evident by the presence of amplifiable β2-microglobulin mRNA (Fig. 1a). All samples tested were positive for β2-microglobulin mRNA. When we examined the same samples for the *SYT-SSX* translocation product, the only sample of cDNA that was positive by PCR was from the synovial sarcoma cell line (Fig. 1b). The cDNA from dermal neurofibromas, plexiform neurofibromas, and MPNSTs were negative for the SYT-SSX translocation product.

DISCUSSION

In the study by O'Sullivan et al. [31], which was based on analysis of formalin-fixed, paraffin-embedded tissues, they reported that 2/3 dermal neurofibromas and 15/20 MPNSTs were positive for the t(X;18) translocation. The positive neurofibromas were an atypical neurofibroma and a cellular neurofibroma, which were from patients who did not have clinical features of NF1. Six of the 15 MPNSTs that were positive for the t(X;18) translocation were from patients with NF1, while the remaining 9 patients did not have NF1. In our analysis of frozen tumor samples from NF1 patients, none of the MPNSTs, plexiform neurofibromas, or

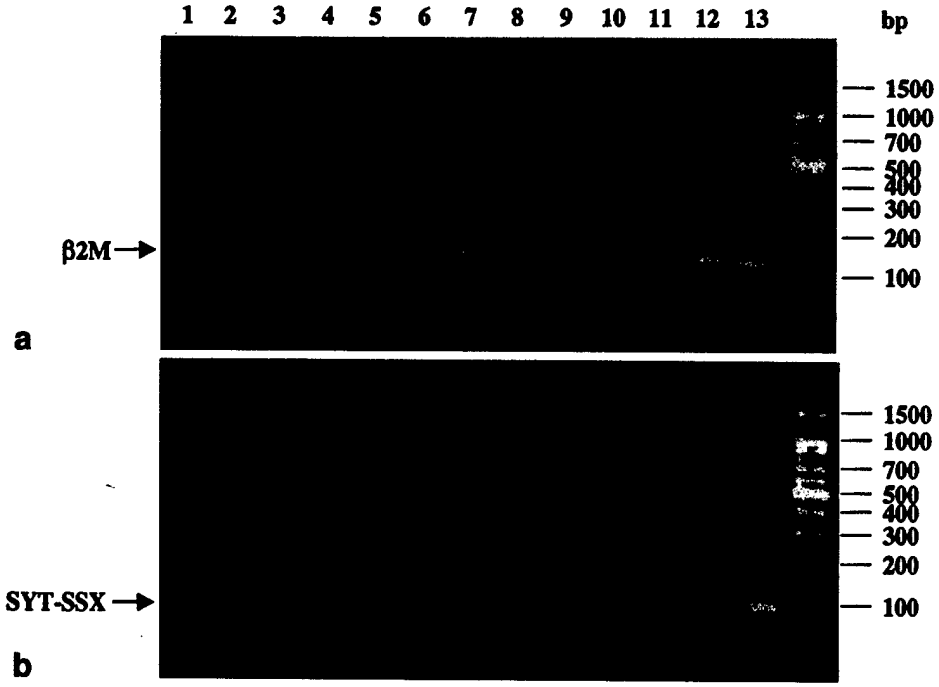

Figure 1. Polymerase chain reaction (PCR) amplification of β2-microglobulin and SYT-SSX cDNA. The water control is in **lane 1**, cDNA derived from the SYN792 cell line is in **lane 13**, cDNA derived from plexiform neurofibromas is in **lanes 2, 3, 11,** and **12**, and cDNA derived from malignant peripheral nerve sheath tumors (MPNSTs) is in **lanes 4–10**. **a:** Results of amplification of β2-microglobulin cDNA. The PCR product is indicated by the arrow (β2M). **b:** Results of amplification of SYT-SSX cDNA. The PCR product is indicated by the arrow (SYT-SSX).

dermal neurofibromas were found to be positive for the t(X;18) translocation.

There have been additional prior reports of looking for the t(X;18) translocation in spindle cell sarcomas, including MPNSTs [33–35]. These studies demonstrate the difficulty in making a diagnosis based solely on the histology and immunohistochemistry of a spindle cell sarcoma, and illustrate how a genetic test can provide more diagnostic information. As in our study, van de Rijn et al. [33] observed that 12/12 MPNSTs in their study were negative for the t(X;18) translocation. In addition, there was a lesion that had histologic, immunohistologic, and ultrastructural features indiscriminate for the diagnosis of synovial sarcoma or MPNST. The lesion was positive for SYT-SSX, so it was rediagnosed as a synovial sarcoma. In the study by Hiraga et al. [34], four out of four MPNSTs from patients with NF1 were negative for SYT-SSX, and six out of seven MPNSTs from patients without NF1 were negative for SYT-SSX. The positive MPNST was reassessed by additional examination of the tissue, including electron microscopy and immunohistochemistry. On the basis of the new data and because the MPNST was not associated with a large nerve and was S-100 negative, it was classified as a synovial sarcoma. This study also contained five unclassified tumors, three of which were positive for SYT-SSX. These were subsequently diagnosed as synovial sarcoma. Another case report demonstrated the t(X;18) chromosomal translocation in a sarcoma with histological features of a MPNST but raised the question of whether the lesion was a MPNST or a synovial sarcoma with histological features of a MPNST [35].

The challenges in classifying these spindle cell tumors from only a histological and immunohistochemical analysis are well known. By using these analyses in combination with genetic tests, such as the RT-PCR assay for the t(X;18) translocation, more precise classification of spindle cell sarcomas may be made. Our results demonstrate that the t(X;18) translocation is absent from neurofibromas and is not a marker for MPNST in patients with NF1.

ACKNOWLEDGMENTS

The authors thank Bryna McConarty for her expert technical assistance with the SYN792 cell line. The authors acknowledge the generous support of the United States Army Medical Research and Materiel Command (USAMRMC), project NF980007.

REFERENCES

1. Cawthon R, Weiss R, Xu G, et al. A major segment of neurofibromatosis type 1 gene: cDNA sequence, genomic structure and point mutations. Cell 1990;62:193–201.

2. Wallace MR, Marchuk DA, Anderson LB, et al. Type 1 neurofibromatosis gene: identification of a large transcript disrupted in three patients. Science 1990;249:182–186.
3. Viskochil D, Buchberg AM, Xu G, et al. Deletions and a translocation interrupt a cloned gene at the neurofibromatosis type 1 locus. Cell 1990;62:187–192.
4. Riccardi VM. Neurofibromatosis: Phenotype, Natural History, and Pathogenesis. Baltimore: Johns Hopkins University Press, 1992.
5. Legius E, Marchuk DA, Collins FS, Glover TW. Somatic deletion of the neurofibromatosis type 1 gene in a neurofibrosarcoma supports a tumor suppressor gene hypothesis. Nat Genet 1993;3:122–126.
6. Rasmussen SA, Overman J, Thomson SA, et al. Chromosome 17 loss-of-heterozygosity studies in benign and malignant tumors in neurofibromatosis type 1. Genes Chromosomes Cancer 2000;28:425–431.
7. Schmidt H, Taubert H, Meye A, et al. Gains in chromosomes 7, 8q, 15q and 17q are characteristic changes in malignant but not in benign peripheral nerve sheath tumors from patients with Recklinghausen's disease. Cancer Lett 2000;155:181–190.
8. Birindelli S, Perrone F, Oggionni M, et al. Rb and TP53 pathway alterations in sporadic and NF1-related malignant peripheral nerve sheath tumors. Lab Invest 2001;81: 833–844.
9. Liapis H, Marley EF, Lin Y, Dehner LP. p53 and Ki-67 proliferating cell nuclear antigen in benign and malignant peripheral nerve sheath tumors in children. Pediatr Dev Pathol 1999;2:377–384.
10. Halling KC, Scheithauer BW, Halling AC, et al. p53 expression in neurofibroma and malignant peripheral nerve sheath tumor. An immunohistochemical study of sporadic and NF1-associated tumors. Am J Clin Pathol 1996;106: 282–288.
11. Kourea HP, Orlow I, Scheithauer BW, Cordon-Cardo C, Woodruff JM. Deletions of the *INK4A* gene occur in malignant peripheral nerve sheath tumors but not in neurofibromas. Am J Pathol 1999;155:1855–1860.
12. Kourea HP, Cordon-Cardo C, Dudas M, Leung D, Woodruff JM. Expression of p27(kip) and other cell cycle regulators in malignant peripheral nerve sheath tumors and neurofibromas: the emerging role of p27(kip) in malignant transformation of neurofibromas. Am J Pathol 1999;155: 1885–1891.
13. Dos Santos NR, De Bruijn DRH, Van Kessel AG. Molecular mechanisms underlying human synovial sarcoma development. Genes Chromosomes Cancer 2001;30:1–14.
14. Haagensen CD, Stout AP. Synovial sarcoma. Ann Surg 1944;120:826–842.
15. Pack GT, Ariel IM. Synovial sarcoma (malignant synovioma). A report of sixty cases. Surgery 1950;28:1047–1084.
16. Batsakis JA, Enzinger FM, Tannenbaum M. Synovial sarcomas of the neck. Arch Otolaryngol Head Neck Surg 1967;85:327–331.
17. Roth JA, Enzinger FM, Tannenbaum M. Synovial sarcoma of the neck: a follow-up study of 24 cases. Cancer 1975;35: 1243–1253.
18. Schmookler BM, Enzinger FM, Brannon RB. Orofacial synovial sarcoma: a clinicopathologic study of 11 new cases and review of the literature. Cancer 1982;50:269–276.
19. Witkin GB, Miettinen M, Rosai J. A biphasic tumor of the mediastinum with features of synovial sarcoma: a report of four cases. Am J Surg Pathol 1989;13:490–499.
20. Rosen G, Forscher C, Lowenbraun S, et al. Synovial sarcoma. Uniform response of metastases to high dose ifosfamide. Cancer 1994;73:2506–2511.
21. Limon J, Dal Cin P, Sandberg AA. Translocations involving the X chromosome in solid tumors: presentation of two sarcomas with t(X;18)(q13;p11). Cancer Genet Cytogenet 1986;23:87–91.
22. Kawai A, Woodruff J, Healy JH, et al. *SYT-SSX* gene fusion as a determinant of morphology and prognosis in synovial sarcoma. N Engl J Med 1998;338:153–160.
23. Antonescu CR, Kawai A, Leung DH, et al. Strong association of *SYT-SSX* fusion type and morphologic epithelial differentiation in synovial sarcoma. Diagn Mol Pathol 2000;9:1–8.
24. Tsuji S, Hisaoka M, Morimitsy Y, et al. Detection of SYT-SSX fusion transcripts in synovial sarcoma by reverse transcription-polymerase chain reaction using archival paraffin-embedded tissues. Am J Pathol 1998;153:1807–1812.
25. Nilsson G, Skytting B, Xie Y, et al. The SYT-SSX1 variant of synovial sarcoma is associated with a high rate of tumor cell proliferation and poor clinical outcome. Cancer Res 1999;59:3180–3184.
26. de Leeuw B, Balemans M, Olde Weghuis D, et al. Molecular cloning of the synovial sarcoma–specific translocation (X;18)(p11.2;q11.2) breakpoint. Hum Mol Genet 1994;3: 745–749.
27. Clark J, Rocques PJ, Crew AJ, et al. Identification of novel genes *SYT* and *SSX*, involved in the t(X;18)(p11.2;q11.2) translocation found in human synovial sarcoma. Nat Genet 1994;7:502–508.
28. Crew AJ, Clark J, Fisher C, et al. Fusion of *SYT* to two genes, *SSX1* and *SSX2*, encoding proteins with homology to the Kruppel-associated box in human synovial sarcoma. EMBO J 1995;14:2333–2340.
29. de Leeuw B, Balemans M, Olde Weghuis D, et al. Identification of two alternative fusion genes, *SYT-SSX1* and *SYT-SSX2*, in t(X;18)(p11.2;q11.2)-positive synovial sarcomas. 1995;4:1097–1099.
30. Skytting BT, Nilsson G, Brodin B, et al. A novel fusion gene, *SYT-SSX4*, in synovial sarcoma. J Natl Cancer Inst 1999;91:974–975.
31. O'Sullivan MJ, Kyriakos M, Zhu X, et al. Malignant peripheral nerve sheath tumors with t(X;18). A pathologic and molecular genetic study. Mod Pathol 2000;13:1253–1263.
32. Neurofibromatosis. Natl Inst Health Consens Dev Conf Consens Statement 1987;6:1–7.
33. van de Rijn M, Barr FG, Collins MH, et al. Absence of SYT-SSX fusion products in soft tissue tumors other than synovial sarcoma. Am J Clin Pathol 1999;112:43–49.
34. Hiraga H, Nojima T, Abe S, et al. Diagnosis of synovial sarcoma with the reverse transcriptase-polymerase chain reaction: analyses of 84 soft tissue and bone tumors. Diagn Mol Pathol 1998;7:102–110.
35. Vang R, Biddle DA, Harrison WR, Heck K, Cooley LD. Malignant peripheral nerve sheath tumor with a t(X;18). Arch Pathol Lab Med 2000;124:864–867.

Executive summary statement: MPNST symposium, Aspen 06/2002 (organizer, **David Viskochil**)

Summary – MPNST Symposium, Aspen, June 7 & 8, 2002

Goal: To develop rational approaches to prevention and effective treatment of malignant peripheral nerve sheath tumors (MPNSTs) in individuals with neurofibromatosis type 1 (NF1).

Objectives:
1. Identify those individuals with NF1 who are at highest risk to develop MPNST.
2. Implement screening protocols for early detection of MPNST in NF1 patients.
3. Evaluate genetic and biologic processes that contribute to the development and progression of peripheral nerve sheath tumors in NF1.
4. Assess the use of neo-adjuvant chemotherapy in the treatment of MPNST.

Strategy: Identify and develop NF1-sarcoma centers with dedicated personnel to identify, screen, and treat individuals with NF1 and MPNST in a uniform way. This would entail the development of protocols, recruitment of patients, application of standards of care, collection of biologic specimens and implementation of treatment protocols. These centers would also be involved in applied and basic research focused on the pathophysiology of MPNSTs, including tissue evaluation, genetic analyses, and the development of animal models. Translational research would include the use of the mouse model for MPNST to develop more effective treatment modalities for MPNST in NF1 patients.

Design:

1. Identify those individuals with NF1 who are at highest risk to develop MPNST.

The prevalence of MPNST among NF1 has been estimated to be 2-to-5% from cross-sectional studies, but recent investigations indicate the lifetime risk is closer to 10%. In addition, there may be subgroups in the NF1 population who are at substantially higher risk, and those not in the high-risk population may have a substantially lower risk. A prospective case-control study is proposed to identify factors that are associated with high risk for MPNST in NF1 patients.

A case-control approach will be used to compare NF1 patients who have confirmed MPSNT to NF1 patients without MPNST. Possible differentiating features that will be evaluated include burden, type and location of plexiform neurofibromas, constitutional large-deletion genotype, family history of sarcoma, therapeutic radiation, and NF1-related neuropathy. NF1-related MPNST cases between 18 and 35 would be recruited for detailed medical and family histories, physical examination, whole-body imaging, and *NF1* mutation analysis to detect large deletion (~10% of NF1 patients). Controls with NF1 but without MPNST would be matched for age and gender. A study that includes 100 cases and 300 controls would have a power of 0.84 to demonstrate a 3-fold increase in the frequency of a factor that occurs in 5% of the controls.

2. Implement screening protocols for early detection of MPNST in individuals with NF1.

At present, histologic evaluation of the entire tumor is the only reliable means of distinguishing MPNSTs from the more common, benign plexiform neurofibromas in individuals with NF1. As with most sarcomas, complete surgical excision predicts better outcome, and this is optimized by early detection. Magnetic resonance imaging locates the site and extent of the lesion, but it does not reliably detect malignancy. Biopsy may miss the site of malignngncy or fail to identify the highest grade of malignancy in a heterogenoeous lesion. Recent advances in imaging technology

provide opportunities to evaluate the role of 18Fluorodeoxyglucose positron emission tomography in the diagnosis of MPNSTs. We propose a 5-year, collaborative, prospective study to determine whether ^{18}FDG PET can reliably diagnose MPNST in NF1 patients who have symptoms associated with peripheral nerve sheath tumors..

NF1 patients aged 6-75 years who have a plexiform neurofibroma and 1 or a combination of manifestations (persistent pain lasting more than 1 month, change in texture from soft to hard, rapid increase in size, neurological deficit) will be eligible to enroll in the study. The site and extent of each PNST will be documented by clinical evaluation and MRI scanning. All participants will undergo ^{18}FDG PET. Patients with positive ^{18}FDG PET will undergo tru-cut/open targeted biopsy with MRI and PET registration. The tumor will be excised and the grade will be confirmed on histology. The patient will receive further treatment and follow-up based on the grade of the tumor and clinical need. Individuals with negative ^{18}FDG PET will have tru-cut/open biopsy of the plexiform neurofibroma. If the biopsy is negative for malignancy they will be followed clinically every 6 months for 5 years. Our second goal is to determine whether PET is able to detect asymptomatic second primary tumors in individuals with MPNST and NF1. All participants will undergo ^{11}C-methionine PET in addition to ^{18}FDG PET in centers that have on-site chemistry facilities. Methionine has been useful in detecting low-grade tumors in the central nervous system and may allow a rapid test (within 30 minutes post-injection) to evaluate MPNST formation in plexiform neurofibromas.

3. Evaluate tumor tissue for molecular changes important in malignant transformation of PNSTs.

The factors most important in transforming benign PNST to MPNST have not been identified. In general, both alleles of the *NF1* gene are inactivated in proliferating Schwann cells in benign peripheral nerve sheath tumors. Other molecular changes must occur to transition from the benign to malignant state. A group of studies to evaluate MPNST specimens is proposed.

Immunohistochemical markers and biochemical studies would be performed on all MPNST tissue that has been surgically removed. Peripheral blood lymphocytes, serum, paraffin blocks, fresh frozen tissue, and live cells from the tumor would also be processed for study. These tissue specimens would be stored and distributed through a tissue repository for NF1-related tumors that has already been established at Washington University in St. Louis. This facility would serve as a repository for all biopsy samples and any tumors excised in protocols outlined in objectives 2 and 4.

Specific aims to be addressed focus on the following; determination of molecular markers that distinguish benign versus malignant PNSTs, identification of specific genes that are differentially expressed in MPNSTs, identification of specific genetic changes in MPNSTs that may be associated with clinical outcomes, identification of molecular changes that distinguish MPNST from other spindle cell sarcomas, and determination of molecular markers that distinguish NF1-related MPNSTs from sporadic MPNSTs. The Tissue Core will be comprised of multiple laboratories devoted to the immunohistochemical and molecular analysis of MPNSTs in addition to the pathology lab that will process and store specimens by standard protocols.

4. Assess neo-adjuvant chemotherapy in the treatment of stage III/IV MPNSTs.

Present approaches to treatment of MPNST are not effective, and 5-year survival is currently 40% or less. Among all protocols, surgical excision is the mainstay of therapy. Adjuvant chemotherapies have not been rigorously applied in a coordinated effort. Taking cues from the benefit that has been demonstrated for neo-adjuvant therapy in patients with Ewings sarcoma, we

propose to undertake similar trials for stage III & IV MPNSTs. This study will include MPNST patients who have NF1 as well as those who do not have NF1, because we do not know if the response will differ between these groups.

Patients 18 years or older with high-grade MPNST that is greater than 5 cm in diameter and staged as III or IV will be eligible for this multicenter study. Subjects will be stratified for the presence or absence of NF1. Patients will be treated with 2 cycles of neo-adjuvant chemotherapy (ifosfamide and adriamycin) prior to surgical resection. The primary objective of this trial is to determine the response rate of the tumor based on volumetric imaging studies, dynamic MR, PET scanning, and histology. Responding patients would be continued on therapy, whereas non-responders would proceed to surgical resection with post-operative radiation. Secondary objectives include the identification of molecular differences that correlate with responsive tumors versus non-responsive tumors, and determination of EFS and OS with this regimen.

A diagram outlining the 4 proposed studies is attached. There are 2 cores; an administrative core with clinical coordinators and statistical and database support, and a tissue core for multiple biologic studies. We envision regional academic institutions that can combine successful sarcoma services with NF1 Clinics as regional centers that will carry out the main work effort outlined in the 4 studies. Interaction between each center to rigorously obtain clinical information and perform standard protocols is imperative to the success of the Program. It is likely that subjects would travel to the regional center for initial evaluations and tumor surgery.

The topic of animal models was not discussed in detail at the MPNST Symposium, although presentations from the NNFF International Consortium for the Molecular Biology of NF1 and NF2 (Aspen, June 9-12) clearly demonstrated the development of a model for MPNST in mice. These tumors are highly reproducible, and it could potentially provide a way to screen novel therapies for the treatment and/or prevention of MPNSTs. Correlation between human and murine MPNST is required. Importantly, a rational basis for the selection of candidate therapeutic agents is imperative to optimally screen mice for "breakthrough" therapies, before initiating human protocols. We anticipate linking the NF1-Sarcoma Program described herein with a mouse core(s) in the development and implementation of future protocols.

Chairs

Jan Friedman
David Gutmann
Lee Helman
Rosalie Ferner
David Viskochil

Participants (see attached list)

Michael O'Doherty
Michael Smith
Abhijit Guha
Arie Perry
Cheryl Coffin
Jonathan Lucas
Karen Albritton
Harry Joe
Minesh Mehta
George Demetri
Ian Judson
Bruce Korf
Judy Small
Gareth Evans
Victor Mautner

Acknowlegment: National Neurofibromatosis Foundation, Inc., Peter Bellermann
University of Utah, Kathy Moran

Published manuscript: Ferner R and Gutmann D. Meeting Report; International consensus statement on malignant peripheral nerve sheath tumors in neurofibromatosis 1 Cancer Research 2002:62;1573-1577. (Acknowledgement to **David Viskochil**)

[*Cancer Research* 62, 1573-1577, March 1, 2002]

Meeting Report

International Consensus Statement on Malignant Peripheral Nerve Sheath Tumors in Neurofibromatosis 1[1]

Rosalie E. Ferner[2] and David H. Gutmann[3]
Division of Clinical Neurosciences, Department of Neuroimmunology, Guy's King's and St. Thomas' School of Medicine, London, SE1 1UL United Kingdom

ABSTRACT

Neurofibromatosis 1 (NF1) is an autosomal dominant tumor predisposition syndrome in which affected individuals have a greatly increased risk of developing malignant peripheral nerve sheath tumors (MPNSTs). These cancers are difficult to detect and have a poor prognosis. Because patients may present to specialists from widely differing disciplines, the association with NF1 is often not appreciated, and there is no cohesive pattern of care. A multidisciplinary group of 33 clinicians and scientists with specialist knowledge in MPNST and NF1 reviewed the current published and unpublished data in this field, and distilled their collective experience to produce a consensus summary on MPNST in NF1. The known clinical, pathological, and genetic information on MPNST in NF1 was collated, and a database was established to record information in a uniform manner. Subgroups with a higher risk of developing MPNST were identified within the NF1 population. The consortium formulated proposals and guidelines for clinical and pathological diagnosis, surgical management, and medical treatment of MPNST in individuals with NF1. A multidisciplinary team approach to the management of this complex disorder is advocated. Progress can be made by adopting the guidelines proposed by this consortium and by widespread dissemination of standardized information. Collaborative research should be promoted with the aim of harnessing advances in molecular genetics to develop targeted therapies for MPNST in people with NF1.

Introduction

NF1[4] is an autosomal dominant neurocutaneous disorder, with an estimated birth incidence of 1 in 2500 (1) . The *NF1* gene on chromosome 17q 11.2 was identified by positional cloning, and its protein product, neurofibromin, functions as a tumor suppressor (2, 3, 4) . One of the functions of neurofibromin is to reduce cell proliferation by accelerating the inactivation of the proto-oncogene *p21-ras,* which has a pivotal role in mitogenic intracellular signaling pathways (4) . The cardinal and defining features of NF1 are café au lait macules, neurofibromas, skinfold freckling, iris Lisch nodules, and characteristic osseous dysplasia (5) . The complications of the disorder are legion and may involve any of the body systems (6) .

Individuals affected with NF1 harbor an increased risk of developing both benign and malignant tumors, supporting the classification of NF1 as a tumor predisposition syndrome. The most common tumor in individuals with NF1 is the neurofibroma, a heterogeneous benign peripheral nerve sheath tumor (7 , 8) . Neurofibromas may appear as discrete, dermal neurofibromas, focal cutaneous or s.c. growths, dumbbell-shaped intraforaminal spinal tumors, or nodular or diffuse plexiform neurofibromas. Plexiform neurofibromas are composed of the same cell types as dermal neurofibromas but have an expanded extracellular matrix and often have a rich vascular supply. They develop along a nerve and may involve multiple branches, nerve roots, and plexi. Impingement on surrounding structures may cause functional compromise, and soft tissue and bone hypertrophy may occur (9) .

Plexiform neurofibromas were clinically visible in 30% of 125 NF1 patients in a South Wales population study (10) . Forty four percent of plexiform neurofibromas (32 of 72 patients) were diagnosed before 5 years of age in one clinic-based study (11) suggesting that many plexiform neurofibromas are congenital lesions. Multiple plexiform neurofibromas occur in 9–21% of cases (10, 11, 12) . Although MPNST can develop in individuals in the general population, individuals with NF1 have a significantly increased risk. These tumors arise frequently in preexisting plexiform neurofibromas, which are very uncommon in people who do not have NF1. MPNSTs are often difficult to detect, metastasize to the lung, liver, brain, soft tissue, bone, regional lymph nodes, skin, and retroperitoneum, and have a poor prognosis (13) . Because patients with MPNSTs may present to specialists from widely differing disciplines, the association with NF1 is often not appreciated, and there is no consistent or widely accepted pattern of care.

Aims.

In this unique meeting, the aim was to establish an international, multidisciplinary consortium of experts on MPNST and NF1. The purpose was to collate the known clinical and genetic information about these tumors and to set up a standardized database to record information in a uniform manner. In addition, the goal was to formulate guidelines for clinical and pathological diagnosis, surgical management, and medical treatment. Moreover, strategies were proposed

for developing targeted therapies for NF1-associated MPNSTs, taking into account the recent advances in molecular biology.

Materials and Methods

An international, multidisciplinary group of clinicians and scientists with a specialist interest in soft tissue sarcomas (MPNST) and NF1 was invited. Invitations were sent to clinicians working in specialist soft tissue sarcoma centers or large neurofibromatosis clinics and to individuals with research publications in these fields. The current knowledge in this field was reviewed based on personal expertise and the medical literature. Subsequently, the specialists pooled their collective experience to produce a consensus group summary on MPNST in NF1.

Results

Clinical Consensus Group.

It is generally accepted that MPNSTs occur in about 2–5% of NF1 patients compared with an incidence of 0.001% in the general population (13) . However, there may be differences in cross-sectional *versus* longitudinal determinations of risk for MPNST, and the lifetime risk for MPNST could be as high as 10% (14) . The majority of patients present in the second and third decades of life, and tend to be younger than their counterparts with MPNSTs in the general population (13) . We have also identified MPNSTs in NF1 patients as young as 7 years and as old as 63 years of age. Clinicians should be alerted to the possible diagnosis of MPNST when a patient with NF1 develops unremitting pain not otherwise explained, rapid increase in size of a plexiform neurofibroma, change in consistency from soft to hard, or a neurological deficit.

Most NF1-associated MPNSTs appear to arise within preexisting plexiform neurofibromas. This observation suggests that individuals with NF1 and plexiform neurofibromas warrant increased surveillance for development of MPNST, and those with many or very extensive plexiform neurofibromas may have the highest risk. However, the natural history of plexiform neurofibromas has not been clearly defined, and these tumors may undergo periods of rapid growth followed by periods of relative quiescence. As such, rapid growth is not always a prelude to malignancy. This issue is currently being addressed by an international study using clinical assessment and volumetric MRI (Clinical Coordinator, Bruce Korf, Boston, MA).

There is no evidence that dermal neurofibromas or flat superficial plexiform neurofibromas undergo malignant transformation, and they do not require close monitoring. Nodular plexiform tumors associated with large peripheral nerve sheaths and extensive tumors involving the brachial, lumbar, or sacral plexus may give rise to MPNSTs and, therefore, merit heightened awareness. Plexiform neurofibromas, which are more centrally located and are more extensive, appear to have a higher likelihood of undergoing malignant change. Individuals with a "neurofibromatous" neuropathy might also have an increased risk of developing MPNST, because they develop dermal neurofibromas in early childhood and have diffuse plexiform involvement of the spinal nerve roots and peripheral nerves (15) .

Patients in whom a microdeletion of the *NF1* locus is detected tend to have higher numbers of discrete dermal neurofibromas at earlier ages and might have a higher incidence of MPNST than the overall NF1 population (16) . The increased risk of MPNST in this group could be readily tested by comparing the frequency of *NF1* microdeletions detected by fluorescence *in situ* hybridization of peripheral blood lymphocytes in NF1 patients with and without MPNST.

MPNSTs are often difficult to detect, because the clinical indicators of malignancy may also be features of active, benign plexiform neurofibromas. A MRI should be performed to locate the site, extent, and change in size of the plexiform neurofibroma, but it does not reliably determine malignant transformation. The diffuse nature of the plexiform neurofibroma may preclude total removal because of impingement on surrounding structures and neurological deficit.

PET with the glucose analogue ^{18}FDG is a dynamic imaging technique, which permits the visualization and quantification of glucose metabolism in cells and reflects the increase in metabolism in malignant tumors (17 , 18) . A retrospective study of 18 NF1 patients demonstrated that ^{18}FDG PET is a potentially useful, noninvasive method for detecting malignant change in plexiform neurofibromas (19) . However, the distinction between low-grade MPNSTs and benign plexiform neurofibromas was not clear in all of the cases. It is recommended that a prospective study with clinical, radiological, and pathological correlation be undertaken to evaluate the value of ^{18}FDG PET in the detection of malignant change in NF1. The new tracer ^{18}F-thymidine, which detects DNA turnover, might be helpful in distinguishing low-grade MPNSTs from active, benign plexiform neurofibromas in future PET-based studies.

Scrupulous documentation of information on NF1 patients with MPNST will play a vital part in optimizing the management of this condition. Data should be recorded in a standardized database, which should be circulated to sarcoma units and to specialists in neurology, genetics, surgery, and oncology, who are likely to encounter these patients. Demographic details, confirmation of the diagnosis of NF1, history of cancer in the individual and family, clinical and radiological features of the MPNST, and pathological description of the tumor need to be included. Documentation of treatment modalities and outcome is essential. It is anticipated that molecular analysis of constitutional DNA and tumor material may play a pivotal role in determining therapeutic protocols.

Pathology Consensus Group.

The options for diagnosis include fine needle aspiration, Tru-Cut needle biopsy, open incisional biopsy, and excisional biopsy. Fine needle aspiration is inadequate for the assessment of tumor type and grade, because dissociated tumor cells are obtained and architectural relationships lost. Tru-Cut needle biopsy is the method of choice when undertaken in a multidisciplinary team setting using expert radiological, surgical, and pathological advice. If sufficient tissue cores are taken and the specimen is sent fresh, techniques can be used such as imprint cytology to ensure that tumor tissue is present. Representative fresh tissue cores can be snap frozen in liquid nitrogen for molecular biological studies and research.

An open incisional biopsy provides more tissue for diagnosis and ancillary studies, but the sample is limited to one site. For this reason, it is necessary to ensure that the sample is representative and includes the areas suspected of malignancy. The combination of open incisional biopsy with multiple Tru-Cut needle biopsies from different areas may overcome this difficulty. This technique should be carefully planned so that future surgical resection margins are not compromised. An excisional biopsy should be reserved for small, superficially located tumors, which can be resected with a clear margin. This provides the most material for diagnosis and research. The technique of targeted biopsy using ^{18}FDG PET and magnetic resonance registration is being developed in specialist centers and may be of potential benefit in the management of this group of heterogeneous tumors.

The minimum histological examination should comprise sections stained with conventional tinctorial stains including H&E and reticulin. In addition, immunohistochemical stains for S100 protein, the skeletal muscle markers desmin and myogenin, and a proliferation marker (MIB1) are required. Other spindle cell tumors may be excluded with appropriate immunohistochemical markers. In the future, there might be a place for the routine application of stains for known tumor suppressor genes or oncogenes (*p53, erbB2, p16,* and *p27*), for molecular analysis of NF1 and NF2 expression, and for determination of RAS activity (see "Molecular Biology Consensus Group").

The pathological features of MPNST reveal a fusiform or globoid mass associated with a nerve. Necrosis, pseudocystic change, or hemorrhage may be found. Histologically, the tumor is composed of spindle cells arranged in cellular fascicles (20) . Divergent differentiation may occur, including rhabdomyoblastic change encountered in the malignant triton tumor variant (20 , 21) .

The pathological criteria for malignancy include invasion of surrounding tissues by tumor cells, vascular invasion, marked nuclear pleiomorphism, necrosis, and the presence of mitoses (20) . Even a single mitotic figure may be significant, particularly in a tumor with hypercellularity and nuclear atypia. The significance of the mitoses depends on the prognostic value of increased cell proliferation. Therefore, the most clinically relevant question is how best to determine malignant transformation in these tumors. The methods available for assessing growth rate include direct counting of observed mitotic figures, the estimation of proliferation index using immunostains, flow cytometry, other molecular techniques, or the detection of an imbalance between apoptosis and proliferation. The accurate prediction of biological behavior may depend on the interpretation of a combination of histological and immunohistochemical features.

There is a histological spectrum of peripheral nerve sheath tumors ranging from the clearly benign to the clearly malignant, and it is often possible to distinguish between high-grade and low-grade tumors. However, a significant number of tumors, the so-called "atypical neurofibromas" do not fit into any defined grading system (20 , 22 , 23) . These may be locally aggressive but are less likely to metastasize. In addition, there are a few histologically low-grade tumors that behave aggressively. The application of molecular techniques to determine the gene expression profiles of gene expression in these tumors may help pathologists to predict biological behavior and outcome more accurately. The correlation with new imaging techniques may also help to resolve this issue.

Surgery Consensus Group.

The aim of surgery is complete removal of the lesion with tumor-free margins (13) . Biopsy of the lesion is essential before surgery is undertaken (see "Pathology Group" statement). Small lesions should be widely resected, and larger tumors should be as widely excised as possible (=" src="/math/ge.gif" border=010 cm) to avoid centripetal spread. Reconstruction of the nerve after surgery for brachial and lumboscaral plexus lesions is not advocated, because it does not restore useful function and may compromise the adequacy of the surgical excision. Amputation may be indicated for extensive tumors and for MPNST, which recur after apparently adequate excision.

Patients should have baseline MRI 2–3 months after surgery. Additional imaging studies and their timing will depend on the patient symptoms and the nature of the primary tumor, ^{18}FDG PET might be a useful screening investigation in the future, because it provides both a local and a body-wide scan within a single investigation for this group of "at-risk" patients.

Oncology Consensus Group.

It is not clear whether patients with NF1 and MPNST have a different clinical course or response to treatment compared with their counterparts in the general population. The current management of MPNST should be identical to that of any other soft tissue tumor in that successful treatment depends on complete surgical excision. Radiotherapy provides local

control and may delay the onset of recurrence but has little effect on long-term survival. Adjuvant radiotherapy should be given wherever possible for intermediate- to high-grade lesions and for low-grade tumors after a marginal excision. Chemotherapy for adult soft tissue sarcomas is usually confined to the treatment of metastatic disease. Few drugs have been shown to be effective, and treatment comprises single agent doxorubicin or a combination of doxorubicin and ifosfamide (24) . Although such treatment is not curative, it may achieve useful palliation for many patients, and complete, long-lasting remissions are observed in rare instances. Moreover, it may be useful in the preoperative setting to downstage patients with unresectable primaries.

MPNST appears to be of intermediate chemosensitivity, less responsive than synovial sarcoma, but more chemosensitive than refractory diseases such as alveolar soft part sarcoma. The partial response rate with the best available chemotherapy is likely to be in the range of 25–30% (24) . Controversy surrounds the use of adjuvant chemotherapy. A meta-analysis has shown a significant benefit at 10 years in terms of progression-free survival for both local and distant relapse (25) . However, the magnitude of any overall survival benefit is small (4% and not statistically significant). Chemotherapy might be used to improve local disease control for marginally resected lesions at sites where an adequate dose of radiotherapy is difficult to deliver.

Recent advances in sarcoma therapy have resulted from an improved understanding of the molecular biology of individual diseases. The discovery of mutations in the *c-kit* gene, resulting in overexpression of a constitutively activated c-kit molecule in gastrointestinal stromal tumors, has been of paramount therapeutic importance. This has not only resulted in CD117 overexpression becoming the hallmark diagnostic test for this disease but has lead to a new form of treatment for a disease that was hitherto untreatable. The receptor tyrosine kinase inhibitor STI571 (Glivec) is a potent inhibitor of KIT and has been reported to result in dramatic tumor regressions in these patients, which thus far appear to be durable (26) .

Similarly, it is the hope that new agents, which target the RAS-RAF- mitogen-activated protein/ERK kinase-extracellular signal-regulated kinase pathway, may prove effective against MPNST in NF1. In these tumors, loss of the inhibiting function of neurofibromin results in increased p21-ras signaling. Anti-RAS pathway drugs include farnesyl transferase inhibitors, which block the ability of RAS to reach the membrane where it is activated (27) . However, there are now specific inhibitors of targets downstream of RAS, such as mitogen-activated protein/ERK kinase, that are also being developed for clinical study. Given the success of Glivec, it is clear that tyrosine kinase inhibitors can be developed that are both selective and effective, and hopefully one of these agents will prove effective against MPNSTs.

Molecular Biology Consensus Group.

Significant progress has been made in recent years in elucidating the molecular genetics and biology of MPNST in NF1. Surgical specimens and cell lines from patients with MPNST and NF1 exhibit loss of *NF1* gene (neurofibromin) expression and high levels of RAS activity (28, 29, 30) . Studies of benign neurofibromas from NF1 patients have demonstrated that loss of *NF1* gene expression and increased RAS activation alone is not sufficient for MPNST formation, and that additional genetic alterations (p27-Kip1, p53, and p16) are required for malignant transformation (31, 32, 33, 34, 35) . The generation of mice with targeted mutations in the *NF1* gene has confirmed this notion in that loss of *NF1* expression appears to be sufficient for the formation of tumors with pathological features of plexiform neurofibromas, whereas MPNST development is dependent on functional inactivation of p53 (36 , 37) .

Our ability to more accurately predict tumor behavior and response to therapy is likely to derive from studies aimed at defining the molecular changes seen in these tumors. A variety of different genetic alterations have been reported in MPNSTs, but it is not clear that any of these are causally related to tumorigenesis or malignant progression. Moreover, it is not known whether a subset of these changes will predict the clinical course or define whether a specific form of therapy is likely to be more efficacious. Additional research is required to define the intracellular signaling pathway abnormalities primarily responsible for plexiform neurofibroma or MPNST growth, and to delineate which specific downstream effectors of RAS mediate RAS mitogenic signaling. Similarly, research efforts to define the genetic changes in addition to *NF1* loss that are required for plexiform neurofibroma malignant transformation also may identify additional therapeutic targets for MPNST drug design. These studies have the potential to identify gene expression profiles that are specifically associated with particular MPNST subtypes or plexiform neurofibromas most likely to undergo malignant change ("molecular fingerprint").

The importance of an international tissue bank for MPNSTs to facilitate basic science and translational research cannot be overstated. This would involve storing fresh-frozen specimens, corresponding normal nerve specimens when available, and normal tissue or blood, as well as paraffin sections. These specimens need to be well characterized pathologically and to be linked to molecular, pathological, and clinical-epidemiological patient data. Both NF1-associated and sporadic MPNSTs should be stored in this tumor bank to determine whether the noted molecular and clinical-epidemiological characteristics are similar in these two groups.

Conclusions.

MPNST is a devastating complication of NF1, which should be managed by multidisciplinary teams of clinicians and scientists with expertise in the diagnosis and treatment of this disease. Clinical and molecular genetic studies should identify NF1 patients who are at high risk of developing MPNST. The establishment of an international database will

permit the standardized recording of clinical, pathological, and treatment data, and outcome measures. The development of imaging methods such as PET scanning will aid in distinguishing MPNST from benign plexiform neurofibromas. Recent advances in molecular genetics have provided exciting opportunities to develop targeted therapies for these tumors, which will be helped by the establishment of an international tissue bank. Our ability to translate these advances into rational clinical trials represents the challenge for the immediate future.

Appendix 1

Medical Consensus Group. Gareth Evans, Department of Medical Genetics, St. Mary's Hospital, Manchester, United Kingdom; Rosalie Ferner, Department of Clinical Neurosciences, GKT School of Medicine, Guy's Hospital, London, United Kingdom; Jan M. Friedman, Division of Medical Genetics, University of British Columbia, Vancouver, Canada; Susan Huson, Department of Medical Genetics, Churchill Hospital, Oxford, United Kingdom; Viktor Mautner, Department of Neurology, Klinikum Nord, Ochsenzoll, Hamburg, Germany; Michael O'Doherty, Clinical PET Center, GKT School of Medicine, St. Thomas' Hospital, London, United Kingdom; David Viskochil, Division of Medical Genetics, University of Utah, Salt Lake City, UT.

Surgery Consensus Group. Rolfe Birch, Peripheral Nerve Injury Unit, Royal National Orthopaedic Hospital, London, United Kingdom; Ivo DeWever, Department of Surgical Oncology, University Hospital, Leuven, Belgium; Rheinhard Friedrich, Department of Surgery, University Hospital, Hamburg-Eppendorf, Germany; Henk Giele, Department of Plastic Surgery, Radcliffe Infirmary, Oxford, United Kingdom; Robert Grimer, Department Of Orthopaedics, Royal Orthopaedic Hospital, Birmingham, United Kingdom; Jonathan Lucas, Soft Tissue Tumor Unit, Department of Orthopaedics, Guy's and St. Thomas' Hospitals, London, United Kingdom; Michael Smith, Soft Tissue Tumor Unit, Department of Orthopaedics, Guy's and St. Thomas' Hospitals, London, United Kingdom; Meirion Thomas, Sarcoma and Melanoma Unit, Royal Marsden Hospital, London, United Kingdom.

Pathology Consensus Group. Cheryl Coffin, Division of Pediatric Pathology, University of Utah School of Medicine, Salt Lake City, UT; Susan Robinson, Department of Neuropathology, King's College Hospital, London, United Kingdom; Ann Sandison, Department of Pathology, Charing Cross Hospital, London, United Kingdom; Susan Standring, Division of Neuroscience, Guy's King's and St. Thomas' School of Medicine, London, United Kingdom; Andreas von Deimling, Department of Neuropathology Charité, Humboldt University, Berlin, Germany.

Oncology Consensus Group. Adrian Jones, Department of Radiotherapy, Churchill Hospital, Oxford, United Kingdom; Ian Judson, CRC Center for Cancer Therapeutics, Institute of Cancer Research, Sutton, United Kingdom; Chris Mitchell, Department of Pediatric Oncology, John Radcliffe Hospital, Oxford, United Kingdom; Rif Pamukcu, Cell Pathways, Inc., Horsham, PA; Mike Stevens, Department of Pediatric Oncology, Birmingham Children's Hospital, Birmingham, United Kingdom; Jeremy Whelan, The Meyerstein Institute of Oncology, The Middlesex Hospital, London, United Kingdom.

Molecular Biology Consensus Group. Abhijit Guha, Labatts Brain Tumor Center, The Hospital for Sick Children, Toronto, Ontario, Canada; David Gutmann, Department of Neurology, Washington University School of Medicine, St. Louis, MO; Chris Jones, Department of Pathology, University of Wales College of Medicine, Cardiff, United Kingdom; Eric Legius, Center for Human Genetics, University Hospital, Leuven, Belgium; Anne Mudge, MRC Laboratory for Molecular Biology, University College, London, United Kingdom; Thorsten Rosenbaum, Children's Hospital, Heinrich-Heine University, Dussledorf, Germany; Meena Upadhyaya, Institute of Medical Genetics, University of Wales College of Medicine, Cardiff, United Kingdom.

ACKNOWLEDGMENTS

We thank Bruce Korf for critical insights during the preparation of this document and J. M. Friedman for editorial comments. Susan Huson proposed the topic for this consensus meeting. Rosalie E. Ferner and David H. Gutmann organized the MPNST Consensus Group with assistance from Meena Upadhyaya, David Viskochil, and Roberta Tweedy (British Neurofibromatosis Association).

FOOTNOTES

The costs of publication of this article were defrayed in part by the payment of page charges. This article must therefore be hereby marked *advertisement* in accordance with 18 U.S.C. Section 1734 solely to indicate this fact.

[1] Supported by Wellcome Trust, The British Neurofibromatosis Association, and Cell Pathways, Inc. RFN1RFN1

[2] To whom requests for reprints should be addressed, at Division of Clinical Neurosciences, Department of Neuroimmunology, Second Floor Hodgkin Building, Guy's King's and St. Thomas' School of Medicine, London Bridge, London SE1 1UL, United Kingdom. Phone: 44-207-848-6122; Fax: 44-207-848-6123; E-mail: rosalie.ferner@kcl.ac.uk. RFN2RFN2

[3] D. H. G. was the leader of the following working groups: Medical Consensus Group, Surgery Consensus Group, Pathology Consensus Group, Oncology Consensus Group, and Molecular Biology Consensus Group. Members of the groups are listed in the Appendix. RFN3RFN3

[4] The abbreviations used are: NF1, neurofibromatosis 1; MPNST, malignant peripheral nerve sheath tumor; MRI, magnetic resonance imaging; ^{18}FDG, ^{18}F-fluorodeoxyglucose; PET, positron emission tomography. RFN4

Received 10/ 9/01; accepted 1/ 4/02.

REFERENCES

1. Huson, S. M., Clark, P., Compston, D. A. S., and Harper, P. S. A genetic study of von Recklinghausen neurofibromatosis in South East Wales. 1: prevalence, fitness, mutation rate, and effect of parental transmission on severity. J. Med. Genet., *26:* 704–711, 1991.
2. Viskochil D., Buchberg A. M., Xu G., Cawthon R. M., Stevens J., Wolff R. K., Culver M., Carey J. C., Copeland N. G., Jenkins N. A., White R., O'Connell P. Deletions and a translocation interrupt a cloned gene at the neurofibromatosis type 1 locus.. Cell, *62:* 187-192, 1990.
3. Wallace M. R., Marchuk D. A., Anderson L. B., Letcher R., Odeh H. M., Saulino A. M., Fountain J. W., Brereton A., Nicholson J., Mitchell A. L., Brownstein B. H., Collins F. S. Type 1 neurofibromatosis gene: identification of a larger transcript disrupted in three NF1 patients.. Science (Wash. DC), *249:* 181-186, 1990.
4. Xu G. F., O'Connell P., Viskochil D., Cawthon R., Robertson M., Culver M., Dunn D., Stevens J., Gesteland R., White R., Weiss R. The neurofibromatosis type 1 gene encodes a protein related to GAP.. Cell, *62:* 599-608, 1990.
5. National Institutes of Health Consensus Development Conference Statement Neurofibromatosis. Arch. Neurol., *45:* 575–578, 1988.
6. Ferner R. E. Clinical aspects of neurofibromatosis 1. Upadhyaya M. Cooper D. N. eds. . Neurofibromatosis 1 from Genotype to Phenotype, *:* 21-38, Bios Scientific Publishers Ltd. Oxford 1998.
7. von Recklinghausen, F. D. Über die Multiplen Fibrome der Haut und Ihre Beziehung zu den Multiplen Neuromen. Berlin: A Hirschwald, 1882.
8. Harkin J. C. Pathology of nerve sheath tumors.. Ann. NY Acad. Sci., *486:* 147-154, 1986.
9. Korf B. R., Huson S. M., Needle M., Ratner N., Rutkowski L., Short P., Tonsgard J., Viskochil D. Report of the working group on neurofibroma4-27, The National Neurofibromatosis Foundation, Inc. 1997.
10. Huson S. M., Harper P. S., Compston D. A. S. Von Recklinghausen Neurofibromatosis.. A clinical and population study in South East Wales. Brain, *111:* 1355-1381, 1988.
11. Waggoner D. J., Towbin J., Gottesman G., Gutmann D. H. A clinic-based study of plexiform neurofibromas in neurofibromatosis 1.. Am. J. Med. Genet., *92:* 132-135, 2000.
12. Friedman J. M., Birch P. H. Type 1 neurofibromatosis.. A descriptive analysis of the disorder in 1, *728patients.Am.J.Med.Genet.,70:* 138-143, 1997.
13. Ducatman B., Scheithauer B., Piepgras D., Reiman H. M., Ilstrup D. M. Malignant peripheral nerve sheath tumors: a clinicopathologic study of 120 cases.. Cancer (Phila.), *57:* 2006-2021, 1986.
14. McGaughran J., Harris D. I., Donnai D., Teare D., McLeod R., Kingston H., Super M., Harris R., Evans D. G. R. A clinical study of type 1 neurofibromatosis in North West England.. J. Med. Genet., *36:* 197-203, 1999.
15. Ferner R. E., Upadhyaya M., Osborn M., Hughes R. A. C. Neurofibromatous neuropathy.. J. Neurol., *243:* S20 1996.
16. Leppig K. A., Kaplan P., Viskochil D., Weaver M., Ortenberg J., Stephens K. Familial neurofibromatosis 1 microdeletions: cosegregation with distinct facial phenotype and early onset of cutaneous neurofibromata.. Am. J. Med. Genet., *73:* 197-204, 1997.
17. Strauss, L. G., and Conti, P. S. The applications of PET in clinical oncology. J. Nucl. Med. *32:* 623–648, 1991.
18. Lucas J. D., O'Doherty M. J., Wong J. C. H., Bingham J. B., McKee P. H., Fletcher C. D. M., Smith M. A. Evaluation of fluorodeoxyglucose positron emission tomography in the management of soft tissue sarcomas.. J. Bone Joint Surg. Br. Vol., *80:* 441-447, 1998.
19. Ferner R. E., Lucas J. D., O'Doherty M. J., Hughes R. A. C., Smith M. A., Cronin B. F., Bingham J. B. Evaluation of ^{18}fluorodeoxyglucose positron emission tomography in the detection of malignant peripheral nerve sheath tumors in neurofibromatosis 1.. J. Neurol. Neurosurg. Psychiatry, *68:* 353-357, 2000.
20. Enziger, F. M., and Weiss, S. W. Benign tumors of peripheral nerves: malignant tumors of the peripheral nerves. *In:* W. Sharon, Weiss and J. R., Goldblum (eds.), Soft Tissue Tumors, Ed. 4, pp. 1111–1263. St. Louis, MO: Mosby, 2001.
21. Masson, P. Recklinghausen's Neurofibromatosis. Sensory Neuromas and Motor Neuromas. Libman Anniversary Volumes 2, pp. 793–802. New York: New York International Press, 1932.
22. Lin, B. T-Y., Weiss, L. M., and Medeiros, L. J. Neurofibroma and cellular neurofibroma with atypia. A report of 14 tumors. Am. J. Surg. Pathol., *21:* 1443–1449, 1997.
23. Coffin C. M., Dehner L. P. Cellular peripheral neural tumors (neurofibromas) in children and adolescents: a clinicopathological and immunohistochemical study.. Pediatr. Pathol., *10:* 351-361, 1990.
24. Santoro A., Tursz T., Mouridsen H., Verveij J., Steward W., Somers R., Buesa J., Casali P., Spooner D., Rankin E. Doxorubicin versus CY VADIC verses doxorubicin plus ifosfamide in first-line treatment of

advanced soft tissue sarcomas: a randomized study of the EORTC Soft Tissue and Bone Sarcoma Grou. p. J. Clin. Oncol., *13:* 1537-1545, 1995.

25. Sarcoma Meta-analysis Collaboration. Adjuvant chemotherapy for localised resectable soft-tissue sarcoma in adults: meta-analysis of individual data. Lancet, *350:* 1647–1654, 1997.
26. Van Oosterom A. T., Judson I., Verweij J., Di Paola E., Van Glabbeke M., Dimitrijevic S., Nielsen O. STI571, an active drug in metastatic gastro-intestinal stromal tumors (GIST) an EORTC Phase I study.. Proc. Am. Soc. Clin. Oncol., *20:* 1a 2001.
27. Cox A. D. Farnesyltransferase inhibitors: potential role in the treatment of cancer.. Drugs, *61:* 723-732, 2001.
28. Guha A., Lau N., Huvar I., Gutmann D., Provias J., Pawson T., Boss G. Ras-GTP levels are elevated in human peripheral nerve tumors.. Oncogene, *12:* 507-513, 1996.
29. Basu T. N., Gutmann D. H., Fletcher J. A., Glover T. W., Collins F. S., Downward J. Aberrant regulation of ras proteins in malignant tumor cells from type 1 neurofibromatosis patients.. Nature (Lond.), *356:* 663-664, 1992.
30. DeClue J. E., Papageorge A. G., Fletcher J. A., Diehl S. R., Ratner N., Vass W. C., Lowy D. R. Abnormal regulation of mammalian p21ras contributes to malignant tumor growth in von Recklinghausen's (type 1) neurofibromatosis.. Cell, *69:* 265-273, 1992.
31. Kluwe L., Friedrich R. E., Mautner V. F. Allelic loss of the NF1 gene in NF1-associated plexiform neurofibromas.. Cancer Genet. Cytogenet., *113:* 65-69, 1999.
32. Rutkowski J. L., Wu K., Gutmann D. H., Boyer P. J., Legius E. Genetic and cellular defects contributing to benign tumor formation in neurofibromatosis type 1.. Hum. Mol. Genet., *9:* 1059-1066, 2000.
33. Sherman L. S., Atit R., Rosenbaum T., Cox A. D., Ratner N. Single cell Ras-GTP analysis reveals altered Ras activity in a subpopulation of neurofibroma Schwann cells but not fibroblasts.. J. Biol. Chem., *275:* 30740-30745, 2000.
34. Nielsen G. P., Stemmer-Rachamimov A. O., Ino Y., Moller M. B., Rosenberg A. E., Louis D. N. Malignant transformation of neurofibromas in neurofibromatosis 1 is associated with CDKN2A/p16 inactivation.. Am. J. Pathol., *155:* 1879-1884, 1999.
35. Kourea H. P., Cordon-Cardo C., Dudas M., Leung D., Woodruff J. M. The emerging role of $p27^{kip}$ in malignant transformation of neurofibromas.. Am. J. Pathol., *155:* 1885-1891, 1999.
36. Cichowski K., Shih T. S., Schmitt E., Santiago S., Reilly K., McLaughlin M. E., Bronson R. T., Jacks T. Mouse models of tumor development in neurofibromatosis type 1.. Science (Wash. DC), *286:* 2172-2176, 1999.
37. Vogel K. S., Klesse L. J., Velasco-Miguel S., Meyers K., Rushing E. J., Parada L. F. Mouse tumor model for neurofibromatosis 1.. Science (Wash. DC), *286:* 2176-2179, 1999.

Human Genomic Profiling Ratio Plots – tumor 38628: years 2000 and 2003.

University of Utah
School of Medicine

Molecular Cytogenetics Research and Development

Client: Dr. Viskochil Date: 06-11-03
Patient Sample: 2002
Control Sample: Promega Male Genomic

Human Genomic Profiling Analysis Report

The following table summarizes the results derived from your microarray experiments. For each chromosome, observed losses are indicated in red in the left column while observed gains are indicated in blue in the right column. Please note that only deviations of losses and gains are reported.

Ch #	Loss	Gain
1	More pronounced loss of 1p	
2		
3	Slight loss 3pterq21	Slight gain 3q25->qter
4		slight gain 4p14->p11
5	Significant Loss 5q12->q32, q35	Significant gain 5pter->q12, q33
6		Slight gain 6q
7		Slight gain 7
8		
9	Slight loss 9pter->p11 and 9q31->q34	Slight gain 9q12q31
10		
11	Loss of entire 11	
12		
13	Significant loss of entire 13 chromosome	
14		
15	Slight loss 15q25->q26	
16	Significant loss 16q13-q22, Less significant loss 16qter, possible homozygous loss 16q	Slight gain 16p
17	Slight loss 17pter->q21	Slight gain 17q21->qter
18		Slight gain 18p11.2->qter
19	Slight loss 19q13.1->q13.3	
20	Slight loss 20p13->p12 and 20p11.2	
21	Slight loss entire chromosome	
22		
X		
Y		

Comments: Please note that copy number changes at single clones have been associated with single locus polymorphisms

SCHOOL OF MEDICINE RM. 201
30 N 1900 E · SALT LAKE CITY · UT 84132
TEL: 801.587.3582 · FAX: 801.585.5241

University of Utah
School of Medicine

Molecular Cytogenetics Research and Development

Client: Dr. Viskochil Date: 06-11-03
Patient Sample: T2000
Control Sample: Promega Male Genomic

Human Genomic Profiling Analysis Report

The following table summarizes the results derived from your microarray experiments. For each chromosome, observed losses are indicated in red in the left column while observed gains are indicated in blue in the right column. Please note that only deviations of losses and gains are reported.

Ch #	Loss	Gain
1	Slight loss of 1p	
2		Slight gain of 2
3		Slight gain 3q25->qter
4		Slight gain 4q
5	Loss 5q12->q32, q35	Slight gain 5pter->q12, q33
6	Slight loss 6p	Slight gain 6q
7		Slight gain 7
8		
9	Slight loss 9pter->p11 and 9q31->q34	Slight gain 9q12q31
10		
11	Loss of entire 11	
12	Slight loss of 12p13->p11.1	
13	Significant loss of entire 13 chromosome	
14		Slight gain 14q13->q32
15	Slight loss 15q25->q26	
16	Significant loss 16q13-q22, Less significant loss 16qter, possible homozygous loss 16q	Slight gain 16p
17	Slight loss 17pter->q21	Slight gain 17q21->qter
18		Slight gain 18p11.2->qter
19	Slight loss 19q13.1->q13.3	
20	Slight loss 20p13->p12 and 20p11.2	
21	Slight loss entire chromosome	
22		
X		
Y		

Comments: Please note that copy number changes at single clones have been associated with single locus polymorphisms

SCHOOL OF MEDICINE RM. 201
30 N 1900 E · SALT LAKE CITY · UT 84132
TEL: 801.587.3582 · FAX: 801.585.5241

University of Utah
School of Medicine

Molecular Cytogenetics Research and Development
Client: Dr. Viskochil Date: July 17, 2003
Patient Sample: 2000
Control Sample: Promega Male Genomic

Human Genomic Profiling Ratio Plots

Included in this document you will find the microarray data from your test samples. Each ratio plot comprises of normalized data from two independent arrays such that the normalized data from the array in which the test sample was labeled in Cy3 is shown in red while the normalized data from the array in which the test sample was labeled in Cy5 is shown in blue. Individual spots along the ratio plot represent the normalized ratio of individual clones linearly ordered such that the left-most clone is consistent with the p-arm terminus while the right-most clone is consistent with the q-arm terminus. Since the normalized Cy5: Cy3 ratio was computed for both arrays, a loss of a particular clone is manifested as the simultaneous deviation of the ratio plots from a modal value of 1.0, with the red ratio plot showing a positive deviation (upward) while the blue ratio plot shows a negative deviation at the same locus (downward). Conversely, DNA copy number gains show the opposite pattern.

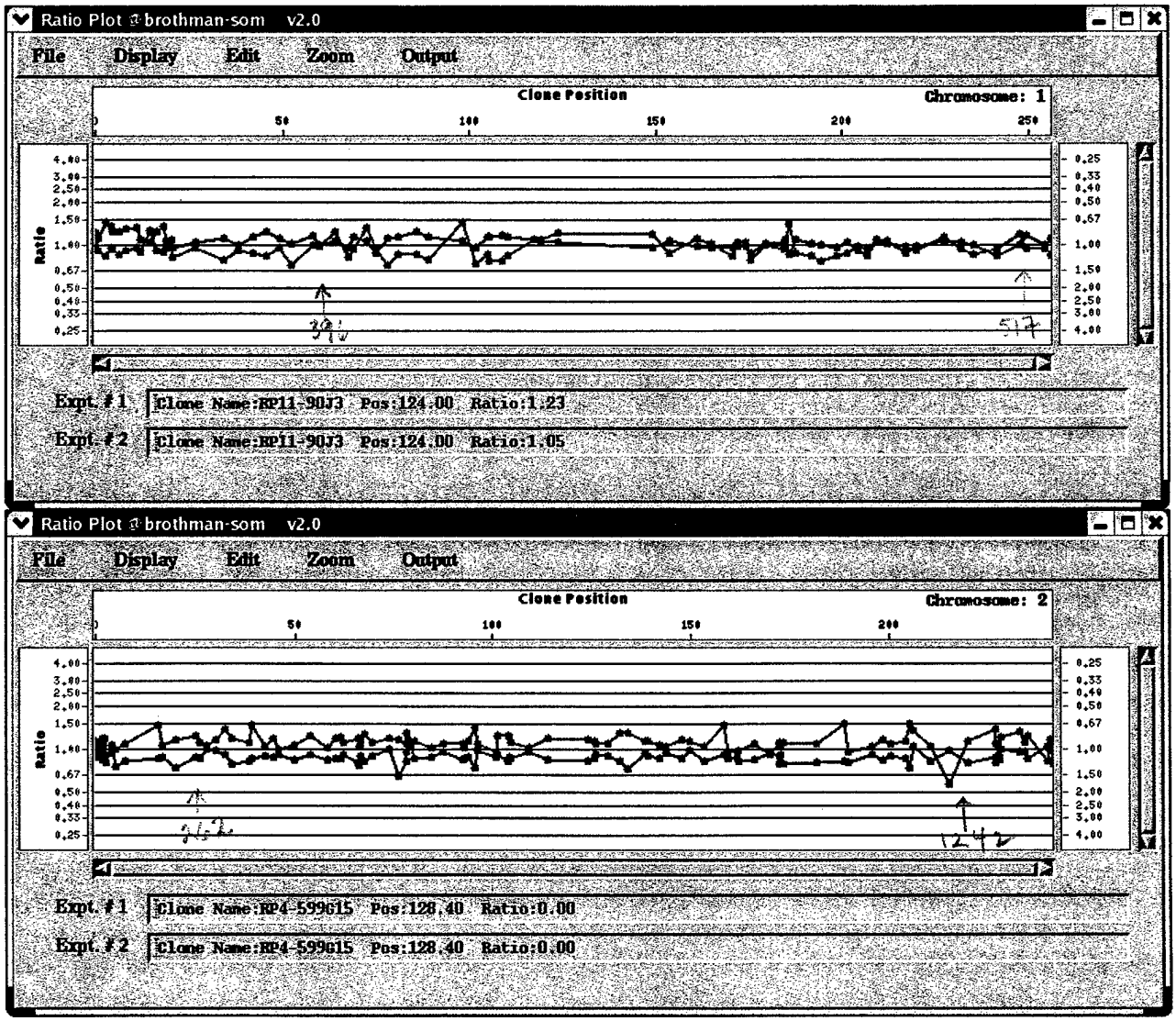

SCHOOL OF MEDICINE RM. 201
30 N 1900 E · SALT LAKE CITY · UT 84132
TEL: 801.587.3582 · FAX: 801.585.5241

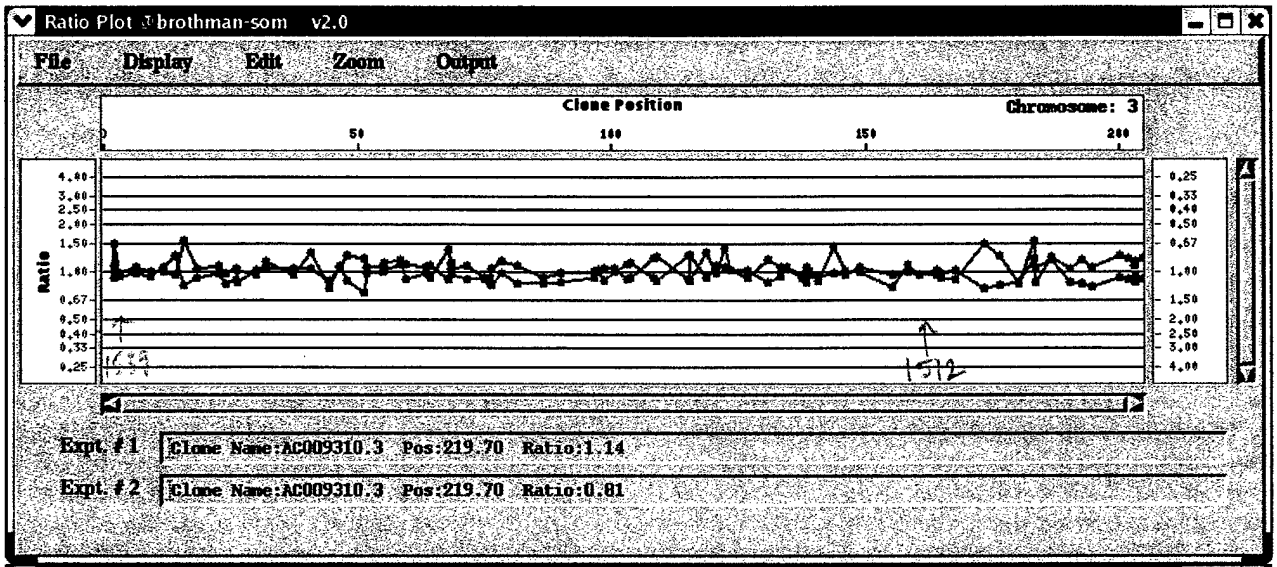

gain
3&25 -
8 loss

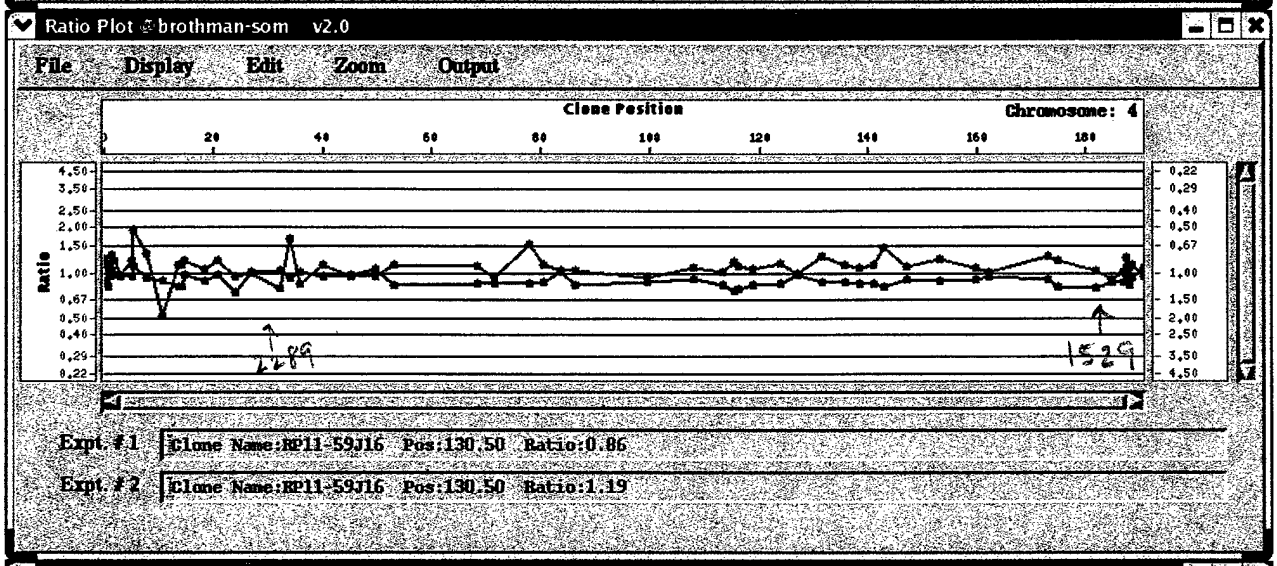

gain
4&8?

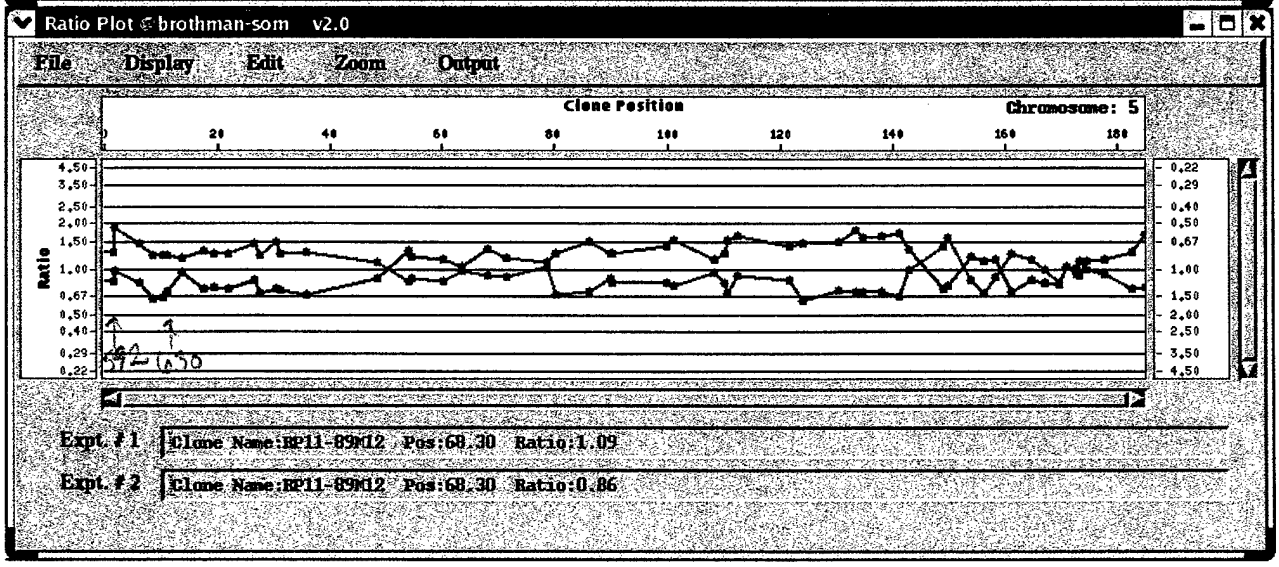

gain
5p

loss
5q

SCHOOL OF MEDICINE RM. 201
30 N 1900 E · SALT LAKE CITY · UT 84132
TEL: 801.587.3582 · FAX: 801.585.5241

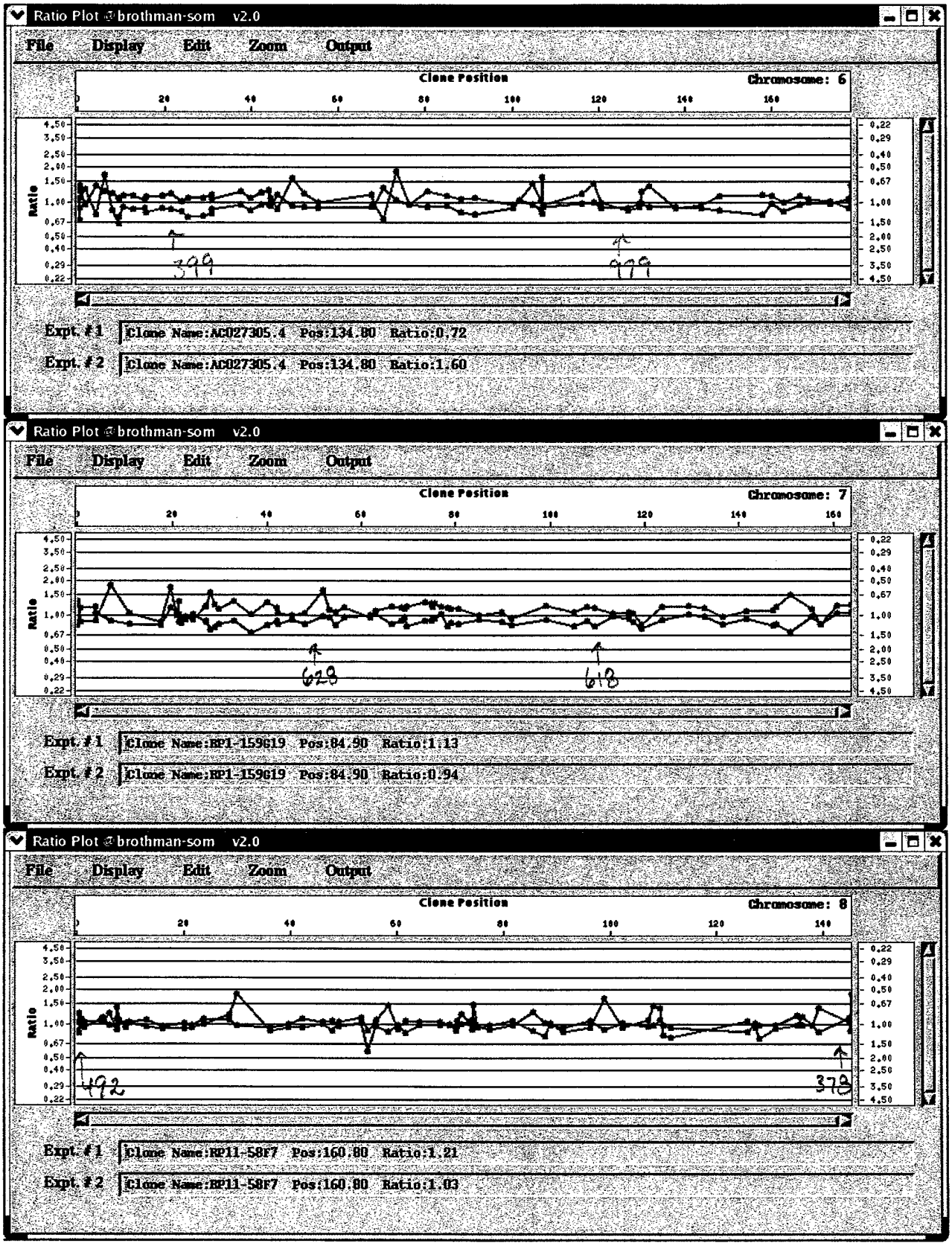

SCHOOL OF MEDICINE RM. 201
30 N 1900 E · SALT LAKE CITY · UT 84132
TEL: 801.587.3582 · FAX: 801.585.5241

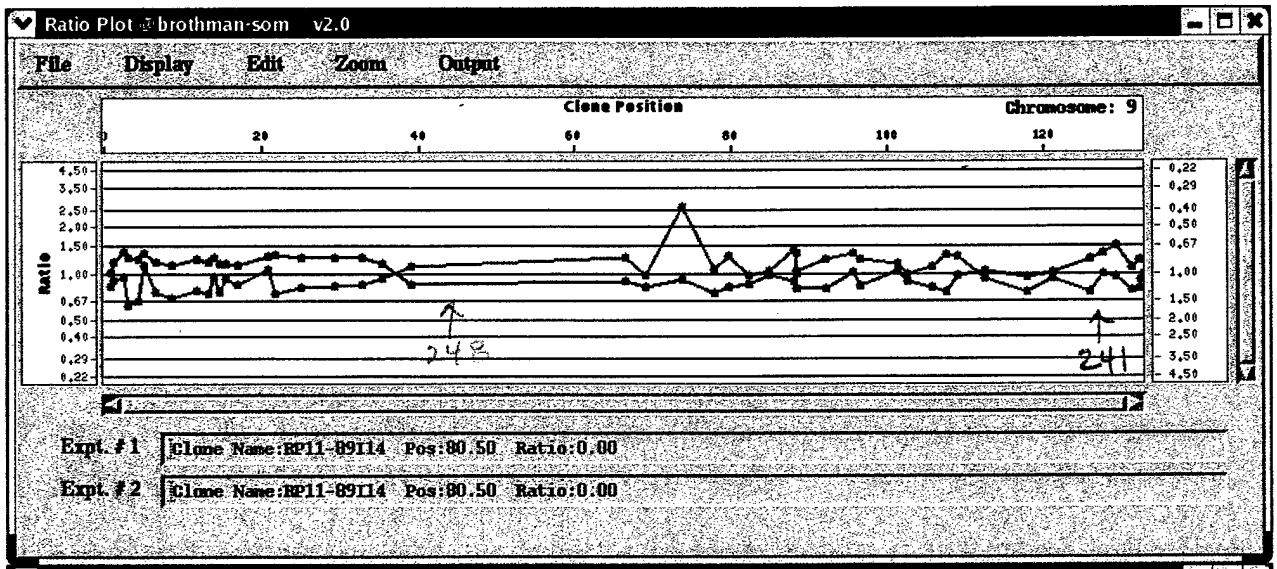

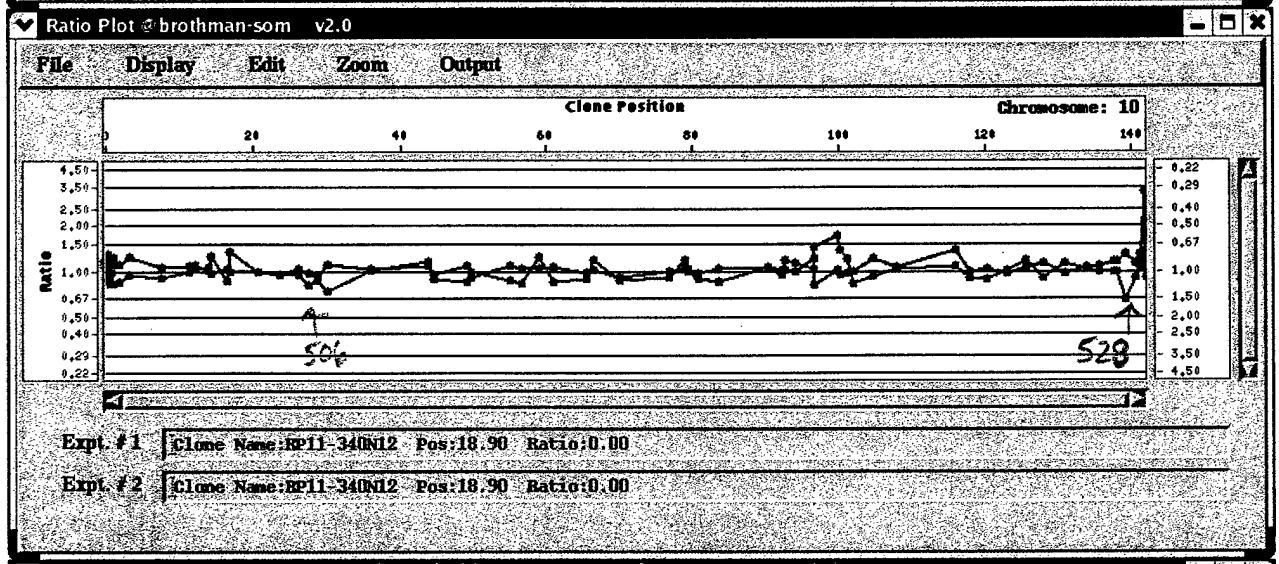

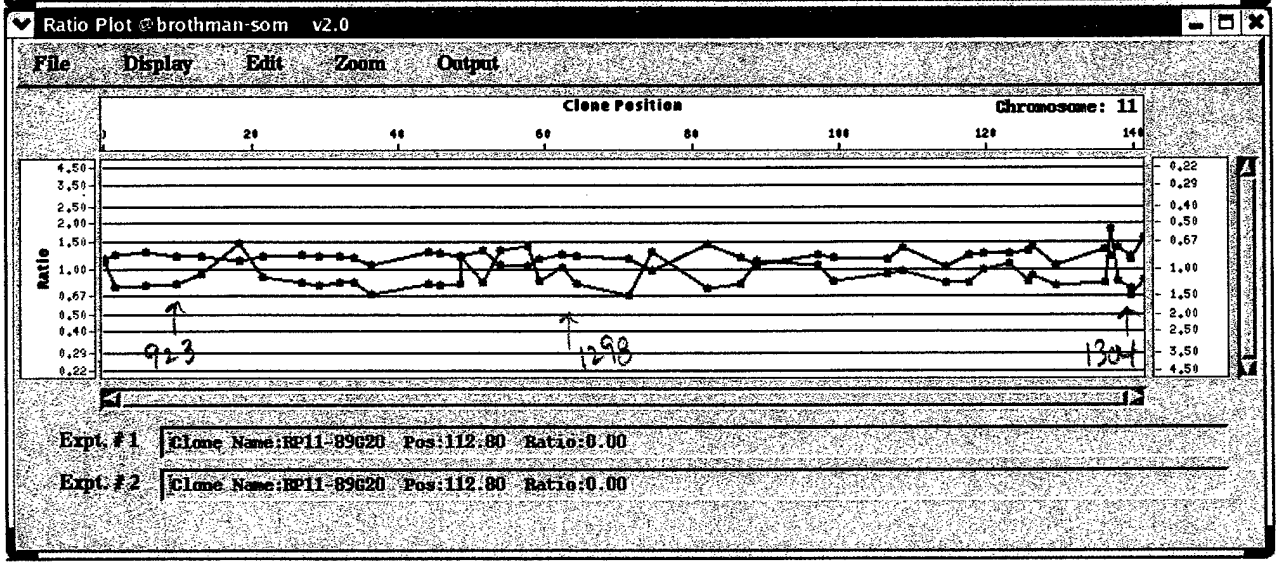

SCHOOL OF MEDICINE RM. 201
30 N 1900 E · SALT LAKE CITY · UT 84132
TEL: 801.587.3582 · FAX: 801.585.5241

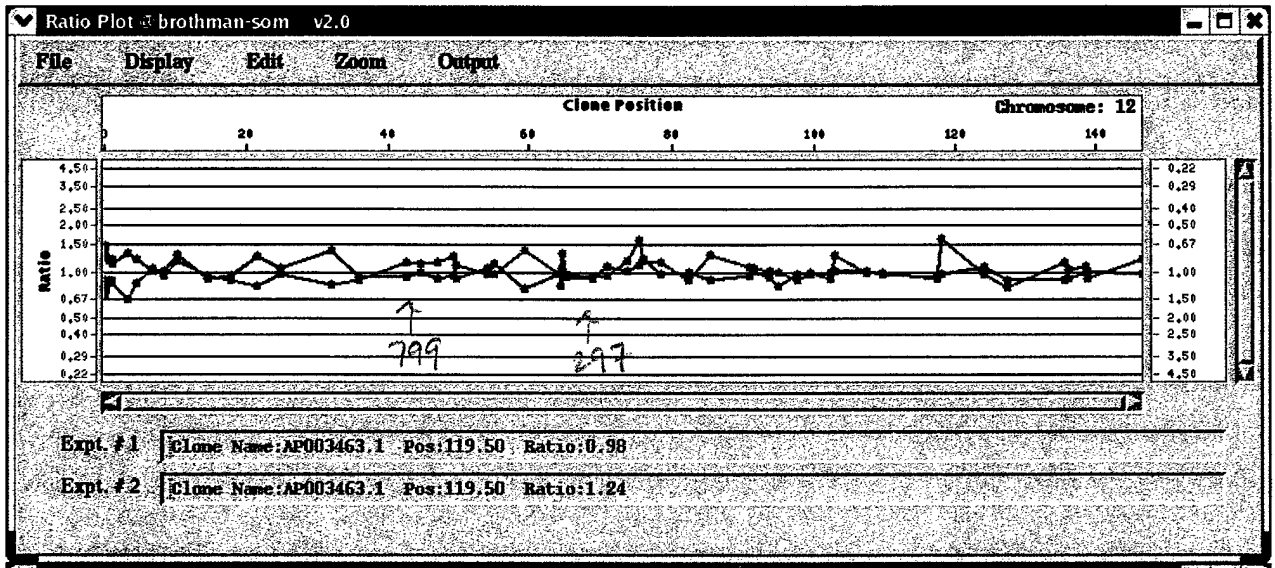

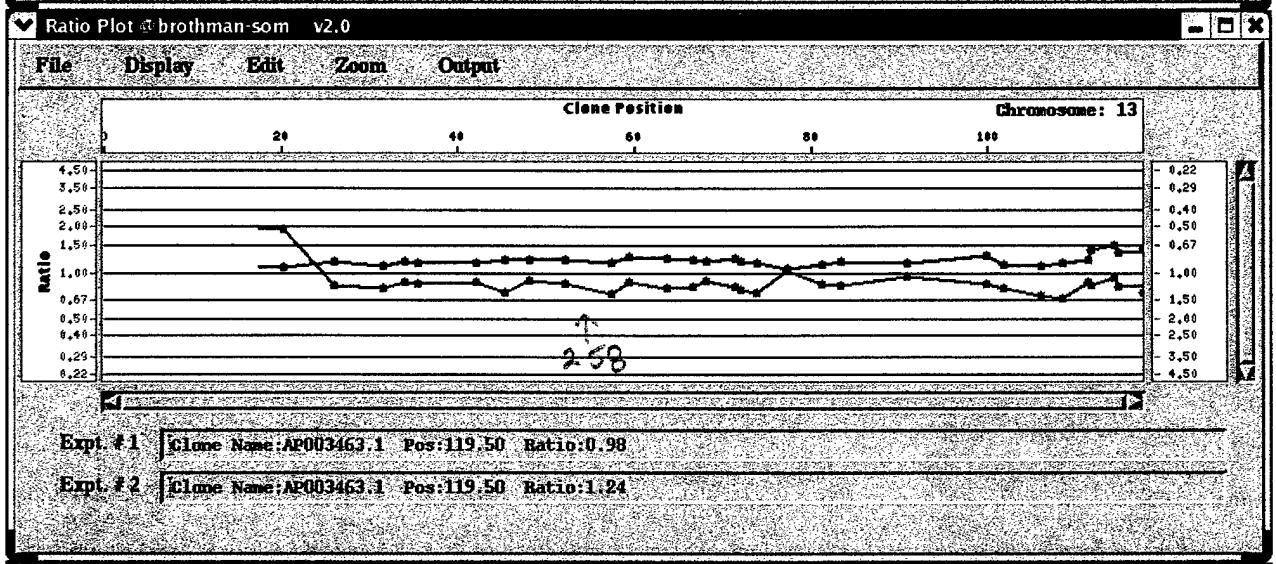

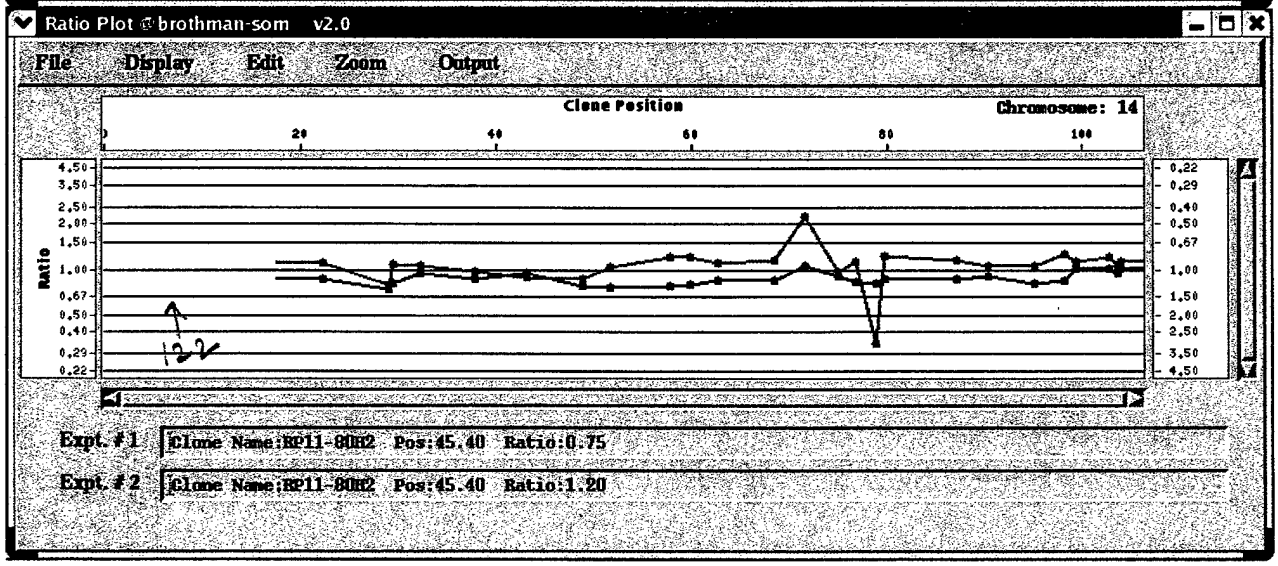

SCHOOL OF MEDICINE RM. 201
30 N 1900 E · SALT LAKE CITY · UT 84132
TEL: 801.587.3582 · FAX: 801.585.5241

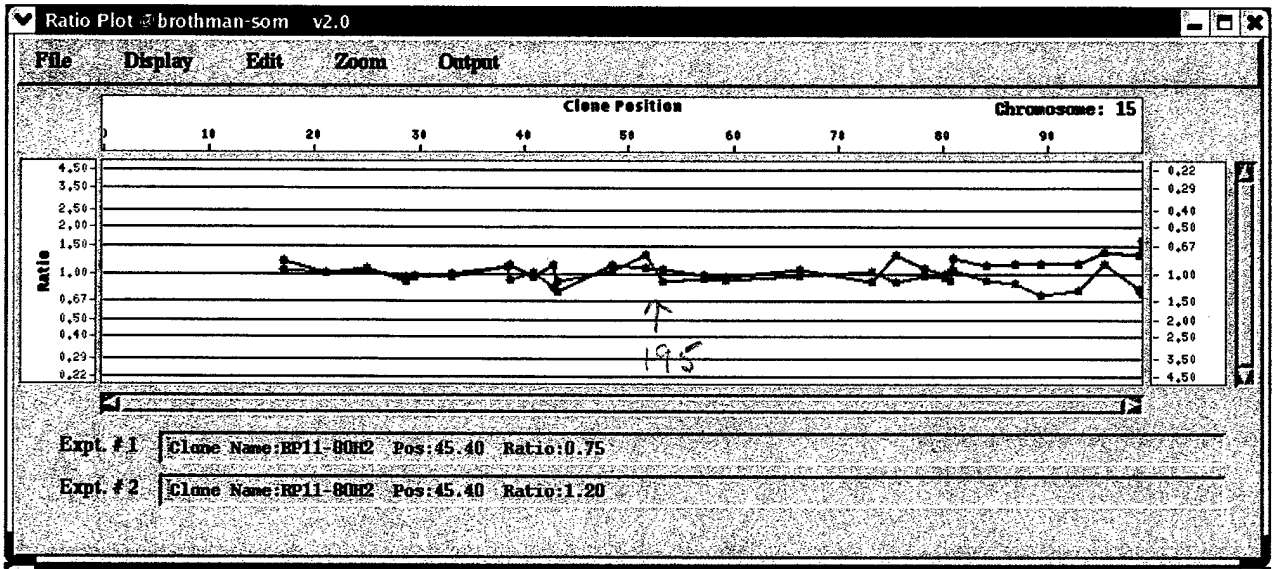

loss 15q

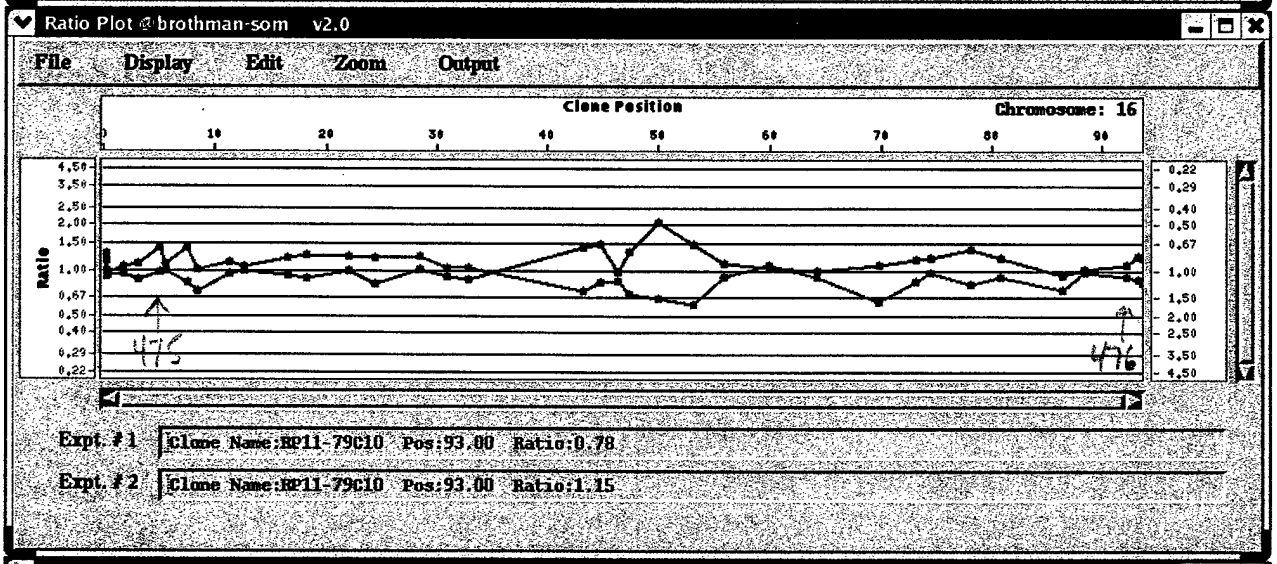

gain 16p

loss 16q

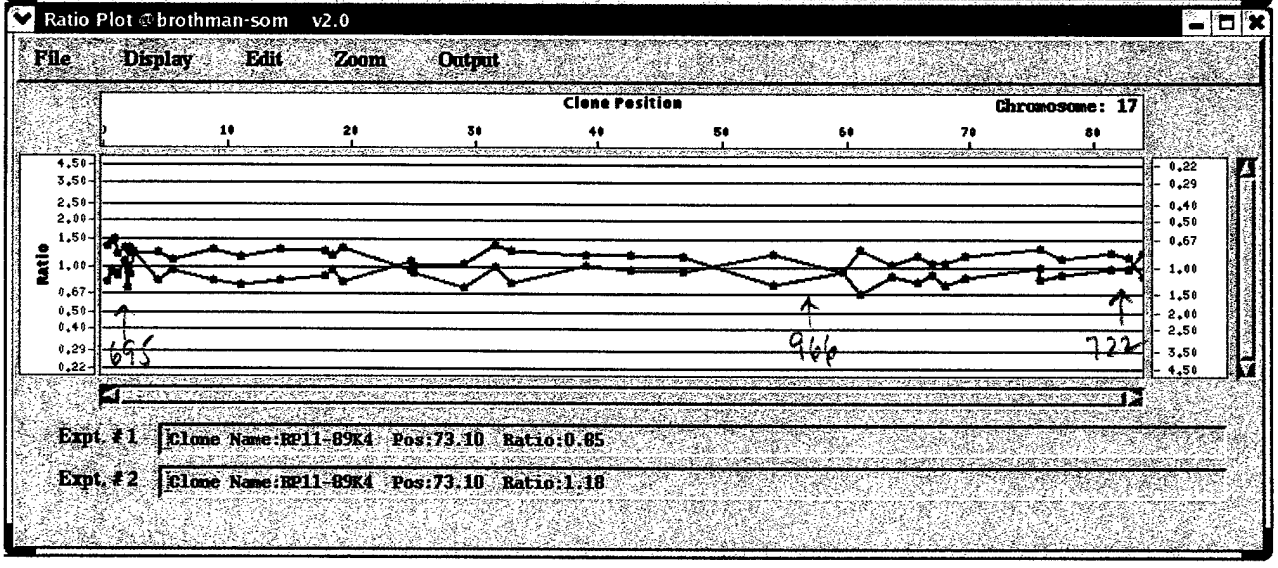

slight 17p loss

slight gain

SCHOOL OF MEDICINE RM. 201
30 N 1900 E · SALT LAKE CITY · UT 84132
TEL: 801.587.3582 · FAX: 801.585.5241

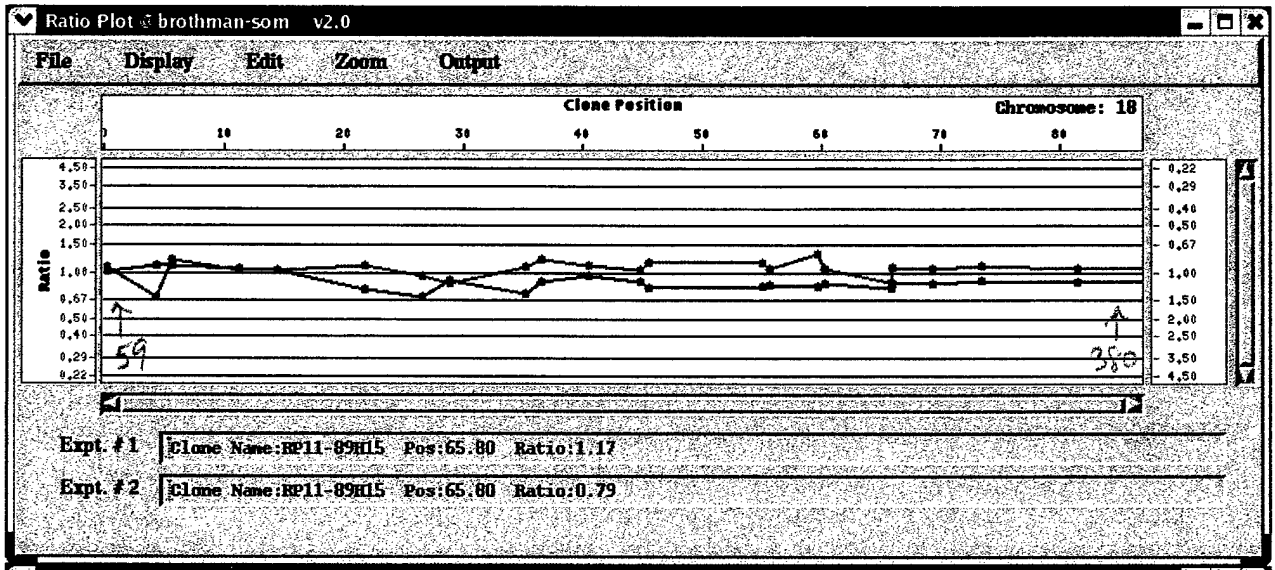

Right gain

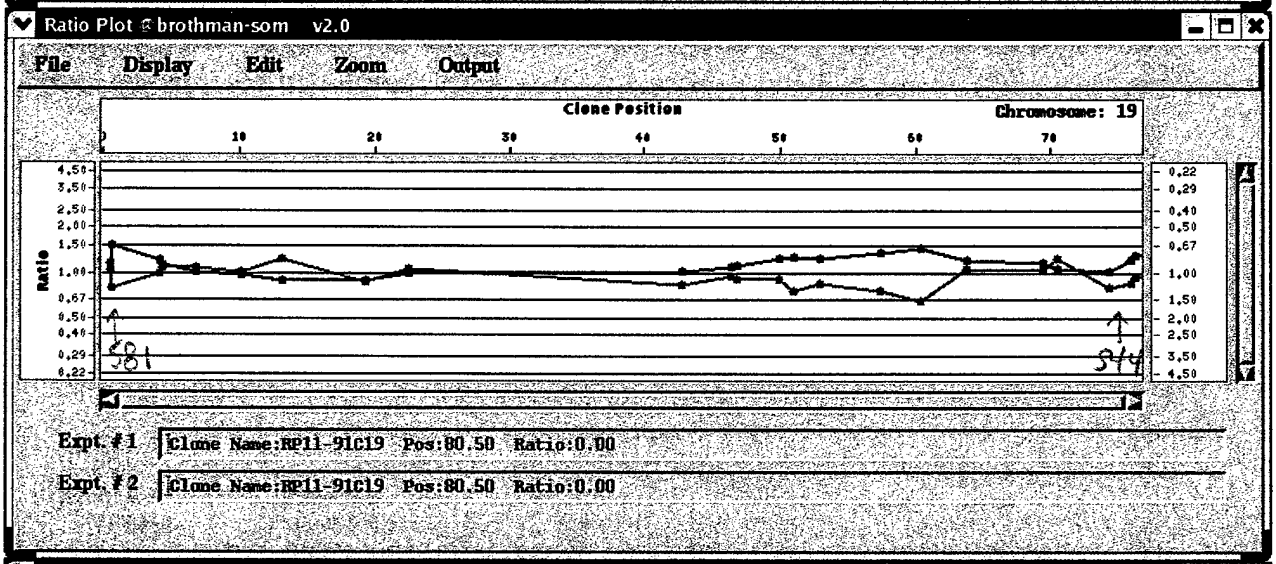

Right Loss 19p

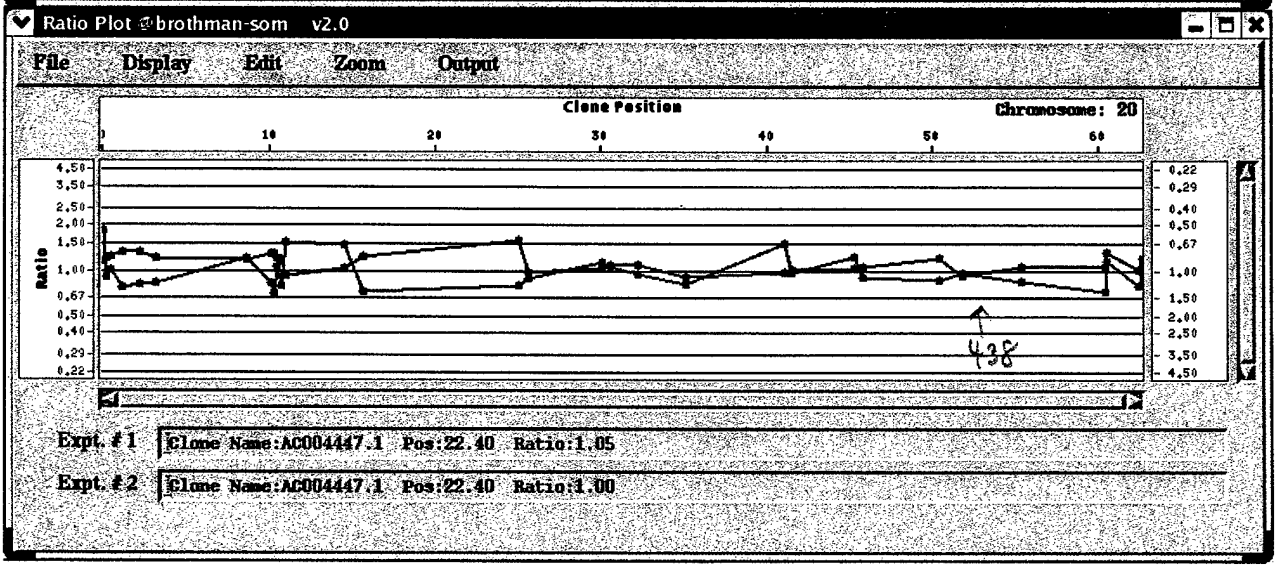

loss 20p

SCHOOL OF MEDICINE RM. 201
30 N 1900 E · SALT LAKE CITY · UT 84132
TEL: 801.587.3582 · FAX: 801.585.5241

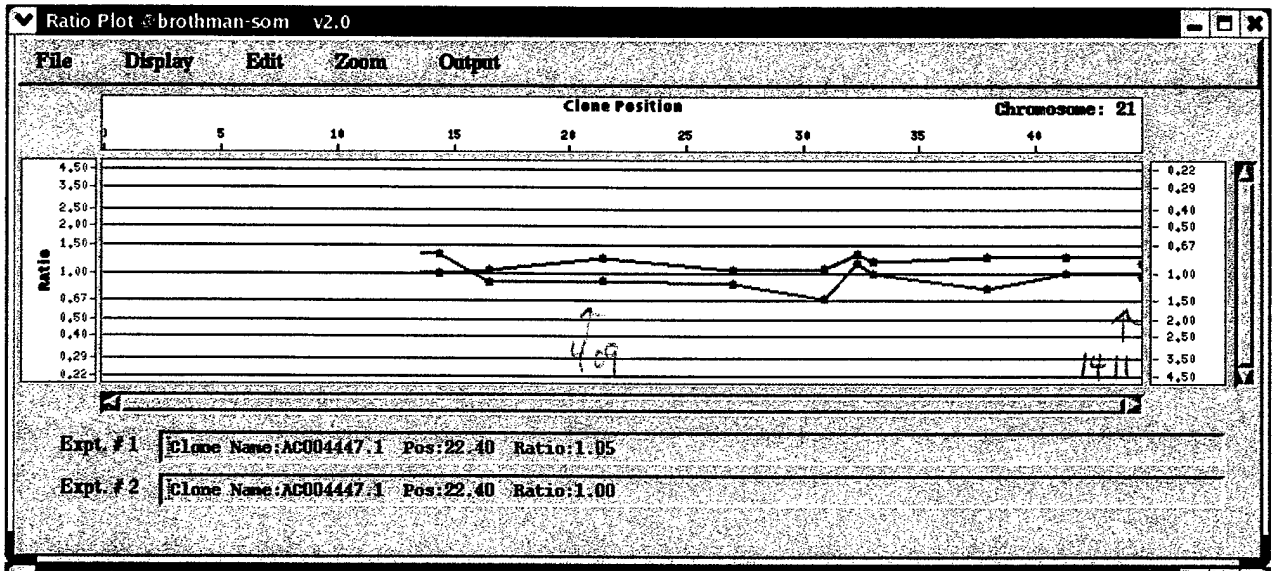

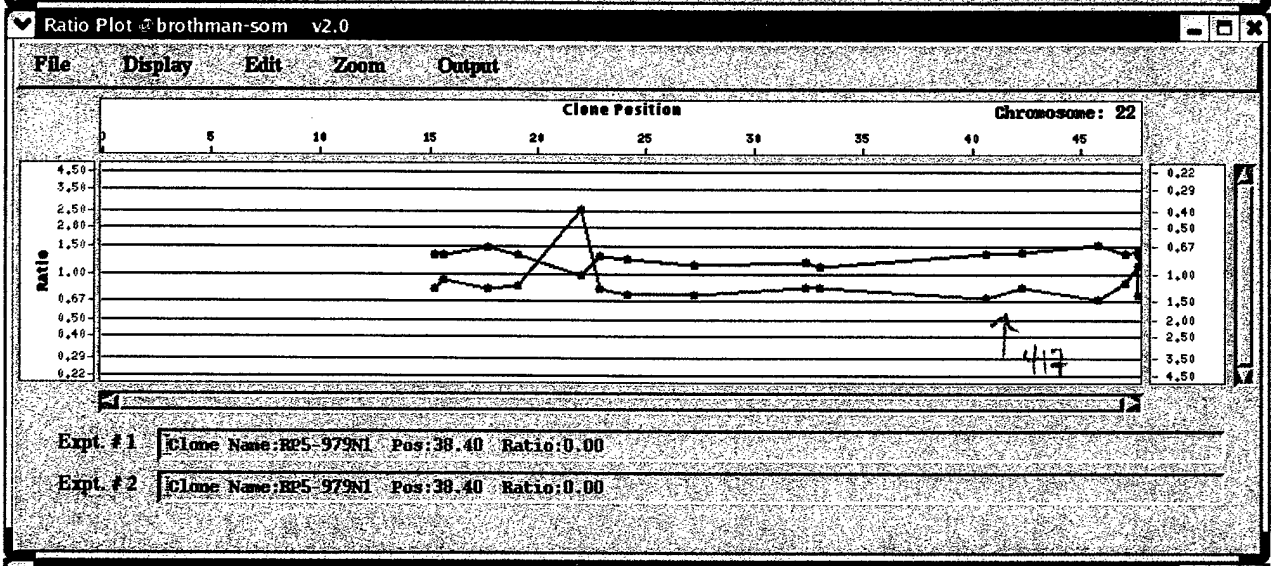

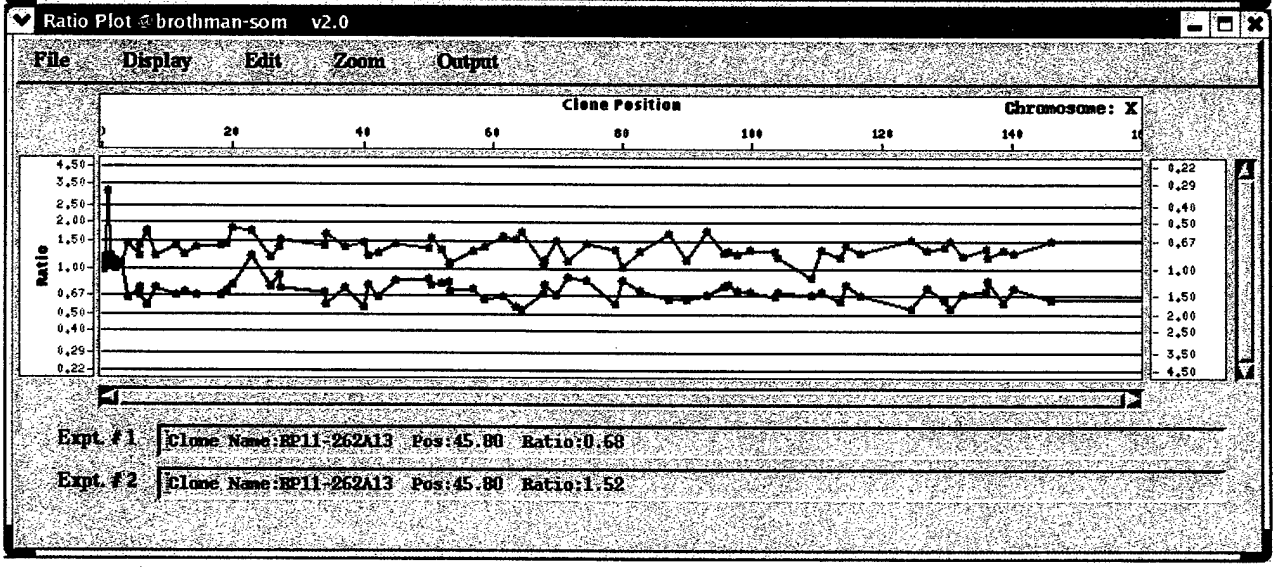

SCHOOL OF MEDICINE RM. 201
30 N 1900 E · SALT LAKE CITY · UT 84132
TEL: 801.587.3582 · FAX: 801.585.5241

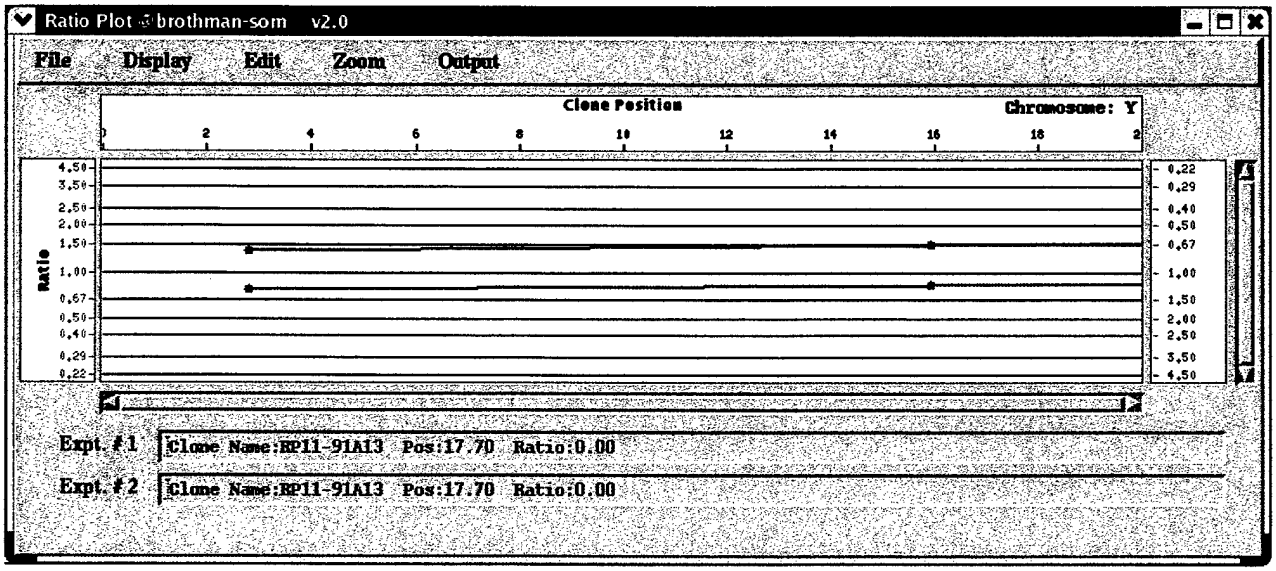

SCHOOL OF MEDICINE RM. 201
30 N 1900 E · SALT LAKE CITY · UT 84132
TEL: 801.587.3582 · FAX: 801.585.5241

University of Utah
School of Medicine

Molecular Cytogenetics Research and Development
Client: Dr. Viskochil Date: 03-07-07
Patient Sample: 2002
Control Sample: Promega Male Genomic

Human Genomic Profiling Ratio Plots

Included in this document you will find the microarray data from your test samples. Each ratio plot comprises of normalized data from two independent arrays such that the normalized data from the array in which the test sample was labeled in Cy3 is shown in red while the normalized data from the array in which the test sample was labeled in Cy5 is shown in blue. Individual spots along the ratio plot represent the normalized ratio of individual clones linearly ordered such that the left-most clone is consistent with the p-arm terminus while the right-most clone is consistent with the q-arm terminus. Since the normalized Cy5: Cy3 ratio was computed for both arrays, a loss of a particular clone is manifested as the simultaneous deviation of the ratio plots from a modal value of 1.0, with the red ratio plot showing a positive deviation (upward) while the blue ratio plot shows a negative deviation at the same locus (downward). Conversely, DNA copy number gains show the opposite pattern.

loss
1p

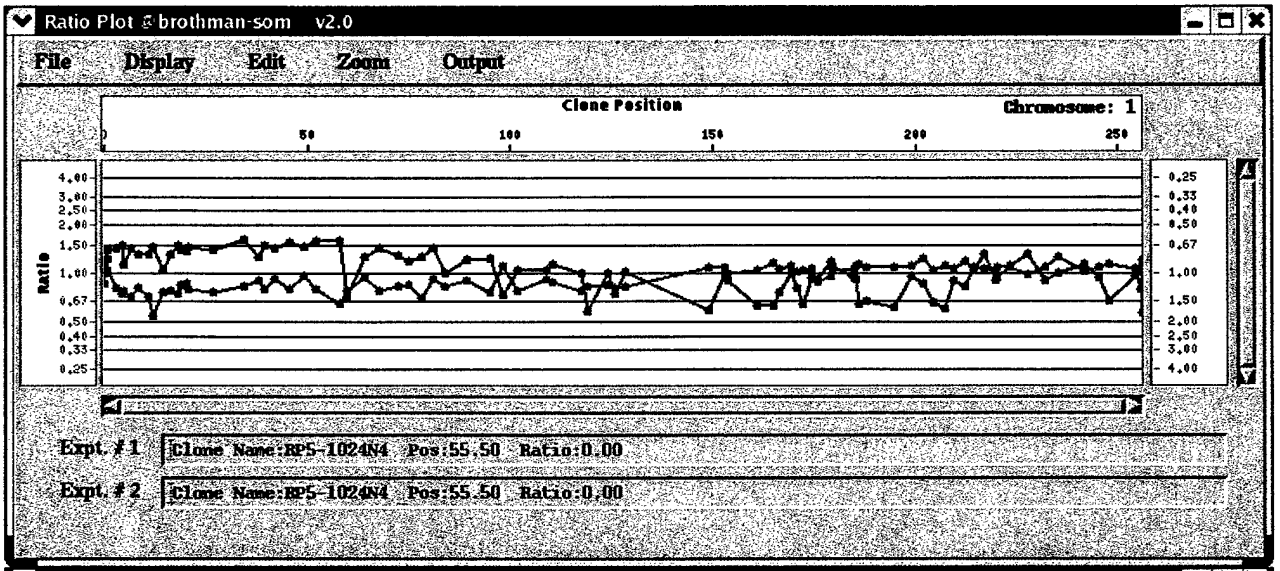

nl

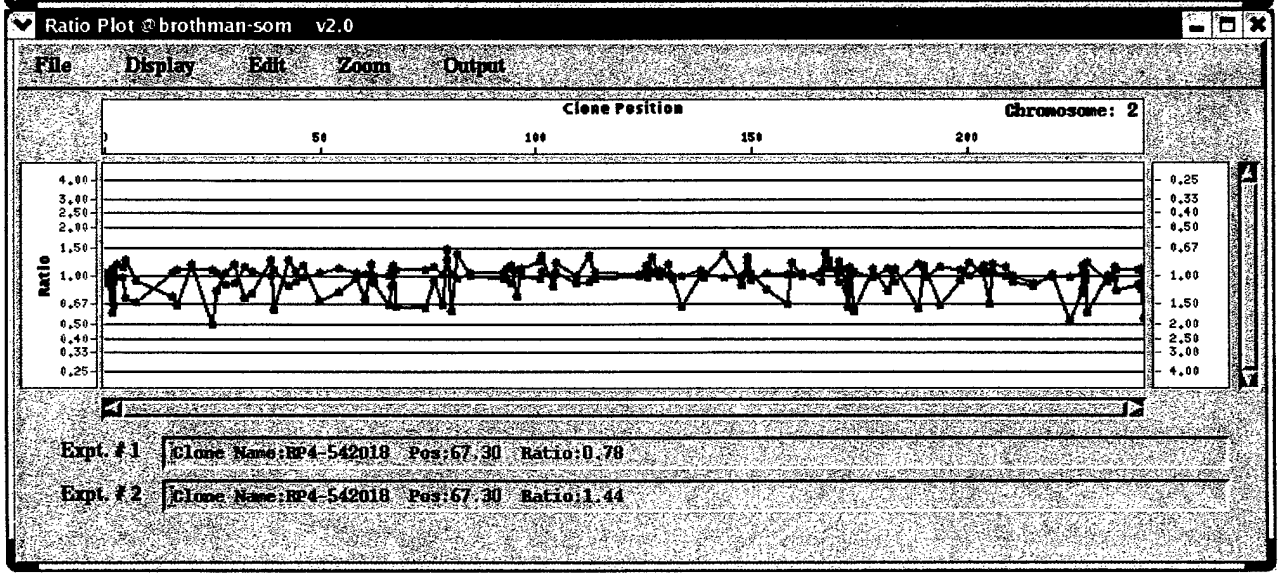

SCHOOL OF MEDICINE RM. 201
30 N 1900 E · SALT LAKE CITY · UT 84132
TEL: 801.587.3582 · FAX: 801.585.5241

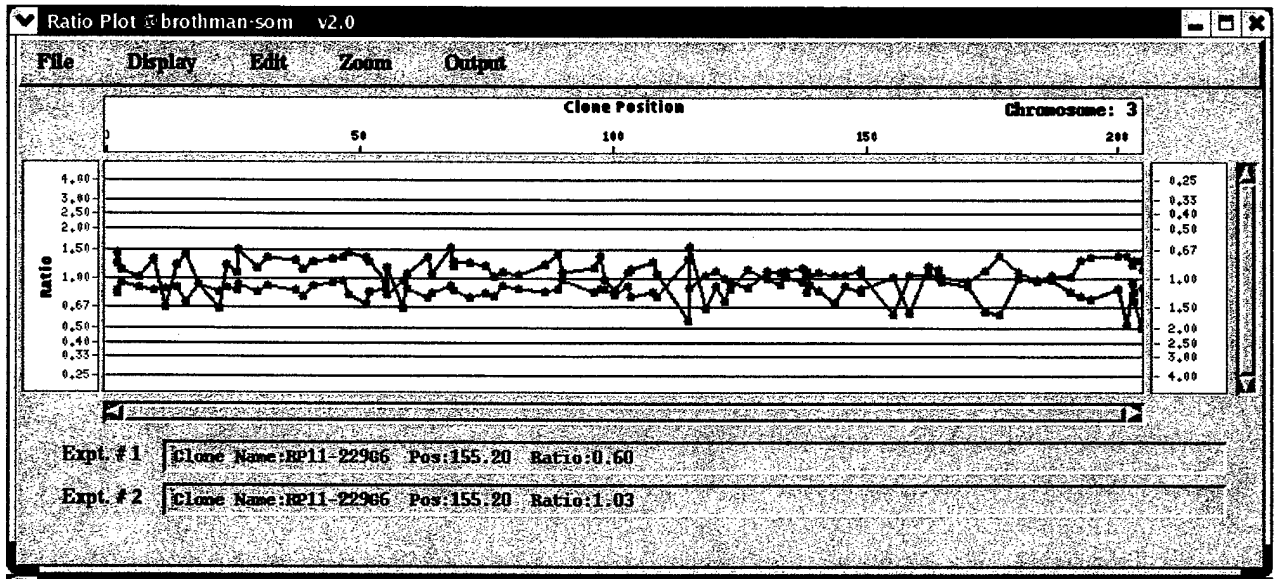

loss 3p
gain
3q

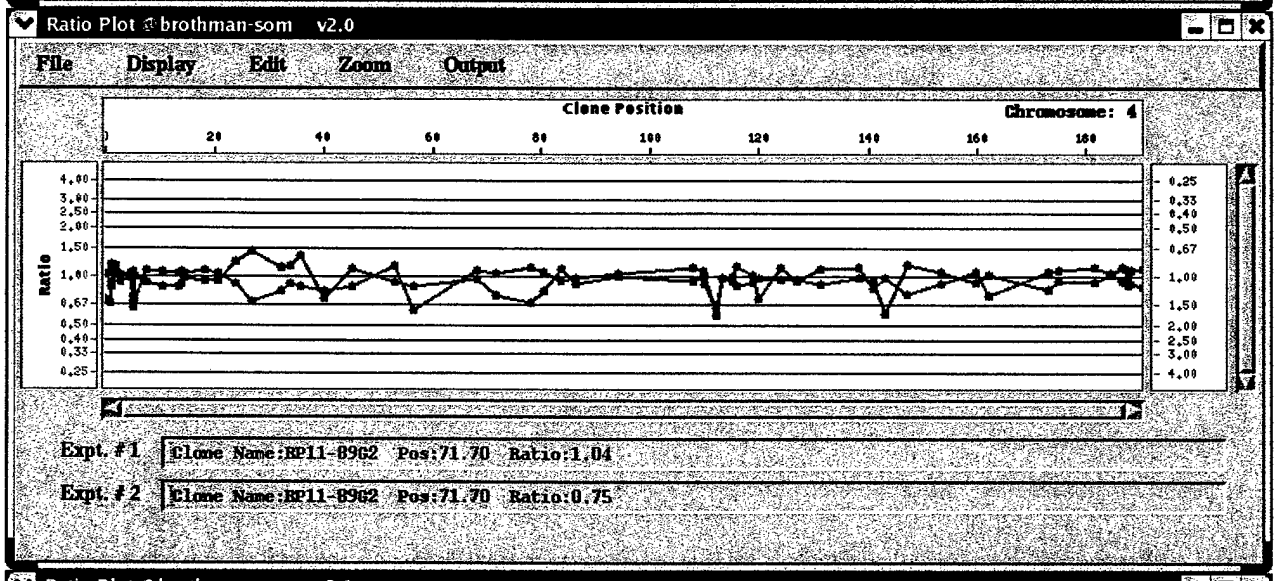

4p
loss

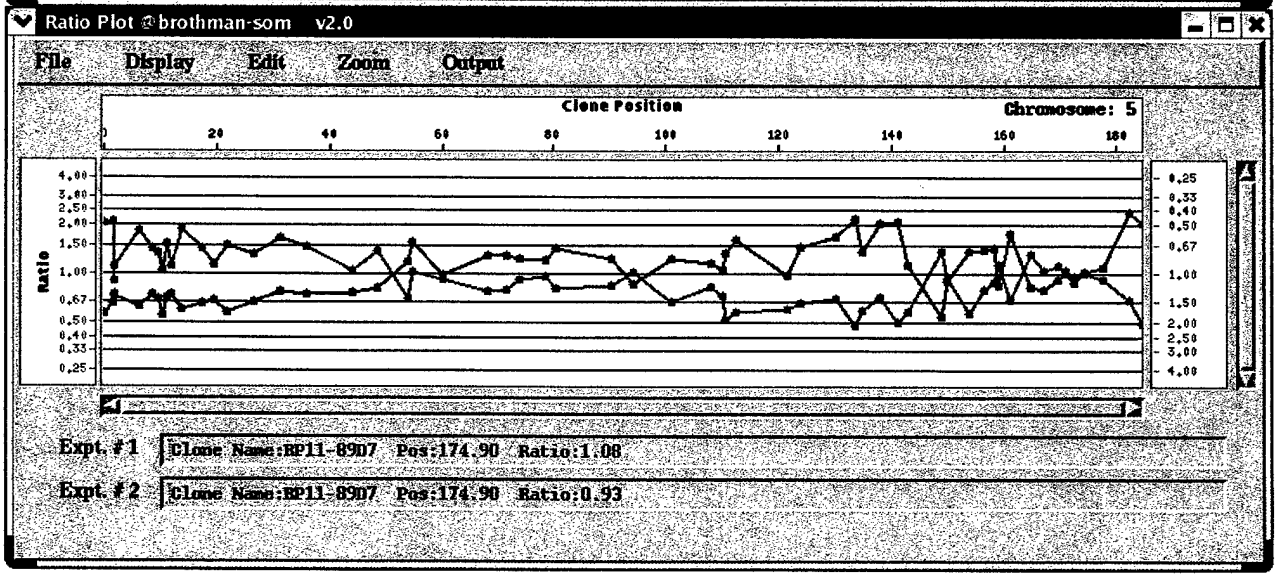

gain
5p
loss
5q

SCHOOL OF MEDICINE RM. 201
30 N 1900 E · SALT LAKE CITY · UT 84132
TEL: 801.587.3582 · FAX: 801.585.5241

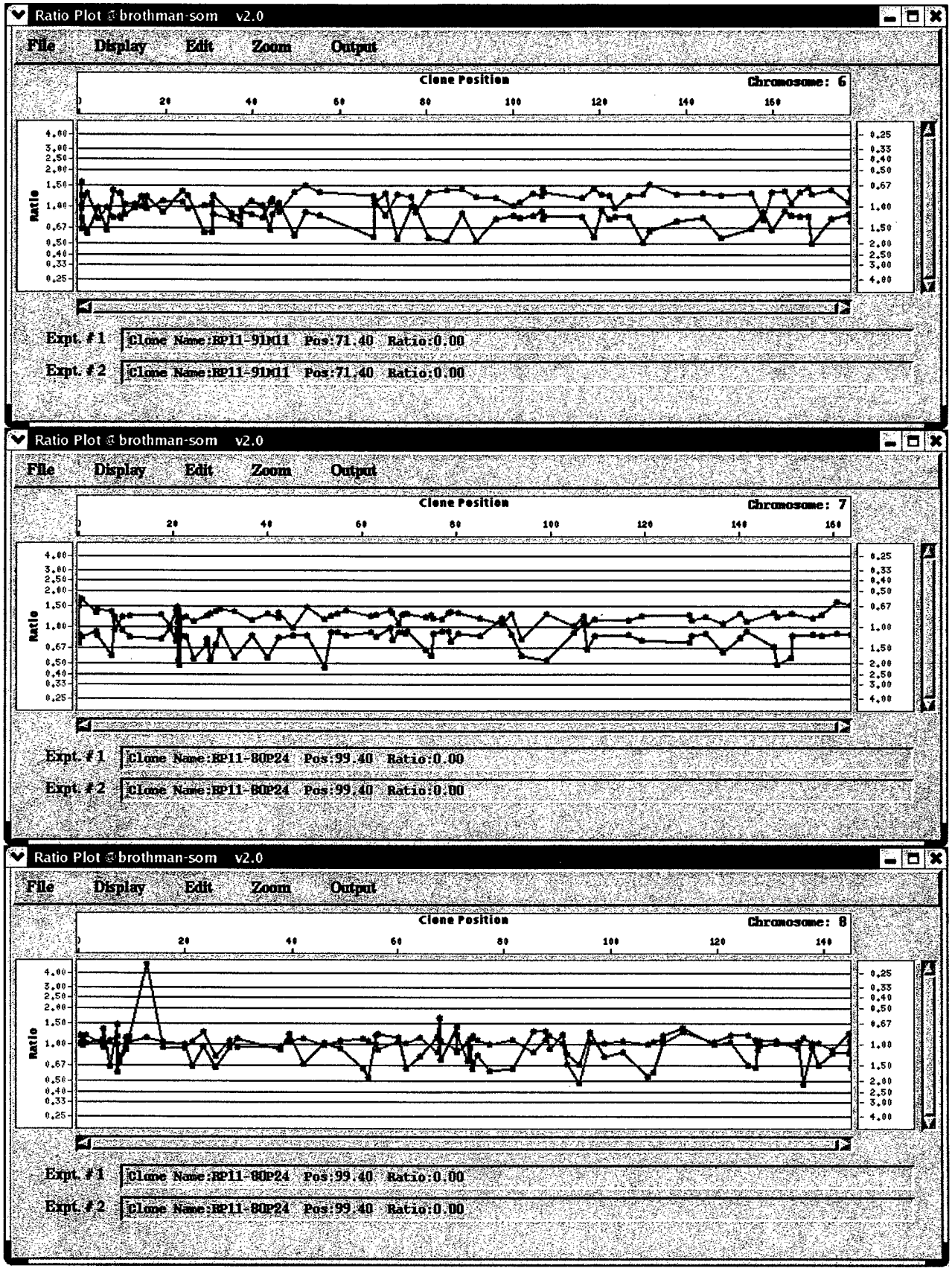

SCHOOL OF MEDICINE RM. 201
30 N 1900 E · SALT LAKE CITY · UT 84132
TEL: 801.587.3582 · FAX: 801.585.5241

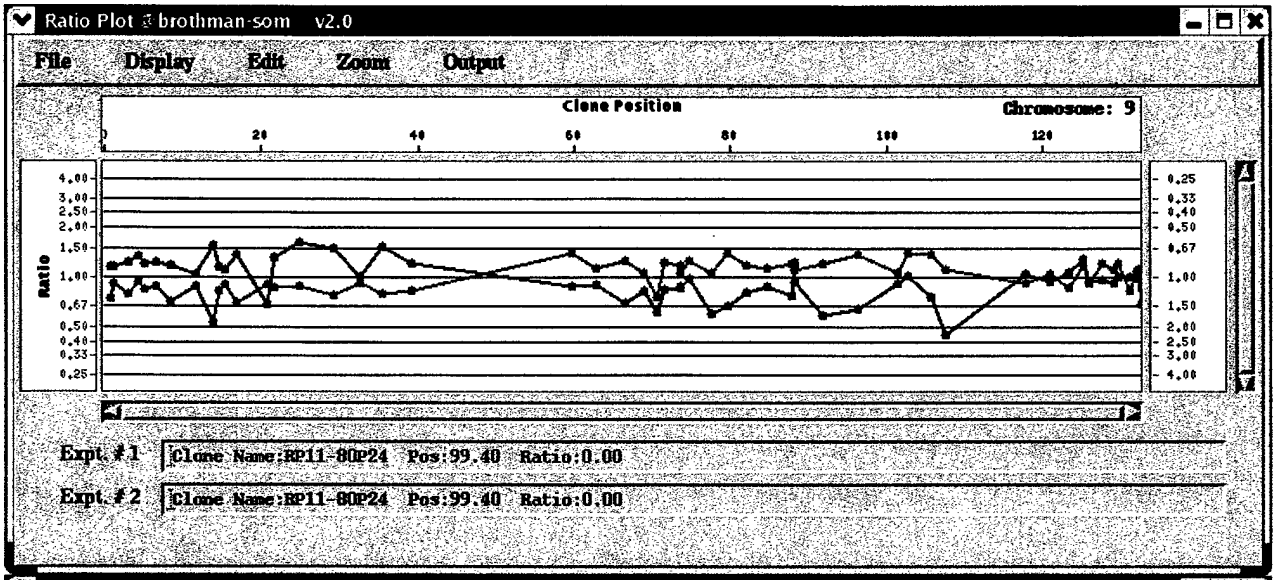

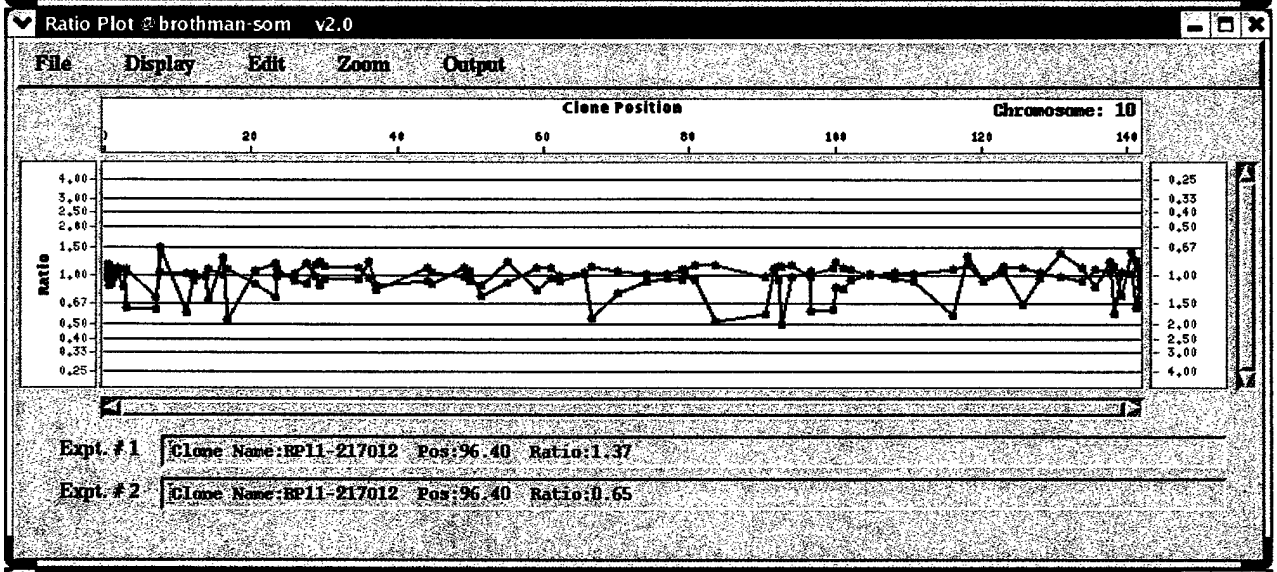

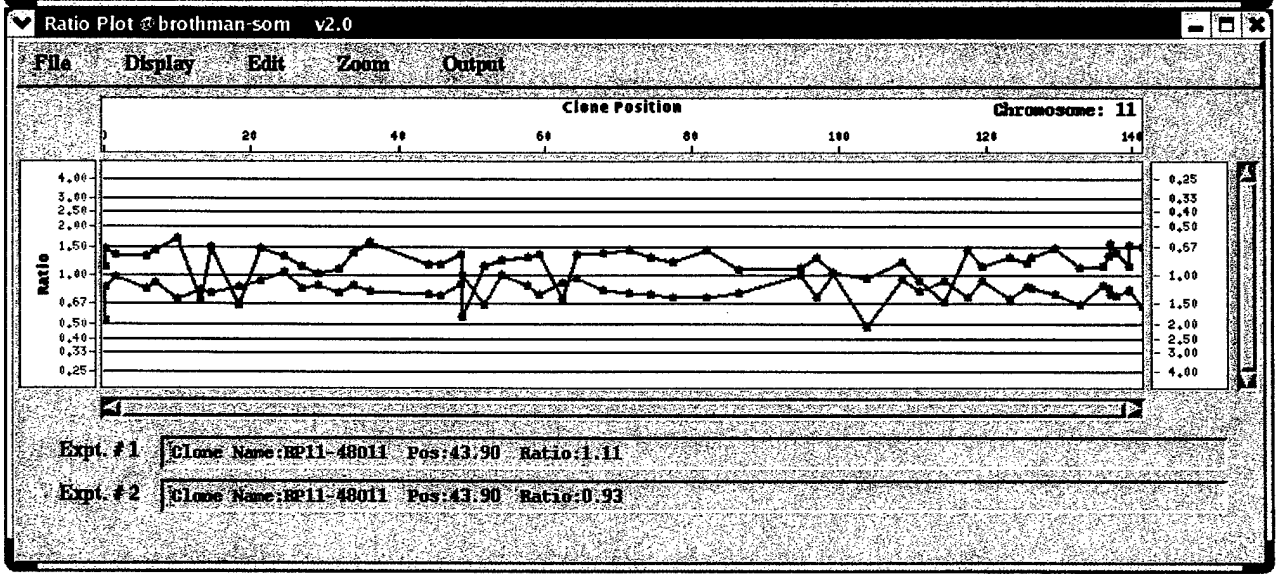

SCHOOL OF MEDICINE RM. 201
30 N 1900 E · SALT LAKE CITY · UT 84132
TEL: 801.587.3582 · FAX: 801.585.5241

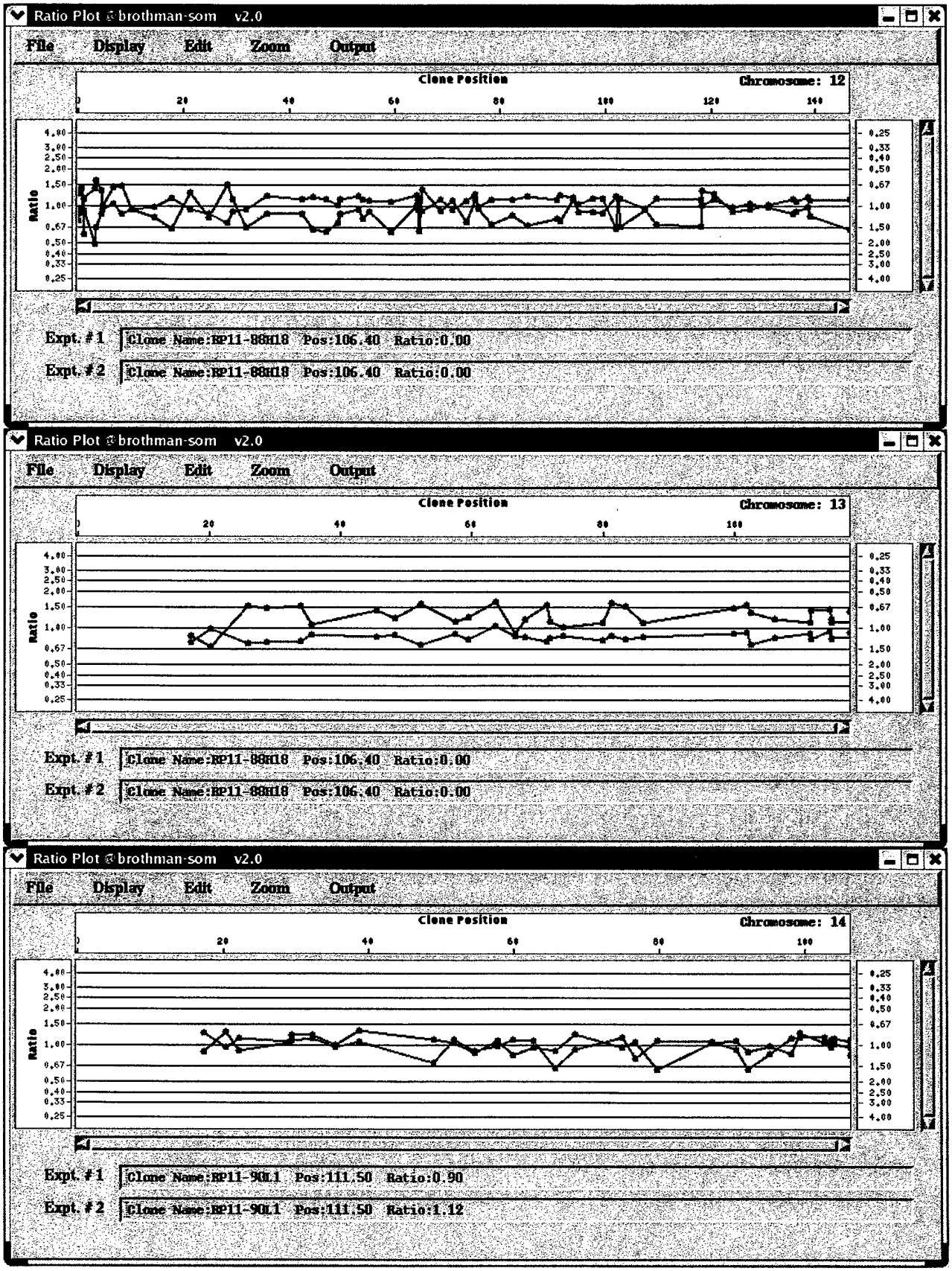

SCHOOL OF MEDICINE RM. 201
30 N 1900 E · SALT LAKE CITY · UT 84132
TEL: 801.587.3582 · FAX: 801.585.5241

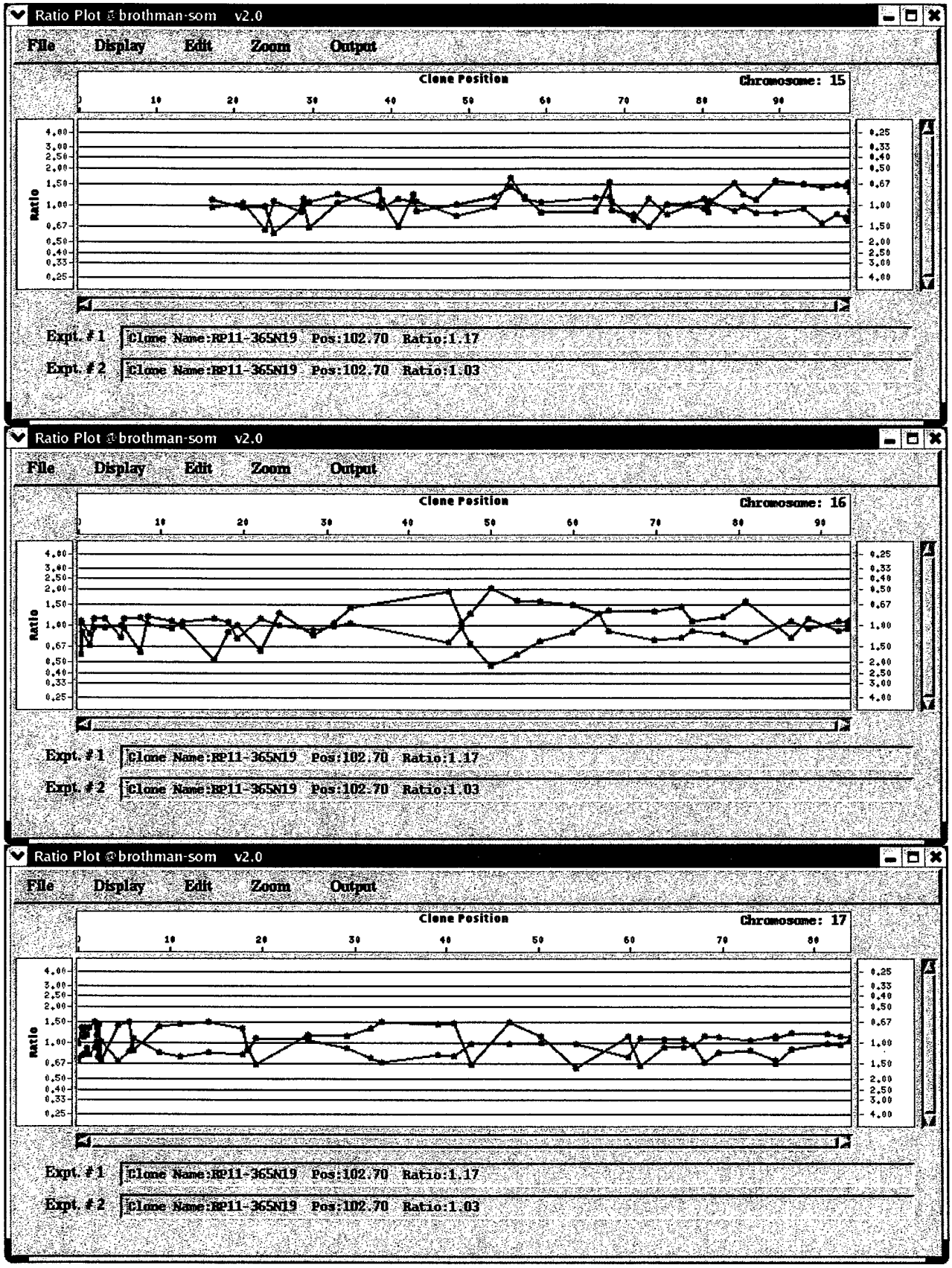

15q-

loss
16 qter

loss
17p
gain
17q

SCHOOL OF MEDICINE RM. 201
30 N 1900 E · SALT LAKE CITY · UT 84132
TEL: 801.587.3582 · FAX: 801.585.5241

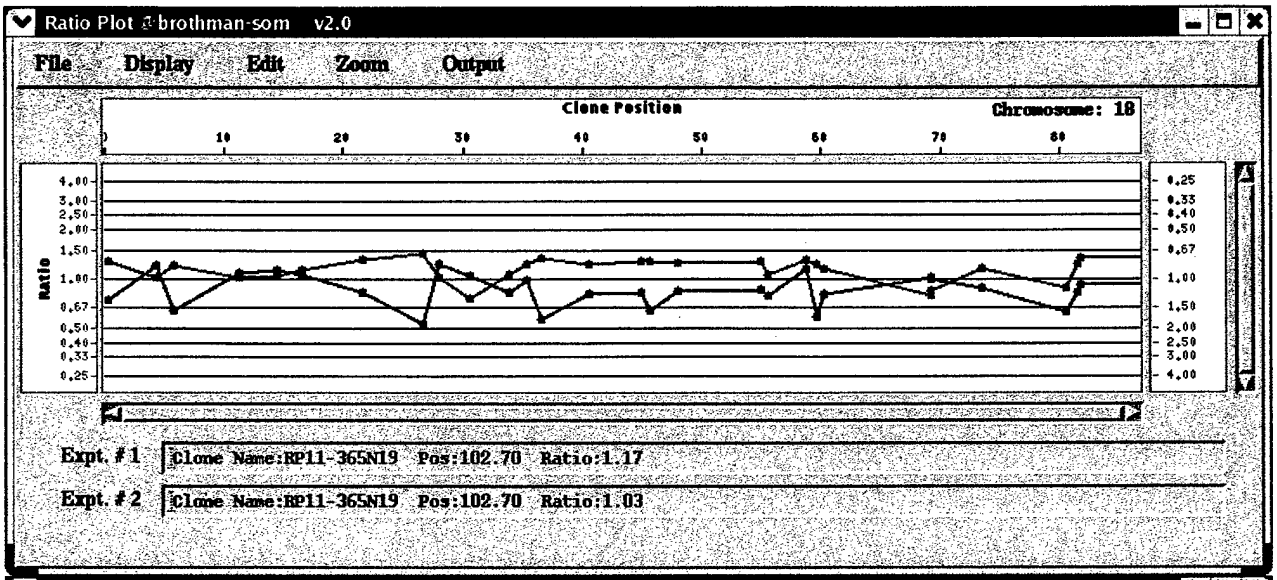

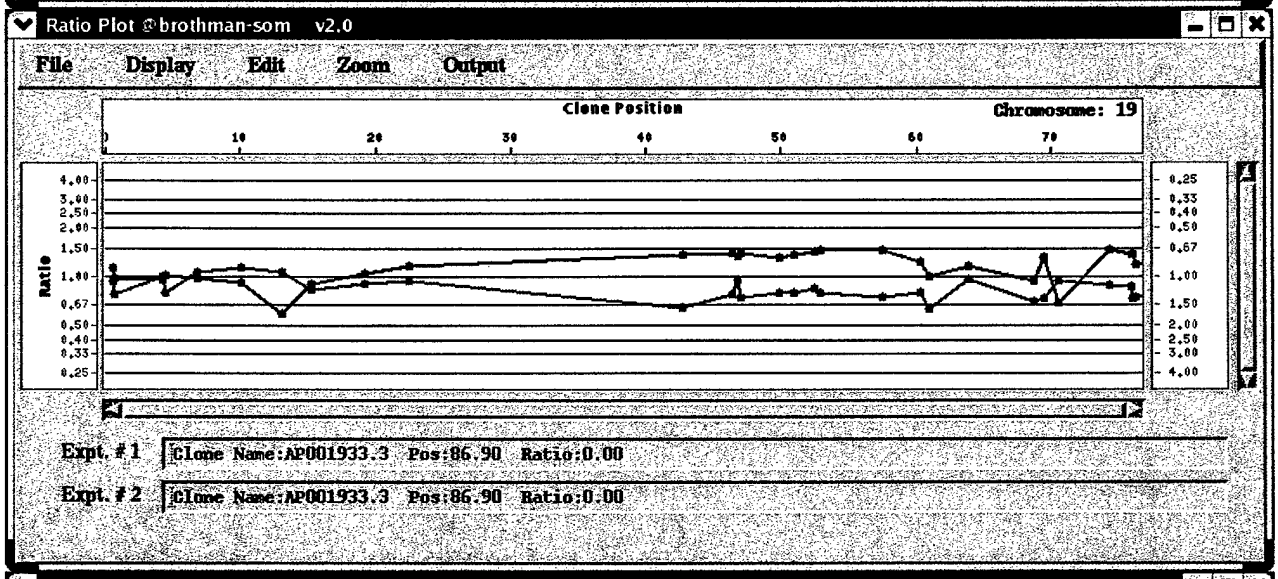

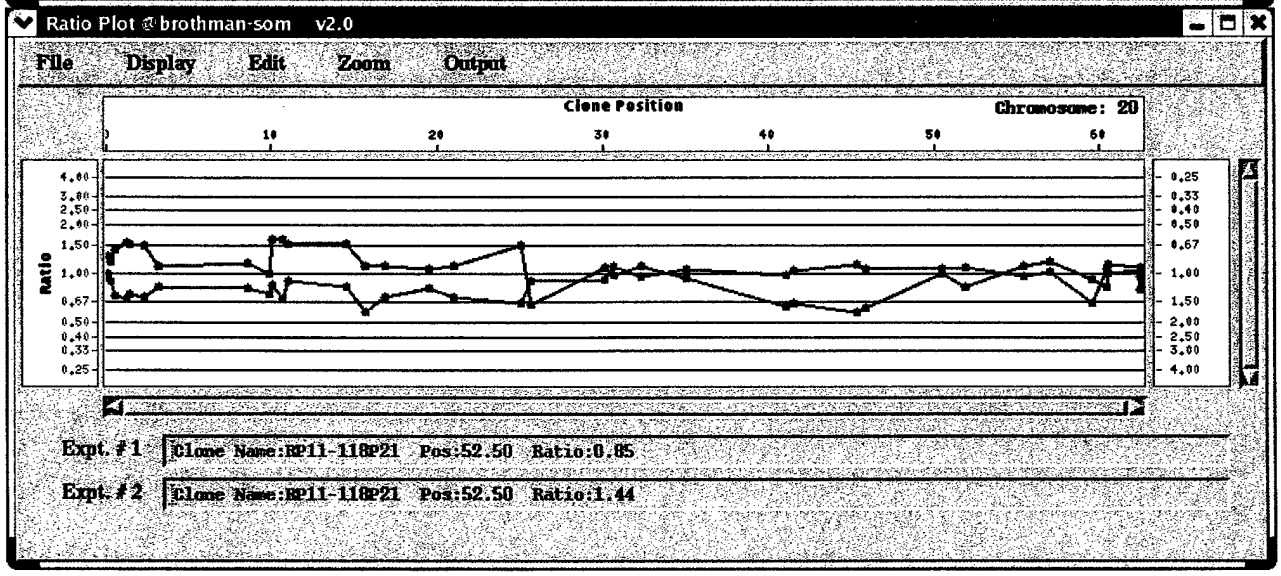

SCHOOL OF MEDICINE RM. 201
30 N 1900 E · SALT LAKE CITY · UT 84132
TEL: 801.587.3582 · FAX: 801.585.5241

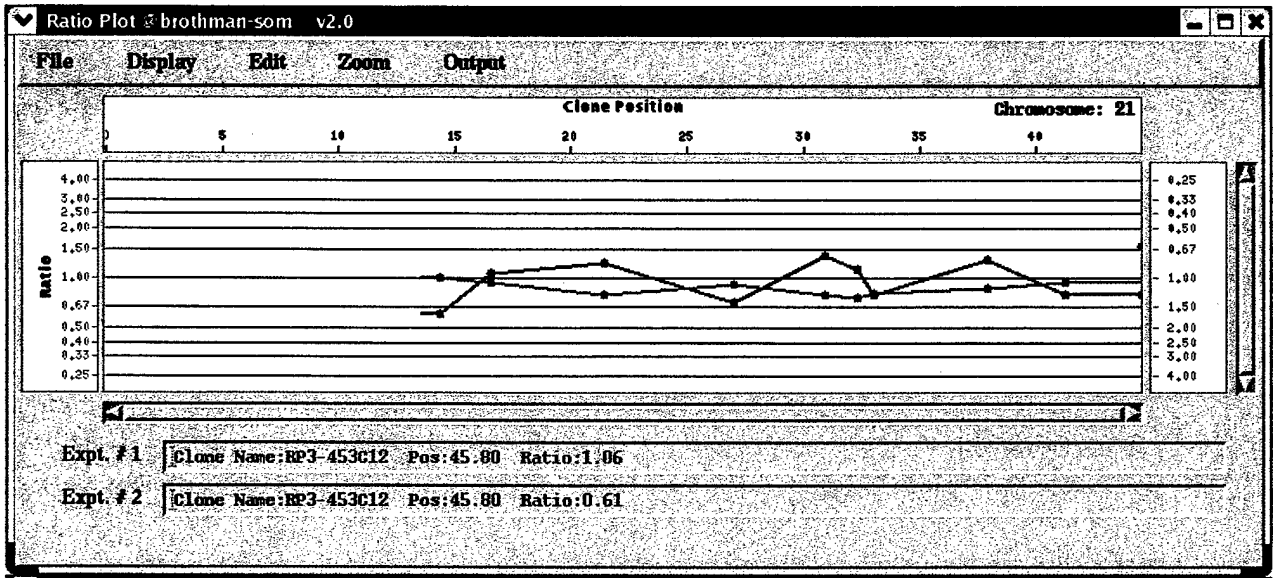

loss

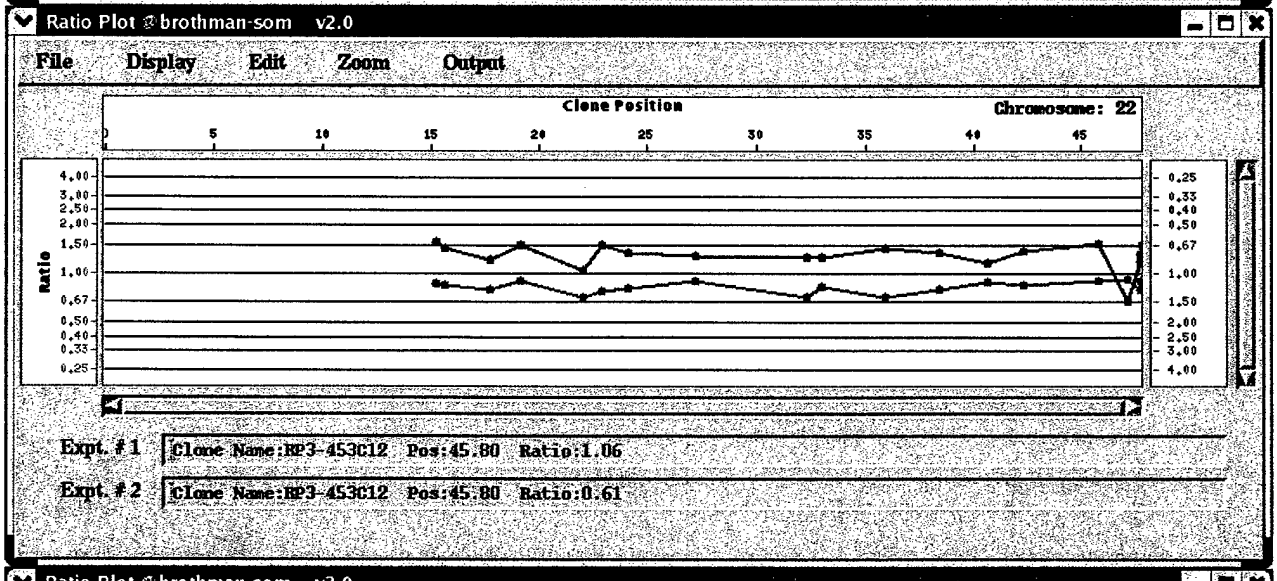

loss

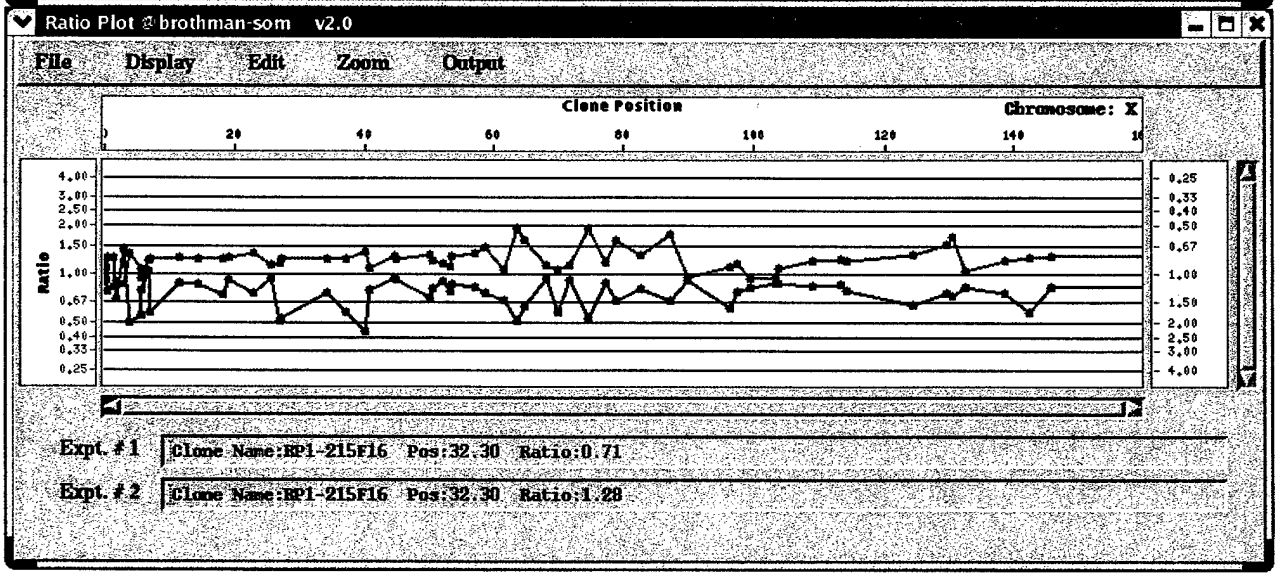

gain

SCHOOL OF MEDICINE RM. 201
30 N 1900 E · SALT LAKE CITY · UT 84132
TEL: 801.587.3582 · FAX: 801.585.5241

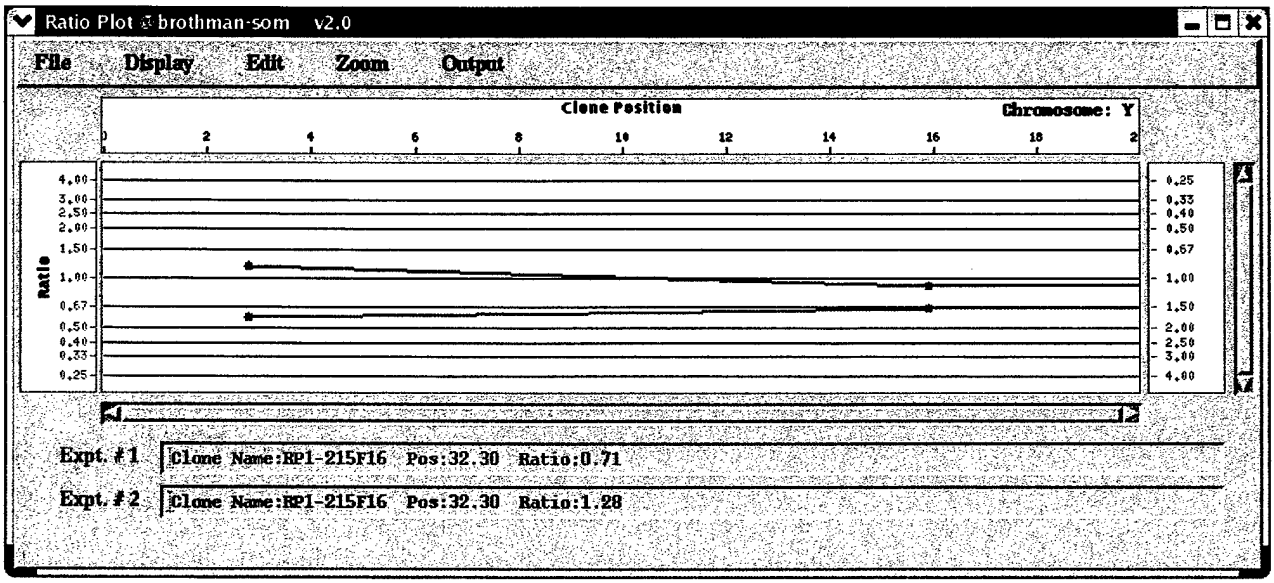

1055

SCHOOL OF MEDICINE RM. 201
30 N 1900 E · SALT LAKE CITY · UT 84132
TEL: 801.587.3582 · FAX: 801.585.5241

Accepted commentary: **Viskochil D**. It takes 2 to tango: Mast cells and Schwann cells in neurofibromas. J Clinical Investigation 2003:in press.

It takes two to tango: mast cell and Schwann cell interactions in neurofibromas

David H. Viskochil

Department of Pediatrics, School of Medicine, University of Utah, Salt Lake City, Utah, USA

Neurofibromas are benign tumors comprised primarily of Schwann cells and fibroblasts. Mast cell infiltration is a well-known phenomenon; however, their role in tumor pathogenesis has been enigmatic. In an elegant set of experiments using cells derived from a murine model of neurofibromatosis 1 (NF1), Yang et al. (see the related article beginning on page 1851) dissect the molecular pathways involved in mast cell migration to neurofibromin-deficient Schwann cells. These results set the stage for rational development of therapeutics that could influence the multicellular microenvironment of neurofibromas to inhibit the development and/or progression of these tumors in human NF1.

J. Clin. Invest. **112**:1791–1793 (2003). doi:10.1172/JCI200320503.

In an *Original article series* published through the March of Dimes Birth Defects Foundation in 1981, Vic Riccardi outlined his "NF cellular interaction hypothesis," implicating the mast cell as a major player neurofibroma formation (1). He was attempting to explain the variable expression of neurofibromatosis 1 (NF1) by cellular interactions and the finding of high numbers of mast cells in neurofibromas when he posited that "the mast cell now is seen *not* as a secondary arrival in a developing neurofibroma but as an *inciting* factor contributing in a primary, direct fashion to tumor development." It has taken over 20 years, but in this issue of the *JCI*, Yang et al. (2) clearly set the record straight by identifying the molecular mechanisms underlying mast cell infiltration of neurofibromas. The authors demonstrated that the inciting factor for mast cell migration is Kit ligand and that it is hypersecreted from *Nf1*$^{-/-}$ Schwann cell populations. Nevertheless, that Riccardi hypothesized paracrine events involving the mast cell as a major player in neurofibroma formation is a testament to his intuition regarding the pathogenesis of this complex genetic condition.

Yang and colleagues were intrigued by the seminal observations of Zhu et al. (3) of neurofibroma formation in mice expressing the conditional deletion of *Nf1*, whereby double inactivation of the gene *Nf1*$^{-/-}$ in Schwann cells could only induce neurofibroma formation in the context of a heterozygous *Nf1*$^{+/-}$ genetic background. This supports the paracrine model for neurofibromas; other cells in these mixed-cell tumors must be haploinsufficient for neurofibromin to support proliferation. Yang et al. (2) have taken these observations a step further by dissecting the cell types and the molecular mechanisms by which the tumor microenvironment contributes to neurofibroma formation. Through a set of elegant experiments, they have delineated a complex biological system and provided a model demonstrating not just who the major players are in this process, but how those players interact in concert to develop neurofibromas (Figure 1).

Address correspondence to: David H. Viskochil, 50 North Medical Drive, Room 2C412, School of Medicine, University of Utah, Salt Lake City, Utah 84112, USA. Phone: (801) 581-8943; Fax: (801) 585-7252; E-mail: DAVE.VISKOCHIL@hsc.utah.edu.

Conflict of interest: The author has declared that no conflict of interest exists.

Nonstandard abbreviations used: neurofibromatosis 1 (NF1); malignant peripheral nerve sheath tumor (MPNST).

Neurofibroma microenvironment

The basic components of an evolving neurofibroma are: (i) *Nf1*$^{-/-}$ Schwann cells, which act as tumorigenic instigators (4–7); (ii) *Nf1*$^{+/-}$ mast cells, which act as inducers (2); and (iii) *Nf1*$^{+/-}$ fibroblasts, Schwann cells, perineural cells, and endothelial cells, which act as the responders (8). The pathways involved in neurofibroma formation identified by Yang et al. (2) involve Kit ligand (secreted by *Nf1*$^{-/-}$ Schwann cells), c-Kit receptor (expressed by mast cells), α4β1 integrin (a mast cell surface protein), VCAM-1 (an endothelial receptor for α4β1 integrin), Ras (a substrate for neurofibromin), and the class I_A-PI3K-Rac2 pathway (mast cell transduction downstream of activated Ras). The primary observation of Yang et al. is the enhanced migration of neurofibromin haploinsufficient mast cells toward the double-inactivated, *Nf1*$^{-/-}$ Schwann cells that secrete five times the normal levels of Kit ligand. According to this paradigm, in human neurofibromas, a "second hit," or somatic mutation of the normal *NF1* tumor suppressor gene allele in heterozygous Schwann cells as a random event, is the initiating event which sets the stage for mast cells to induce neurofibroma formation by paracrine/autocrine mechanisms.

Mast cells and neurofibromas

The presence of mast cells in human neurofibromas, initially reported in 1911 by Greggio (9), is well known to clinical pathologists. Additional studies have since supported the finding of mast cells in peripheral nerve trunks (10, 11), peripheral nerve tumors (12–14), and neurofibromas in neurofibromatosis 1 (15–17). The potential involvement of the c-Kit receptor and its ligand (18, 19) in the formation of neurofibromas has also been reported, but Yang et al. (2) are the first investigators to evaluate living cells of different genetic backgrounds in order to demonstrate *how* increased mast cells populate neurofibromas. Now that a plausible mechanism has been established for the migration of mast cells to developing neurofibromas, it is important to dissect potential mechanisms whereby mast cells can induce cells in the microenvironment to either tolerate or enhance cell proliferation. Because we know that neurofibromas, like other tumors, are complex tissues

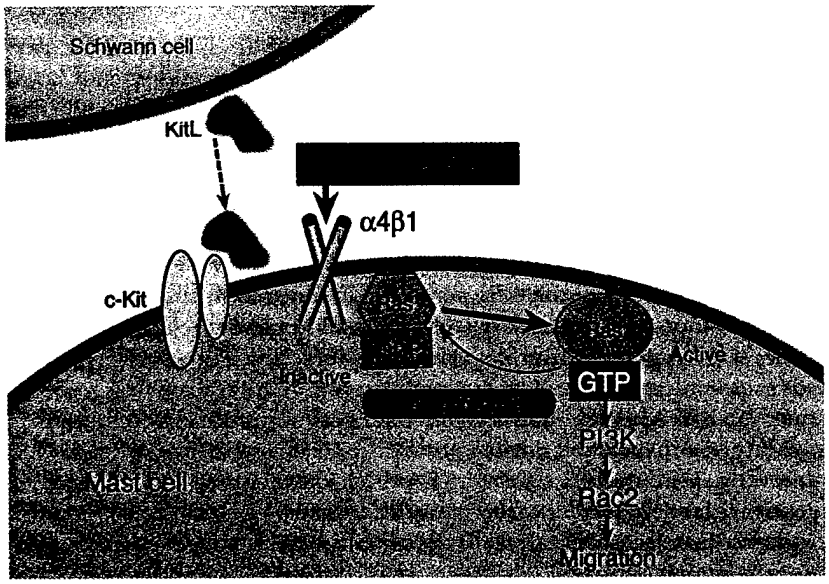

Figure 1
Illustration depicting the molecular pathways involved in mast cell recruitment to neurofibromas. A neurofibromin-deficient Schwann cell ($Nf1^{-/-}$) secretes five times the normal Kit ligand, which serves as a chemoattractant for mast cells expressing c-Kit. Mast cell migration is mediated by the Ras/PI3K/Rac2 signal transduction pathway, which is enhanced in $Nf1^{+/-}$ cells. Although not shown, endothelial cells also play a role in mast cell migration through the interaction of the endothelial cell VCAM-1 receptor and α4β1 integrin of the mast cell. Heterozygous inactivation of *Nf1* promotes rapid mast cell haptotaxis specifically on α4β1 integrins in response to KitL. It is known that mast cells are activated in neurofibromas and degranulate; however it is yet to be determined if and how the presence of mast cells induces tumor progression. Figure courtesy of D. Wade Clapp, Indiana University School of Medicine. KitL, Kit ligand.

with interactions between genetically altered Schwann cells, mast cells, and other supporting coconspirators lead to cancer development (20), it now becomes important to determine the role mast cells play in the microenvironment of NF1-related peripheral nerve sheath tumors.

Mast cells in cancer

Mast cell secretions are known to be integral components of wound healing and tissue repair, even in the peripheral nervous system. In addition to their role in inflammation, mast cells provide mitogens for fibroblasts, endothelial cells, and nerve cells to enhance tissue remodeling, and they are also now being recognized as potential epigenetic contributors to cancer (21). It will be important to establish the functions of the mast cell after it has migrated to the Kit ligand–secreting Schwann cells. In addition to secreting mitogenic and angiogenic substances, including basic FGF, VEGF, histamine, heparin, prostaglandins, leukotrienes, and proteolytic enzymes, mast cells may also have novel cell-to-cell interactions (22) or other unknown functions that could induce neurofibromas. Thus, the development of medical treatment targeted to mast cell function may be a rational approach to decreasing neurofibroma formation in NF1. In a pilot study, Riccardi used ketotifen as a stabilizer of mast cells to demonstrate less small-vessel bleeding in surgical excisions of neurofibromas (23). He followed up this study with a controlled multiphase trial of ketotifen in 27 patients, assessing pain and itching associated with neurofibromas, and showed a response (24) that was reviewed as encouraging, but not definitely beneficial (25). Given that specific paracrine pathways have yet to be defined in the microenvironment of NF1-related neurofibromas, Yang et al. (2) appropriately point out that therapeutic agents that target the migration of mast cells (i.e., inhibition of c-kit activity and adhesion to α4β1 integrin) may hold promise in the early treatment and/or prevention of neurofibromas.

Mast cells: missing in action

There is one caveat to bear in mind in regard to the role $Nf1^{+/-}$ mast cells may play as they nestle into their newfound microenvironment. With respect to the role of inflammation in cancer and the recognition that mast cells are one of the inflammatory cell types involved in protumor actions (26), it should be acknowledged that neurofibromas are benign tumors, especially the dermal neurofibromas, which never progress to malignancy. It is also important to recognize that the neurofibromas that develop in the mouse models are not dermal neurofibromas, but are more like human plexiform neurofibromas. These tumors often progress to malignant peripheral nerve sheath tumors (MPNSTs); however, unlike in other tumor model systems where inflammatory cells are in excess in tumor microenvironments, there are relatively few mast cells in MPNSTs (ref. 27; H. Zhou, personal communication). Is it possible that an influx of mast cells, drawn by a small cohort of malignant $Nf1^{-/-}$ Schwann cells, induces fibroblasts to synthesize the plethora of extracellular matrix seen in dermal neurofibromas, which could then serve as a "glue" to corral the deviant Schwann cells? By this reasoning, only when mast cells are lost, as seen in the MPNSTs, would there be diminution of the anti-cancer effects of mast cells in maintaining the benign nature of neurofibromas. Thus, until the paracrine/autocrine paradigm is deciphered in neurofibroma formation, it behooves the NF1 research community to continue working toward the identification of mast cell signals (inducers) that specify responses from the microenvironment before implementing clinical trials using agents that inhibit mast cell migration toward the tumorigenic Schwann cell. To this end, Yang and colleagues (2) will likely make more outstanding contributions both to the NF1 research field and to the work of those who are dissecting the roles of inflammation and the microenvironment in cancer.

1. Riccardi, V.M. 1981. Cutaneous manifestation of neurofibromatosis: Cellular interaction, pigmentation, and mast cells. In *Birth defects: original article series*. Volume 17. R. Blandau, N. Paul, and F. Dickman, editors. Alan R. Lis Inc. New York, New York, USA. 129–145.
2. Yang, F.-C., et al. 2003. Neurofibromin-deficient Schwann cells secrete a potent migratory stimulus for *Nf1*$^{+/-}$ mast cells. *J. Clin. Invest.* **112**:1851–1861. doi:10.1172/JCI200319195.
3. Zhu, Y., Ghosh, P., Charnay, P., Burns, D.K., and Parada, L.F. 2002. Neurofibromas in NF1: Schwann cell origin and role of tumor environment. *Science.* **296**:920–922.
4. Kluwe, L., Friedrich, R., and Mautner, V.F. 1999. Loss of NF1 allele in Schwann cells but not in fibroblasts derived from an NF1-associated neurofibroma. *Genes Chromosomes Cancer.* **24**:283–285.
5. Serra, E., et al. 2000. Schwann cells harbor the somatic NF1 mutation in neurofibromas: evidence of two different Schwann cell subpopulations. *Hum. Mol. Genet.* **12**:3055–3064.
6. Rutkowski, J.L., Wu, K., Gutmann, D.H., Boyer, P.J., and Legius, E. 2000. Genetic and cellular defects contributing to benign tumor formation in neurofibromatosis type 1. *Hum. Mol. Genet.* **12**:1059–1066.
7. Muir, D., Neubauer, D., Lim, I.T., Yachnis, A.T., and Wallace, M.R. 2001. Tumorigenic properties of neurofibromin-deficient neurofibroma Schwann cells. *Am. J. Pathol.* **158**:501–513.
8. Fialkow, P.J., Sagebiel, R.W., Gartler, S.M., and Rimoin, D.L. 1971. Multiple cell origin of hereditary neurofibromas. *N. Engl. J. Med.* **284**:298–300.
9. Greggio, H. 1911. Les cellules granuleuses (Mastzellen) dans les tissus normaux et dans certaines maladies chirurgicales. *Arch. Med. Exp.* **23**:323–375.
10. Gamble, H.J., and Goldby, S. 1961. Mast cells in peripheral nerve trunks. *Nature.* **189**:766–767.
11. Olsson, Y. 1971. Mast cells in human peripheral nerve. *Acta Neurol. Scand.* **47**:357–368.
12. Baroni, C. 1964. On the relationship of mast cells to various soft tissue tumours. *Br. J. Cancer.* **18**:686–690.
13. Pineda, A. 1965. Mast cells – their presence and ultrastructural characteristics in peripheral nerve tumors. *Arch. Neurol.* **13**:372–382.
14. Isaacson, P. 1976. Mast cells in benign nerve sheath tumours. *J. Pathol.* **119**:193–196.
15. Giorno, R., Lieber, J., and Claman, H.N. 1989. Ultrastructural evidence for mast cell activation in a case of neurofibromatosis. *Neurofibromatosis.* **2**:35–41.
16. Carr, N.J., and Warren, A.Y. 1993. Mast cell numbers in melanocytic naevi and cutaneous neurofibromas. *J. Clin. Pathol.* **46**:86–87.
17. Nurnberger, M., and Moll, I. 1994. Semiquantitative aspects of mast cells in normal skin and in neurofibromas of neurofibromatosis types 1 and 5. *Dermatology.* **188**:296–299.
18. Hirota, S., et al. 1993. Possible involvement of c-kit receptor and its ligand in increase of mast cells in neurofibroma tissues. *Arch. Pathol. Lab. Med.* **117**:996–999.
19. Bedache, A., Muja, N., and De Vries, G.H. 1998. Expression of Kit in neurofibromain-deficient human Schwann cells: role in Schwann cell hyperplasia associated with type 1 neurofibromatosis. *Oncogene.* **17**:795–800.
20. Hannahan, D., and Weinberg, R.A. 2000. The hallmarks of cancer. *Cell.* **100**:57–70.
21. Coussens, L.M., and Werb, Z. 2001. Inflammatory cells and cancer: think different. *J. Exp. Med.* **193**:F23–F26.
22. Greenberg, G., and Burnstock, G. 1983. A novel cell-to-cell interaction between mast cells and other cell types. *Exp. Cell. Res.* **147**:1–13.
23. Riccardi, V.M. 1987. Mast-cell stabilization to decrease neurofibroma growth. *Arch. Dermatol.* **123**:1011–1016.
24. Riccardi, V.M. 1993. A controlled multiphase trial of ketotifen to minimize neurofibroma-associated pain and itching. *Arch. Dermatol.* **129**:577–581.
25. Meyer, L.J. 1993. Drug therapy for neurofibromatosis? *Arch. Dermatol.* **129**:625–626.
26. Coussens, L.M., and Werb, Z. 2002. Inflammation and cancer. *Nature.* **420**:860–867.
27. Johnson, M.D., Kamso-Pratt, J., Federspiel, C.F., and Whetsell, W.O. 1989. Mast cell and lymphoreticular infiltrates in neurofibromas. Comparison with nerve sheath tumors. *Arch. Pathol. Lab. Med.* **113**:1263–1270.

Tumbling down a different pathway to genetic instability

Haiwei H. Guo and Lawrence A. Loeb

Joseph Gottstein Cancer Research Laboratory, Department of Pathology, University of Washington, Seattle, Washington, USA

Ulcerative colitis (UC), a chronic inflammatory condition associated with a predisposition to colon cancer, is frequently characterized by DNA damage in the form of microsatellite instability (MSI). A new report links inflammation in UC with increases in the DNA repair enzymes 3-methyladenine DNA glycosylase and apurinic/apyrimidinic endonuclease, and, paradoxically, with increased MSI (see the related article beginning on page 1887). These findings may represent a novel mechanism contributing to MSI in chronic inflammation.

J. Clin. Invest. **112**:1793–1795 (2003). doi:10.1172/JCI200320502.

Address correspondence to: Lawrence A. Loeb, Department of Pathology, K-072 HSB, 1959 NE Pacific Street, University of Washington, Seattle, Washington 98195-7705, USA. Phone: (206) 543-6015; Fax: (206) 543-3967; E-mail: laloeb@u.washington.edu.

Conflict of interest: The authors have declared that no conflict of interest exists.

Nonstandard abbreviations used: ulcerative colitis (UC); chromosomal instability (CI); microsatellite instability (MSI); base excision repair (BER); 3-methyladenine DNA glycosylase (AAG); apurinic/apyrimidinic endonuclease (APE1); apurinic/apyrimidinic (AP); reactive oxygen species (ROS); polymerase β (polβ).

Ulcerative colitis, genetic instability, and cancer

A longstanding question in cancer research is the strong association between certain chronic inflammatory conditions and the concomitant elevated risk for malignancy in affected tissues. Understanding the molecular mechanisms driving the progression to cancer may not only provide more effective means of prevention but also shed light on mechanisms of carcinogenesis. Ulcerative colitis (UC), which affects as many as 6 per 100,000 people in the United States, is a relapsing form of chronic inflammatory disease of the large bowel. Patients with more than a 10-year history of disease have a 20- to 30-fold greater risk of developing colorectal cancer (1). Both chromosomal instability (CI) and microsatellite (short, repetitive nucleotide sequences in DNA) instability (MSI) are present in UC and can be detected early in dysplastic, premalignant tissues (2, 3). What are the sources of these changes in DNA sequence? Chromosomal changes are frequent in cancer and MSI has been clearly documented as a result of mutations in mismatch repair enzymes in the hereditary nonpolyposis colon cancer syndrome. MSI is also observed in many other malignancies (4). Accumulation of mutations in microsatellites could be the result of alterations in enzymes that normally guarantee DNA stability, thus leading to a mutator phenotype (4). Existing hypotheses postulate that excess amounts of free radicals found in inflamed UC tissues overwhelm DNA repair pathways, leading to the accumulation of damaged DNA (5), or that mismatch repair pathways are inactivated, either directly by oxidative stress (6) or by hypermethylation (7). In the traditional view, members of DNA repair pathways are heroic players, stoically laboring against the overwhelming tide of genetic insults thrown their way.

Abstract for submitted proposal to the NINDS. PI: **D. Viskochil**. MPNSTs in NF1: 3 clinical trials. Submitted October 1, 2003.

Mail Message

Novell.

Close Previous Next Forward Reply to Sender Reply All Move Delete Read Later Properties

From: Dave Viskochil
To: Terri Nielsen-Rogers
Date: Monday - January 26, 2004 9:39 AM
Subject: abstract

ABSTRACT MPNST-NF1 NINDS 09-03.doc (20992 bytes) [View] [Save As]

this is the abstract for a submission to NINDS - proposal mumber is 1 R01 NS049454-01.

thanks

Title: MPNST in NF1: A Multicenter Clinical Trial

Malignant peripheral nerve sheath tumors (MPNSTs) are sarcomas originating in the peripheral nervous system, specifically the nerve sheath. The association of MPNST with neurofibromatosis type 1 (NF1) is well-established; approximately ½ of those who develop MPNST have NF1, and, for those who have NF1, there is a 10% life-time risk to develop a MPNST. The clinical manifestations of this condition do not readily identify a subgroup of individuals with NF1 who are at higher risk to develop MPNST. Furthermore, there is not an effective surveillance protocol for early detection of MPNST, nor is there effective medical treatment for management of this malignancy once it is detected. This proposal is comprised of 3 clinical trials to address each of these issues.

Specific aim 1 uses a cross-sectional, case-control approach to compare clinical, genetic and environmental features that differentiate those individuals with NF1 who develop MPSNTs from those who do not develop MPNSTs. *It tests the hypothesis that a subgroup of individuals with NF1 can be identified whom are at higher risk to develop MPNST.* Specific aim 2 will assess the predictive value of ^{18}Fluorodeoxyglucose positron emission tomography (^{18}FDG PET) in the early detection of MPNST. *It tests the hypothesis that ^{18}FDG PET can discriminate between MPNST and benign plexiform neurofibroma in symptomatic patients with NF1.* Specific aim 3 is a novel phase II trial of neoadjuvant chemotherapy in patients with sporadic and NF1-associated MPNSTs. *It tests the hypothesis that neoadjuvant chemotherapy has activity (results in tumor shrinkage) in the treatment of high-grade MPNST.* In addition, a tumor repository will be expanded to process and perform standard neuropathologic testing on tumor tissue acquired through each clinical trial. An administrative core will be developed to optimize recruitment of individuals with these relatively rare tumors, facilitate data sharing between participating centers, and enhance data analysis for each clinical trial.

Published manuscript: Muknopadhyay D, Anan S, Lee R, Kennedy S, **Viskochil D**, Davidson N. C-> U Editing of neurofibromatosis 1 mRNA occurs in tumors that express both the type II transcript and aobec-1, the catalytic subunit of the apolipoprotein B mRNA-editing enzyme. Am J Hum Genet. 2002:70;38-50.

Am. J. Hum. Genet. 70:38–50, 2002

C→U Editing of Neurofibromatosis 1 mRNA Occurs in Tumors That Express Both the Type II Transcript and apobec-1, the Catalytic Subunit of the Apolipoprotein B mRNA–Editing Enzyme

Debnath Mukhopadhyay,[1] Shrikant Anant,[1] Robert M. Lee,[1] Susan Kennedy,[1] David Viskochil,[3] and Nicholas O. Davidson[1,2]

Departments of [1]Medicine and [2]Pharmacology and Molecular Biology, Washington University Medical School, St. Louis; and [3]Department of Pediatrics, Division of Medical Genetics, University of Utah Health Science Center, Salt Lake City

C→U RNA editing of neurofibromatosis 1 (NF1) mRNA changes an arginine (CGA) to a UGA translational stop codon, predicted to result in translational termination of the edited mRNA. Previous studies demonstrated varying degrees of C→U RNA editing in peripheral nerve–sheath tumor samples (PNSTs) from patients with NF1, but the basis for this heterogeneity was unexplained. In addition, the role, if any, of apobec-1, the catalytic deaminase that mediates C→U editing of mammalian apolipoprotein B (apoB) RNA, was unresolved. We have examined these questions in PNSTs from patients with NF1 and demonstrate that a subset (8/34) manifest C→U editing of RNA. Two distinguishing characteristics were found in the PNSTs that demonstrated editing of NF1 RNA. First, these tumors express apobec-1 mRNA, the first demonstration, in humans, of its expression beyond the luminal gastrointestinal tract. Second, PNSTs with C→U editing of RNA manifest increased proportions of an alternatively spliced exon, 23A, downstream of the edited base. C→U editing of RNA in these PNSTs was observed preferentially in transcripts containing exon 23A. These findings were complemented by in vitro studies using synthetic RNA templates incubated in the presence of recombinant apobec-1, which again confirmed preferential editing of transcripts containing exon 23A. Finally, adenovirus-mediated transfection of HepG2 cells revealed induction of editing of apoB RNA, along with preferential editing of NF1 transcripts containing exon 23A. Taken together, the data support the hypothesis that C→U RNA editing of the NF1 transcript occurs both in a subset of PNSTs and in an alternatively spliced form containing a downstream exon, presumably an optimal configuration for enzymatic deamination by apobec-1.

Introduction

Neurofibromatosis type 1 (NF1 [MIM 162200]) is a dominantly inherited disease affecting ~1/3,500 individuals worldwide. The *NF1* gene has been mapped and characterized extensively, and several features of interest have emerged in relation to its altered function in disease. The *NF1* gene spans ~350 kb on chromosome 17q11.2 and encodes 60 exons, which are ubiquitously transcribed (Li et al. 1995). The nuclear NF1 transcript is ~11 kb and encodes neurofibromin, a tumor-suppressor–gene product of 2,818 residues, which contains a region of ~366 amino acids that functions as a GTPase-activating protein (GAP) (reviewed in Cichowski and Jacks 2001). GAP activity has been demonstrated for neurofibromin—more specifically, in the context of Ras activation, both in vitro and in vivo—and is postulated to be an important feature of the loss of function accompanying mutations in the *NF1* gene (Basu et al. 1992; DeClue et al. 1992; Nakafuku et al. 1993; Bollag et al. 1996; Guha et al. 1996; Lau et al. 2000; Sherman et al. 2000).

Although the disorder becomes fully penetrant at a relatively early age, the clinical features of NF1 are quite variable even between affected siblings. In addition, as many as half of the newly diagnosed cases of NF1 represent new mutations, a feature likely accounted for by the high spontaneous-mutation rate at this locus (Andersen et al. 1993; Ars et al. 2000). Taken together, the range of mutations and the phenotypic variability suggest that modifier genes may play a significant role in the natural history of this disease (Skuse and Ludlow 1995). An important consideration in understanding the potential mechanisms for exerting phenotypic variability in this disease is the role of RNA processing of transcripts arising from somatic and germline mutations in the *NF1* gene; for example, alterations in mRNA splicing have been demonstrated to occur in ~50% of pa-

Received August 23, 2001; accepted for publication October 5, 2001; electronically published November 27, 2001.

Address for correspondence and reprints: Dr. Nicholas O. Davidson, Box 8124, Gastroenterology Division, Washington University School of Medicine, 660 South Euclid Avenue, St. Louis, MO 63110. E-mail: NOD@IM.WUSTL.EDU

0002-9297/2002/7001-0006$15.00

tients with NF1 (Park and Pivnick 1998), suggesting an important mechanism for amplifying the phenotypic variability alluded to above.

Another posttranscriptional mechanism, C→U editing of RNA, was postulated for inactivation of the GAP function of NF1 some years ago, by Skuse and colleagues (Skuse et al. 1996; Skuse and Cappione 1997). These investigators identified a C→U change, occurring at nt 3916 in the NF1 transcript, that changes a genomically templated arginine (CGA) to a UGA stop codon in the edited mRNA (Skuse et al. 1996; Skuse and Cappione 1997). The edited transcript encodes a truncated protein product that terminates in the amino-terminal portion of the GAP-related domain and would thus result in functional inactivation of the tumor-suppressor function of neurofibromin (Skuse et al. 1996; Ashkenas 1997; Cappione et al. 1997; Skuse and Cappione 1997). Nevertheless, certain features of these original findings were unexplained. The level of C→U editing of NF1 RNA, for example, was quite variable (4%–17%) among the tumors examined, with a trend suggesting that the more malignant tumors demonstrated higher levels of editing (Skuse et al. 1996; Skuse and Cappione 1997). In addition, the enzymatic factors mediating this C→U change were not identified, and the relationship, if any, to editing of intestinal apolipoprotein B (apoB) (*APOB* [MIM 107730]) mRNA, the prototype example of C→U deamination of nuclear RNA, was not resolved. In particular, C→U editing of mammalian intestinal apoB RNA demonstrates absolute dependence on the expression of the catalytic deaminase, apobec-1 (*APOBEC-1* [MIM 600130]) (Hirano et al. 1996; Morrison et al. 1996), whereas preliminary studies by Skuse et al. (1996) revealed no clear evidence that apobec-1 plays a role in the editing of NF1 RNA.

We have reexamined these questions through analysis of peripheral nerve–sheath tumor samples (PNSTs) from 34 patients with NF1. The majority, 26 of 34, of tumors demonstrated low levels of C→U RNA editing, in the range of 0%–2.5%, with 10 of these 26 demonstrating <1% editing, the limits of reliable detection of the assay. However, the remaining 8 of the 34 tumors demonstrated 3%–12% C→U editing of NF1 RNA, which was reproducible and validated by sequencing of the cDNA products. These tumors demonstrated two distinguishing characteristics. First, these PNSTs express apobec-1 mRNA, the catalytic deaminase of the holoenzyme that edits apoB RNA (Teng et al. 1993; Lau et al. 1994; Yamanaka et al. 1994; Davidson and Shelness 2000), suggesting an important role for apobec-1 in the context of a target beyond apoB RNA. Second, NF1 RNA from these PNSTs contains increased proportions of an alternatively spliced exon, 23A, downstream of the edited base in which editing occurs preferentially. These findings, together with results of both in vivo and in vitro experiments with apobec-1, strongly suggest an important mechanistic linkage between NF1 RNA splicing and C→U editing and provide a basis for understanding the heterogeneity of posttranscriptional regulation of *NF1* expression.

Material and Methods

Tissue Procurement

The use of human tumor and normal adjacent tissue in this investigation was reviewed and approved by the institutional review boards of the University of Chicago Hospitals, the University of Utah Hospital, Massachusetts General Hospital, Harvard University Hospital, and Washington University School of Medicine. Samples of PNSTs were collected from a total of 34 patients with NF1, whose clinical diagnosis was based on National Institutes of Health consensus-conference criteria (National Institutes of Health Consensus Development Conference 1988). No attempt was made to identify familial versus sporadic cases. In addition, paired normal and tumor samples were obtained from 11 patients (without NF1) undergoing surgical resection for colon adenocarcinoma. The majority of these samples were moderately differentiated tumors located in the proximal, mid, or descending colon. Each was snap-frozen in liquid nitrogen and was stored at −80°C until processed. Frozen tissue sections were stained with hematoxylin and eosin to confirm the histological composition of these specimens.

Endogenous Editing of NF1 mRNA

Total RNA and genomic DNA from the NF1 and colon-cancer tissues was isolated by TRIzol reagent (LifeTechnologies). First-strand cDNA was synthesizedby Superscript II reverse transcriptase (RT) (LifeTechnologies) primed with random hexamers. PCR was performed with *Pyrococcus woesei* DNA polymerase (Roche Molecular Biochemicals), to amplify NF1 cDNA flanking the edited base (fig. 1), by primers SA61 (5′- CAAGGAGAACTCCCTATAGCG-ATG-3′; 5′ at nt 3650) and SA64 (5′-CTGTTCTGAGG-GAAACGCTGG-3′; 5′ located at nt 4201). An aliquot of each PCR was analyzed by agarose-gel electrophoresis to monitor yield and the integrity of the product. Typical yield was 0.4–0.5 μg/50 μl PCR. To selectively amplify NF1 mRNA containing exon 23A, primer RML33 (5′-TGTAGCTTTATTCAGTAGGGAGTGG-CAAG-3′; 5′ located at nt 4142) was substituted for SA64, in the PCR (fig. 1). To determine the proportions of NF1 mRNA containing exon 23 A, 10 μCi α[^{32}P]-dCTP (3,000 Ci/mmol) was included in the reaction, and the products were analyzed by 8% native PAGE and were quantitated by phosphorimaging (Molecular Dynamics). Genomic DNA corresponding to exon 22

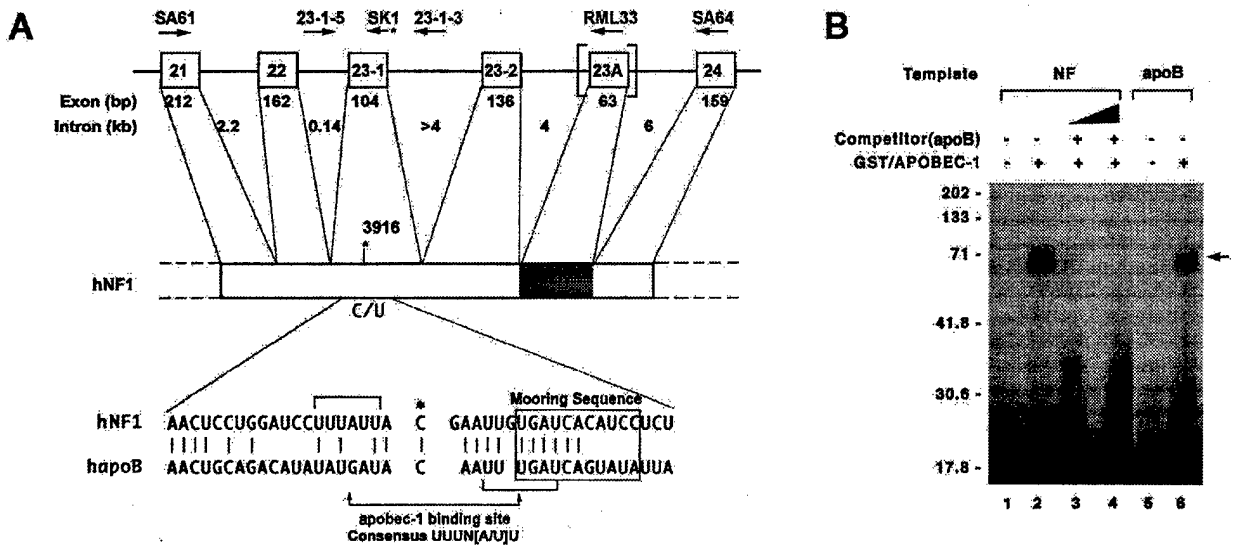

Figure 1 *A*, Organization of *NF1*. *Top*, Exons 21–24 of *NF1*, along with exon and intron sizes. The alternatively spliced exon 23A is within the vertical brackets, and the corresponding region in NF1 mRNA is shaded. Identities, orientations, and locations of the various primers are indicated above the exon and intron designations. *Bottom*, Alignment of 41-nt region (nt 3896–3936) of NF1 mRNA surrounding the edited base, compared to human apoB mRNA (hapoB). The edited C in both sequences is indicated by an asterisk (*), and sequence identity is indicated by vertical lines. The apobec-1 binding site and mooring sequence are indicated by horizontal brackets and a box, respectively. *B*, apobec-1, a NF1 RNA–binding protein. UV cross-linking was performed by incubating 250 ng GST/APOBEC-1 with either a 550-nt [^{32}P]-labeled NF1 RNA (NF [lanes 1–4]) containing exon 23A (nt 3650–4201) or a 105-nt [^{32}P]-labeled apoB RNA (apoB [lanes 5 and 6]), flanking the edited base. After treatment with RNaseT1 and UV irradiation, the cross-linked products were analyzed by 10% SDS-PAGE. For competition analysis, 50- (lane 3) and 100-fold (lane 4) excess of cold apoB RNA was added to the reaction. The results shown are representative of three such experiments. Molecular-weight markers are indicated to the left of the gel, and the location of the cross-linked GST/APOBEC-1 band is indicated by the arrow to the right of the gel.

was amplified by primers 23-1-5 (5′-AAAAACACGGTTCTATGTGAAAAG-3′, located in intron 22) and 23-1-3 (5′-TTTGTATCATTCATTTTGTGTGTA-3′, located in intron 23-1), located in the adjacent introns (fig. 1). Primer-extension analysis was employed to determine the extent of editing of NF1 RNA at nt 3916, by primer SK1 (5′- CATGTTGCCAATCAGAGGATGTG-3′, located at nt 3949) (Skuse et al. 1996), which is complementary to a 23-nt region 12 nt downstream of the edited base. The primer SK1 is that used by Skuse et al. (1996). [^{32}P]-labeled SK1 primer was annealed to 10 ng NF1 cDNA flanking the edited base. Primer extension was conducted in the presence of 0.05 μM each of dATP, dCTP, and TTP and 1.6 μM ddGTP, in the presence of T7 DNA polymerase. In this assay, the radiolabeled primer extends to the first upstream C (at nt 3916) and undergoes chain termination, giving an extension product of 34 nt. If the C at nt 3916 is edited to T, the products extend to the next upstream C, at nt 3908, giving an extension product of 42 nt. The primer-extension products were resolved by PAGE with 10% acrylamide containing 8 M urea, followed by phosphorimaging. We have validated and characterized this assay extensively in the context of editing of apoB RNA (Giannoni et al. 1994; Anant et al. 1998; Madsen et al. 1999). Standardization of the assay was undertaken by use of mixtures of NF1 cDNA containing known quantities of C3916 and T3916 products from sequence-validated templates constructed from previously amplified NF1 cDNA (550 bp), in which a T at nt 3916 was introduced by mutagenesis. Known quantities of PCR product were used to establish the optimal conditions for primer extension. This established that the reliable limits of detection with 10 ng template correspond to 1% U (data not shown). Levels of apparent editing <1% were considered background "primer read through." All assays included a C standard and a T standard, for reference.

In Vitro RNA-Editing Assay

Synthetic templates were prepared to yield transcripts that either included (550 nt) or did not include (487 nt) exon 23A and that contained a C at nt 3916. A 20-fmol sample of each RNA was individually incubated in a buffer containing 20 mM HEPES. HCl pH 7.8, and 100 mM KCl, at 30°C for 4 h, in the presence of 250 ng glutathione-S-transferase (GST)/apobec-1 and 50 μg of

a 30% ammonium sulfate precipitate of bovine liver S-100 extracts (MacGinnitie et al. 1995). The RNA was extracted, subjected to primer extension with [^{32}P]-labeled SK1 primer (see above), and subsequently analyzed, under denaturing conditions, by PAGE with 8% polyacrylamide gel containing 8 M urea. Editing of RNA was quantitated by phosphorimager analysis (Molecular Dynamics).

Protein-Truncation Assay

NF1 cDNA encoding exons 21–24 was amplified by RT-PCR, as described above, with primers NF-PPT-5′ (5′-GGGTGTAATACGACTCACTATAGGCCACC*ATGG-AGCAGAAACTCATCTCTGAA*CAAGGAGAACTCC-CTATAGCGATGGCTC-3′; T7 promoter is underlined, and myc-tag is boldface italic) and SA64. NF-PTT-5′ was designed to contain an upstream T7 promoter and a myc epitope tag, in frame with the NF1 cDNA. These primers were designed so that the region amplified contained the same numbers of methionine residues in the translation products from transcripts either with or without exon 23A. The full-length product (~22 kD) contains six methionine residues, whereas the truncated protein (~11 kD) contains five. The RT-PCR products were subjected to coupled transcription-translation (Promega) with rabbit reticulocyte lysates in the presence of translation-grade [^{35}S]-methionine (Amersham-Pharmacia), according to the manufacturer's recommendations. The translation reaction was subsequently immunoprecipitated with anti-myc monoclonal antibody 9E-10 (Santa Cruz Biotechnology) and was analyzed by gradient 10%–20% SDS-PAGE and autoradiography.

Detection of apobec-1 and apobec-1 Complementation Factor (ACF) mRNA

RT-PCR was conducted by use of primers, listed below, for apobec-1 and ACF. First-strand cDNA synthesis was undertaken as described above, using random-hexamer priming; cDNA amplification used gene-specific primers located in the 5′ and 3′ regions of the coding

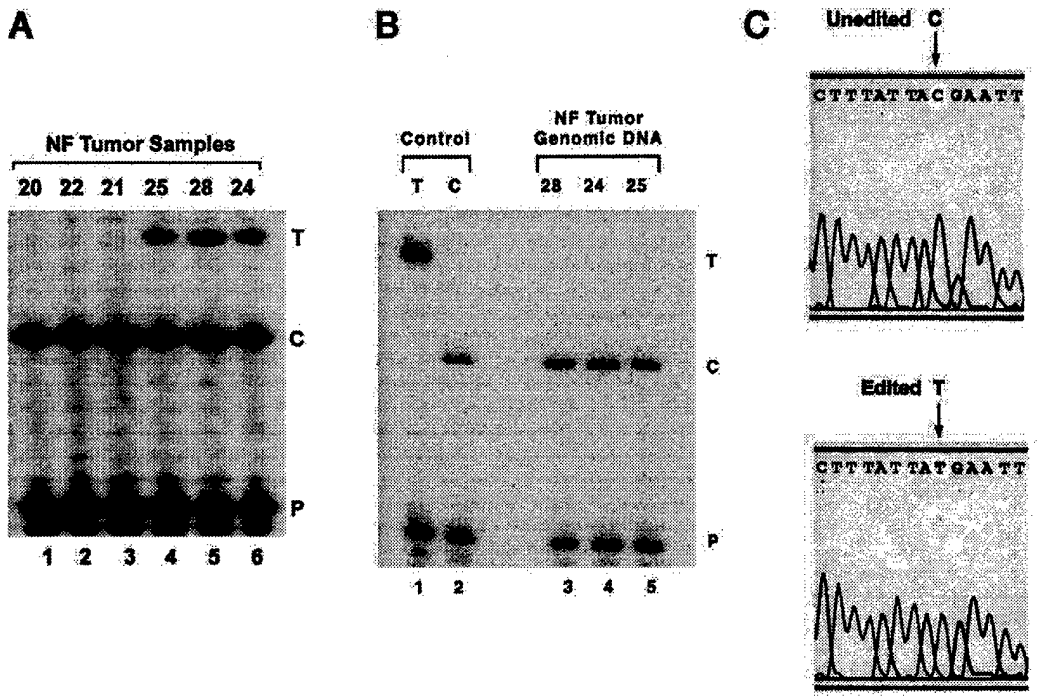

Figure 2 NF1 mRNA undergoing C→U editing in a subset of neurofibromatosis-related PNSTs. *A*, Total RNA extracted from neurofibromatosis tumor tissue—and extent of editing of NF1 mRNA, as determined by primer-extension assay as described in the "Material and Methods" section. The primer-extension products were separated on a gel of 10% polyacrylamide containing urea and were autoradiographed. A representation of experiments performed in triplicate for 34 neurofibromatosis tumor samples is shown. The locations of the primer (P) and of unedited (C) and edited (T) primer-extension products are indicated to the right of the gel. *B*, C→U editing, which is shown not to be a somatic mutation. Genomic DNA flanking exon 23-1 was amplified by PCR using intron-specific primers and subsequently was subjected to primer-extension analysis. As controls, PCR products containing either C or T at nt 3916 of NF1 cDNA were also analyzed. The locations of the primer (P) and of unedited (C) and edited (T) primer-extension products are indicated to the right of the gel. *C*, Editing at nt 3916 of NF1 RNA, confirmed by sequencing of individual cDNA clones. The locations of the unedited (*Unedited C; top*) and edited (*Edited T; bottom*) nucleotide in a representative clone are indicated by arrows above the gels.

Table 1

C→U Editing of NF1 RNA in PNSTs

Category and Sample	Histology	Editing (%) Mean	SD	Range (n = 3)	Expression apobec-1	ACF
No editing (<1% U):						
NF20	Plexiform	.64	.34	.3–1.0	–	+
NF22	Triton tumor	.65	.35	.3–.9	–	+
NF6	Neurofibroma	.66	.43	.2–1.1	–	+
NF35	Glioblastoma	.68	.22	.45–.9	–	+
NF21	Malignant schwannoma	.69	.65	.2–1.3	–	+
NF3	Neurofibroma	.72	.65	.1–1.4	–	+
NF4	Neurofibroma	.72	.68	.1–1.5	–	+
NF2	Neurofibroma	.86	.65	.75–1.1	–	+
NF18	Malignant schwannoma	.95	.65	.9–1.3	–	+
NF5	Neurofibroma	.99	.56	.95–1.7	–	+
NF7	Malignant schwannoma	1.01	.46	.9–1.5	–	+
NF17	Neurofibroma	1.08	.24	.85–1.5	–	+
NF13	Neurofibroma	1.14	.65	.75–1.8	–	+
NF8	Malignant schwannoma	1.15	.75	.65–1.9	–	+
NF16	Neurofibroma	1.15	.49	.55–1.7	–	+
NF9	Neurofibroma	1.24	.43	.8–1.7	–	+
NF27	Malignant schwannoma	1.35	.36	.9–1.7	–	+
NF23	Neurofibroma	1.37	.54	.75–1.9	–	+
Low editing (<2.5% U):						
NF14	White matter	1.48	.39	1.0–1.9	–	+
NF34	Glioblastoma	1.52	.43	1.1–1.95	–	+
NF11	Neurofibroma	1.57	.54	1.0–2.1	–	+
NF1	Neurofibroma	1.58	.58	1.0–2.2	–	+
NF30	Ganglioneuroma	1.83	.16	1.65–2.1	–	+
NF15	Peripheral nerve	1.85	.86	1.1–2.5	–	+
NF31	Schwannoma	1.99	.38	1.5–2.5	–	+
NF19	Neurofibroma	2.36	1.03	1.33–3.4	–	+
NF10	Neurofibroma	3.16	.98	2.2–4.1	+	+
NF33	Glioblastoma	3.18	.68	2.6–3.9	+	+
NF26	Nonmalignant schwannoma	3.48	.62	2.8–4.2	+	+
NF32	Neurofibroma	5.06	.89	4.1–5.9	+	+
Bona-fide editing (>3% U):						
NF29	Granulomatous cell	5.52	1.08	4.3–6.7	+	+
NF25	Malignant schwannoma	10.35	2.53	8.1–12.5	+	+
NF24	Malignant schwannoma	12.02	3.12	8.9–15.3	+	+
NF28	Ganglioneuroblastoma	12.65	1.65	10.5–14.8	+	+

sequence. PCR cycling conditions for apobec-1 and ACF were 95°C for 3 min, 1 cycle; 95°C for 30 s, 55°C for 1 min, and 72°C for 1 min, 30 cycles; and 72°C for 10 min. As a control, glyceraldehyde-3-phosphate dehydrogenase (GAPDH) mRNA was simultaneously amplified by the indicated primers. The amplified products were sequenced on both strands to confirm their identity. Primers used are as follows: for GAPDH, primers 5′-TCGGAGTCAACGGATTTGGTCG-3′ and GAP 5′-AGGCAGGGATGATGTTCTGGAGAG-3′; for apobec-1, primers SA146 5′-GACGACGACAAGGGATCCATGAGTTCCGAGACAGGC-3′ and SA147 5′-GGAACAAGACCCGTCGACTCATTTCAACCCTGTGGCCCACAG-3′; and, for ACF, primers ACF2 5′-CTCGAGTCAGAAGGTGCCATATCCATC-3′ and ACF6 5′-CAGATATTAGAAGAGATTTGTC-3′. The primer pairs for apobec-1 generate a full-length cDNA, whereas the primers for ACF generate an amplicon of 447 bp. Where indicated in the text, nested PCR was undertaken for apobec-1, by use of the primers listed below, which yield a product of 273 bp (nt 116–388). Primers used for nested PCR were as follows: JM-8 5′-ACCCCAGAGAACTTCGTAAAGAGGCC-3′ and JM-9 5′-CCGAGCTACGTAGATCACTAGAGTCA-3′.

UV Cross-Linking of NF1 and apoB RNAs to apobec-1

NF1 cDNA flanking the edited base (fig. 1) was amplified by primers SA61 and SA64, subcloned into plasmid pGEM-3zf(+) (Promega) and was sequenced to confirm the presence of wild-type sequence. The plasmid was linearized with restriction endonuclease *Kpn*I and was sub-

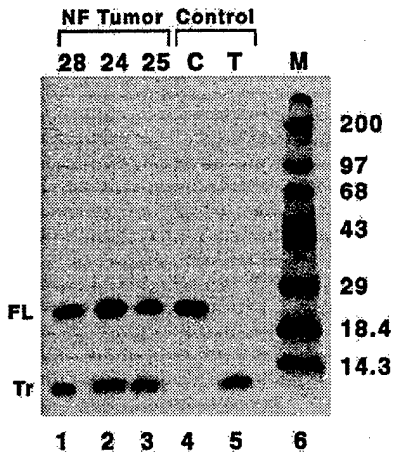

Figure 3 Protein-truncation assay. NF1 cDNA flanking the edited base was amplified by primers NF-PTT-5′ and SA64, as described in the "Material and Methods" section. The RT-PCR products were subjected to in vitro coupled transcription/translation in the presence of [^{35}S] methionine. The translation products were immunoprecipitated with α-myc-tag antibody and were resolved by 10%–20% SDS-PAGE. The locations of the full-length (FL) and truncated (Tr) translation products, which correspond to the unedited and edited NF1 mRNA, respectively, are indicated to the left of the gel. Control reactions were undertaken by use of a synthetic, sequence-validated template containing either C or T at nt 3916. The results shown are representative of three such experiments.

jected to in vitro transcription with SP6 RNA polymerase, in the presence of α[^{32}P]-CTP (3,000 Ci/mmol). The [^{32}P]-labeled NF1 RNA (50,000 cpm, at 4 × 10^8 cpm/μg) was incubated with 25 ng recombinant GST/APOBEC-1 (MacGinnitie et al. 1995) for 15 min at room temperature, in a buffer containing 10 mM HEPES pH 8.0, 100 mM KCl, 1 mM EDTA, 0.25 mM DTT, and 2.5% glycerol. The reaction was then sequentially treated with RNase T1 (final concentration, 1 unit/μl) and heparin (final concentration, 5 mg/ml), followed by UV irradiation (250 mJ/cm^2) in a Stratalinker (Stratagene). As control, RNA binding was performed with a 105-nt rat apoB RNA that previously had been demonstrated to bind apobec-1 (Anant et al. 1995; Nakamuta et al. 1995; Anant and Davidson 2000). Competition analysis was performed with radiolabeled NF1 RNA and 5- and 10-fold excess of cold apoB RNA, as described in detail elsewhere (Anant et al. 1995).

Adenovirus-Mediated Infection of HepG2 Cells

Recombinant adenovirus expressing either rat apobec-1 or a control, lacZ cDNA, were cloned as described elsewhere (Kozarsky et al. 1996) and were titered to a multiplicity of infection (MOI) of 10^9–10^{10} pfu/ml. HepG2 cells were infected with 3 × 10^3–MOI recombinant adenovirus and cell lysates, and total RNA was prepared for analysis after 48 h. Primer-extension analysis was performed to quantitate C→U editing of endogenous NF1 and apoB RNA, as outlined above and as described in detail elsewhere (Giannoni et al. 1994). Cell lysates were analyzed by denaturing SDS-PAGE and western blotting, to demonstrate, as described elsewhere (Anant and Davidson 2000), the presence of apobec-1, by rabbit anti–apobec-1 IgG.

Results

NF1 RNA Sequence Alignment Flanking the Edited Base at nt 3916

The *cis*-acting elements regulating C→U editing of apoB RNA have been extensively characterized and include an AU-rich bulk-RNA context, a mooring sequence 3′ of the edited base, and efficiency elements both upstream and downstream (Shah et al. 1991; Backus and Smith 1992; Driscoll et al. 1993; Backus et al. 1994; Anant et al. 1995; Hersberger and Innerarity 1998; Anant and Davidson 2000). Alignment of an ~40-nt stretch of NF1 RNA sequence flanking nt 3916 reveals ~50% identity with apoB RNA, as has been noted elsewhere (Skuse et al. 1996), including 6 of 11 matches in the region corresponding to the mooring sequence (fig. 1). More recently, a consensus apobec-1 binding motif, UUUN[A/U]U, has been identified in both apoB RNA and other validated targets of high-affinity binding by apobec-1 (Anant and Davidson 2000). Further inspection of the NF1 RNA sequence flanking the edited base reveals this consensus apobec-1 binding site immediately upstream of the targeted cytidine (fig. 1). Therefore, we examined directly the ability of recombinant apobec-1

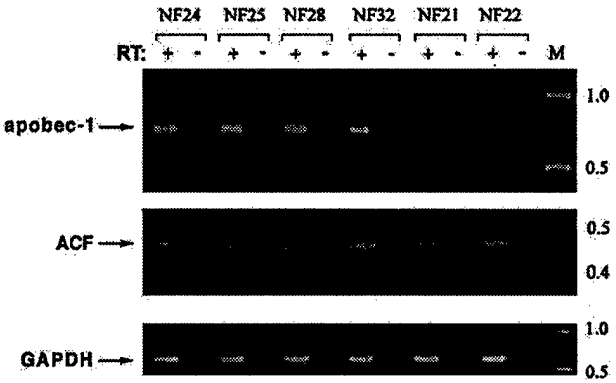

Figure 4 apobec-1 mRNA, expressed in a subset of neurofibromatosis tumors. RT-PCR by gene-specific primers ("+" lanes) was performed to amplify apobec-1, ACF, and GAPDH (*top*, *middle*, and *bottom*, respectively). As a control, PCR without prior RT ("−" lanes) was performed. The locations of molecular-weight standards are indicated to the right of the gel.

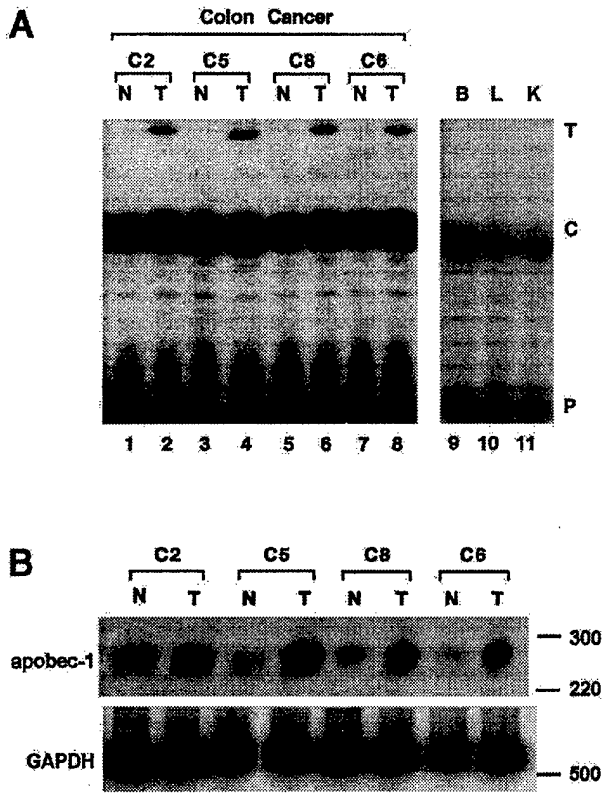

Figure 5 Editing of NF1 mRNA in colon cancers. *A*, Endogenous editing of NF1 RNA, as determined by primer-extension analysis and described in figure 2*A*. The data demonstrate increased editing in colon tumor tissue (lanes T), compared to matched normal control tissue (lanes N). In addition, no editing (<1% U) was observed in NF1 mRNA from normal brain (lane B), liver (lane L), or kidney (lane K). *B*, apobec-1 mRNA expression induced in colon cancers. RT-PCR was performed in the presence of $\alpha[^{32}P]$-dCTP, by use of primers specific for apobec-1 and GAPDH, to amplify a 274- and a 510-bp fragment, respectively. Increased expression of apobec-1 is observed in colon tumor tissue (lanes T), compared to paired normal tissue (lanes N). The locations of the molecular-weight (in bp) markers are indicated to the right of the gel.

to bind synthetic NF1 RNA template, using UV cross-linking. The data demonstrate that apobec-1 binds NF1 RNA (fig. 1*B*) and that this binding is competed by apoB RNA (fig. 1*B*, lanes 3 and 4).

C→U Editing of RNA of NF1 Samples

RNA from 34 PNSTs was subjected to primer-extension assay, to detect C→U editing of NF1 RNA, and the reaction products were analyzed by urea PAGE and phosphorimaging. A representative series of samples is shown in figure 2*A*. Several of the samples (24, 25, and 28; see fig. 2*A*) demonstrated 12%–16% C→U editing of RNA, similar to the values and range noted by Skuse and colleagues (Skuse et al. 1996; Cappione et al. 1997). However, having established, by using synthetic RNA templates (data not shown), the limits of detection, we were able to exclude bona fide editing in samples in which there was less than ~1% U (samples 20–22; see fig. 2*A*). This technical point is also emphasized in the results of primer-extension analysis of genomic DNA from the most extensively edited tumors, in which there is no detectable T in either of the sample lanes or in the control C template (fig. 2*B*). Direct sequencing of the cDNA products confirmed the presence of a T in the edited cDNA, corresponding to nt 3916 (fig. 2*C*). The cumulative results for the 34 samples assayed are listed in table 1. The findings demonstrate that a subset (8/34) of tumors manifest C→U editing of RNA (defined as >3% U) and that the remainder (26/34) demonstrate either very low levels (1%–2.5% U [in the case of 16/34]) or undetectable (<1% U [in the case of 10/34]) editing activity. These findings suggest that C→U editing of NF1 RNA is not a universal finding in tumors but, rather, appears to be confined to a subset of samples.

C→U Editing of NF1 RNA: Detection by Protein-Truncation Assay

The products of the initial round of RT-PCR were amplified in-frame with a myc-tag and T7 promoter and were used to program a coupled in vitro transcription/translation reaction mixture. Both full-length and truncated products were recovered (fig. 3). The molar incorporation of $[^{35}S]$-methionine into immunoprecipitable protein products revealed the observed proportion of full-length to truncated protein products to be ~10:1, close to the value expected on the basis of C→U editing (i.e., ~10%–15%) of NF1 RNA in the respective sample of origin.

Tumors Demonstrating C→U Editing: Expression of apobec-1 mRNA

The expression of gene products associated with the machinery for editing of apoB RNA was investigated as a potential variable contributing to the heterogeneity observed in C→U editing of NF1 RNA. Two gene products in particular were examined. These correspond to apobec-1, the catalytic deaminase responsible for C→U editing of apoB, and ACF, the competence factor that supports site-specific deamination of apoB RNA by apobec-1 (Teng et al. 1993; Lellek et al. 2000; Mehta et al. 2000). apobec-1 mRNA was detectable in all eight tumors that manifest >3% C→U editing (fig. 4 and table 1). In all cases, the amplification products were sequenced, to confirm the identity of apobec-1 (data not shown). Tumor samples that demonstrated either no C→U editing (samples 21 and 22; see fig. 2*A*) or very low (i.e., ~1%–2%) levels did not yield a detectable product for apobec-1 mRNA (fig. 4 and table 1), even when nested PCR was used. More-

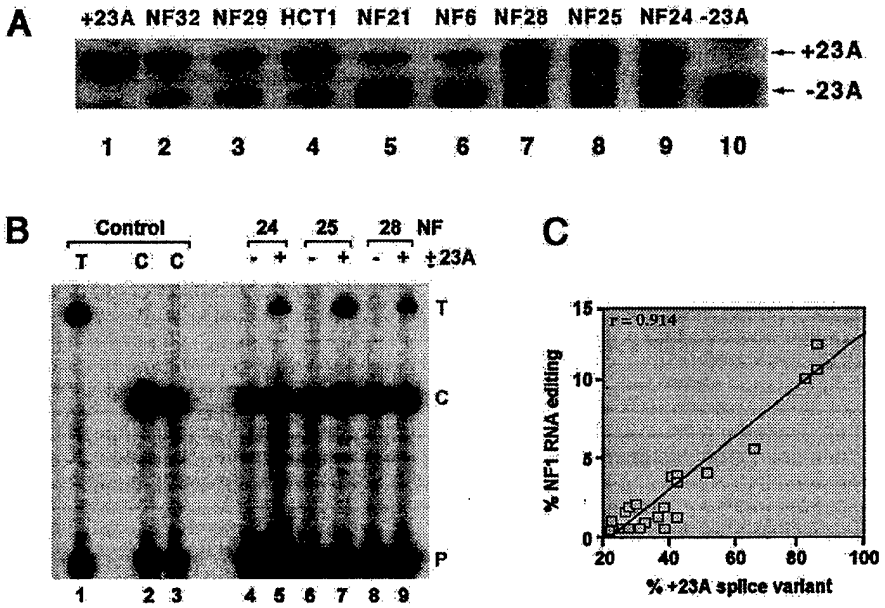

Figure 6 Preferential editing of NF1 mRNA containing exon 23A. *A*, Levels of alternative splicing of exon 23A in various tumor samples, as determined by RT-PCR and described in the "Material and Methods" section. As controls, PCRs were performed with synthetic RNA templates either containing (+23A) or lacking (−23A) exon 23A. The results shown are representative of experiments performed in triplicate, with all the tumor and normal samples. *B*, RT-PCR products of NF1 RNA containing (+23A) and lacking (−23A) the alternatively spliced exon, which were purified by electrophoresis and which subsequently were subjected to primer-extension analysis. As a control, primer-extension analysis was performed with cDNA templates containing only either a C or a T at nt 3916. The results shown are representative of three such experiments. *C*, Correlation between editing of NF1 RNA and inclusion of exon 23A (data are percent of total amount). This correlation was significant ($P < .001$).

over, normal tissue from sites in which apobec-1 is not detectable (e.g., liver, kidney, and brain) demonstrated <1% C→U editing of NF1 RNA (fig. 5). The observation that remains unexplained is the apparent lack of apobec-1 expression in tumors demonstrating very low (i.e., ~1%–2%) levels C→U editing (fig. 4 and table 1). We speculate that this finding may be due to the mixed cellular composition typically found in the PNSTs, in which editing of NF1 RNA occurs in a small subset of cells and in which apobec-1 mRNA is below detection limits. ACF mRNA, by contrast, was detected in all samples (fig. 4 and table 1), a finding consistent with previous reports that its expression is ubiquitous in humans (Lellek et al. 2000; Mehta et al. 2000). As an additional control, all RNA samples supported amplification of GAPDH mRNA (fig. 4).

Non-Neuronal Tumors Expressing apobec-1 and Demonstrating Editing of NF1 RNA

In humans, apobec-1 is normally confined to the luminal gastrointestinal tract (Teng et al. 1993; Yamanaka et al. 1994; Funahashi et al. 1995). Human colorectal cancers, however, have been demonstrated to express increased levels of apobec-1 mRNA, compared to normal adjacent mucosa (Lee et al. 1998). NF1 RNA was amplified from these tumors as well as from the adjacent normal tissue and was subjected to primer-extension assay. The results demonstrate higher levels of C→U editing of RNA in the tumor samples (4%–8% U), compared to paired normal tissue, and confirm the increase in apobec-1 mRNA abundance (1%–3% U) (figs. 5*A* and *B*). These findings suggest that C→U editing of NF1 RNA is not confined to tumors arising from Schwann-like cells but may be a feature of tumors that support apobec-1 expression; however, a more extensive survey of tumors of the gastrointestinal tract will be required, to allow us to formally examine the implications of editing of NF1 RNA, in relation to apobec-1–gene expression.

Editing of NF1 RNA: Occurrence in Transcripts Containing Exon 23A

To further pursue the mechanisms underlying the heterogeneity of C→U editing of NF1, transcripts were selectively amplified (by a strategy reviewed both in the "Material and Methods" section and in fig. 1), to examine alternative splicing of exon 23A, downstream of the edited base. As illustrated in figure 6*A*, these samples reveal a range of proportions of this alternatively spliced

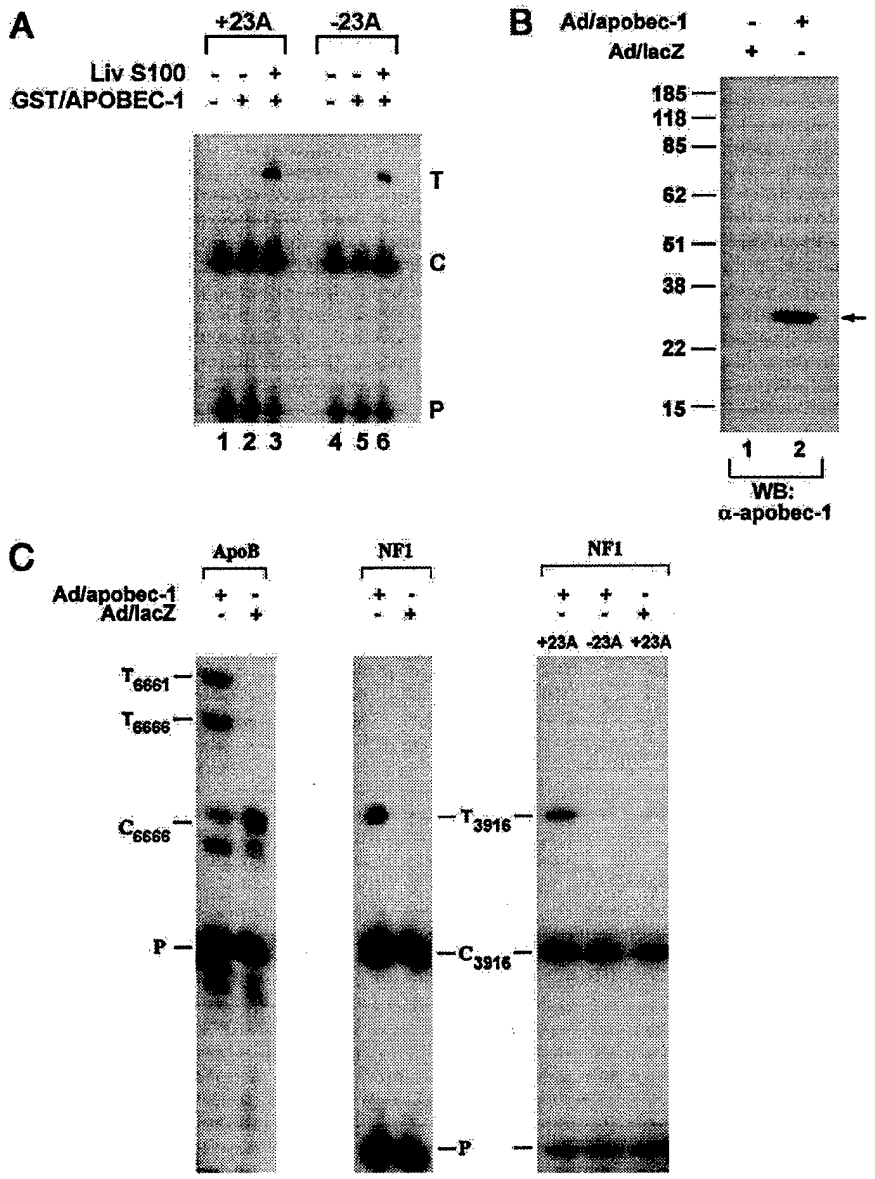

Figure 7 apobec-1 mediation of C→U editing of NF1 RNA. *A*, Assays of in vitro editing of RNA, performed with 20 fmol synthetic NF1 RNA either containing (+23A) or lacking (−23A) exon 23 A, in the presence of 250 ng recombinant GST/APOBEC-1 and 50 μg bovine liver extract (Liv S100). After in vitro incubation, the RNA was extracted, and cDNA was prepared for analysis by primer extension (see the "Material and Methods" section). The mobilities of the primer (P) and of the unedited (C) and edited (T) cDNA are indicated to the right of the gel. *B*, Adenovirus-mediated expression of apobec-1. HepG2 cells, from a human hepatoma cell line, were infected with recombinant adenovirus encoding either apobec-1 (Ad/apobec-1) or the bacterial β-galactosidase (Ad/lacZ). Forty-eight hours after infection, cell lysates were prepared and were subjected to western blot analysis with rabbit α-apobec-1 IgG. Migration of the 27-kD apobec-1 immunoreactive band is indicated by an arrow to the right of the gel, and molecular-weight standards are indicated to the left of the gel. *C*, Total RNA extracted from HepG2 cells infected with either Ad/apobec-1 or Ad/lacZ and subjected to RT-PCR for amplification of apoB (*left panel*) and NF1 (*middle panel*) mRNAs flanking the edited base. Primer-extension analysis was performed and was analyzed by PAGE with 8% acrylamide containing urea. To differentiate the editing of RNA in the two alternatively spliced NF1 transcripts (lanes ±23A), the PCR products were fractionated through agarose gels, and the two products were isolated and were individually subjected to primer-extension analysis (*right panel*). The locations of the primer and of unedited (C) and edited (U) primer-extension products, for both apoB and NF1, are indicated to the left or right of the gels. This is a representative of three independent assays.

exon. These amplicons were individually isolated and were subjected to primer-extension analysis, and the extent of C→U editing was determined. As indicated in figure 6*B*, C→U editing was found only in transcripts containing exon 23A. This approach was applied to the range of tumors studied, and the results demonstrated a strong positive correlation between the relative proportions of exon 23A–containing transcripts and the extent of C→U editing of RNA (fig. 6*C*). These findings strongly suggest a functional relationship between the presence of exon 23A and the editing of NF1 RNA.

apobec-1 as the Mediator of C→U Editing of NF1 RNA In Vivo and In Vitro

We employed two complementary approaches to confirm the suspected role of apobec-1 in C→U editing of NF1. In the first approach, we incubated synthetic NF1 transcripts that contained the unedited cytidine at nt 3916 and that either included (+23A) or lacked (−23A) the alternatively spliced downstream exon, with apobec-1 and S100 extracts. The results of these assays (fig. 7*A*) reveal that C→U editing of NF1 RNA can be reproduced in vitro and that transcripts containing exon 23A are more extensively edited (12% ± 1.7% U; $n = 3$), compared to transcripts lacking this alternatively spliced exon (3.9% ± 0.8% U; $n = 3$; $P < .001$). In the second approach, we used adenovirus-mediated transduction of apobec-1 to demonstrate a gain of function in cell culture. For this purpose, we turned to HepG2 cells, a human liver–derived cell line that expresses apoB RNA and NF1 mRNA but that does not express endogenous apobec-1 (Giannoni et al. 1994). HepG2 cells were infected with either adenovirus apobec-1 or lacZ, and cell lysates were prepared for protein and RNA extraction 48 h later. The results confirm the efficient induction of editing of apoB RNA after introduction of apobec-1 (see the western blot in fig. 7*B*) and reveal C→U editing at the canonical site (nt 6666), as well as hyperediting of upstream cytidines (C6661), as noted elsewhere (Sowden et al. 1996; Yamanaka et al. 1996) (fig. 7*C*, *left*); RNA from these same cells demonstrated C→U editing of NF1 RNA (fig. 7*C*, *middle*), with no such change, in either transcript, after lacZ transfection. Further analysis of these NF1 RNA species reveals that C→U editing was detectable only in transcripts containing exon 23A (fig. 7*C*, *right*), confirming and extending findings from the tumors analyzed above.

Discussion

Several mechanisms exist for amplification of the repertoire of genes encoded in chromosomal DNA. Posttranscriptional regulation encompasses one such level of control and includes editing of RNA, which has recently emerged as an important restriction point in the species- and tissue-specific modulation of gene expression (Maas and Rich 2000). The central conclusion of the present study demonstrates that C→U editing of NF1 RNA occurs in a subset of tumor samples that have at least two distinguishing characteristics that distinguish them from those tumors in which editing of RNA does not occur; these characteristics are (1) the presence of apobec-1 mRNA and (2) the preferential inclusion of a downstream exon, 23A, in the edited transcript. The findings (*a*) add support to the hypothesis that, in the regulation of mRNA metabolism, apobec-1 may play a role beyond that of its originally identified target, apoB, and (*b*) provide evidence that alternative splicing of NF1 RNA may be an important component of C→U editing of this transcript. Each of these observations merits additional discussion.

apobec-1 is an RNA-specific cytidine deaminase whose expression, in humans, is confined to the luminal gastrointestinal tract (Hadjiagapiou et al. 1994; Lau et al. 1994). apobec-1 functions as a dimeric subunit component of a multicomponent holoenzyme and mediates site-specific deamination of a single cytidine in the nuclear apoB transcript. This C→U RNA-editing reaction results in the production of a truncated protein, apoB48, required for intestinal lipid transport (Chen et al. 1987; Powell et al. 1987; Teng et al. 1993). Accordingly, the finding that apobec-1 mRNA is expressed in neuronal tumors from patients with NF1 represents the first demonstration, in humans, of apobec-1 expression in cells other than epithelial cells lining the gastrointestinal tract (Hadjiagapiou et al. 1994; Lau et al. 1994). apobec-1 mRNA expression is widespread in the mouse and rat, and C→U RNA editing activity can be demonstrated in tissue extracts from numerous organs (Greeve et al. 1993; Nakamuta et al. 1995; Hirano et al. 1997; Qian et al. 1997). Nevertheless, the mechanism by which apobec-1 expression is confined to the gastrointestinal tract in humans has not been clarified. Analyses undertaken by several groups have revealed few informative features of the proximal promoter region of the human *APOBEC-1* gene, and no additional insight has been gained through comparative analyses of the murine, rat, and human loci (Greeve et al. 1993; Nakamuta et al. 1995; Hirano et al. 1997; Qian et al. 1997). apobec-1 mRNA expression has been examined in a number of human carcinomas (Greeve et al. 1999), in light of the phenotype associated with forced overexpression of apobec-1 in transgenic animals, in which promiscuous C→U RNA editing of other target transcripts has been associated with hepatocellular carcinoma (Yamanaka et al. 1996, 1997). These studies, in human cancer tissues, concluded that apobec-1 mRNA is detectable only in cancers arising in the luminal gastrointestinal tract (Greeve et al. 1999), a finding that previously had been noted in normal tissue (Greeve et al. 1993; Hadjiagapiou et al. 1994; Lau et al. 1994). Ac-

cordingly, overexpression of apobec-1 does not appear to be a general feature of malignancy; this said, the factors that permit expression of apobec-1 mRNA in a subset of PNSTs from patients with NF1 will require additional investigation.

In considering the possibility that apobec-1 was involved in C→U editing of NF1, we were intrigued by the earlier observations, by Skuse and colleagues, that the NF1 RNA region flanking the edited base contains only ~50% identity to the canonical apoB RNA sequence, particularly within an 11-nt motif referred to as the "mooring sequence" (Backus and Smith 1992; Skuse et al. 1996). We suspected, as did Skuse and colleagues, that this degree of mismatch would severely impair the efficiency of C→U RNA editing (Skuse et al. 1996). This suspicion is consistent with the finding that C→U editing of NF1 RNA produces ≤20% UGA (edited RNA)—in contrast to the situation with intestinal apoB mRNA, in which, typically, >90% exists in the UAA (edited) form (Chen et al. 1987; Powell et al. 1987). The mechanisms accounting for these quantitative differences remain to be elucidated but include, in addition to structural features of the transcript that are associated with the optimal nucleotide sequence, distinctive requirements for *trans*-acting factors.

The functional significance, if any, of C→U editing of NF1 RNA remains unresolved; in particular, it is widely recognized that second-hit somatic mutations occur in the wild-type *NF1* allele in many PNSTs in patients with neurofibromatosis (reviewed in Cichowski and Jacks 2001). Furthermore, it should be emphasized that, with the exception of C→T changes at nt 3916, we did not systematically exclude somatic mutations in the PNSTs investigated in this study; nevertheless, at least from a theoretical standpoint, the finding that a subset of tumors from patients with NF1 demonstrate C→U RNA editing supports the hypothesis that modifier genes (in this case, apobec-1) may play a role in the heterogeneity of molecular defects. The corollary hypothesis is that C→U editing of NF1 RNA creates a translational stop codon, potentially leading to premature truncation of neurofibromin. We attempted to demonstrate the presence of a truncated protein corresponding to the edited mRNA in cell lysates from clonal intestinal-cancer cell lines supporting >15% C→U editing, but we were successful only in identifying the full-length form of the protein (data not shown). Whether this reflects technical limitations of the reagents or other explanations is currently unknown. Thus, the question of whether the edited NF1 RNA encodes a truncated protein in vivo is still unresolved.

Studies of NF1 mRNA in affected patients have revealed an ~50% incidence of splicing abnormalities (Park and Pivnick 1998). The majority of these splicing defects are predicted to result in protein truncations, and the current findings are certainly consistent with this general expectation; however, the results from this recent survey of splicing abnormalities in NF1 failed to reveal any specific feature associated with exon 23A, nor was there any particular clustering of alternative splice defects, which would favor inclusion of this exon (Costa et al. 2001). Exon 23A itself plays an important role in the function of neurofibromin, as inferred from targeted deletion of this region in mice, which results in a learning deficit (Costa et al. 2001). These findings suggest that there may be important parallels between the murine and human genes for NF1, parallels that could be investigated with surrogate models. Indeed, an important series of questions emerging from current studies concerns the possibility that C→U editing of NF1 RNA may be experimentally approached by murine models. This is an attractive possibility, since our lab and others have generated mutant strains in which apobec-1 has been deleted through homologous recombination. Additionally, the auxiliary subunit of the enzyme that edits apoB RNA recently has been cloned (Lellek et al. 2000; Mehta et al. 2000), and its role in alternative splicing and C→U editing of NF1 RNA will be of interest. In this regard, studies have demonstrated that an apobec-1–related RNA-specific deaminase, ADAR2, which mediates A→I editing of double-stranded RNA, also plays a role in alternative splicing (Rueter et al. 1999); this function will need to be examined in the context of apobec-1 and NF1 RNA. These and other issues related to the molecular mechanisms of posttranscriptional regulation will be the focus of future reports.

Acknowledgments

This work was supported by National Institutes of Health (NIH) grants HL-38180 and DK-56260 and NIH Digestive Disease Research Core Center grant DK-52574 (all to N.O.D.). The authors acknowledge the generous assistance of Drs. David N. Louis (Massachusetts General Hospital, Boston) and Priscilla Short (University of Chicago Hospitals) for their provision of samples for these analyses. In addition, the authors acknowledge their colleagues, Valerie Blanc, Libby Newberry, and Jeffrey Henderson, for their valuable insights and discussion.

Electronic-Database Information

Accession numbers and the URL for data in this article are as follows:

Online Mendelian Inheritance in Man (OMIM), http://www.ncbi.nlm.nih.gov/Omim/ (for NF1 [MIM 162200], APOB [MIM 107730], and APOBEC-1 [MIM 600130])

References

Anant S, Davidson NO (2000) An AU-rich sequence element (UUUN[A/U]U) downstream of the edited C in apolipopro-

tein B mRNA is a high-affinity binding site for Apobec-1: binding of Apobec-1 to this motif in the 3′ untranslated region of c-myc increases mRNA stability. Mol Cell Biol 20: 1982–1992

Anant S, MacGinnitie AJ, Davidson NO (1995) apobec-1, the catalytic subunit of the mammalian apolipoprotein B mRNA editing enzyme, is a novel RNA-binding protein. J Biol Chem 270:14762–14767

Anant S, Yu H, Davidson NO (1998) Evolutionary origins of the mammalian apolipoproteinB RNA editing enzyme, apobec-1: structural homology inferred from analysis of a cloned chicken small intestinal cytidine deaminase. Biol Chem 379:1075–1081

Andersen LB, Fountain JW, Gutmann DH, Tarle SA, Glover TW, Dracopoli NC, Housman DE, Collins FS (1993) Mutations in the neurofibromatosis 1 gene in sporadic malignant melanoma cell lines. Nat Genet 3:118–121

Ars E, Serra E, Garcia J, Kruyer H, Gaona A, Lazaro C, Estivill X (2000) Mutations affecting mRNA splicing are the most common molecular defects in patients with neurofibromatosis type 1. Hum Mol Genet 9:237–247

Ashkenas J (1997) Gene regulation by mRNA editing. Am J Hum Genet 60:278–283

Backus JW, Schock D, Smith HC (1994) Only cytidines 5′ of the apolipoprotein B mRNA mooring sequence are edited. Biochim Biophys Acta 1219:1–14

Backus JW, Smith HC (1992) Three distinct RNA sequence elements are required for efficient apolipoprotein B (apoB) RNA editing in vitro. Nucleic Acids Res 20:6007–6014

Basu TN, Gutmann DH, Fletcher JA, Glover TW, Collins FS, Downward J (1992) Aberrant regulation of ras proteins in malignant tumour cells from type 1 neurofibromatosis patients. Nature 356:713–715

Bollag G, Clapp DW, Shih S, Adler F, Zhang YY, Thompson P, Lange BJ, Freedman MH, McCormick F, Jacks T, Shannon K (1996) Loss of NF1 results in activation of the Ras signaling pathway and leads to aberrant growth in haematopoietic cells. Nat Genet 12:144–148

Cappione AJ, French BL, Skuse GR (1997) A potential role for NF1 mRNA editing in the pathogenesis of NF1 tumors. Am J Hum Genet 60:305–312

Chen SH, Habib G, Yang CY, Gu ZW, Lee BR, Weng SA, Silberman SR, Cai SJ, Deslypere JP, Rosseneu M, Gotto AM, Li WH, Chan L (1987) Apolipoprotein B-48 is the product of a messenger RNA with an organ-specific in-frame stop codon. Science 238:363–366

Cichowski K, Jacks T (2001) NF1 tumor suppressor gene function: narrowing the GAP. Cell 104:593–604

Costa RM, Yang T, Huynh DP, Pulst SM, Viskochil DH, Silva AJ, Brannan CI (2001) Learning deficits, but normal development and tumor predisposition, in mice lacking exon 23a of Nf1. Nat Genet 27:399–405

Davidson NO, Shelness GS (2000) Apolipoprotein B: mRNA editing, lipoprotein assembly, and presecretory degradation. Annu Rev Nutr 20:169–193

DeClue JE, Papageorge AG, Fletcher JA, Diehl SR, Ratner N, Vass WC, Lowy DR (1992) Abnormal regulation of mammalian p21ras contributes to malignant tumor growth in von Recklinghausen (type 1) neurofibromatosis. Cell 69: 265–273

Driscoll DM, Lakhe-Reddy S, Oleksa LM, Martinez D (1993) Induction of RNA editing at heterologous sites by sequences in apolipoprotein B mRNA. Mol Cell Biol 13:7288–7294

Funahashi T, Giannoni F, DePaoli AM, Skarosi SF, Davidson NO (1995) Tissue-specific, developmental and nutritional regulation of the gene encoding the catalytic subunit of the rat apolipoprotein B mRNA editing enzyme: functional role in the modulation of apoB mRNA editing. J Lipid Res 36: 414–428

Giannoni F, Bonen DK, Funahashi T, Hadjiagapiou C, Burant CF, Davidson NO (1994) Complementation of apolipoprotein B mRNA editing by human liver accompanied by secretion of apolipoprotein B48. J Biol Chem 269:5932–5936

Greeve J, Altkemper I, Dieterich JH, Greten H, Windler E (1993) Apolipoprotein B mRNA editing in 12 different mammalian species: hepatic expression is reflected in low concentrations of apoB-containing plasma lipoproteins. J Lipid Res 34:1367–1383

Greeve J, Lellek H, Apostel F, Hundoegger K, Barialai A, Kirsten R, Welker S, Greten H (1999) Absence of APOBEC-1 mediated mRNA editing in human carcinomas. Oncogene 18:6357–6366

Guha A, Lau N, Huvar I, Gutmann D, Provias J, Pawson T, Boss G (1996) Ras-GTP levels are elevated in human NF1 peripheral nerve tumors. Oncogene 12:507–513

Hadjiagapiou C, Giannoni F, Funahashi T, Skarosi SF, Davidson NO (1994) Molecular cloning of a human small intestinal apolipoprotein B mRNA editing protein. Nucleic Acids Res 22:1874–1879

Hersberger M, Innerarity TL (1998) Two efficiency elements flanking the editing site of cytidine 6666 in the apolipoprotein B mRNA support mooring-dependent editing. J Biol Chem 273:9435–9442

Hirano K, Min J, Funahashi T, Davidson NO (1997) Cloning and characterization of the rat apobec-1 gene: a comparative analysis of gene structure and promoter usage in rat and mouse. J Lipid Res 38:1103–1119

Hirano K, Young SG, Farese RV Jr, Ng J, Sande E, Warburton C, Powell-Braxton LM, Davidson NO (1996) Targeted disruption of the mouse apobec-1 gene abolishes apolipoprotein B mRNA editing and eliminates apolipoprotein B48. J Biol Chem 271:9887–9890

Kozarsky KF, Bonen DK, Giannoni F, Funahashi T, Wilson JM, Davidson NO (1996) Hepatic expression of the catalytic subunit of the apolipoprotein B mRNA editing enzyme (apobec-1) ameliorates hypercholesterolemia in LDL receptor-deficient rabbits. Hum Gene Ther 7:943–957

Lau N, Feldkamp MM, Roncari L, Loehr AH, Shannon P, Gutmann DH, Guha A (2000) Loss of neurofibromin is associated with activation of RAS/MAPK and PI3-K/AKT signaling in a neurofibromatosis 1 astrocytoma. J Neuropathol Exp Neurol 59:759–767

Lau PP, Zhu HJ, Baldini A, Charnsangavej C, Chan L (1994) Dimeric structure of a human apolipoprotein B mRNA editing protein and cloning and chromosomal localization of its gene. Proc Natl Acad Sci USA 91:8522–8526

Lee RM, Hirano K, Anant S, Baunoch D, Davidson NO (1998) An alternatively spliced form of apobec-1 messenger RNA is overexpressed in human colon cancer. Gastroenterology 115:1096–1103

Lellek H, Kirsten R, Diehl I, Apostel F, Buck F, Greeve J (2000) Purification and molecular cloning of a novel essential component of the apolipoprotein B mRNA editing enzyme-complex. J Biol Chem 275:19848–19856

Li Y, O'Connell P, Breidenbach HH, Cawthon R, Stevens J, Xu G, Neil S, Robertson M, White R, Viskochil D (1995) Genomic organization of the neurofibromatosis 1 gene (NF1). Genomics 25:9–18

Maas S, Rich A (2000) Changing genetic information through RNA editing. Bioessays 22:790–802

MacGinnitie AJ, Anant S, Davidson NO (1995) Mutagenesis of apobec-1, the catalytic subunit of the mammalian apolipoprotein B mRNA editing enzyme, reveals distinct domains that mediate cytosine nucleoside deaminase, RNA binding, and RNA editing activity. J Biol Chem 270:14768–14775

Madsen P, Anant S, Rasmussen HH, Gromov P, Vorum H, Dumanski JP, Tommerup N, Collins JE, Wright CL, Dunham I, MacGinnitie AJ, Davidson NO, Celis JE (1999) Psoriasis upregulated phorbolin-1 shares structural but not functional similarity to the mRNA-editing protein apobec-1. J Invest Dermatol 113:162–169

Mehta A, Kinter MT, Sherman NE, Driscoll DM (2000) Molecular cloning of apobec-1 complementation factor, a novel RNA-binding protein involved in the editing of apolipoprotein B mRNA. Mol Cell Biol 20:1846–1854

Morrison JR, Paszty C, Stevens ME, Hughes SD, Forte T, Scott J, Rubin EM (1996) Apolipoprotein B RNA editing enzyme-deficient mice are viable despite alterations in lipoprotein metabolism. Proc Natl Acad Sci USA 93:7154–7159

Nakafuku M, Nagamine M, Ohtoshi A, Tanaka K, Toh-e A, Kaziro Y (1993) Suppression of oncogenic Ras by mutant neurofibromatosis type 1 genes with single amino acid substitutions. Proc Natl Acad Sci USA 90:6706–6710

Nakamuta M, Oka K, Krushkal J, Kobayashi K, Yamamoto M, Li WH, Chan L (1995) Alternative mRNA splicing and differential promoter utilization determine tissue-specific expression of the apolipoprotein B mRNA-editing protein (Apobec1) gene in mice: structure and evolution of Apobec1 and related nucleoside/nucleotide deaminases. J Biol Chem 270:13042–13056

National Institutes of Health Consensus Development Conference (1988) Neurofibromatosis: conference statement. Arch Neurol 45:575–578

Park VM, Pivnick EK (1998) Neurofibromatosis type 1 (NF1): a protein truncation assay yielding identification of mutations in 73% of patients. J Med Genet 35:813–820

Powell LM, Wallis SC, Pease RJ, Edwards YH, Knott TJ, Scott J (1987) A novel form of tissue-specific RNA processing produces apolipoprotein-B48 in intestine. Cell 50:831–840

Qian X, Balestra ME, Innerarity TL (1997) Two distinct TATA-less promoters direct tissue-specific expression of the rat apo-B editing catalytic polypeptide 1 gene. J Biol Chem 272:18060–18070

Rueter SM, Dawson TR, Emeson RB (1999) Regulation of alternative splicing by RNA editing. Nature 399:75–80

Shah RR, Knott TJ, Legros JE, Navaratnam N, Greeve JC, Scott J (1991) Sequence requirements for the editing of apolipoprotein B mRNA. J Biol Chem 266:16301–16304

Sherman LS, Atit R, Rosenbaum T, Cox AD, Ratner N (2000) Single cell Ras-GTP analysis reveals altered Ras activity in a subpopulation of neurofibroma Schwann cells but not fibroblasts. J Biol Chem 275:30740–30745

Skuse GR, Cappione AJ (1997) RNA processing and clinical variability in neurofibromatosis type I (NF1). Hum Mol Genet 6:1707–1712

Skuse GR, Cappione AJ, Sowden M, Metheny LJ, Smith HC (1996) The neurofibromatosis type I messenger RNA undergoes base-modification RNA editing. Nucleic Acids Res 24:478–485

Skuse GR, Ludlow JW (1995) Tumour suppressor genes in disease and therapy. Lancet 345:902–906

Sowden M, Hamm JK, Smith HC (1996) Overexpression of APOBEC-1 results in mooring sequence-dependent promiscuous RNA editing. J Biol Chem 271:3011–3017

Teng B, Burant CF, Davidson NO (1993) Molecular cloning of an apolipoprotein B messenger RNA editing protein. Science 260:1816–1819

Yamanaka S, Poksay KS, Arnold KS, Innerarity TL (1997) A novel translational repressor mRNA is edited extensively in livers containing tumors caused by the transgene expression of the apoB mRNA-editing enzyme. Genes Dev 11:321–333

Yamanaka S, Poksay KS, Balestra ME, Zeng GQ, Innerarity TL (1994) Cloning and mutagenesis of the rabbit ApoB mRNA editing protein: a zinc motif is essential for catalytic activity, and noncatalytic auxiliary factor(s) of the editing complex are widely distributed. J Biol Chem 269:21725–21734

Yamanaka S, Poksay KS, Driscoll DM, Innerarity TL (1996) Hyperediting of multiple cytidines of apolipoprotein B mRNA by APOBEC-1 requires auxiliary protein(s) but not a mooring sequence motif. J Biol Chem 271:11506–11510

Published manuscript: Packer R, Gutmann D, Rubenstein A, **Viskochil D**, Zimmerman R, Vezina G, Small J, Korf B. Plexiform neurofibromas in NF1. Toward biologic-based therapy. Neurology 2002:58;1461-1470.

CME

Plexiform neurofibromas in NF1

Toward biologic-based therapy

R.J. Packer, MD; D.H. Gutmann, MD, PhD; A. Rubenstein, MD; D. Viskochil, MD, PhD; R.A. Zimmerman, MD; G. Vezina, MD; J. Small, PhD; and B. Korf, MD, PhD

Abstract—Neurofibromatosis type 1 (NF1) is one of the most common neurogenetic diseases affecting adults and children. Neurofibromas are one of the most common of the protean manifestations of NF1. Plexiform neurofibromas, which will frequently cause cosmetic abnormalities, pain, and neurologic deficits, are composed of "neoplastic" Schwann cells accompanied by other participating cellular and noncellular components. There is increasing evidence that loss of *NF1* expression in neoplastic Schwann cells is associated with elevated levels of activated RAS, supporting the notion that the *NF1* gene product, neurofibromin, acts as a growth regulator by inhibiting ras growth-promoting activity. In addition, there is increasing evidence that other cooperating events, which may be under cytokine modulation, are important for neurofibroma development and growth. Treatment of plexiform neurofibromas has been empiric, with surgery being the primary option for those with progressive lesions causing a major degree of morbidity. The efficacy of alternative treatment approaches, including the use of antihistamines, maturation agents, and antiangiogenic drugs, has been questionable. More recently, biologic-based therapeutic approaches, using drugs that target the molecular genetic underpinnings of plexiform neurofibromas or cytokines believed important in tumor growth, have been initiated. Evaluation of such trials is hindered by the unpredictable natural history of plexiform neurofibromas and difficulties in determining objective response in tumors that are notoriously large and irregular in shape. Innovative neuroimaging techniques and the incorporation of quality-of-life scales may be helpful in evaluation of therapeutic interventions. The ability to design more rational therapies for NF1-associated neurofibromas is heavily predicated on an improved understanding of the molecular and cellular biology of the cells involved in neurofibroma formation and growth.

NEUROLOGY 2002;58:1461–1470

Neurofibromatosis type 1 (NF1) is one of the most common neurogenetic diseases affecting children and adults, occurring in 1 per 3,500 to 4,000 individuals.[1,2] NF1 is transmitted as an autosomal dominant disorder with a spontaneous mutation rate, estimated to be as high as 50%. NF1 has protean manifestations and can involve the central and peripheral nervous systems as well as the skin, bone, endocrine, gastrointestinal, and vascular systems. Diagnostic criteria for NF1 highlight these diverse manifestations and include pigmentary lesions (café-au-lait macules, skin fold freckling, and Lisch nodules), neurofibromas, optic pathway gliomas, and bony dysplasias. Despite the frequent occurrence of symptomatic neurofibromas in patients with NF1, these lesions have not been well studied and treatment options are limited. New insights into the molecular pathogenesis of tumors in patients with NF1 have opened innovative avenues for treatment.

Clinical aspects. Neurofibromas are benign peripheral nerve sheath tumors characterized by unpredictable patterns of growth, variable cellular composition, and diverse appearances.[1-5] Nearly all adults with NF1 will develop neurofibromas at some time during their lives. Classified as World Health Organization grade 1 tumors, such lesions may be present at birth or develop at any time during life. Clinically, neurofibromas may present as discrete tumors (dermal neurofibromas), diffuse tumors, plexiform neurofibromas, or tumors associated with spinal nerve sheaths (spinal neurofibromas). Neurofibromas are composed of neoplastic Schwann cells, perineural-like cells, and fibroblasts in a matrix of collagen fibers and mucosubstances.[4] Growth of neurofibromas is initially along the course of nerve fibers. If the tumor arises from a relatively large nerve, it may be enclosed by the thickened epineurium and be confined to the nerve (a discrete

From the Departments of Neurology and Pediatrics (Dr. Packer) and Radiology (Neuroradiology) (Dr. Vezina), Children's National Medical Center, George Washington University, Washington, DC; Department of Neurology (Dr. Gutmann), Washington University School of Medicine, and Neurofibromatosis Program, St. Louis Children's Hospital, St. Louis, MO; Department of Neurology (Dr. Rubenstein), Mount Sinai School of Medicine, and National Neurofibromatosis Foundation (Dr. Small), New York, NY; Department of Pediatrics (Dr. Viskochil), University of Utah, Salt Lake City; Department of Radiology (Neuroradiology) (Dr. Zimmerman), Children's Hospital of Philadelphia and University of Pennsylvania; and Harvard–Partners Center for Genetics and Genomics (Dr. Korf), Massachusetts General Hospital, Boston.

Received July 27, 2001. Accepted in final form December 24, 2001.

Address correspondence and reprint requests to Dr. Roger J. Packer, Center for Neuroscience and Behavioral Medicine, Department of Neurology, Children's National Medical Center, 111 Michigan Ave. NW, Washington, DC 20010; e-mail: rpacker@cnmc.org

lesion). Tumors arising from small nerves may spread diffusely into the dermis and soft tissue. Plexiform neurofibromas involve multiple nerves or fascicles and are expanded by tumor cells and collagen.

Solitary plexiform neurofibromas may occur in patients without other stigmata of NF1. In a recent review, 8 of 124 patients with plexiform neurofibromas had no other evidence of NF1.[5] The pathogenesis of such lesions is unclear, but they may result from mosaicism of *NF1* or a related gene. Although the majority of patients with localized forms of NF1 have no affected relatives with the disease, there are infrequent reports of patients with localized NF1 having children with findings diagnostic of NF1. Although genetic testing for some of the mutations of the *NF1* gene exists, there is no evidence that such testing will be helpful in diagnosing NF1 in patients with isolated plexiform neurofibromas.

Discrete dermal neurofibromas tend to arise from a sensory nerve but may present as an exophytic or subcutaneous tumor. Dermal neurofibromas may cause discomfort or itching but are rarely associated with neurologic deficit. Their pattern of growth is often unpredictable, with periods of gradual sustained enlargement followed by apparent growth arrest. Hormonal influence may modulate their growth, as these tumors more frequently demonstrate increased growth during puberty and pregnancy. However, they do not transform into malignant tumors.[8]

Plexiform neurofibromas are slow-growing tumors, which may be present at birth or may become apparent later in life. Their incidence in patients with neurofibromatosis has not been well established, but they probably occur in anywhere between 25 and 50% of patients, with most series suggesting an incidence of 25 to 30%.[2,3] These tumors arise in various regions of the body, including the trunk, limbs, head, and neck. In all of these areas, they can cause dysfunction including cosmetic abnormalities, pain, and functional deficits. Plexiform neurofibromas can remain silent for many years and may be revealed only by imaging studies. Some tumors may grow to large sizes prior to clinical detection; in one study of 126 individuals 16 years of age or older with NF1, plexiform neurofibromas were found in the chest of 20% of patients and in the abdomen and pelvis of 44%.[2] Spinal cord compression with associated neurologic dysfunction can occur, and masses that stretch along the peripheral nerve may cause nerve damage and resultant neurologic dysfunction. Plexiform neurofibromas can also present as congenital or early developmental lesions and result in severe cosmetic abnormalities or neurologic impairment; orbital lesions may compress the optic nerves, causing visual loss.

In contrast to discrete neurofibroma, plexiform neurofibromas often result in morbidity caused by continued tumor growth.[6,7] Diffuse or plexiform neurofibromas are typically associated with multiple nerves and can grow to large proportions, affecting an entire limb or body segment. These lesions often have a rich vascular network and may result in hemorrhage. In addition, the underlying bone may be stimulated to grow and result in limb length discrepancies or dysplasia; the latter is seen frequently in the orbital region (sphenoid wing dysplasia). Plexiform neurofibromas may also occasionally exhibit malignant transformation and mutate into malignant peripheral nerve sheath tumors.[7-11] These spindle cell sarcomas tend to be poorly responsive to therapy, can metastasize, and are associated with a low 5-year survival rate.

Spinal neurofibromas are often difficult to classify as either discrete or diffuse lesions.[11] Although they can involve multiple nerve roots, they may also appear as discrete compact lesions. The incidence of spinal neurofibromas in patients with NF1 has not been well delineated by prospective studies done in patients of different ages, but such lesions are thought to be quite common, are often multiple along the spine, and can cause motor or sensory deficits as they grow. Most spinal neurofibromas are located within the vertebral foramina and cause problems by compression of the nerve roots. In some patients, they are found essentially along all vertebral regions, and it can be difficult to determine which lesion is symptomatic. A familial form of NF1, manifest by café-au-lait spots and multiple spinal neurofibromas symmetrically affecting multiple spinal nerve roots, but with little other stigmata or NF1, has been described.[12]

Biologic aspects. There are several impediments that have limited progress in designing optimal therapies for NF1-associated neurofibromas, including a more complete understanding of 1) the contribution of each cell type in a neurofibroma to its genesis and continued growth, 2) the specific consequences of absent *NF1* gene function on cell growth control, and 3) the role of additional genetic and biologic factors that influence neurofibroma formation and growth. Histologically, dermal and plexiform neurofibromas are composed of "neoplastic" Schwann cells accompanied by a varying number of other participating cellular and noncellular components. Embedded in a rich mucosubstance collagen matrix are both nonneoplastic Schwann cells that retain one functional *NF1* allele (*NF1*+/−), "neoplastic" Schwann cells lacking *NF1* gene expression, as well as *NF1*+/− fibroblasts, perineurial cells, and mast cells. Although it is presumed that the *NF1*-deficient Schwann cell is the "neoplastic" component of this tumor, *NF1*+/− fibroblasts and mast cells might also contribute to tumorigenesis.

A number of recent studies have demonstrated that the "neoplastic" Schwann cells lack *NF1* gene expression by multiple methods including loss of heterozygosity, RNA and protein expression, and fluorescent in situ hybridization (FISH).[13-19] The *NF1* gene codes for a large cytoplasmic protein, termed neurofibromin, which functions in part as a tumor suppressor (negative growth regulator) by inactivating the RAS signaling molecule.[20,21] In many cells,

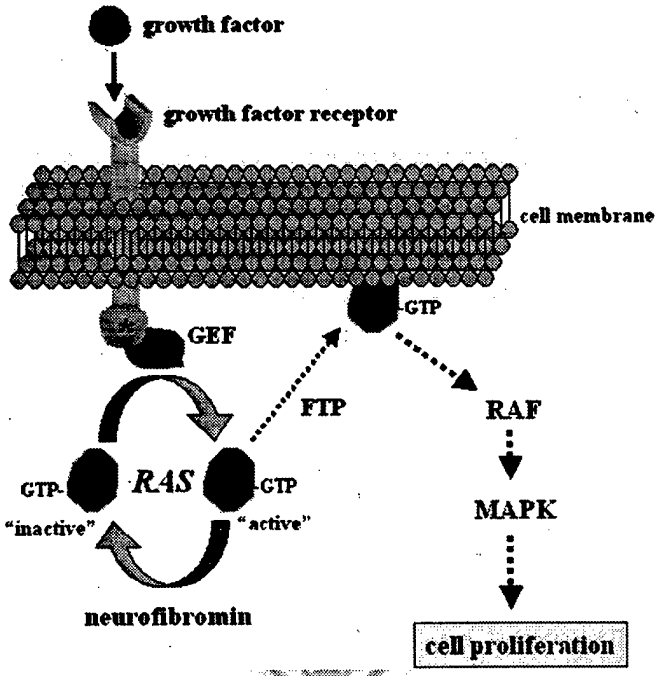

Figure 1. Growth regulatory pathways important for neurofibromatosis type 1 (NF1)-associated neurofibroma formation and progression. The binding of a mitogenic growth factor, such as epidermal growth factor (EGF) or fibroblast growth factor (FGF), to its specific receptor (EGF-R and FGF-R) results in receptor activation (denoted by asterisk). This activation recruits guanine nucleotide exchange factors (GEF) to the cell membrane, where they can accelerate the conversion of inactive GDP-bound RAS to its active GTP-bound form. Activation of RAS is associated with an additional post-translational modification mediated by farnesyltransferase proteins (FTP) that facilitates the translocation of RAS to the cell membrane, where it can initiate the cascade of activating interactions involving its specific downstream effectors (e.g., RAF and MAPK) that culminate in increased cell proliferation. Neurofibromin functions as a negative growth regulator (tumor suppressor) by accelerating the conversion of active GTP-bound RAS to its inactive GDP-bound form.

activation of RAS results from the binding of specific mitogenic growth factors (e.g., epidermal growth factor, fibroblast growth factor, etc.) to their cognate receptors (epidermal and fibroblast growth factor receptors). This association results in recruitment of specific activators of RAS to the cell membrane and the initiation of a cascade of signaling events (such as RAF and MAPK activation) that culminate in increased cell proliferation (figure 1). Neurofibromin functions to inactivate RAS and prevents RAS mitogenic signaling, resulting in reduced cell proliferation. Loss of neurofibromin as a consequence of inactivation of both copies of the *NF1* gene in the "neoplastic" Schwann cells is associated with elevated levels of activated RAS.[22] In another "benign" tumor type common in NF1, the optic nerve glioma, loss of the *NF1* gene product, neurofibromin, is likewise associated with increased RAS pathway activation.[23]

In contrast, neurofibroma-derived fibroblasts do not demonstrated elevated RAS activity.[23] However, in vitro studies suggest that neurofibroma-associated human fibroblasts or mouse *NF1*+/− fibroblasts may contribute to the pathogenesis of this tumor.[23] In this regard, mouse fibroblasts with one functioning *NF1* allele (*NF1*+/−), analogous to the fibroblasts in the human neurofibromas, display abnormal wound healing and continued fibroblast proliferation in

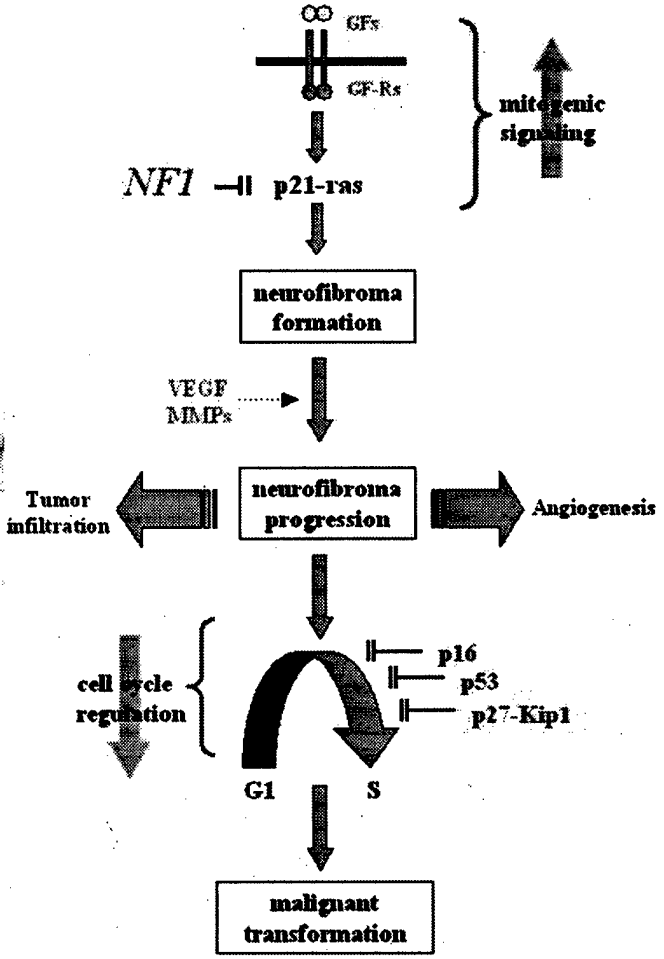

Figure 2. Additional factors may also contribute to tumor formation or progression. In this model of neurofibroma pathogenesis, the increased mitogenic signaling that results from inactivation of the NF1 *tumor suppressor and increased RAS activation is sufficient to initiate neurofibroma formation. Neurofibroma progression may result from additional genetic or biologic changes that increase the expression of vascular growth factors (GF; e.g., vascular endothelial growth factor [VEGF]) or matrix metalloproteinase enzymes (MMP) to promote angiogenesis and tumor infiltration. Last, malignant transformation requires further genetic changes that inactivate key cell cycle regulators, like the p16, p53, or p27-Kip1 tumor suppressors. Loss of these cell cycle regulators results in increased cell proliferation and the accumulation of additional genetic changes important for malignant transformation. Green denotes pathways and molecules that promote increased cell proliferation; red denotes molecules that reduce cell growth. GF-R = growth factor receptor.*

vivo.[24] These results argue that the non-neoplastic fibroblast is not "normal" and may contribute to the development of the neurofibroma by responding aberrantly to proliferative signals imparted by "neoplastic" Schwann cells.

Less is known about the contribution of the mast cell to the development of the neurofibroma. Although some patients describe itching in regions that later develop cutaneous neurofibromas, no direct role for the mast cell has been demonstrated. Mouse *NF1*+/− mast cells exhibit abnormal growth properties and dysregulated RAS signaling.[25] Further studies will be required to determine whether the mast cell plays a direct role in neurofibroma tumor formation or whether it represents an "innocent bystander" cell trapped within the tumor.

Although loss of *NF1* function in Schwann cells is associated with neurofibroma formation, there is abundant evidence that additional cooperating events may be important for neurofibroma genesis and growth. These changes include increased expression of growth factors and growth factor receptors, including epidermal and platelet-derived growth factor receptors[26,27] and vascular endothelial growth factor,[28] which may promote new blood vessel formation. In addition, neurofibroma-derived Schwann cells can invade chick allantoic membranes and survive as explants in rat sciatic nerve.[29,30] The angioinvasive properties of neurofibroma-derived Schwann cells may result from increased production of proteins that break down the extracellular matrix, such as matrix metalloproteinases (MMP), whose expression is elevated in neurofibromas.[31] These results suggest that other biologic properties in addition to cell growth are altered in human neurofibromas (figure 2).

As benign plexiform neurofibromas can transform into malignant peripheral nerve sheath tumors (MPNST), studies have focused on identifying cooperating genetic events that might be associated with malignant transformation (see figure 2). Functional inactivation of several key cell cycle regulators, including p53, p27-Kip1, and p16, have been identified in MPNST compared with their benign neurofibroma counterparts.[32-38] Loss of the function or expression of these cell cycle regulators results in increased cell proliferation and might permit the accumulation of additional genetic mutations important for malignant transformation. In support of the notion that alterations in cell cycle growth regulators are critical for MPNST formation, two groups have demonstrated that mice with targeted mutations in the *NF1* and p53 genes develop MPNST when both the *NF1* and p53 genes are inactivated.[39,40]

Treatment. Historically, the treatment of patients with plexiform neurofibromas in NF1 has been empiric. Patients have been followed clinically and radiographically, with intervention reserved for those who are symptomatic or those with clear-cut tumor enlargement. The majority of patients requiring intervention have been treated by surgery; however, because of the infiltrative nature of the tumors, outcome after surgery is often suboptimal, with a high incidence of tumor regrowth. In one series of 168 tumors operated on in patients collected from a large multidisciplinary institutional NF1 clinic, 74 cases were found to progress after surgery.[41] Factors associated with progression after surgery included younger age at the time of diagnosis, subtotal tumor resection, and a nonextremity location. As can be expected, extent of resection and tumor location are often inter-related, as tumors of the face may be difficult to excise because of concerns over postoperative cosmesis and tumors of the mediastinum and spine may insinuate with vital structures and thus be less amenable to total resection. In this series, patients younger than 10 years were more likely to have tumor progression than older patients after surgery; the reason(s) for such an association remains unclear but may be partially related to an increase in growth of the tumor at the time of puberty.

Because of concerns about malignant transformation, radiation therapy has not been widely used for plexiform neurofibromas. Over the last three decades, nonsurgical management has focused on the use of a variety of different drugs (see the table). However, despite clinical interest and need, there has been a paucity of clinical trials for patients with plexiform neurofibromas in NF1. The earliest therapeutic trials were aimed at targets thought to be integral in the progression of plexiform neurofibromas, such as mast cell function and angiogenesis. More recent approaches have targeted the "neoplastic" Schwann cell or the role of fibroblasts in tumor progression.

The first studies were performed with the antihistamine agent ketotifen fumarate.[42-44] These innovative studies, focused predominantly on superficial, primarily dermal, neurofibromas, used clinical criteria for eligibility. All patients with symptoms of itching and/or pain were eligible for the study. Treatment was aimed at improving symptomatology, especially relieving itching due to the neurofibroma. The first trial, using a double-blind crossover design, treated 20 patients (mean age 30.5 years); not all patients had clear-cut NF1, as patients with isolated neurofibromas could be entered if they had pruritus or dysesthetic pain. The second study was an open-label trial of 25 patients (mean age 27.1 years) with symptomatic neurofibromas. Eligible patients were to have progressive or continually symptomatic lesions causing discomfort or disability; radiographic progression was not a necessity for patient entry.

Because of the variability of entry criteria and the subjective endpoints, based primarily on patient self-reporting, evaluation of the efficacy of ketotifen fumarate is difficult. Patients entered in the ketotifen fumarate studies were evaluated for both change in clinical symptomatology, using a disability score, and change in size of the lesion, either by direct or by radiographic measurement. The investigators of the

Table *Clinical trials in patients with neurofibromatosis type 1 and plexiform neurofibromas*

Agent studied	Eligibility criteria	No. enrolled	Outcome measures	Results
Ketotifen fumarate in phase II	Symptomatic lesions	45 in 2 trials	Self-reporting symptomatic relief; change in size	Symptomatic relief in some; ↓ pruritis ± dysesthetic pain; no clear shrinkage
Retinoic acid or interferon-α in noncomparative phase II	Progressive lesions	57	Direct CT/MR measure; time to progression	86% retinoic, 96% interferon-α stable at 18 mo; symptomatic improvement in 14%, minor shrinkage in 5 (8%)
Thalidomide in phase I	Symptomatic lesions	20; 12 evaluable	Toxicity; efficacy a secondary endpoint	2 had dose-limiting toxicity; 4 had tumor shrinkage; 5 had symptomatic improvement
Oral farnesyl protein transferase inhibitor in phase I	Symptomatic lesions	17	Toxicity; efficacy a secondary endpoint	Well tolerated; no shrinkage seen

study concluded that ketotifen fumarate resulted in symptomatic relief of pruritus or dysesthetic pain or both in a subset of patients and improvement in the disability score.[42-44] However, radiographic response and clinical shrinkage of tumor were not well documented. These trials were performed primarily in the pre-MRI era, and only a subset of patients was evaluated by CT. In addition, owing partially to availability of the drug, the study treated predominantly teenagers and adults.

The largest prospective treatment trial for plexiform neurofibromas performed to date was a randomized noncomparative phase II trial that treated 57 evaluable patients with either *cis*-retinoic acid or interferon-α. Retinoic acid was used for its maturation effects and α-interferon for its nonspecific anti-inflammatory and anti-angiogenic properties. This study entered both children and adults. The median age of patients was 11 years (mean age 5.4 years), skewing the population to a relatively young patient group. This trial was designed to enter only patients with progressive plexiform neurofibromas. Patients were to have unequivocal radiographic progression or evidence of tumor growth by direct measurement within 1 month prior to entry, but some patients were entered on the basis of increasing clinical symptomatology. There was no stratification based on tumor location or age. Although the majority of patients had plexiform neurofibromas of the head and neck (n = 35), others had growths of the chest and spine (n = 9) or viscera (n = 8). Patients on study were to have direct measurements of tumor size and repeat neuroimaging evaluations, by either CT or MRI, every 3 months while on treatment. Standard oncologic phase II response criteria were used to evaluate for efficacy: That is, a complete response was considered total resolution of all lesions; a partial response, a >50% decrease in the sum of the greatest perpendicular diameters of measurable lesions; a minor response, a 25 to 50% decrease in the sum of the greatest perpendicular diameters of measurable lesions; and stable disease, a ≤25% decrease in measurable lesion size.

At 18 months of follow-up, 86% of patients treated with retinoic acid and 96% of patients treated with interferon were considered to be at least stable (P. Phillips, Children's Hospital of Philadelphia, personal communication, 2002). Three patients treated with retinoic acid and two treated with interferon had a 10 to 20% reduction in surface measurement; however, no patient had a demonstrable radiographic response. Symptomatic/physiologic improvement was noted in 14% (eight patients) of the population, with five of the symptomatic improvements occurring in those who had received interferon. Symptomatic improvement included relief of pain, resolution of bradycardia in a patient with a vagal nerve tumor, and, in one patient, a resolution of orthopnea.

A phase I study utilizing thalidomide, again targeting antiangiogenesis as a means to control neurofibroma growth, has been recently completed for patients with progressive plexiform neurofibromas.[45] As this was a phase I study, patients were required to have symptomatic lesions not amenable to treatment by conventional measures but did not require evidence of radiographic progression prior to study entry. The predominant aim of the study was to determine the toxicity of the agent used and the maximal tolerated dose of the agent safely deliverable; clinical and radiographic efficacy were secondary endpoints. An intrapatient dose escalation of the thalidomide was performed, and 20 patients, between the ages of 6 and 41 years (mean age 16.5 years) at the time of treatment, were entered on study. Eight of the 20 patients abandoned the study for a variety of reasons, including 2 being lost to follow-up, 2 having a MPNST on biopsy, and 2 for acute dose-limiting toxicity including neuropathy and hives. Interestingly, although efficacy was not a primary endpoint, four patients were noted to have a decrease in size of their lesions (by either radiographic or direct surface measure) and five had symptomatic improvement. Building on the results of these two previous studies, which used interferon and thalidomide, and the concept that antiangio-

genic compounds may be synergistic, there is interest in combining the agents to achieve greater efficacy.

The second phase I study used an oral farnesyl protein transferase inhibitor in 17 patients with plexiform neurofibromas (B. Widemann, National Cancer Institute, personal communication, 2002). Farnesyl protein transferase inhibitors block the post-translational isoprenylation of RAS and other farnesylated proteins.[46] The RAS proteins are integral to mitogenic cell signaling pathways, and proper farnesylation is essential for the function of RAS proteins. As described previously, neurofibromin, the product of the *NF1* gene, contains a domain capable of inactivating RAS by accelerating RAS-GTP hydrolysis (see figure 1). Decreased levels of neurofibromin have been associated with constitutively activated RAS-GTP status; thus, inhibition of RAS farnesylation may inhibit growth of tumors in patients with NF1. This was the first study to directly aim at the molecular genetic underpinnings of aberrant Schwann cells. The study used the criterion of a partial response as a measure of efficacy, and no patients on the study had a radiographic partial response. A phase II study utilizing a randomized placebo-controlled crossover design with the same agent is ongoing.

Another promising agent, 5-methyl-1-phenyl-2-(1*H*)-pyridone (Pirfenidone, Marnac, Dallas, TX), is already in clinical trials in adults with progressive plexiform and spinal neurofibromas. Pirfenidone is a broad-spectrum antifibrotic drug that modulates actions of cytokines such as platelet-derived growth factor, fibroblast growth factor, epidermal growth factor, intracellular adhesion molecules, and transforming growth factor-β1.[47,48] Inhibition of these cytokines decreases proliferation and collagen matrix synthesis in human fibroblasts. The antifibrotic effects of pirfenidone have been documented in vitro and in animal experiments in vivo and have been used in human fibrosing conditions.[49] The histopathology of neurofibromas is characterized by slender spindle cells with abundant extracellular matrix of dense, wavy collagen fibers and mucoid material. The pirfenidone treatment approach is designed to affect the potential growth-promoting effects of fibroblasts in plexiform neurofibromas, which may have an important role in the pathogenesis of these tumors. Recent work from laboratories at the Children's National Medical Center has demonstrated significant overexpression of fibroblast growth factor and platelet-derived growth factor in five plexiform neurofibromas by gene expression profiling, increasing the rationale for the use of pirfenidone.

Because of concerns over both short-term and long-term toxicities, including mutagenesis, conventional chemotherapy has not been widely employed in patients with progressive plexiform neurofibromas. Based on promising results in patients with desmoid tumors, the combination of vincristine and methotrexate is under study for plexiform neurofibromas in patients with NF1.[50]

A major issue in all of these studies comprises the entry criteria used. Although the one prospective randomized phase II study attempted to enter only those patients with progressive tumors, a subset of patients, even on that study, were entered because of clinical progression without documented radiographic progression. This variability in entry criteria makes evaluation of the efficacy of agents across studies difficult, especially given the erratic natural history of plexiform neurofibromas.

At the current time, a study evaluating the natural history of plexiform neurofibromas is ongoing (B.R. Korf, unpublished results). This study was designed to enter 300 patients with plexiform neurofibromas stratified by both age (patients younger or older than 18 years) and location (patients were stratified as regards having tumors of the head or neck, trunk and extremities externally visible, or trunk and extremities not externally visible). An interesting and somewhat unexpected finding of this study is that the majority of patients entered on study, to date, are younger than 18 years at the time of entry. This natural history study is utilizing a variety of criteria to determine if the tumor progresses, including volumetric radiographic measurements. A major goal of the study is to determine the incidence of progression of plexiform neurofibromas over a finite period of time. Data concerning this important issue are scant, and without more information, evaluating future phase II studies will be difficult. An updated listing of institutional review-approved studies in the United States supported by the National Neurofibromatosis Foundation is available at their web site (www.nf.org).

Clinical trial design. As noted, given the unpredictable natural history of plexiform neurofibromas and their infiltrative nature, clinical trial design becomes a major issue in evaluating approaches for patients with plexiform neurofibromas as well as comparing results across studies. Although such lesions do grow, it may be difficult to apply standard oncologic criteria to assess the efficacy of an agent. In most pediatric and adult oncologic trials evaluating new means of therapy for patients (phase II trials), efficacy is assessed by the ability of the agent either to increase survival or progression-free survival or to result in shrinkage of the tumor.

To date, no study in patients with NF1 has demonstrated objective (radiographic) responses in the ≥50% range. This may be because of the indolent nature of the plexiform neurofibromas and the unlikeliness of any treatment to cause such a dramatic response in the tumor growth. Alternatively, it may be caused by the lack of efficacy of agents used. Another possible reason for the inability to document tumor response is the difficulty in measuring the size of plexiform neurofibromas and determining a change in size over time. Plexiform neurofibromas are notori-

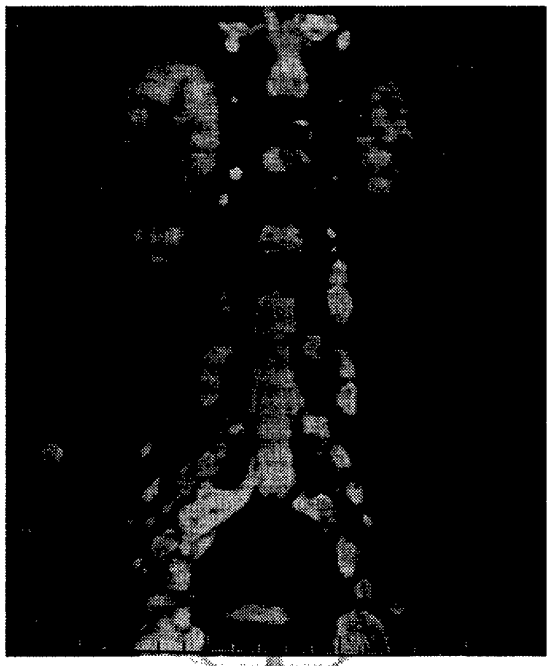

Figure 3. A 20-year-old man with lumbosacral plexiform neurofibromas. Inversion recovery coronal T2-weighted MRI of the lumbar–sacral junction reveals extensive fusiform enlargement of most of the visualized nerve roots. There is good contrast definition between the neurofibromas and the surrounding soft tissues; however, contrast between the neurofibromas and the subarachnoid fluid is poor. Central foci of low T2 signal within each nerve root ("target" sign) are a typical finding in plexiform neurofibroma.

ously large and irregular in shape, and standard two-dimensional imaging by either CT or more recently by MRI is quite difficult (figures 3 and 4).

In the aforementioned ongoing natural history study of patients with NF1, the reproducibility of volumetric MR data analysis is being analyzed. If such analysis is found to be reproducible and easily performable, it may be of major utility. Other imaging techniques have not been widely used in the evaluation of patients with NFI and plexiform neurofibromas. MR neurography is a high-resolution means to evaluate peripheral nerves and may, in the future, be of utility in evaluation of response for patients on treatment trials for plexiform neurofibromas.[51] However, at this point, the technique is relatively cumbersome and is useful predominantly for small lesions. The size of plexiform neurofibromas may make this technique, in its current state, impossible to apply to clinical studies. PET has been evaluated in intracranial lesions in patients with NF1 (the majority thought to be low-grade astrocytomas), but the utility of this technique has not been evaluated in patients with plexiform neurofibromas. PET may be helpful in identifying malignant change in plexiform neurofibromas.[52]

In attempts to overcome the issue of the erratic nature of plexiform neurofibromas, other trial designs have been investigated for patients with progressive lesions. One approach is to use the endpoint of progression-free survival, instead of objective response, as a measure for efficacy. Although this is a rational endpoint, it does not negate the problem of the erratic natural history of the disease. The use of a randomized, crossover, double-blinded, placebo-controlled study design does overcome some of these issues, as patients serve as their own controls for endpoints such as time to progression. Because there is no other standard, effective treatment for plexiform neurofibromas and these tumors may remain quiescent, even after rapid growth for a period of time, the use of a placebo arm could be postulated. Such study designs are still predicated on the concept that the population to be studied is uniform and that demonstration of progression denotes that the tumor will continue to progress over a finite period of time. This assumption has never been formally demonstrated and may, indeed, not be true for plexiform neurofibromas in patients with NF1.

Because plexiform neurofibromas often are indolent and may cause increasing dysfunction, even without clear-cut evidence of radiographic progression, other methods have been explored to determine the efficacy of an agent. In the early trials with ketotifen, a symptomatic score was developed primarily

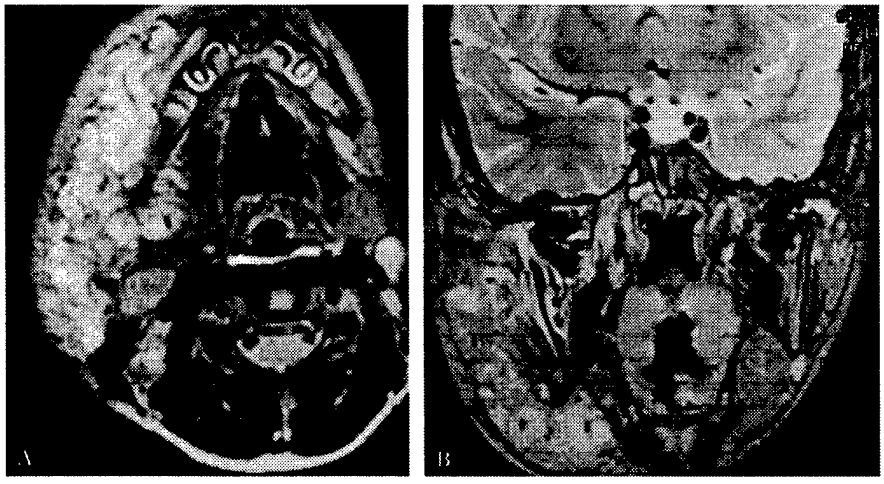

Figure 4. Extensive facial plexiform neurofibroma in an 8-year-old boy. Inversion recovery axial (A) and coronal fat-suppressed T2-weighted (B) MRI reveal extensive involvement of the subcutaneous and deep soft tissues of nearly the entire right side of the face. Accurate demarcation of the plexiform neurofibroma from surrounding fatty tissue, lymph nodes, and salivary glands cannot be made because of their similar contrast characteristics.

to determine the effect of the drug on pruritus and, to a lesser extent, pain.[53,54] Although a variety of neurologic rating scales have been used for patients with neurologic impairments, none has been reproducibly applied to patients with NF1, much less for patients with NF1 and plexiform neurofibromas. If such scales are to be used to capture the diverse manifestations of compromise caused by the plexiform neurofibromas, the scale must measure not only the neurologic impairment but also the impact of the plexiform neurofibromas on other issues such as pain, ambulation, discomfort, general well-being, and functional independence. There has been recent interest in utilizing quality-of-life scales for this type of assessment because of their ease in reporting and the breadth of information captured. A variety of different quality-of-life scales are under evaluation or have been suggested as possible outcome measures for patients on studies. The Health-Related Quality-of-Life Scale is a multi-attribute scale that evaluates the health status of attributes such as sensation, mobility, emotion, cognition, self-care, and fertility.[53] It also has measures of vision, hearing, speech, ambulation, dexterity, emotion, and cognition. The Health-Related Quality-of-Life Scale can be used in patients ranging from 6 years of age through adulthood. For children between 6 and 12 years, a parental form of the scale is available, whereas for patients older than 12 years, a self-reporting form is used. A similar, somewhat less detailed scale is the Rand 36-Item Health Survey.[54] This scale also evaluates physical functioning, mental health, and cognition. Still another potential scale is the NIH Impact of Pediatric Illness Scale (F. Balis, National Cancer Institute, personal communication, 2002). This questionnaire has been developed to assess the effects of chronic illness and treatment on the everyday behavior of children and evaluate adaptive behavior, emotional functioning, physical status, and CNS symptoms. The assessment usually takes <30 minutes but is limited by its lack of application to older patients. None of the aforementioned scales has been validated in patients with plexiform neurofibromas in NF1.

Future directions. Despite the difficulties in evaluating the efficacy of agents, a variety of studies utilizing biologically based approaches are either underway or soon to begin for patients with plexiform neurofibromas associated with NF1. The ability to design more rational therapies for NF1-associated neurofibromas and, for that matter, other manifestations of NF1 is heavily predicated on an improved understanding of the molecular and cellular biology of the cells involved in neurofibroma formation and growth. Some of these insights possibly derived from further experiments are more easily addressed utilizing mouse models and derivative cells and will likely provide critical insights into human tumors. There is still, however, a basic lack of fundamental information regarding neurofibromas in patients with NF1. Further studies will require access to tumor specimens and necessitate the development of multicenter-coordinated collection systems to provide these tissues to scientists. Key questions that still must be addressed include 1) What genetic or protein expression changes are associated with neurofibroma formation? 2) What cells participate in neurofibroma formation? and 3) What biologic markers correlate with tumor growth or arrest in response to therapy? Although paraffin-embedded specimens are of utility and can be used for FISH and immunohistochemistry-based analysis, their utility for RNA and protein activity studies is limited. Fresh snap-frozen tissue or similarly obtained tissue will be required for large-scale gene expression profiling to identify transcripts associated with tumor formation and progression. Gene expression profiling experiments afford the opportunity to identify potential transcripts that might serve as surrogate markers for tumor growth and response to therapy. In addition, fresh tissue is required to develop xenographs or primary culture models for in vitro preclinical models of human neurofibromas suitable for rapid screening of potential rational therapies.

The advances in the laboratory must be coupled with greater uniformity in the improved design of the clinical studies needed. Definition of what constitutes progressive disease has to be agreed upon to standardize criteria for patient entry. More refined means of assessment, be they volumetric analysis, other forms of neuroimaging, or quality-of-life scales, have to be validated before they can be used as determinants of the efficacy of agents. Future clinical trials, given the number of patients available for treatment, will necessitate the development of multi-institutional or national trial structures. A better understanding of the natural history of plexiform neurofibromas is required to determine the optimum time for initiation of treatment and the types of treatment most likely to succeed. However, independent of all these hurdles, there is a clear clinical need to expeditiously develop well-designed, statistically sound studies for children and adults with NF1 and plexiform neurofibromas. Potential therapies are already available, and the number is likely to increase as more is learned about the pathogenesis of NF1.

Acknowledgment

The authors thank the National Neurofibromatosis Foundation for its support.

References

1. Friedman JM, Gutmann DH, MacCollin M, et al. Neurofibromatosis: phenotype, natural history and pathogenesis. 3rd ed. Baltimore: Johns Hopkins University Press, 1999.
2. Huson SM, Harper PS, Compston DAS. Von Recklinghausen neurofibromatosis: a clinical and population study in southeast Wales. Brain 1988;111:1355–1381.
3. Korf BR. Plexiform neurofibromas. Am J Med Genet 1999;89:31–37.
4. Woodruff JM, Lourea HP, Louis DN, Scheitauer BW. Neurofibroma. In: Kleihues P, Cavenee WK, eds. World Health Orga-

nization classification of tumours, pathology and genetics of tumors of the nervous system. Lyon: IARC Press, 2000:167–168.
5. Ruggieri M, Huson S. The clinical and diagnostic implications of mosaicism in the neurofibromatosis. Neurology 2001;56: 1433–1443.
6. Korf BR. Malignancy in neurofibromatosis type 1. Oncologist 2000;5:477–485.
7. Waggoner DJ, Towbin J, Gottesman G, Gutmann DH. A clinic-based study of plexiform neurofibromas in neurofibromatosis 1. Am J Med Genet 2000;92:132–135.
8. King AA, DeBaun MR, Riccardi VM, Gutmann DH. Malignant peripheral nerve sheath tumors in neurofibromatosis 1. Am J Med Genet 2000;93:388–392.
9. Wanebo JE, Malik JM, VandenBerg SR, et al. Malignant peripheral nerve sheath tumors. Cancer 1993;71:1247–1253.
10. Thakkar SD, Feigen U, Mautner VF. Spinal tumours in neurofibromatosis type 1: an MRI study of frequency, multiple and variety. Neuroradiology 1999;41:625–629.
11. Poyhonen M, Leisti E-L, Kytola S, Leisti J. Hereditary spinal neurofibromatosis: a rare form of NF1? J Med Genet 1997;34: 184–187.
12. Coleman SD, Williams CA, Wallace MR. Benign neurofibromas in type 1 neurofibromatosis (NF1) show somatic deletions of the NF1 gene. Nat Genet 1995;11:90–92.
13. Kluwe L, Friedrich R, Mautner VF. Loss of *NF1* allele in Schwann cells but not in fibroblasts derived from an NF1-associated neurofibroma. Genes Chromosomes Cancer 1999; 24:283–285.
14. Perry A, Roth KA, Banerjee R, Fuller CE, Gutmann DH. *NF1* deletions in S-100 protein-positive and negative cells of sporadic and neurofibromatosis 1 (NF1)-associated plexiform neurofibromas and MPNSTs. Am J Pathol 2001;159:57–61.
15. Rutkowski J, Wu K, Gutmann DH, et al. Multiple mechanisms of benign tumor formation in neurofibromatosis type 1. Hum Mol Genet 2000;9:1056–1066.
16. Sawada S, Florell S, Purandare SM, et al. Identification of *NF1* mutations in both alleles of a dermal neurofibroma. Nat Genet 1996;14:110–112.
17. Serra E, Puig S, Otero D, et al. Confirmation of a double hit model for the *NF1* gene in benign neurofibromas. Am J Hum Genet 1997;61:512–519.
18. Serra E, Rosenbaum T, Winner U, et al. Schwann cells harbor the somatic *NF1* mutation in neurofibromas: evidence of two different Schwann cell subpopulations. Hum Mol Genet 2000; 9:3055–3064.
19. Xu G, O'Connell P, Viskochil D, et al. The neurofibromatosis type 1 gene encodes a protein related to GAP. Cell 1990;62: 599–608.
20. Ballester R, Marchuk DA, Boguski M, et al. The *NF1* locus encodes a protein functionally related to mammalian GAP and yeast IRA proteins. Cell 1990;63:851–859.
21. Sherman LS, Atit R, Rosenbaum T, et al. Single cell Ras-GTP analysis reveals altered ras activity in a single population of neurofibroma Schwann cells but not fibroblasts. J Biol Chem 2000;275:30740–30745.
22. Lau N, Feldkamp MM, Roncari L, et al. Loss of neurofibromin is associated with activation of ras/MAPK and PI3-K/Akt signaling in a neurofibromatosis 1 astrocytoma. J Neuropathol Exp Neurol 2000;59:759–767.
23. Kopelovich L, Rich RF. Enhanced radiotolerance to ionizing radiation is correlated with increased cancer proneness of cultured fibroblasts from precursor states in neurofibromatosis patients. Cancer Genet Cytogenet 1986;22:203–210.
24. Akit RP, Crowe MJ, Greenhalgh DG, et al. The NF1 tumor suppressor regulates skin wound healing, fibroblast proliferation, and collagen deposition by fibroblasts. J Invest Dermatol 1999;112:835–842.
25. Ingram DA, Yang F-C, Travers JB, et al. Genetic and biochemical evidence that haploinsufficiency of the Nf1 tumor suppressor gene modulates melanocyte and mast cell fates in vivo. J Exp Med 2000;191:181–187.
26. Perisio PM, Brooks JJ. Expression of growth factors and growth factor receptors in soft tissue tumors: implications for the autocrine hypothesis. Lab Invest 1989;60:245–253.
27. DeClue JE, Heffelfinger S, Benbenuto G, et al. Epidermal growth factor receptor expression in neurofibromatosis type 1-related tumors and NF1 animal models. J Clin Invest 2000; 105:1233–1241.
28. Arbiser JL, Flynn E, Barnhill RL. Analysis of vascularity of human neurofibromas. J Am Acad Dermatol 1998;38:950–954.
29. Sheela S, Riccardi VM, Ratner N. Angiogenic and invasive properties of neurofibroma Schwann cells. J Cell Biol 1990; 111:645–652.
30. Muir D, Neubauer D, Lim IT, et al. Tumorigenic properties of neurofibromin-deficient neurofibroma Schwann cells. Am J Pathol 2001;158:501–513.
31. Muir D. Differences in proliferation and invasion by normal, transformed and NF1 Schwann cell cultures are influenced by matrix metalloproteinase expression. Clin Exp Metast 1995; 13:303–314.
32. Birindelli S, Perrone F, Oggionni M, et al. Rb and TP53 pathway alterations in sporadic and NF1-related malignant peripheral nerve sheath tumors. Lab Invest 2001;81:833–844.
33. Liapis H, Marley EF, Lin Y, Dehner LP. p53 and Ki-67 proliferating cell nuclear antigen in benign and malignant nerve sheath tumors in children. Pediatr Dev Pathol 1999;2:377–384.
34. Kindblom LG, Ahlden M, Meis-Kindblom JM, Stenman G. Immunohistochemical and molecular analysis of p53, mdm2, proliferating cell nuclear antigen and Ki67 in benign and malignant nerve sheath tumors. Virchows Arch 1995;427:19–26.
35. Halling KC, Scheithauer BW, Halling AC, et al. p53 expression in neurofibroma and malignant peripheral nerve sheath tumor: an immunohistochemical study of sporadic and NF1-associated tumors. Am J Clin Pathol 1996;106:282–288.
36. Nielsen GP, Stemmer-Rachamimov AO, Ino Y, et al. Malignant transformation of neurofibromas in neurofibromatosis 1 is associated with CDKN2A/p16 inactivation. Am J Pathol 1999;155:1879–1884.
37. Kourea HP, Cordon-Cardo C, Dudas M, et al. Expression of p27-Kip and other cell cycle regulators in malignant peripheral nerve sheath tumors and neurofibromas: the emerging role of p27-Kip in malignant transformation of neurofibromas. Am J Pathol 1999;155:1885–1891.
38. Koureau HP, Orlow I, Scheithauer BW, et al. Deletions of the INK4A gene occur in malignant peripheral nerve sheath tumors but not in neurofibromas. Am J Pathol 1999;155:1855–1860.
39. Cichowski K, Shih TS, Schmitt E, et al. Mouse models of tumor development in neurofibromatosis type 1. Science 1999; 286:2172–2176.
40. Vogel KS, Kleese LJ, Velasco-Miguel S, et al. Mouse tumor model for neurofibromatosis type 1. Science 1999;286:2176–2179.
41. Needle MN, Cnaan A, Dattilo J, et al. Prognostic signs in the surgical management of plexiform neurofibroma: the Children's Hospital of Philadelphia experience, 1974–1994. J Pediatr 1997;131:678–682.
42. Riccardi VM. Mast-cell stabilization to decrease neurofibroma growth. Arch Dermatol 1987;123:1011–1016.
43. Riccardi VM. A controlled multiphase trial of ketotifen to minimize neurofibroma-associated pain and itching. Arch Dermatol 1993;129:577–581.
44. Riccardi VM. The potential role of trauma and mast cells in the pathogenesis of neurofibromas. In: Ishibashi Y, Hori Y, eds. Tuberous sclerosis and neurofibromatosis: epidemiology, pathophysiology, biology and management. New York: Elsevier, 1990:167–190.
45. Gupta A, Cohen B, Ruggierri P, et al. A phase I study of thalidomide for the treatment of plexiform neurofibroma in patients with neurofibromatosis 1 (NF1). Neurology 2000;54: 12–13. Abstract.
46. Yan N, Ricca C, Fletcher J, et al. Farnesyl transferase inhibitors block the neurofibromatosis type 1 (NF1) malignant phenotype. Cancer Res 1995;55:3569–3575.
47. Gurujeyalakshmi G, Hollinger MA, Giri SN. Pirfenidone inhibits PDGF isoforms in bleomycin hamster model of lung fibrosis at the translational level. Am J Physiol 1999;276: L311–L318.
48. Iyer SN, Gurujeyalakshmi G, Giri SN. Effects of pirfenidone on procollagen gene expression at the transcriptional level in bleomycin hamster model of lung fibrosis. J Pharmacol Exp Ther 1998;189:211–218.

49. Raghu G, Johnson WC, Lockhart D, Mageto Y. Treatment of idiopathic pulmonary fibrosis with a new antifibrotic agent, pirfenidone: results of a prospective, open-label phase II study. Am J Respir Crit Care Med 1999;159:1061–1069.
50. Lachner H, Urban C, Kerbl R, et al. Noncytotoxic drug therapy in children with unresectable desmoid tumors. Cancer 1997;80:334–340.
51. Maravilla KR, Bowen BC. Imaging of the peripheral nervous system: evaluation of peripheral neuropathy and plexopathy. AJNR 1998;19:1011–1023.
52. Ferner RE, Lucas JD, O'Doherty MJ, et al. Evaluation of 18fluorodeoxyglucose positron emission tomography (18FDG PET) in the detection of malignant peripheral nerve sheath tumours arising from within plexiform neurofibromas in neurofibromatosis 1. J Neurol Neurosurg Psychiatry 2000;68:353–357.
53. Gill TM, Feinstein AR. A critical appraisal of the quality-of-life measurements. JAMA 1994;272:619–626.
54. Hays RD, Sherbourne C, Manzel E. The Rand 36-item health survey 1.0. Health Econ 1993;2:217–227.

Neuro *Images*

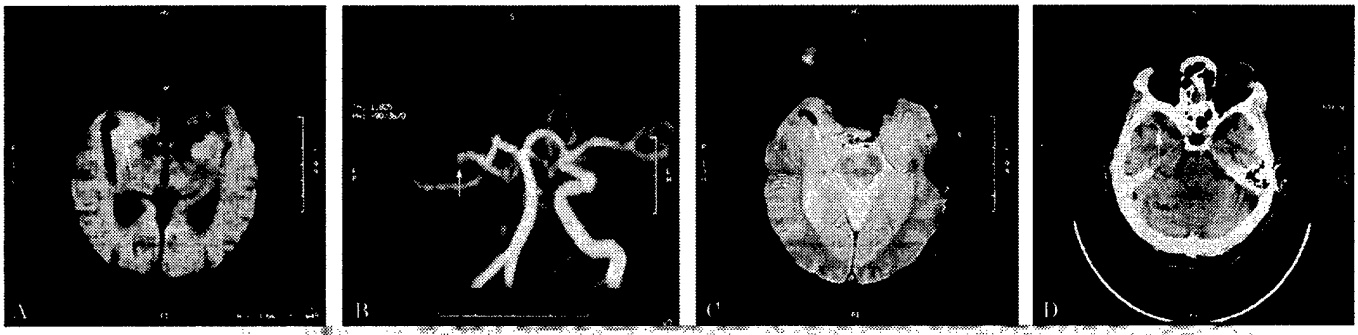

Figure. (A) Hyperintense region is seen in the right middle cerebral artery (MCA) territory on diffusion-weighted imaging compatible with an acute infarct (arrow). (B) MR angiography shows occlusion of the right internal carotid artery with partial cross-filling of the right MCA and signal loss at the right M1 segment (arrow). (C) GRE reveals the susceptibility artifact of acute thromboembolism in the right MCA (arrow). (D) Nonenhanced CT depicts a right hyperdense MCA sign (arrow).

The hypointense MCA sign

J.A. Chalela, MD, J.B. Haymore, RN, MS, ACNP,
M.A. Ezzeddine, MD, L.A. Davis, RN, MSN, S. Warach, MD, PhD,
Bethesda, MD

A 74-year-old woman with history of hypertension and atrial fibrillation arrived at the hospital 20 minutes after a sudden onset of left hemiparesis. On examination, she was alert and oriented, had a right gaze preference, left homonymous hemianopia, left hemineglect, and dense left hemiparesis.

An emergent MRI and CT of the brain were obtained. An acute ischemic stroke was noted in the right middle cerebral artery (MCA) territory (figure, A). Intracranial MR angiography revealed a complete occlusion of the right internal carotid artery with partial cross-filling of the right MCA terminating at the right M1 (see figure, B) Gradient echo imaging (GRE) revealed a hypointense ovoid signal in the distal right sylvian fissure (see figure, C). A nonenhanced CT scan of the brain showed a right hyperdense MCA sign in the same territory (see figure, D).

The hyperdense MCA sign on CT is a well-characterized radiologic finding that may indicate acute vessel occlusion. Hypointense signals on GRE that are within vascular cisterns may also indicate acute thrombosis and should not be confused with acute hemorrhage, which may have similar characteristics.[1] Defining features of the hypointense MCA sign on GRE include unilateral susceptibility changes that exceed the vessel diameter of the contralateral and susceptibility changes confined to vascular cisterns. Further evidence to support this conclusion is a corresponding vessel occlusion on MR angiography, homolateral perfusion deficit, and hyperdense MCA sign on CT.[2] Distinguishing between the hypointense MCA sign indicating intraluminal occlusion and a hypointense region of intraparenchymal hemorrhage has important therapeutic implications in the acute stroke patient.

1. Linfante I, Llinas R, Caplan L, Warach S. MRI features of intracerebral hemorrhage within 2 hours from symptom onset. Stroke 1999;30:2263–2267.
2. Flacke S, Urbach H, Keller E, et al. Middle cerebral artery (MCA) susceptibility sign at susceptibility-based perfusion MR imaging: clinical importance and comparison with hyperdense MCA sign at CT. Radiology 2000;215:476–482.

See also page 1512

Technical Abstract in proposal to the US Army Medical Research and Materiel Command NFRP02 (Log#NF020074; September, 17, 2002; PI: **David H. Viskochil**)

TECHNICAL ABSTRACT

Immunohistochemical and Genetic Analyses in Peripheral Nerve Sheath Tumors in NF1
David Viskochil, M.D., Ph.D., Investigator-Initiated Research Award

Background: Malignant peripheral nerve sheath tumor (MPNST) is a sarcoma arising from the peripheral nerve sheath, and its association with neurofibromatosis type 1 (NF1) is well-established. A number of biochemical pathways have been shown to be altered in association with MPNSTs, but the mouse model provides compelling evidence to promote p53 as the most important contributor to malignant transformation. There have been relatively few studies that have focused on the correlation of p53 immunohistochemical staining with *TP53* mutation analysis in human MPNSTs. This correlation needs to be explored, without losing sight of the potential for contributions from other disrupted pathways in malignant transformation. Extensive chromosome analysis, combined with comparative genomic hybridization (CGH), has identified but a few candidate loci harboring candidate genes that may be involved in the altered cellular biology of MPNSTs. A novel technique, CGH microarray, which provides a higher resolution screen of genome imbalances, has not been applied to the study of tumor progression in PNSTs.

Objectives: This project is devoted to the study of peripheral nerve sheath tumors, plexiform neurofibromas and MPSNTs, with respect to NF1. It is divided in 3 parts. The first objective is to develop a better understanding of the role p53 plays in PNST progression. The second objective is to expand our knowledge base of underlying genetic imbalances that arise during "malignant transformation." The third objective is to implement a high-throughput germ-line *NF1* mutation screen to better screen the NF1 population for mutations that may predispose one to develop an MPNST.

Specific Aims: 1.) To determine the immunohistochemical and genetic changes in p53 and *TP53* in the evolution of plexiform neurofibromas to MPNSTs. 2.) To evaluate genomic DNA from PNSTs to identify unbalanced chromosomal regions harboring candidate genes that may contribute to malignant transformation in PNSTs. 3.) To apply high-throughput DNA sequencing to identify *NF1* germline mutations, and to determine if mutation class is associated with an increased risk for MPNST.

Study Design: Archived and prospectively acquired plexiform neurofibromas and MPNSTs will be profiled with a panel of immunohistochemical markers, including a more robust set of p53 antibodies that can distinguish wild-type, mutant and phosphorylated p53. Staining will be correlated with plexiform neurofibromas, low-grade MPNSTs and high-grade MPNSTs. Mutation analysis will be performed on tumor DNA for *TP53* to correlated the presence of mutation with the staining patterns. Spectral Genomics™ has developed a human genome array of 1003 non-overlapping clones that allow quantification of test-DNA hybridization at an average resolution of 3 megabases. CGH microarray analysis will be performed on DNA extracted from plexiform neurofibromas and MPNSTs. Genome imbalances from tumor specimens will be identified and correlated with tumor grades and immunohistochemistry expression profiles. NF1 patients enrolled in this study will be screened with high-throughput cDNA and genomic DNA sequencing protocols for *NF1* mutations. Classes of *NF1* mutations will be correlated with the presence of MPNST.

Relevance: Plexiform neurofibromas are relatively common in NF1, affecting up to 20% of all individuals. Only a subset of these benign tumors undergo malignant transformation, however, neither genetic nor immunohistochemical markers are presently available to signal which plexiform tumors are at risk to evolve into MPSNTs. In addition, there is not an effective surveillance protocol for early detection of MPNST, nor is there effective medical treatment for the malignancy once it has arisen. A better understanding of the pathophysiology of PNSTs is essential for the development of rational adjuvant therapies to complement present day standard of care.

Technical Abstract in proposal to the US Army Medical Research and Materiel Command NFRP03 (Log#NF030073; August, 23, 2003; PI: **David H. Viskochil**)

Technical Abstract in the Body of Submitted Proposal for Clinical Trial Development Award to the NFRP03 in 2003. Log #NF030073.

A major goal of this CTDA proposal is to optimize subject recruitment in each of the clinical trials. Using the prevalence estimate for NF1 as 1 in 3,500 individuals in the population at large coupled with the cross-sectional estimate of 5% affected by MPNST, we acknowledge that few centers will have more than 2 patients with MPNST and NF1 in any given year. We anticipate 1 in 1,750,000 people will develop MPNST and NF1 on an annual basis, thus the populations of the US, Canada, and Europe will provide a maximum of 50 cases per year. Our goal is to recruit at least 2/3 of this cohort for enrollment in at least 1 of the 3 clinical trials. By developing a well-publicized network of NF1 Clinic Centers and Sarcoma Centers, we plan to offer enrollment to every individual in North America and Europe who has MPNST and NF1 into the case-control trial to identify risk factors for MPNST (**clinical trial project 1**). Based on inclusion and exclusion criteria, some individuals will be eligible for the clinical trial of neoadjuvant chemotherapy, and this will be offered to them as a treatment option (**clinical trial project 3**). Subjects with symptomatic peripheral nerve sheath tumors will be offered enrollment in the PET scanning surveillance study, but this is limited to specific centers where PET scanning is available (**clinical trial project 2**). Nevertheless, those who have MPNST detected as part of clinical trial project 2 will be offered enrollment in projects 1 and 3. Finally, a portion of every MPNST that is biopsied or resected will be sent to the tumor repository at Washington University for routine analysis and storage. This core will be administered by Mark Watson, and clinicopathologic studies will be performed under the guidance of Arie Perry. The availability of tissue samples that are processed in a standardized way may provide the most significant outcome of this multi-center proposal. Distribution of this material to other laboratories that are performing research related to NF1 and/or MPNSTs may provide further insight to their molecular pathology.